Master's thesis

NTNU
Norwegian University of Science and Technology
Faculty of Engineering
Department of Energy and Process Engineering

Signe Truyen Ryssdal

High Temperature Heat Pumps in Integrated Energy Systems

Master's thesis in Energy and Process Engineering
Supervisor: Trygve Magne Eikevik
December 2020

NTNU
Norwegian University of
Science and Technology

Signe Truyen Ryssdal

High Temperature Heat Pumps in Integrated Energy Systems

Master's thesis in Energy and Process Engineering
Supervisor: Trygve Magne Eikevik
December 2020

Norwegian University of Science and Technology
Faculty of Engineering
Department of Energy and Process Engineering

NTNU
Norwegian University of
Science and Technology

Norwegian University of Science and Technology

Faculty of Engineering
Department of Energy and Process Engineering

MASTER'S THESIS

for

Student Signe Truyen Ryssdal

Autumn 2020

High temperature heat pumps in integrated energy systems

Høytemperatur varmepumper i integrerte energisystemer

Background and objective

A combined cooling, heating and power generation system meets the need of low-carbon neighborhood to fully absorb renewable energy. A development of load peak-shaving technology of renewable energy based on solar energy with thermal energy storage (TES), as well as the new solar-thermal converting devices, with high-temperature heat pump and compact energy storage system (PCM). At the scenario of 100% clean energy, to achieve a high proportion of renewable energy acceptance by energy supply system in large public buildings or small-scale neighborhoods. In such systems it is necessary to develop high temperature electric heat pump using green or natural working fluid, which the hot side outlet temperature can reach to 100°C, the temperature rise can exceed 50°C, and the COP of the heating system can exceed 3.5. Evaluate a heat pump that fulfills these requirements and analyze how it functions with the other part of the combined cooling, heating, and power generation system.

The following tasks are to be considered:

1. Literature review on combined cooling, heating, and power generation systems and high temperature heat pumps
2. Define the case for the investigation with the integrated heat pump system
3. Develop the simulation model
4. Evaluate the potential of the high temperature heat pump with natural working fluids
5. Make a draft scientific paper of the main results in the thesis
6. Make proposal for further work

Abstract

This thesis is a part of the first stage in the project «Key technologies and demonstration of combined cooling, heating, and power generation for low-carbon neighborhoods/buildings with clean energy – ChiNoZEN». An integrated energy system consisting of a PVT-system, a battery for electrical power, a thermal energy storage system, a high-temperature heat pump, and district heating was modelled in Matlab. The heat pump consisted of two compressors installed in parallel, as well as two condensers. The operation of the system was simulated over the course of one year for three Chinese cities: Shanghai, Lanzhou, and Beijing. For every hourly iteration, the heat demand, available electrical power, and available energy in the thermal energy storage system were compared, and the operational mode of the heat pump was decided based on the results. The high-temperature heat pump used Ammonia as its refrigerant and achieved a COP of 3.55, a condensation temperature of 96°C and a temperature lift of 72°C. The heat pump had a maximum capacity of 255.7 kW, and the thermal storage had a maximum capacity of 1000 kWh.

The results from the simulations showed that the system behaved similarly in the three cities during the summer months when temperatures were high and there was little or no demand for space heating. In the colder months, the heat demand in Lanzhou and Beijing was higher than in Shanghai. The heat pump operated on full load providing the thermal energy storage had not reached full capacity. However, when the power supply was insufficient for full load operation, the heat pump operates don part load. It was shut off when the maximum capacity of the thermal energy storage was reached.

The temperatures in the condensers remained relatively constant throughout the year, but a reduction in condenser temperature was observed during part load operation of the heat pump. This led to a lower heat sink temperature. The COP of the system increased during part load operation, likely due to the reduction in condenser temperatures and therefore lower temperature lifts. The annual average heat pump COP was higher than the annual system efficiency for all three cities. This was due to losses in the thermal energy storage system.

The system was able to provide sufficient heat to cover demand for most of the year, although some heat shortages were observed for all three cities during the winter months. The heat shortages happened because of periods with insufficient power to operate the heat pump, so the heat pump was shut off in spite of a high heat demand. The capacities of the thermal and electrical energy storage systems were not high enough to provide a stable heat supply in the periods with high heat demand.

It was found that the area of the PV panels should be increased to produce more power so that the heat pump operation would not be limited by lack of available power. An alternative power source could also be installed to provide more power. Furthermore, the capacity of the battery storage and the thermal energy storage should be increased to provide a more stable supply of heat and electric power than the system currently experiences. Lastly, heat pump parameters such as mass flow rates and size of compressors and heat exchangers should be optimized to increase the overall efficiency.

Sammendrag

Denne oppgaven er en del av første trinn i prosjektet project «Key technologies and demonstration of combined cooling, heating, and power generation for low-carbon neighborhoods/buildings with clean energy – ChiNoZEN». En modell av en to-trinns høytemperaturs varmepumpe som bruker ammoniakk som arbeidsmedium har blitt laget. Varmepumpen består av to kompressorer koblet parallelt, to kondensatorer, en akkumulator, en ekspansjonsventil og en fordamper. Varmepumpen er en del av et integrert energisystem som i tillegg består av solcellepaneler, et batteri for laging av elektrisk energi, et varmebatteri og fjernvarme. Hele energisystemet ble modellert, og driften over et år ble simulert for tre ulike lokasjoner: De kinesiske byene Shanghai, Lanzhou og Beijing. Verdier for varmeetterspørsel, varmepumpens kapasitet, tilgjengelig strøm og tilgjengelig varme i varmebatteriet ble regnet ut for hver time. Driften av varmepumpen i den aktuelle timen ble deretter bestemt basert på etterspørsel og tilgjengelig strøm og varme. COP for varmepumpen er 3,55, fordampingstemperatur er 96°C og den opererer med et temperaturløft på opptil 72°C. Varmepumpen har en maksimal kapasitet på 255,7 kW, og varmebatteriet har en maksimal lagringskapasitet på 1000 kWh.

Resultatene fra simuleringene viste at driften av systemet var relativt lik i alle de tre byene i perioder med høye temperaturer og store mengder stråling fra sola. I disse periodene var det lite behov for varme. I perioder med lavere temperaturer var varmeetterspørselen høyere i Lanzhou og Beijing enn i Shanghai. Varmepumpen opererte med fullast når det var mulig, forutsatt at varmelageret ikke var fullt. Hvis varmelageret var fullt, ble varmepumpen slått av frem til varmelageret var tomt igjen. De gangene det ikke var nok tilgjengelig strøm for at varmepumpen kunne gå på fullast, gikk den på dellast.

Kondensatortemperaturene holdt seg relativt stabile gjennom året, men ble redusert hver gang varmepumpen opererte med dellast. Dette førte til en lavere utgående vanntemperatur på vannet som ble varmet opp av kondensatoren. Varmepumpens virkningsgrad økte når varmepumpen opererte med dellast, sannsynligvis som følge av lavere kondensatortemperaturer og dermed et mindre temperaturløft. Årlig COP for varmepumpen var høyere enn total årlig virkningsgrad for systemet i alle de tre byene. Det er grunnet tap i varmebatteriet.

Det integrerte energisystemet lyktes i å dekke varmebehovet for mesteparten av året, men alle byene opplevde perioder der behov var større enn tilgjengelig varmekapasitet. Dette skjedde fordi varmepumpen ikke alltid kunne operere til tross for stor etterspørsel, fordi det ofte ikke var nok strøm tilgjengelig til å drive varmepumpen. Videre var kapasiteten på både varmebatteri og elektrisk batteri for lav til å kunne gi en jevn mengde varme gjennom perioder med lave temperaturer og høy etterspørsel.

Det ble observert at solcellepanelene bør ha et større areal enn de har i denne simuleringen, slik at de kunne produsere mer elektrisk energi. Eventuelt kan en sekundær strømkilde kobles til systemet. I tillegg må kapasiteten på både elektrisk batteri og varmebatteri økes slik at nok energi alltid er tilgjengelig til å drive kompressoren og til å supplere varme til fjernvarmeanlegget. Verdiene til variabler som massestrøm i tillegg til faste verdier som kompressorstørrelse og areal til varmevekslere bør også optimaliseres for å øke systemets virkningsgrad.

摘要

论文研究是基于“清洁能源低碳社区/建筑冷热电联产关键技术与示范——ChiNoZEN”项目第一阶段的一部分，主要考虑构建一个两级压缩高温氨热泵系统，并使得其 COP 为 3.55、冷凝温度为 96℃、温升可达 72℃。集成能源系统中，除了高温热泵，还包括 PVT 系统、电力电池、热能储存系统和区域供热系统。该系统在上海、兰州和北京三个城市进行了为期一年的模拟运行。热泵的最大容量为 255.7 千瓦，储热器的最大容量为 1000 千瓦时。

文章进一步利用 Matlab 模拟系统性能，其中制冷剂特性通过 Refprop 提供。以每小时为迭代过程单位，比较了蓄热系统的热需求量、可用电功率和可用能，并在此基础上确定了热泵的运行模式。

模拟结果表明，在夏季，系统在北京，上海，兰州这三个城市表现相近，主要由于气温较高，其对集中供暖的需求很少甚至没有。而在较冷的月份，兰州和北京的热需求高于上海。在冬季，热泵无法提供足够的能量来满足这三个城市中的任何一个城市的热量需求，但是可用热量与需求之间的差距最大的是兰州和北京。

上海全年电力供热的缺口为 44795 千瓦时，兰州的是 263130 千瓦时，北京的是 187534 千瓦时。电力供热的短缺主要发生在冬季，此时气温低而热量需求量大。短缺的原因是，在需求量大的时期，由于运行热泵的可用功率很少或没有，热泵只能停机几个小时。如果有更多的电力供应，短缺就会减少。研究表明，如果北京和上海能够随时提供足够的电能使热泵满负荷运行，并且如果储能容量更大，则北京和上海的可用热量和热需求之间的差距可以完全消除。然而，在冬季，兰州的热需求将需要更大的热泵，其容量大于 255 千瓦。

该热泵系统由两台并联安装的压缩机和两台冷凝器组成。冷凝器内的温度全年保持相对恒定，但在热泵部分负荷运行期间，冷凝器温度有所下降，此时将导致散热片温度降低。在部分负荷运行期间，系统的 COP 增加，可能是由于冷凝器温度降低，因此温度升高较低。

研究同时发现，增加太阳能电池板的面积可以产生更大的功率，使得热泵的运行不受可用功率不足的限制。同时也可以考虑安装一个可替代电源来提供更多的电力。此外，应增加电池和热能储存的容量，以提供比当前系统更稳定的热量和电力供应。最后，应优化热泵参数，如质量流量、压缩机和换热器的尺寸，以提高整体效率。

Preface

This specialization project has been carried out as a cooperation between NTNU and SJTU as part of the Double Degree program the two universities share. The work was supposed to be carried out in Shanghai, China, but due to the COVID-19 pandemic, I was unable to return to China. I therefore carried out the work in Norway, and I am very thankful to both universities for how helpful they have been in this unusual situation. People at SJTU and NTNU helped me move my belongings from China to Norway. SJTU changed their courses and mandatory assignments so that it was possible to finish my degree on time even though I could not be in Shanghai, and NTNU provided workspaces and other assistance.

I would like to thank Professor Trygve Magne Eikevik from NTNU for his guidance with this project. His help and willingness to lend me books and explain the things I did not fully understand has been invaluable, and I always feel welcome to pay him I visit in his office. Furthermore, I would like to thank Professor Ruzhu Wang and Doctor Bin Hu from SJTU. They have been very helpful during my time in Shanghai at SJTU. Not only have they helped me with academic issues and welcomed me into their research group, but they have helped me overcome cultural differences and navigate life as a Norwegian in China.

I have now finished five wonderful years of studies at NTNU and SJTU. I would like to thank all the friends I have made throughout the years for making my time as a student so unforgettable. I am grateful for the many opportunities I have had to be a part of various student organizations, and I am especially grateful for my time in Propulse NTNU. My family and friends have always supported me, and they are always there for me if I need something. I would especially like to thank my parents for the incredible life they have given me, full of unconditional love and support.

Table of Contents

List of Figures

List of Tables

List of Equations

List of Abbreviations

BJ	Beijing
CCHP	Combined Cooling, Heating and Power
CFC	Chlorofluorocarbon
CHX	Cascade Heat Exchanger
CO_2	Carbon Dioxide
COP	Coefficient of Performance
COP_{Ca}	Coefficient of Performance for a Carnot cycle
DH	District Heating
GWP	Global Warming Potential
HC	Hydrocarbon
HCFC	Hydrochlorofluorocarbon
HFC	Hydrofluorocarbon
HFO	Hydrofluoroolefin
HP	Heat Pump
HT	High Temperature
HTC	High-temperature cycle
HTHP	High Temperature Heat Pump
HVAC	Heating, Ventilation, and Air-Conditioning
IES	Integrated Energy System
IoT	Internet of Things
K	Kelvin
Kg	Kilogram (unit for mass)
kJ	Kilo joule (unit for energy)
LCA	Life Cycle Assessment
LHT	Latent Heat Transfer
LMTD	Logarithmic Mean Temperature Difference
LR	Load Ratio
LT	Low Temperature
LTC	Low Temperature Cycle
LZ	Lanzhou
MPP	Maximum Power Point
NTNU	Norwegian University of Science and Technology
ODP	Ozone Depletion Potential
Pa	Pascal (unit for pressure)
PCM	Phase Changing Materials
PDF	Portable Document Format
PH diagram	Pressure-enthalpy diagram
PV	Photovoltaics
PVT	Photovoltaic-thermal
SH	Shanghai
SHT	Sensible Heat Transfer
SJTU	Shanghai Jiao Tong University
STC	Standard Test Conditions
VHTHP	Very High Temperature Heat Pump
VPN	Virtual Private Network
W	Watt (unit for power)
kWh	Kilowatthour (unit for energy)

Nomenclature

$\dot{Q}_0$	Refrigeration capacity (Also referred to as $\dot{Q}_e$) [kW]
$\dot{Q}_c$	Heating capacity [kW]
$\dot{m}_R$	Mass flow rate of refrigerant [kg/s]
$\dot{m}_{HW}$	Mass flow rate of water through HT condenser [kg/s]
$\dot{m}_{CW}$	Mass flow rate of water through evaporator [kg/s]
$\dot{m}_{MW}$	Mass flow rate of water through T condenser [kg/s]
$\dot{m}_{DH}$	Mass flow rate of water through district heating [kg/s]
$\dot{W}$	Work done by the compressor [kW]
T_0	Temperature in evaporator [K]
T_c	Temperature in condenser [K]
h	Enthalpy [kJ/kg]
s	Entropy [kJ/kgK]
η	Compressor efficiency [-]
η_{is}	Isentropic efficiency [-]
η_{vol}	Volumetric efficiency [-]
η_{STC}	Efficiency at standard test conditions [-]
Π	Pressure Ratio [-]
U	U-value. Heat transfer coefficient through a material [W/m^2K]
A	Area [m^2]
T	Temperature [K]
T_{HW}	Temperature of water through HT condenser [K]
T_{CW}	Temperature of water through evaporator [K]
T_{MW}	Temperature of water through LT condenser [K]
Θ	Thermal length [K]
r	Operating efficiency [-]
T_{STC}	Temperature at standard test conditions [K]
T_{PV}	Temperature of PV module [K]
TC	Temperature coefficient of the maximum point [%/K]
E	Energy [kWh]
H	Global horizontal radiation [kW/m^2]
PR	Performance ratio [-]
P_{max}	Maximum power point [Wp]
D	Heat Demand [kWh]
C_p	Specific heat capacity at constant pressure [kJ/kgK]

1 Introduction

1.1 Background and motivation

In the past few decades, climate change has been a widely discussed topic. Since the late 1800s, the average global surface temperature has risen about 0.9°C, and most of the warming has taken place during the past 35 years (NASA, 2020). The increase in surface temperature of the Earth is often called "global warming". The effects of the climate change can already be seen through the melting of glaciers, more extreme weather, shift of plant and animal ranges, and more. Global warming happens when the gases in the atmosphere absorb the radiative heat from Earth, preventing the energy from going through the atmosphere and effectively "trapping" it on Earth (NASA, 2019). Many of the gases that contribute to global warming can be found naturally in the atmosphere, but their concentration has increased dramatically due to emission from human activities from the industrial revolution and onwards (NASA, 2019). The effect is similar to the way heat is "trapped" in a greenhouse, and therefore the gases that accumulate in the atmosphere and contribute to global warming are often referred to as "greenhouse gases". To limit the temperature increase, the emission of these gases must be drastically reduced.

Global energy consumption and production account for a big part of annual greenhouse gas emissions, so by changing the way we use energy we can reduce greenhouse gas emissions and slow down global warming. Every year, the International Energy Agency (IEA) publishes their annual World Energy Outlook report, where trends in energy demand and supply are analyzed. According to their Global Status Report from 2017, buildings and construction account for 36% of global energy use and 39% of energy related CO_2 emissions (World Green Building Council, 2017) (World Green Building Council, 2017).Operational emissions, that is emissions from heating, cooling, and lighting of buildings, account for 28% of global emissions (World Green Building Council, 2019). As the world is becoming more developed, the demand for heating and cooling will likely rise, as more people will be financially able to equip their residences with heating and cooling systems.

In 2015, a little more than 20% of global electricity production came from renewable sources (Ritchie and Roser, 2020). This means that almost 80% of the electricity in the world is produced by non-renewable sources. This is in spite of the fact that viable renewable alternatives exist in the market today, such as solar power, hydropower, and wind power.

According to the IEA, heat accounted for 50% of final global energy consumption in 2018, and 40% of global CO2 emissions. 46% of the heat produced was used in buildings, mainly for space and water heating. 50% was used in industrial processes, and the last 4% was used in agriculture. Of all the heat produced in 2018, only 10% came from renewable energy sources (IEA, 2019). Increasing this share by replacing old heating systems with greener, more efficient technologies can contribute greatly to a decrease in global greenhouse gas emissions. Many alternatives exist today, such as district heating systems, solar heaters, and heat pumps.

Another change the world has witnessed in the past years is the rapidly increasing use of the internet in almost everything people do. People use the internet in their work, for entertainment, for research, for news, and most importantly, for communication. The internet facilitates communication not just between humans, but between appliances, products, and devices. The "internet of things" (IoT) has become one of the most important emerging technologies (Nord et al., 2019).

Among the systems facilitated by the internet of things are integrated energy systems (IES). Such systems consist of various energy systems that are connected and operate interdependently of one another. Integrated energy systems have shown significantly higher energy efficiency than typical independent energy supply systems (Li et al., 2017). The implementation of the internet of thigs can optimize the communication between the various components of integrated energy systems. Typical integrated energy systems consist of combined cooling, heating, and power (CCHP), but other combinations also exist. Two of the main benefits of integrated energy systems are the reduced overall cost if the system is properly controlled and the reduced environmental impact due to the higher overall efficiency. To further reduce the environmental impact, renewable energy sources can be integrated into these energy systems.

The challenge that faces humanity with regards to climate change and global warming is the main motivation factor behind this project. The climate is changing rapidly, even though the data show huge potential for reduction in greenhouse gas emissions. Heat pumping technology, coupled with smart energy management systems and local electricity production, can greatly reduce the carbon footprint of the energy sector and give hope for a greener future.

1.2 About the project

This thesis is part of the project «Key technologies and demonstration of combined cooling, heating, and power generation for low-carbon neighborhoods/buildings with clean energy – ChiNoZEN». The ChiNoZEN project supports the transition to a reliable, affordable, publicly accepted, sustainable built environment, aiming at reducing fossil fuel dependency in the face of increasingly scarce resources, growing energy needs, and threatening climate change. The project is funded by the Research Council of Norway and the Ministry of Science and Technology in China, and has a variety of industry and academic partners in China and Norway (NTNU Department of Energy and Process Engineering, 2020).

In this thesis, a model of an integrated energy system will be created in Matlab. The integrated energy system will consist of a solar photovoltaic-thermal system (PVT), a battery for electric energy storage, a high-temperature heat pump, and a thermal energy storage system. Furthermore, the system will be connected to district heating. The operation of the energy system will be simulated for a year in three different locations in China: Shanghai, Lanzhou, and Beijing. The focus of the simulations is the operation of the heat pump. The goal is to investigate how the heat pump operates with the other components of the integrated energy system over the course of one year. Because the work is part of the ChiNoZEN project, ways to improve the existing model will also be suggested.

2 Theory and Literature Review

2.1 High Temperature Heat Pumps

2.1.1 About Heat Pumps

The basic working principle of a heat pump is that it transfers low grade heat from a low temperature heat source to an area with a higher temperature (heat sink). According to the second law of thermodynamics, heat cannot flow from an area with a low temperature to an area with a higher temperature without the addition of work (Klein and Nellis, 2012). Therefore, a heat pump must be supplied with a primary energy source, often electricity, to be able to deliver heat at higher temperatures.

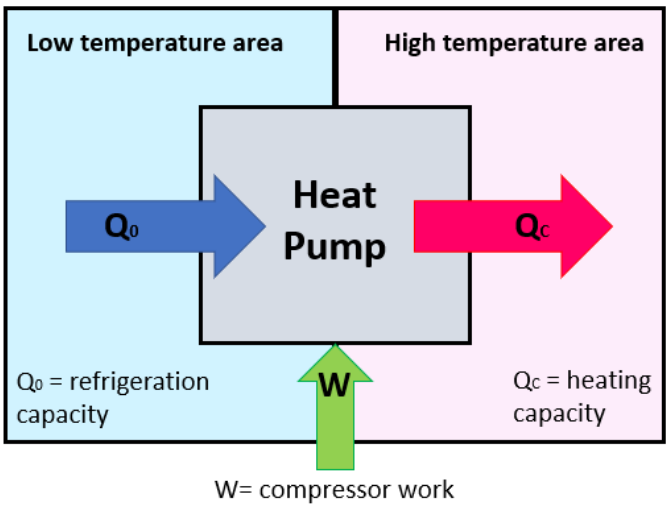

Figure 1: Basic working principle of a heat pump

Heat pumps and refrigeration systems have the same working principle and can be used for heating (heat pumps) or cooling (refrigeration systems). Refrigeration systems are commonly used for air conditioning, refrigeration purposes and freezing purposes. Heat pumps are commonly used for space heating and hot water heating (U.S. Department of Energy, 2018), and high temperature heat pumps have shown great potential in industrial processes. Heat pumps will be the focus of this paper.

2.1.2 The vapor compression cycle

The simplest vapor compression cycles consist of a condenser, a compressor, an evaporator and an expansion valve. Vapor compression systems usually have more components in order to increase their energy efficiency, see chapter 2.1.4.1. However, the working principle can be explained by looking at a simple cycle.

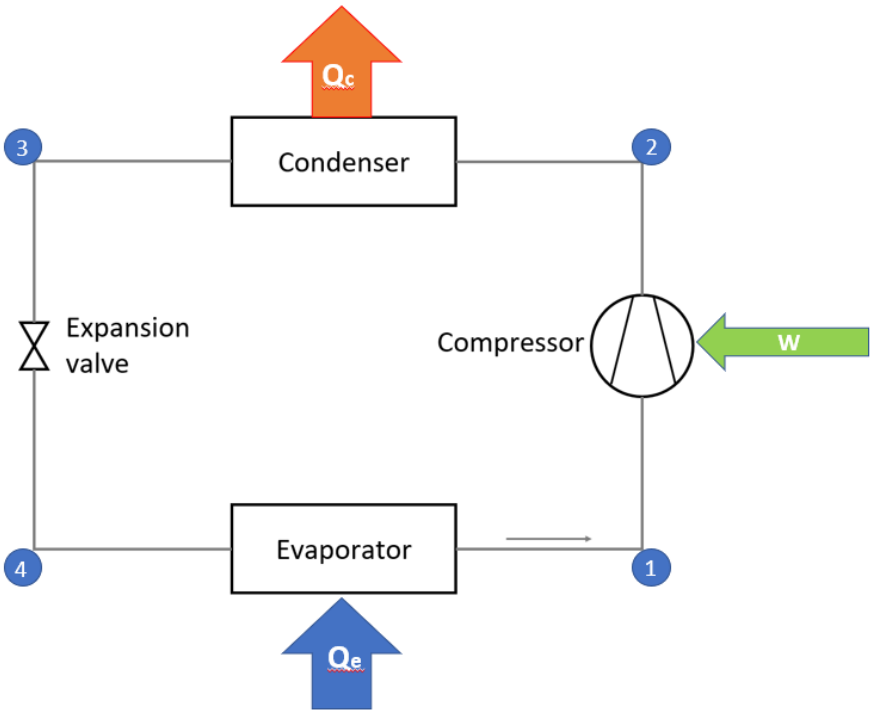

Figure 2: Simple vapor compression cycle

The refrigerant, or working fluid, flows through the heat pump and operates at different temperatures and pressures at different stages in the cycle. At the exit of the evaporator and inlet of the compressor (1) the refrigerant is a vapor with a low temperature at low pressure. The compressor is powered by an external source, often by electricity. The power is transferred into mechanical energy, and the vapor refrigerant is compressed to a higher pressure and temperature. The gas then leaves the compressor and enters the condenser (2), where it changes to a liquid state and releases heat used in processes such as water heating or industrial processes, or to heat indoor spaces. The liquid refrigerant leaves the condenser and enters a throttling valve/expansion valve (3), where temperature and pressure decrease. The refrigerant then enters the evaporator (4) at a temperature lower than the ambient temperature. The evaporator works as a heat exchanger, and as the refrigerants goes through the evaporator, it absorbs heat from the surroundings and evaporates. The refrigerant then exits the evaporator, and the cycle starts again.

A Pressure-enthalpy diagram (PH diagram) can be used to visualize a vapor compression cycle. The diagram shows the pressure and enthalpy of the different stages of the process, see Figure 3. It can be used to graphically find the work, heating capacity and refrigeration capacities of a cycle. Stage (2s) in the cycle visualized below is the state at point (2) if the compression is isentropic.

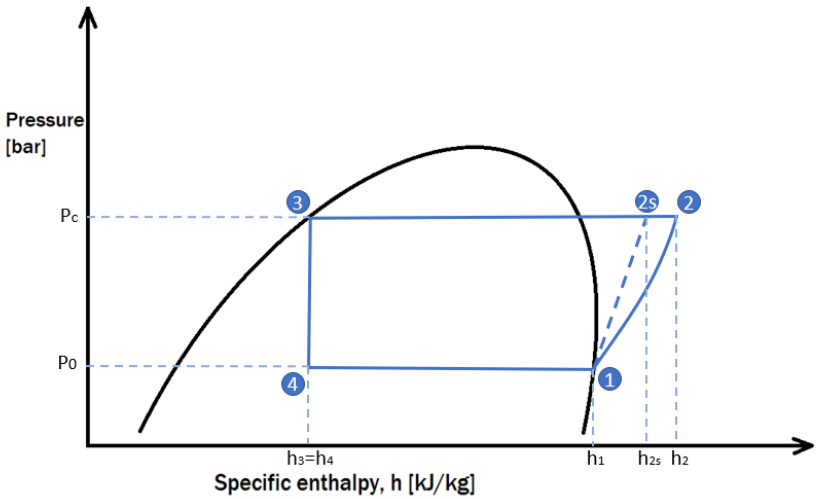

Figure 3: Pressure-enthalpy diagram for a simple vapor compression cycle

Vapor compression heat pumps can achieve large coefficients of performance (COP), which is a measure of a heat pump's energy efficiency, and vapor compression heat pumps can therefore be much more environmentally friendly than electric heating. Due to the wide range of refrigerants available, vapor compression systems can achieve high efficiency in both heating and cooling applications. The downside of vapor compression heat pumps is that they require a power input. In today's heat pumps, this is usually electric power, and the environmental benefit of a heat pump compared to other heating technologies therefore depends on whether the electricity supplied to the system comes from renewable sources or not.

2.1.3 High Temperature Heat Pumps

Because traditional heat pumps can only deliver heat up to a certain temperature, their areas of use are limited. Therefore, heat pumps that can deliver higher temperatures, referred to in literature as High Temperature Heat Pumps (HTHPs) or industrial heat pumps, have become an important area of research.

There is no consensus in literature regarding the temperature levels that distinguish a HTHP from a regular heat pump. In general, authors agree that heat pumps with heat sink temperatures above 100°C can be classified as HTHPs, although lower heat sink temperatures have also been accepted (Arpagaus et al., 2018). Certain authors distinguish between HTHP and Very High Temperature Heat Pumps (VHTHP), a concept introduced by Peureux and Bobelin (Arpagaus et al., 2018, Peureux et al., 2014). VHTHP are heat pumps with heat sink temperatures above 100°C, whereas HTHPs have heat sink temperatures above 80°C. In this paper, there will be no distinction between HTHPs and VHTHPs, and heat pumps with heat sink temperatures above 80°C will be defined as HTHPs.

High temperature heat pumps work in the same way as traditional heat pumps, the only difference being that they can deliver higher heat sink temperatures. Oftentimes, they provide a higher temperature lift than traditional heat pumps. Many high temperature heat pumps use industrial waste heat as their heat source. Industrial waste heat often has a temperature of 30°C-70°C, which is significantly higher than traditional heat sources for heat pumps such as outdoor air, seawater, groundwater, and geothermal heat (Arpagaus et al., 2018). There is a great demand for heat for space heating and

water heating in residential buildings as well as in industrial applications. The industry needs heat for production, processing, and finishing of products. The temperatures needed vary between these categories, and with the products being produced. In Germany, 74% of the total industrial heat demand came from process heat, space heating, and hot water production. If heat pumps with heat sink temperatures of 140°C were utilized, they could cover 32% of the total industrial heat demand in Germany (Arpagaus et al., 2018).

High temperature heat pumps have great potential, especially in the food, paper, and chemical industries. Processes such as drying, pre-heating, boiling, pasteurization, laundering, and coloring can be performed at temperatures below 100°C, and the heat pump technology today is therefore sufficient. For temperatures above 100°C and up to 140°C, there are prototypes under development, and for temperatures above 140°C, research is being conducted (Arpagaus et al., 2018, Bless et al., 2017).

Although high temperature heat pumps have great potential, and already existing heat pumps can be used for various applications today, the use is not widespread. The reasons seem to be mainly based on lack of awareness and knowledge as well as economic disadvantages compared to competing technologies. The technical possibilities of heat pumps and general knowledge about integration and use of high temperature heat pumps is lacking both in the industry and among private users. The payback period for heat pumps is often longer than for gas and oil-fired boilers, and in some places, electricity is more expensive than fossil fuels, making it more desirable form an economic perspective to use fossil fuel fired boilers. (Arpagaus et al., 2018)

However, the world has seen a shift in mentality when it comes to green energy over the past few years, and many countries have implemented measures to increase the share of green energy sources. This can possibly lead to an increase in the use of high temperature heat pumps both for industrial and residential applications.

2.1.4 Efficiency in Heat Pump Systems

2.1.4.1 Energy Efficiency

Many parameters can be used when evaluating a heat pump. The system can be evaluated based on size, costs, environmental impact, or energy efficiency. Oftentimes, heat pump systems are evaluated based on all these factors. In this paper, however, the focus will be on energy efficiency. When evaluating the energy efficiency of a heat pump, the Coefficient of Performance (COP) is the most commonly used indicator. The COP shows the relation between the energy output and the energy consumption of the heat pump. To find the COP, the refrigeration or heating capacity and energy consumption of the compressor must first be calculated.

The refrigeration capacity is a measure of the energy absorbed in the form of heat in the evaporator. It can be found using the following equation:

Equation 1: Refrigeration capacity

$$\dot{\boldsymbol{Q}}_{\boldsymbol{0}} = \dot{\boldsymbol{m}}_{\boldsymbol{R}} \cdot (\boldsymbol{h}_{\boldsymbol{1}} - \boldsymbol{h}_{\boldsymbol{4}})$$

Where $\dot{Q}_0$ is the refrigeration capacity, $\dot{m}_R$ is the circulated refrigerant flow, h_1 is the enthalpy of the refrigerant at the evaporator outlet, and h_4 is the enthalpy of the refrigerant at the inlet of the evaporator.

Similarly, the heating capacity is a measure of the energy released in the condenser. It can be described by the enthalpy difference over the condenser:

Equation 2: Heating capacity

$$\dot{Q}_C = \dot{m}_R \cdot (h_3 - h_2)$$

Where $\dot{Q}_C$ is the heating capacity, h_3 is the enthalpy at the outlet of the condenser, and h_2 is the enthalpy at the inlet of the condenser.

The work done by the compressor can be found using the following equation:

Equation 3: Work done by the compressor

$$\dot{W} = \dot{m}_R \cdot (h_2 - h_1)$$

Where $\dot{W}$ is the work done by the compressor, which is assumed to be equal to the power consumption of the compressor in this thesis, h_2 is the enthalpy at the compressor outlet, and h_1 is the enthalpy at the compressor inlet.

Once the refrigeration and heating capacities as well as the power consumption is determined, the COP can be calculated. The refrigeration and heating capacities describe how much energy the heat pump system can supply to or remove from a space. If the system in question is used for cooling, the refrigeration capacity is used to determine the efficiency of the system. If the heat pump is used for heating, the heating capacity is used. The COP for heating systems is called the heating COP, while the COP used in refrigeration systems is called the cooling COP. Some heat pumps can provide both heating and cooling, and in those systems a combined COP can be found.

Because the focus on this report is high temperature heat pumps used for heating, only the heating COP is relevant, and any further mentions of COP will refer to the heating COP. The heating COP can be found using the following equation:

Equation 4: Heating COP

$$COP = \frac{\dot{Q}_C}{\dot{W}}$$

Multi-stage systems and cascade systems have more than one compressor and will be described in chapter 2.3. The COP for a two-stage system and a cascade system with two cycles is found using the following equation:

Equation 5: COP for two-stage systems

$$COP = \frac{\dot{Q}_{C,total}}{\dot{W}_{C1} + \dot{W}_{C2}}$$

A COP of one, or less than one, means that the heat pump delivers the same amount of energy as, or less energy than, it consumes. In those cases, the heat pump will contribute negatively, and drain energy rather than supplying it. For a heat pump to be effective, it must therefore have a COP greater than one. However, that is the minimum requirement and most heat pumps today have far higher COPs than one. The COP depends on many factors such as the components used in the system, system configurations, temperature lift, and refrigerant selection. With various configurations, high temperature heat pump systems can reach COPs of between 3 and 4.2 (Cao et al.,

2014), and even as high as 8.83 in systems with a high heat source temperature and a low temperature lift (Hu et al., 2019).

2.1.4.2 Other means of measuring efficiency

When deciding on a system solution and a refrigerant to use in a heat pump, one should not solely base the decision on the COP. As mentioned, other factors such as environmental impact and costs are important when designing or installing a heat pump.

The environmental efficiency of a heat pump can be evaluated through an environmental analysis of the whole system, for example a life cycle assessment (LCA). An analysis as such can calculate the total environmental impact of a heat pump, including the environmental costs of production, installation, use, maintenance, and disposal. A heat pump with a high COP delivers more energy in the form of heat than the electricity it consumes but is not necessarily environmentally superior to a heat pump with a lower COP if the production or disposal processes have high energy demands.

Furthermore, a cost analysis will give an impression of the economic efficiency of a heat pump. A heat pump with a high COP might need expensive parts or materials, or it might be difficult or costly to produce and install. If the payback time of a heat pump is much longer than for another heating system, the demand for the heat pump will decrease or completely vanish. Even though the operational costs might decrease with a higher COP, people care about the total costs of their investments. It is therefore important that an increased energy efficiency does not affect the cost efficiency too much.

To summarize, it is important that a heat pump is efficient, not just in energy use, but in environmental impact, costs, and size. To find the heat pump that is best suited for a specific application, a thorough analysis should be conducted where all the abovementioned factors are accounted for. In this project, however, the scope is limited to the energy efficiency. As a result, the COP will be the main way that the efficiency of various heat pump systems will be evaluated.

2.1.5 Effects of load ratio and operational mode on efficiency

The operational mode of the heat pump refers to how the heat pump operates during a certain time interval. Full load operation means that the heat pump continuously operates on maximum capacity. Part load operation means that the heat pump operates on part load, producing less heat than the maximum capacity. No operation means that the heat pump is shut off and does not produce any heat. Intermittent operation means that the heat pump operates in cycles, varying between operating on full or part load and being completely shut off.

Part load operation is achieved by reducing the work of the compressors. Vapor compression systems can use single-speed compressors, or variable-speed compressors. Single-speed compressor operate with a given speed and a given load that cannot be adjusted. Variable-speed compressors, on the other hand, can adjust their speed according to heat demand, and operate on part-load if it is desirable to produce less heat than the maximum capacity. The load ratio (LR) is the ratio of actual heat pump capacity to maximum heat pump capacity:

Equation 6: Load ratio

$$LR = \frac{\dot{Q}_{c,actual}}{\dot{Q}_{c,max}}$$

If a heat pump that can produce 200 kW of heat only produces 50 kW, the load ratio is 0.25 or 25%.

The capacity of the heat pump can be changed in numerous ways. If the heat pump has more than one parallel compressors, one or more compressors can be turned off to reduce the load ratio. In screw compressors, slide regulation, variable volume ratio slide, and speed control can be used to reduce the speed of the compressor. Slide regulation is the most common way of regulating the compressor capacity, and functions by sliding a valve to adjust the volume ratio of the compressor Eikevik (2019).

Uhlmann and Bertsch did a theoretical and experimental study of the startup and shutdown behavior of residential heat pumps. They observed a peak in electrical power right after the heat pump was started up, before the power consumption and heat rate stabilized. This was because refrigerant had accumulated in the evaporator during shutoff time, and because of this the refrigerant that entered the compressor right after startup was in two-phase rather than single-phase gas. They found that while shutdown and startup cycles lead to a slight reduction in efficiency of residential heat pump, cycling of heat pumps do not lead to significant overall losses if the minimal run time was above 15 minutes. The capacities of the heat pumps in the study were between 10 and 17 kW (Uhlmann and Bertsch, 2012).

Man et al. investigated the performance of a ground source heat pump system for cooling and heating. They tested out continuous and intermittent operation modes, and during the tests for the intermittent mode, the system was turned on for 10 hours and off for 14 hours of the day. They found that the COP was slightly higher when during the intermittent operation than during continuous operation, and after 100 hours of operation the COP was 9.37% higher for the intermittent system than the continuous system. This was likely because the temperature of the borehole, which was the heat source, decreased during continuous operation of the heat pump due to cooling from the evaporator. When the heat pump was shut off, the borehole returned to its regular temperature, increasing the heat source temperature when the heat pump restarted. However, the COP of the whole system was much lower due to total system energy consumption (Man et al., 2012).

Han et al. conducted a performance analysis of an air source heating system for an office building. They found that an increasing part load ratio led to an increased performance, up to a certain point. They found that the average COP of the heat pump with higher part load ratio operating range was slightly higher than a heat pump with a lower part load ratio (Han et al., 2016).

Karlsson and Fahlén conducted a study where they analyzed how energy efficiency was affected capacity control. They compared intermittent control and variable-speed control. They found a decrease in efficiency during part load operation for the heat pump with a conventional compressor. But the heat pump with a compressor designed for variable-speed operation had an increase in efficiency during part-load operation. They also found that condensing temperatures decreased and evaporating temperatures increased during part-load operation compared to full-load operation. This was consistent with theoretical research they had done. They assumed that the decrease in COP found during practical experiments for one of the heat pumps came from a reduction in compressor efficiency (Karlsson and Fahlén, 2007).

The articles and theory reviewed did not have a consistent recommendation for the most efficient operational mode. Some research showed that intermittent regulation (on/off regulation) of the heat pump was more efficient than constant operation, however this leads to higher energy consumption during shut down and restart. This was especially clear in the study from Man et al. (2012), where the temperature of the heat source was reduced over time during heat pump operation. It is likely that this effect would have been less dominant if the heat source were a circulating fluid instead of a borehole with little circulation and air change.

Some researchers found that part-load operation was more efficient than full-load operation, but the optimal part load ratio varied with each case. The reasons why part load operation sometimes increased efficiency and sometimes not are complicated and can be explained by a variety of factors. Part load operation leads to a lower temperature difference between the evaporator and compressor, which increases efficiency. Furthermore, less power is necessary to operate the compressor because of the reduced speed. This also leads to increased efficiency. On the other hand, energy use related to regulation of the heat pump increases when the load ratio is changed. Other components than the compressor such as pumps that drive the refrigerant through the system still need to operate, and some studies showed that the share of electricity use from those components increased during part load operation.

The large variations in results show that it can be difficult to predict whether a part load operation or intermittent operation, or a combination, will lead to an increase or reduction in overall efficiency. It likely depends on which factors are included in the calculations and how complicated the system is.

2.1.6 Effect on heat pump performance by basic components

2.1.6.1 Compressors

The compressor is among the most important factors in determining the operation and efficiency of a heat pump. The size of the compressor determines the maximum mass flow rate possible, which is directly related to both power consumption and heat capacity. There are several types of compressors, but the three most common types for heat pumps are piston compressors, screw compressors, and turbo compressors. The type of compressor should be selected based on the displacement volume. A specific compressor has not been selected for this project, and the different types of compressors will therefore not be described further here.

The isentropic and volumetric efficiencies are important factors for the efficiency of the system. The volumetric efficiency takes into account losses due to clearance volume, which is the part of the compressor volume that cannot be compressed due to spatial constraints, as well as losses due to heat exchange between refrigerant and components, pressure drops in valves, leakage losses, and absorption of the gas refrigerant in lubrication oil (Eikevik, 2019).

The isentropic efficiency is the ratio between the theoretical work done in an isentropic compression to the actual work done during compression:

Equation 7: Isentropic efficiency

$$\eta_{is} = \frac{\dot{W}_{is}}{\dot{W}_{shaft}}$$

Where $\dot{W}_{is}$ is the work done by the compressor if the compression process was isentropic and without any losses. $\dot{W}_{shaft}$ is the shaft input to the compressor, or the actual work done by the compressor.

2.1.6.2 Condenser and evaporator

The heat exchangers (condensers and evaporator) can also have a large impact on the efficiency of the compressor. Heat exchange losses can have a large effect on the overall efficiency and can be reduced by adapting the heat exchangers to the specific system. This can be difficult, as a large variety of heat exchanger designs exist. Like with the compressor, no specific heat exchangers are selected for this project, so the different types of heat exchangers will not be further investigated. However, some calculations on the heat exchangers will be done, and the most important values regarding heat exchange in the condenser and evaporator will therefore be presented.

The **heat capacity ($\dot{Q}_c$)** and **refrigeration capacity ($\dot{Q}_e$)** describe the amount of heat or refrigeration the heat pump produces. See Equation 1 and Equation 2.

The **U-value** of the heat exchanger is the heat transfer coefficient and describes the heat transfer through the wall of the heat exchanger in W/m^{2}K. A higher U-value leads to a higher heat transfer rate, which is desirable in heat exchangers.

The **area (A)** of the heat exchangers is the total area of the surfaces where the heat exchange happens. The unit is m^2. Heat exchangers are often made with a goal of having a large surface area to volume-ratio.

The **mass flow rates ($\dot{m}$)** of the refrigerant and heat sink/heat source fluid describe how much mass that passes through a certain point every second. A higher mass flow rate leads to lower heat exchange values.

The **logarithmic mean temperature difference (LMTD)** describes the driving force for heat transfer in the heat exchanger (Connor, 2019). It can be calculated in two ways, as seen in the following equations.

2.1.6.2.1 Equations for the condensers

The equations used to calculate the temperatures and LMTD of the condensers will be presented here. The LMTD can be found using Equation 8.

Equation 8: Logarithmic mean temperature difference in the condenser

$$LMTD_{Condenser} = \frac{\theta_{in} - \theta_{out}}{ln\left(\frac{\theta_{in}}{\theta_{out}}\right)}$$

Where θ_{in} is the difference between the condensation temperature T_c and the inlet temperature of the water to be heated by the condenser ($T_{hw,\,in}$), and θ_{out} (thermal length) is the difference between the condensation temperature and the outlet temperature of the water heated by the condenser ($T_{hw,\,out}$). The thermal lengths can be found with Equation 9 and Equation 10.

Equation 9: Thermal length at condenser inlet

$$\theta_{in} = T_c - T_{hw,in}$$

Equation 10: Thermal length at condenser outlet

$$\theta_{out} = T_c - T_{hw,out}$$

Equation 8Equation 8 assumes that the hot water outlet temperature is known. If the heat capacity $\dot{Q}_c$ is known, the outlet temperature of the water heated by the condenser can be calculated with the following equation:

Equation 11: Outlet temperature of hot water

$$T_{hw,out} = T_{hw,in} + \frac{\dot{Q}_c}{C_{p,hw} \times \dot{m}_{hw}}$$

$C_{p,hw}$ is the specific heat capacity of the hot water at constant pressure, in J/kgK. $\dot{m}_{hw}$ is the mass flow rate of the hot water through the condenser in kg/s, and $\dot{Q}_c$ is the heat capacity in W.

Another way to calculate the LMTD is to use the U-value and the condenser area:

Equation 12: Logarithmic mean temperature difference in the condenser

$$LMTD_{Condenser} = \frac{\dot{Q}_c}{U \times A}$$

Where U is the U-value and A is the heat exchanger surface area. These equations can also be rearranged, combined, and used to find other values such as $\dot{Q}_c$ or T_c.

2.1.6.2.2Equations for the evaporator

The same equations, with slight modifications, can be used to find the outlet temperature of the water from the evaporator and the LMTD of the evaporator. $T_{cw,in}$ and $T_{cw,out}$ are the temperatures of the water being cooled by the evaporator at the inlet and outlet. T_e is the evaporating temperature, and $\dot{Q}_e$ is the refrigeration capacity.

Equation 13: Thermal length at evaporator inlet

$$\theta_{in} = T_{cw,in} - T_e$$

Equation 14: Thermal length at evaporator outlet

$$\theta_{out} = T_{cw,out} - T_e$$

Equation 15: Logarithmic mean temperature difference in the evaporator

$$LMTD_{Evaporator} = \frac{\theta_{in} - \theta_{out}}{ln\left(\frac{\theta_{in}}{\theta_{out}}\right)}$$

Equation 16: Outlet temperature of cold water

$$T_{cw,out} = T_{cw,in} - \frac{\dot{Q}_e}{C_{p,cw} \times \dot{m}_{cw}}$$

Equation 17: Logarithmic mean temperature difference in the evaporator

$$LMTD_{Evaporator} = \frac{\dot{Q}_e}{U \times A}$$

2.2 Refrigerants

2.2.1 Properties of refrigerants

The refrigerant, or working fluid, of the heat pump is the fluid that circulates through the heat pump system. It is the refrigerant that releases heat in the condenser and absorbs heat in the evaporator. Different refrigerants have different properties, so when designing a heat pump, it is important to select a refrigerant that is suitable for the specific system being designed.

When selecting a refrigerant for a heat pump, many factors must be considered. Among others, one must look at the temperature ranges of the system and corresponding pressures of the refrigerant, volumetric heating capacity, specific volume, and other thermophysical properties. These properties greatly affect the efficiency of the heat pump, so it is important to choose a refrigerant with properties that fit the desired parameters of a certain system (Eikevik, 2019).

Traditionally, the thermophysical properties have been the most important factors when selecting refrigerants for a heat pump. However, in the past few decades, there has been an increased focus on the effect of refrigerants on the atmosphere and the climate. Due to leaks, the refrigerants sometimes escape heat pump and refrigeration systems and are released to the ambient during operation of the heat pump. Furthermore, refrigerants are often improperly disposed of when a heat pump is replaced, and they leak into the atmosphere. Refrigerant can also be released into the atmosphere when the heat pump is installed (Staffell et al., 2012). To quantify the negative effect they have on the environment, refrigerants are now categorized based on their Ozone Depletion Potential (ODP) and Global Warming Potential (GWP) (Arpagaus et al., 2018). The fight against climate change has led to several regulations regarding the environmental impact of refrigerants, such as the Montreal Protocol of 1987 banning refrigerants with high ODPs, the Kyoto Protocol of 1997 that recommended phasing out refrigerants with high GWP, and the Paris accord of 2016 that strongly emphasized the phasing out of harmful synthetic refrigerants (Abas et al., 2018). As a result of these agreements as well as national regulations, ODP and GWP have now become important factors in refrigerant selection.

The ODP describes the refrigerant's ability to deplete the ozone layer by chemically reacting with the ozone molecules in the stratosphere. ODP is defined relative to R11, which means that a refrigerant with an ODP of one will do the same amount of damage to the ozone layer as R11 (Klein and Nellis, 2012). A thinner ozone layer allows for more harmful UV-B radiation to pass through the atmosphere and harm the DNA of plants and animals.

The GWP, on the other hand, describes the effect refrigerants have on the climate and how they contribute to global warming. GWP is defined relative to Carbon Dioxide. Many of the traditional refrigerants are greenhouse gases, and a small amount of gases with a high GWP can contribute significantly more to global warming than larger amounts of CO_2. Refrigerants with an ODP of zero but a high GWP should be avoided due to the negative effects on global warming.

In addition to thermophysical properties, ODP, and GWP, the refrigerant must comply with necessary safety standards. The refrigerant must be compatible with any lubrication

used in the compressor and materials used in the various components in the heat pump system at the given pressures. Furthermore, the toxicity and flammability must be considered. Toxic refrigerants can cause harm in the event of a leak, so if a toxic refrigerant is used, necessary precautions must be taken. Flammable refrigerants should be avoided in systems where there is a risk of ignition, such as in car air conditioning systems. However, they can be used in systems with less risks of accidents, as long as necessary care is taken (Klein and Nellis, 2012).

2.2.2 Types of refrigerants

2.2.2.1 Natural refrigerants

Natural refrigerants are fluids that occur in nature without human intervention. They were widely used in HVAC operations until the 1930s, when higher-performing synthetic refrigerants were invented (Abas et al., 2018). However, due to the high GWP and ODP values of many synthetic refrigerants, natural refrigerants have made a comeback in recent years. Typical examples of natural refrigerants are water (R718), air (R729), ammonia (R717), and CO2 (R744). Hydrocarbons (HC) make up a big group of natural refrigerants that are used in a variety of heat pump applications.

Water (R718)

Water is neither flammable nor toxic and is one of the safest refrigerants. It has shown favorable thermodynamic properties at high temperature applications (Hu et al., 2017b). However, there are certain drawbacks with using water as a refrigerant as well. One of the drawbacks is the high normal boiling point of 100°C. The effect of this is that most of the cycle will happen below atmospheric pressure. This means that air will leak into the system in the event of leaks, instead of refrigerant leaking out of the system. This will increase maintenance costs, as the cycle will have to be evacuated and recharged. Water will also be incompatible with certain materials as it can cause rust. Furthermore, the density of water vapor is low. This means that the necessary swept volume of the compressor and the pressure ratio is higher than for many other refrigerants (Arpagaus et al., 2018).

CO_2 (R744)

CO_2 has an ODP of zero and a GWP of one. It is non-flammable, and not toxic in small concentrations. It is a byproduct of industrial processes and widely available, so using CO_2 can reduce waste and resources. Moreover, the thermophysical properties of CO_2 are very good and favorable for many heat pump applications. The critical temperature is low and the critical pressure is high, which means that most heat pump cycles using CO_2 for heating operate in the transcritical range. Because of the temperature glide that a refrigerant experiences during transcritical heat rejection, CO_2 is considered a good refrigerant for water heating systems (Nekså et al., 1998, Brodal and Jackson, 2019).

Ammonia (R717)

Ammonia has been a widely used refrigerant for many years due to its favorable thermophysical properties. For example, it has a high volumetric heating capacity, which means that compressors can be rather small compared to some other refrigerants. However, ammonia has a high pressure at high temperatures, which limits the number of available compressors. Ammonia can be flammable, and it is toxic. Because of this, there exist regulations that must be followed when installing an ammonia heat pump (Bamigbetan et al., 2017).

Hydrocarbons

Several different kinds of hydrocarbons are used as refrigerants, and the properties vary between the different types. However, hydrocarbons share some common properties. In general, hydrocarbons are compatible with metal alloys and polymers that are often used in HFC systems, and they are compatible with the most common synthetic oils (Palm, 2008). There are however some disadvantages. Hydrocarbons are highly flammable, and because of this they can cause great harm in the event of an accident. Extra measures must therefore be taken to avoid possible dangerous situations. One possible measure is to reduce the amount of the refrigerant, as larger amounts of refrigerants pose greater risks. This implies that highly flammable refrigerants should not be used in large systems, but they might be fit for smaller systems (Palm, 2008). Furthermore, the market for hydrocarbon refrigerants is quite small, with the exception of domestic freezers and refrigerators. This limits the choice of compressors commercially available.

2.2.2.2 Synthetic refrigerants

Synthetic refrigerants are fluids that have been developed by humans, and they do not exist naturally. The advantage with synthetic refrigerants is that they often have favorable thermodynamic properties, as many of them have been developed for the sole purpose of being refrigerants. The chemical composition of the synthetic refrigerants can be adjusted to improve their thermodynamic properties. This is not possible to do with natural refrigerants (Bamigbetan et al., 2016).

Traditionally, Chlorofluorcarbons (CFCs) and Hydrochlorofluorcarbons (HCFCs) were the most widely used refrigerant types due to favorable thermophysical properties (RefrigerantHQ, 2019). However, because the chlorine in CFC molecules have been proven to be the main cause of ozone depletion, CFC refrigerants are no longer produced (Klein and Nellis, 2012). In order to reduce the ozone depletion, Hydro Flouride Carbons, or HFC-blends, became a replacement for CFCs in the 1990s (Arpagaus et al., 2018). However, most HFCs have rather high GWP values, and are therefore being phased out (Bamigbetan et al., 2016).

Another class of synthetic refrigerants is the group of so-called "low GWP synthetic refrigerants". These refrigerants have a low calculated GWP value, low flammability, chemical stability, they are non-toxic and have suitable critical temperatures for many heat pump applications. (Abas et al., 2018). Hydrofluoroolefins (HFOs) are in this group, and have been considered good low GWP alternatives to HFCs, HCFCs, and CFCs. Like HFCs, they contain hydrogen, fluoride, and carbon. However, due to a difference in molecular structure HFOs have much shorter atmospheric lifetimes, typically only a few days. This greatly reduces their GWP and makes them good alternatives for heat pump applications. (EFCTC, 2011). However, many of these synthetical refrigerants are rather new, and although they have been excessively studied as refrigerants (for example (Fukuda et al., 2017), (Kondou and Koyama, 2015, Longo et al., 2019, Nawaz et al., 2017, Wu et al., 2018)), there is some uncertainty as to what their true effects on the environment are (Bamigbetan et al., 2019).

2.2.2.3 Properties of selected refrigerants

A comparison of some refrigerant properties can be seen in the table below. The values without an asterisk are from (Standard Norge, 2017), while the values with an asterisk are from (Arpagaus et al., 2018).

Refrigerant	Safety Classification	GWP	ODP	P_{sat}, 40°C [kPa]	P_{sat},110°C [kPa]
Water (R718)	A1*	0*	0*	7.380	143.38
Ethanol	n/a	n/a	0	18.010	313.5
Methanol	n/a	n/a	0	34.70	472.2
R1234ze(Z)	A2*	<1*	0*	290.2	1663
R1233zd(E)	A1*	~0	4.050	215.4	1288
R1224yd(Z)	A1*	<1*	0.00012*	245	1432
Ammonia (R717)	B2L	0	0	1555	7583
R245fa	B1	1030	0	249.6	1574
R600	A3	4	0	379.2	1845
R600a	A3	3	0	530.9	2381

Table 1: Properties of selected refrigerants

The safety classification is made by looking at the refrigerants' flammability and toxicity. The system is illustrated in the table below.

Flammability	**Higher**	A3	B3
	Lower	A2	B2
		A2L	B2L
	No flame propagation	A1	B1
		Lower	**Higher**
		Toxicity	

Table 2: Safety classifications of refrigerants

2.2.3 Refrigerants in high temperature heat pumps

Refrigerants that work well in conventional heat pumps do not necessarily work well in high temperature heat pumps (Bamigbetan et al., 2019). The critical temperature of many conventional refrigerants is often lower than the required heat sink temperature, which means that the heat pump cycle must be transcritical to work under the given operating conditions. In this paper, the focus will be on subcritical cycles, and refrigerants with a low critical temperature will not be considered.

Another challenge with HTHPs is the high condenser temperature, which corresponds to a high condenser pressure in many refrigerants. This can lead to challenges when choosing materials for the heat pump, but the main issue is the performance of the compressor (Bamigbetan et al., 2016). High condenser pressures require compressors that are adapted to high pressures (Bamigbetan et al., 2019), so the choice of compressors is more limited than for conventional heat pumps. Several studies have been performed to find out which refrigerants work well for high temperature heat pumps.

Fakuda et al. looked at R1234ze(E) and R1234ze(Z) as refrigerants for high temperature heat pumps. The former has a GWP of 6, and is seen as a viable alternative for R134a,

which has a GWP of 1430. The latter has been considered an alternative to R245fa because it has very similar thermodynamic properties. They found that R1234ze(E) delivered the best performance at a condensation temperature of 90°C, and that R1234ze(Z) had the highest COP with a condensing temperature of 130°C. They concluded that R1234ze(E) is well suited for general HTHP applications, but that R1234ze(Z) is a better choice when the HTHP operates at higher temperatures. They also found that R1234ze(Z) had much higher irreversible losses at 75°C than at 105°C and 125°C. The losses of R1234ze(Z) were also higher than the losses of R1234ze(E) at 75°C. The high irreversible losses lead to a lower COP and should therefore be reduced as much as possible (Fukuda et al., 2014).

Hu et al. compared the physical and thermodynamic properties of 13 different refrigerants, including R1233ze(E), R1234ze(E), R1234ze(Z), and R718. They found that at condensation temperatures between 100°C and 120°C, the COP was highest for R1233zd(E), followed by R1234ze(E), however many other refrigerants had similar but slightly lower COPs (Hu et al., 2017b).

Many authors have investigated the possibility of using hydrocarbons in high temperature heat pumps. Bamigbetan et al. evaluated natural refrigerants that operated with a heat source of 40°C and a heat sink at 90 and 150°C. They specifically looked into ammonia (R717) and various hydrocarbons (R290, R600, R601) and their mixtures. They considered the refrigerants in a simple cycle, a two-stage cycle, and a cascade cycle. R290 and R717 could not operate subcritically with a condensing temperature of 110°C, and R601 had a suction pressure below atmospheric pressure. The cascade system, on the other hand, showed promising COPs (Bamigbetan et al., 2016).

CO2 has been the object of many studies on natural refrigerants. However, for high temperature applications, it must operate in a transcritical cycle which will not be investigated in this thesis.

The studies show that although some refrigerants are unsuited for high temperature applications due to their thermophysical properties, many refrigerants, both natural and synthetic low GWP, are viable options for HTHPs. It is difficult to compare the refrigerants studied in the abovementioned papers, as the system configurations varied greatly. It can be difficult to know whether it is the refrigerant or the system differences that cause the variations in COP based on the papers alone. However, it is clear that there are many options for HTHP refrigerants.

2.3 System Configurations in heat pumps

2.3.1 General

The simplest vapor compression heat pump system consists of a compressor, a condenser, an expansion valve, and an evaporator, see chapter 2.1.2. However, most systems are expanded or altered in some way to improve the efficiency. There are several ways in which the efficiency of a heat pump system can be improved, and a few of them will be presented in the following paragraphs.

Subcooler

Adding a subcooler after the condenser will reduce the temperature of the refrigerant entering the expansion valve, which reduces the expansion loss of the system. The specific refrigeration capacity, or enthalpy difference in the evaporator, will increase as a result of this. This reduces the mass flow, and therefore also the compressor size

(Eikevik, 2019). Additionally, the heat removed in the subcooler can be used in space or process heating, for example to preheat hot water. Similarly, a de-superheater can be added after the evaporator.

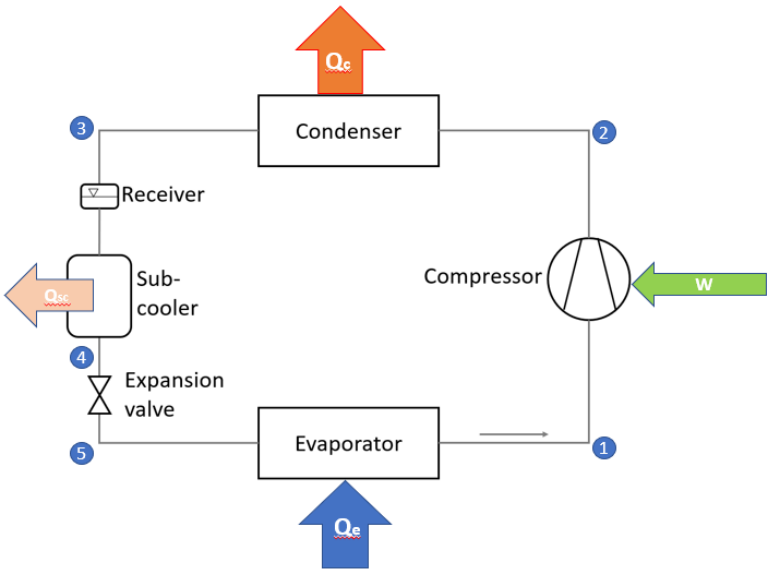

Figure 4: Vapor compression cycle with a subcooler

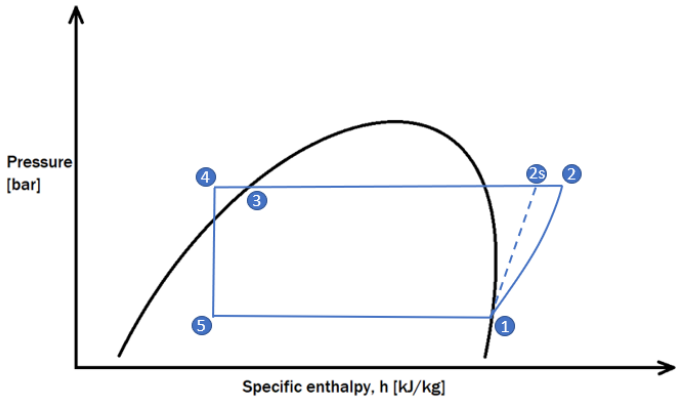

Figure 5: PH-diagram for heat pump with subcooler

Multi-stage compression

A common way to increase efficiency is to use more than one compressor in series. With multi-stage compression, the heat pump will have a low-pressure stage, a high-pressure stage, and one or more intermediate pressure stages. Normally, expansion is also done in several stages, and it is not uncommon to cool the refrigerant between the compressors by mixing it with flash tank gas from flash tanks between the expansion valves (Eikevik, 2019). By compressing in several stages, the pressure ratios in the compressors decrease. As a result, the work done by the compressor decreases, and the compressor uses less energy. However, with several stages, more compressors are needed, and it is important to consider the power use of all compressors when calculating the efficiency of a multi-stage system. Still, improving the isentropic efficiency of a compressor can have a large effect on the efficiency of the system. Therefore, in systems with a large pressure difference between the evaporator and the condenser, a multi-stage system can be very beneficial. The drawback is that investment and maintenance costs will increase due to a greater number of compressors.

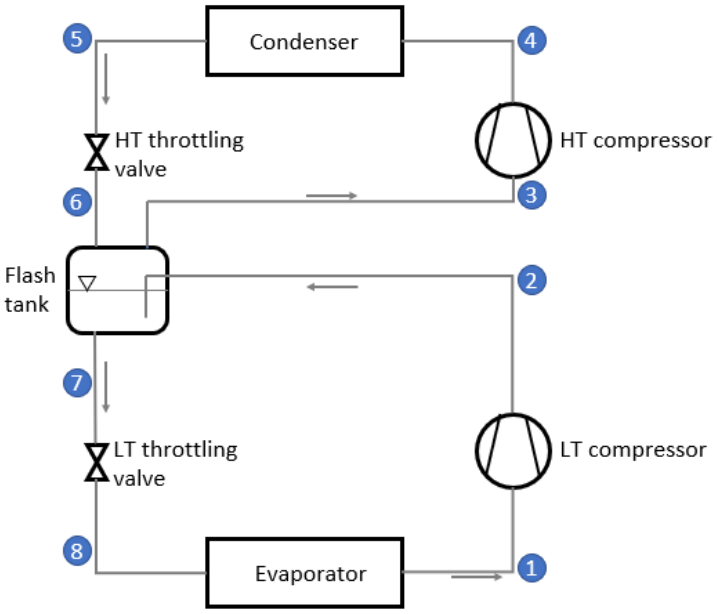

Figure 6: Two-stage vapor compression cycle

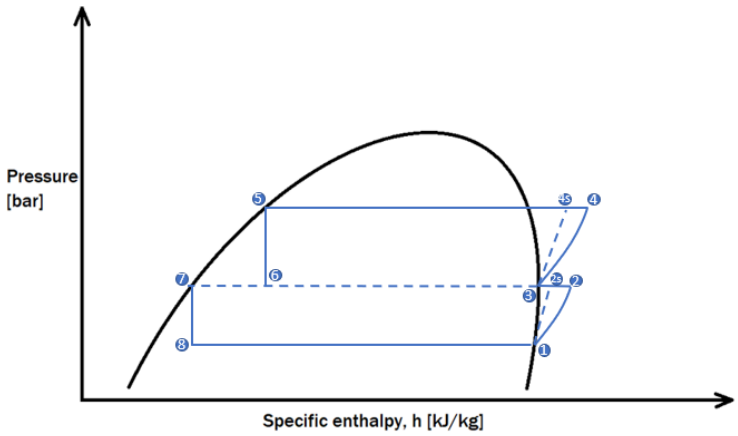

Figure 7: PH diagram for two-stage vapor compression cycle

Economizer

To reduce the expansion loss in a two-stage compression process, an economizer solution could be used. A subcooler is added before the expansion valve, and while most of the refrigerant goes directly through the subcooler, a small amount will go through an expansion valve first. This will reduce the pressure and temperature of the refrigerant, and this will cool the rest of the refrigerant. The part of the refrigerant that is expanded is injected into the refrigerant flow between the compressors, to cool down the refrigerant at the intermediate stage (Taras and Lifson, 2007).

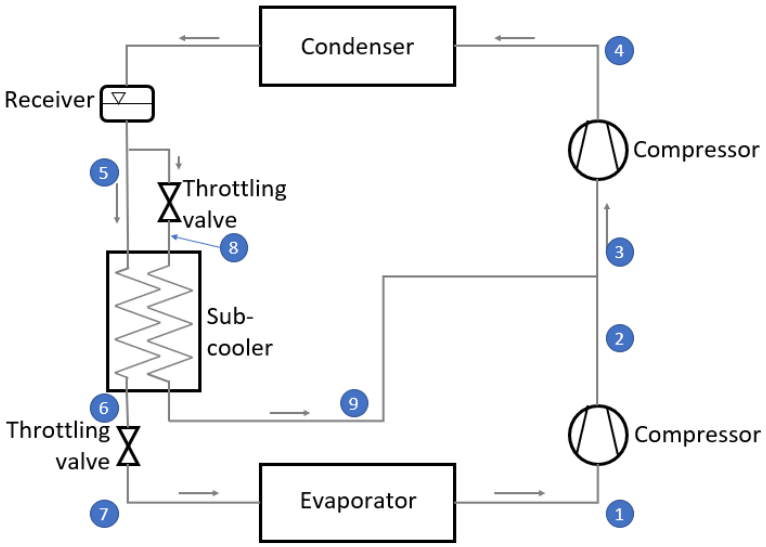

Figure 8: Vapor compression cycle with economizer

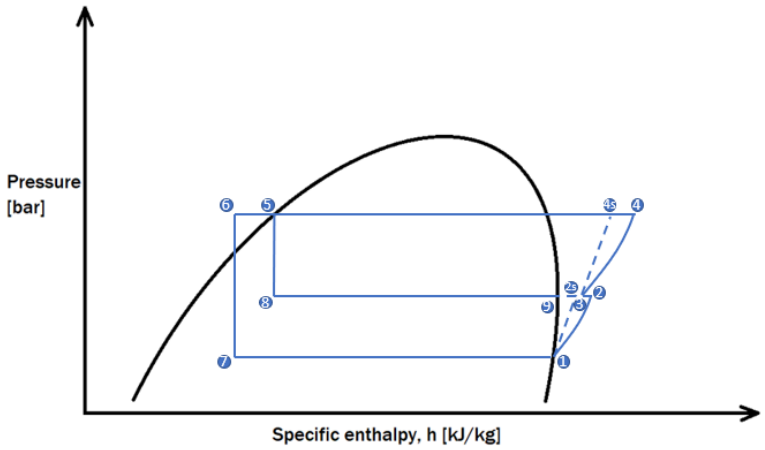

Figure 9: PH diagram of heat pump with economizer

Ejector

Ejectors, or jet pumps, can be used in several ways in heat pump systems. The simplest way is by replacing the expansion valve. The motive fluid flows from the condenser and expands in the motive nozzle. At the same time, a low-pressure suction steam is lead from the evaporator to the ejector. The steams mix in the mixing section and become one steam with almost uniform pressure and speed. The kinetic energy is converted into internal energy in the diffuser, and the pressure at the outlet of the ejector is higher than the suction inlet pressure. The fluid enters a separator, and the liquid will return to the evaporator through an expansion valve while the vapor will go to the compressor. The ejector system uses the expansion loss to increase the inlet pressure of the compressor. This reduces the pressure ratio, and therefore the energy used by the compressor (Sarkar, 2012).

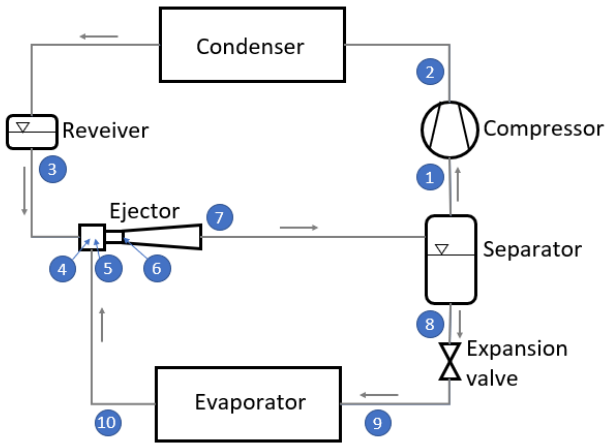

Figure 10: Vapor compression cycle with ejector

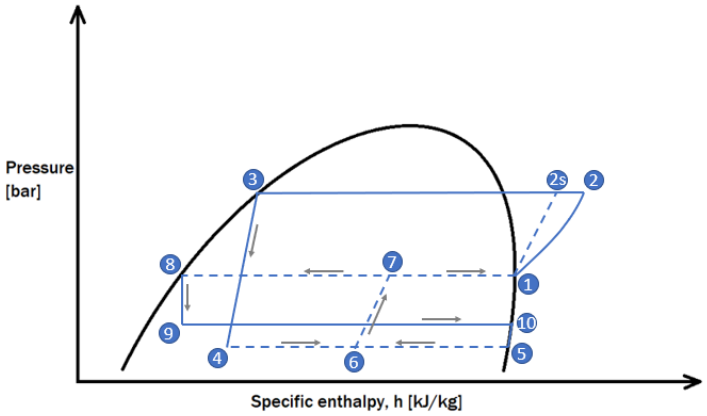

Figure 11: PH diagram of heat pump with ejector

<u>Cascade system</u>

A cascade system is interesting when it comes to high temperature heat pumps, because it allows for large temperature differences with pressure levels that are not too high. A cascade system is two heat pump systems connected by a heat exchanger that acts as a condenser for the low temperature system and an evaporator for the high temperature system. Because the systems are completely separated, they can use different refrigerants (Kim et al., 2013).

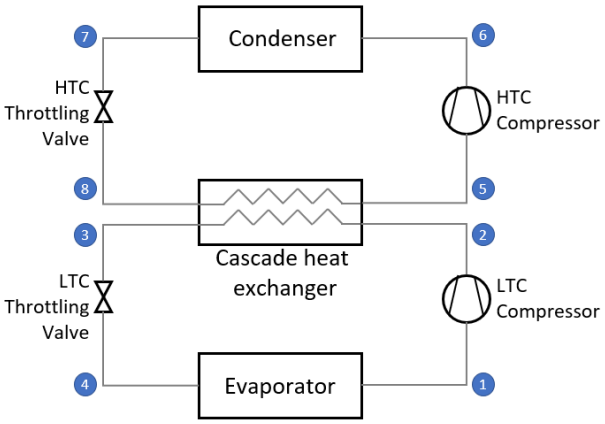

Figure 12: Cascade heat pump system

2.3.2 Improved efficiency for high temperature heat pumps

2.3.2.1 Previous studies

High temperature heat pumps face similar challenges as conventional heat pumps when it comes to energy efficiency, but certain challenges become more prominent as the temperatures rise. One of the challenges that is especially prominent in high temperature systems is that they often demand a large temperature lift, which in turn leads to a large pressure difference across the compressor. This requires a large power input to the compressor and reduces compressor efficiency. Because of this, multiple stage systems and cascade systems can be especially beneficial in HTHPs.

As mentioned above, multi-stage systems compress the refrigerant in several stages, so the pressure ratio over each compressor in multi-stage systems is lower than the pressure ratio of a single-stage system with the same operating conditions. This reduces the compression losses drastically and can ensure a higher isentropic efficiency in the compressors. Furthermore, the power consumption in each compressor is reduced, and in many cases to a lower overall power consumption (Liangdong et al., 2010). Moreover, the separation of liquid and vapor in the flash tank leads to a lower enthalpy in the liquid entering the evaporator, which in turn leads to a higher enthalpy difference across the evaporator and a higher heating capacity, which leads to an increased COP (Hu et al., 2017a).

Hu et al. performed an exergy analysis of multi-stage compression high temperature heat pump systems with R1234ze(Z) as a working fluid. They analyzed and compared performances of a single-stage, two-stage, and three-stage system for 120°C pressurized hot water supply with a constant heat recovered in the evaporator of 420 kW. The waste heat source varied between 50°C and 90°C. They found that the three-stage system had the smallest compressor power consumption regardless of waste heat source temperature, but that the power saving of multiple stages became less significant with increasing waste heat source temperatures. The same was true for exergy efficiency. They also found that COP improved with 12.2% and 19.8% for two-stage and three-stage systems, respectively, when the waste heat source was 50°C. With a waste heat source of 80°C, the COP improved with 6.3% and 9.4% compared to a single-stage system (Hu et al., 2017a).

Mateu-Royo et al. looked at energy performance and volumetric heating capacity of five vapor compression systems using various refrigerants. They looked at single-stage cycle, a single-stage cycle with internal heat exchanger, a two-stage cycle, a two-stage cycle with internal heat exchanger, and a two-stage cycle with intermediate internal heat exchanger. They found that the single stage cycle with internal heat exchanger had the highest performance for temperature lifts of 40 and 60 K. However, for temperature lifts of 80 and 100 K, the two stage cycle with internal heat exchanger had the highest performance (Mateu-Royo et al., 2018). This indicates that the advantages of multiple stages become more prominent as the temperature lift increases.

Hu et al. also investigated and compared three advanced heat pump systems. The first system is a one-cycle two-compressor system. The second system is a two-compressor parallel system. The third system is a two-cycle parallel system. The three systems have different complexities and performance. They found that the exergy efficiency was 5.4% and 11.5% higher for the two-compressor parallel system and the two-cycle parallel system, respectively, than for the one-cycle two-compressor system. The COP was also

higher for the third and second systems. The system COP is largest for the two-cycle parallel system, second largest for the two-compressor parallel system and lowest for the one-cycle two-compressor system for all condenser outlet temperatures. The difference between the COPs, however, seems to decrease as the outlet temperature increases. When the wastewater temperature increases, the heating capacity decreases slightly. This is because mass flow rate decreases, whereas the enthalpy difference in the condenser remains unchanged. It seems that condensing temperature has a stronger influence on heating capacity than evaporating temperature. The system COP is again highest for the two-cycle parallel system and lowest for the one-cycle two-compressor system for all evaporator inlet temperatures, and the difference increases with increasing evaporator inlet temperature (Hu et al., 2019).

Fukuda et al. evaluated the efficiency of two different heat pump configurations using three different refrigerants. They used waste heat at 70°C to get a heat sink temperature of 160°C using a single-stage compression cycle and a two-stage compression extraction cycle. They found that the COP was higher in the two-sage cycle for all refrigerants. The highest- and lowest performing refrigerants were the same in both system configurations, but the difference between the refrigerants decreased in the two-stage system, from a difference between the highest and lowest performing refrigerants of 0.56 in the single-stage system to a difference of 0.14 in the two-stage system (Fukuda et al., 2017).

Cao et al compared different heat pump systems that produced hot water with a temperature of 95°C with a heat source of 45°C. They looked at a single-stage vapor compression heat pump, a two-stage heat pump with external heat exchanger, a two-stage system with refrigerant injection, a two-stage system with refrigerant injection and internal heat exchanger, a two-stage system with flash tank, and a two-stage system with flash tank and intercooler. As expected, the COP of all systems increased with increasing evaporation temperatures and decreased with increasing condensation temperature. The COP was lowest for systems 1 and 2 for all temperatures, followed by systems 3 and 4, and highest for systems 5 and 6 (Cao et al., 2014).

Bamigbetan et al. developed a high temperature heat pump that could deliver heat at 115°C. The system is a cascade heat pump system that uses propane and butane as refrigerants. The COP decreased with increasing temperature lifts, and the average heating COP was 3.5 for the experiment and 3.2 for the simulation, with a temperature lift of 48-78 K. However, with temperature lifts of around 50 K the COP was around 4. The combined COP had an average of 3.4 (Bamigbetan et al., 2019).

Ma et al looked at a cascade system for high temperature heat pumps with the near-zeotropic mixture BY-3 as the lower stage refrigerant and R245fa as the upper stage refrigerant. The COP was slightly lower than 3 with a condensing temperature of 100°C, and around 2.65 when the condensing temperature was 115°C (Ma et al., 2018).

2.3.2.2 Discussion

Because all systems in the abovementioned research are different, in can be difficult to make a good comparison. Specific COPs for systems with such different parameters and refrigerants cannot be compared in a good way. However, it is possible to draw certain conclusions from the trends that emerge from the research.

Firstly, it seems that there should be a certain temperature lift before a multi-stage system is more beneficial than a single-stage system. This is logical, because the

pressure difference between the compressor and evaporator is directly related to the temperature lift. Because the main advantage with multiple stages is the reduction of the compressor losses due to the decreased pressure ratio, it makes sense that the advantages are more prominent in systems with a large pressure difference between the evaporator and the condenser.

However, it seems difficult to find a specific temperature lift below which a multi-stage system is less beneficial than a single-stage system. This is partly because it depends on which refrigerant is used, as the degree to which the pressure changes with the temperature varies between the refrigerants. Additionally, the heat pump systems in the abovementioned articles have different system configurations, and even though many systems have the same number of compression stages, they differ from one another in other ways. For example, an internal heat exchanger may affect the COP.

Furthermore, it seems that if the system has a high enough temperature lift, multiple stages increase the COP of the system compared to a single-stage system. This was found in all the articles that compared single- and multi-stage systems. In the articles that compared two-and three-stage systems, the three-stage systems had a higher COP than the two-stage system. Therefore, the COP may increase with the number of stages. However, it is likely that this only happens up to a certain point. Because each compressor requires power input, there is a limit to how many compressors that can run before the total work added is too high and the COP starts to decrease.

The COP in the cascade systems in the case studies were generally lower than the COP in the multi-stage systems. This implies that from an energy efficiency perspective, multi-stage systems are better suited for high temperature applications than cascade systems. However, cascade systems have several benefits such as the option to use two different refrigerants, which can optimize the pressure ratios of each compressor.

Based on the information in the papers, it seems that multiple stages and cascade systems in general are beneficial in high temperature heat pumps, especially if the temperature lift is high. However, it is evident that other system configurations can have a large effect on system efficiency as well, so multiple stages or cascade cycles should be combined with other energy saving measures such as ejectors, economizers, and other solutions. The use of these system configurations in combination with cascade or multi-stage cycles can yield a high COP in HTHPs.

2.4 Other parts of an integrated energy system

2.4.1 General

As mentioned in the introduction, the most common types of integrated energy systems consist of combined cooling, heating, and power generation (CCHP). The energy performance characteristics of such systems are greatly influenced by the operational strategy and capacity of the equipment (Li et al., 2016). The energy system in this project will have heating and cooling from heat pumps, power generation from PV modules, as well as storage of electrical and thermal energy. The cooling system is neglected in this report. Furthermore, the system will be connected to district heating.

The focus in this thesis will be the operation of the heat pump, and the models of other components are greatly simplified. Consequently, the performance of the whole system and the operational strategy will not be closely evaluated at this stage in the project. In

the following chapters, theory about the other parts of the integrated energy system created in this thesis will be presented.

2.4.2 Thermal Energy Storage

Thermal energy storage systems store thermal energy by heating or cooling a medium so that the stored energy can be used for heating or cooling at a later time (Sarbu and Sebarchievici, 2018). Thermal storage systems have been used by humans for centuries and range from simple systems using ice or hot or cold water to more complex systems with phase changing materials (PCM). Thermal storage systems are primarily used in buildings and industrial processes (Sarbu and Sebarchievici, 2018). The main advantages with thermal storage are increased predictability and increased energy efficiency. Economic efficiency can also be increased by optimizing heat production and taking advantage of fluctuations in electricity prices.

Worldwide, there is a high demand for thermal energy for industrial processes and residential use. At the same time, there is a large amount of excess thermal energy available. In spite of this, it can sometimes be difficult or costly to cover the demand. Furthermore, thermal energy generation often leads to emissions of greenhouse gases (Alva et al., 2018). The reason why a lot of thermal energy is going to waste while at the same time, thermal energy is produced at great economic and environmental costs, is that several gaps between supply and demand exist. The main gaps are that excess thermal energy is often generated at a time when the demand is low, and that the places where thermal energy is needed may be located far away from where the excess thermal energy is produced (Alva et al., 2018).

These problems can be solved or reduces by integrating thermal energy storage systems. If energy is produced at a different time or than when and where it is consumed, it can be stored between the time of production and the time of consumption. Thermal energy storage in the form of hot water storage tanks is found in many homes across the world today. In residential applications, thermal energy storage can ensure a more stable access to thermal energy, and to cheaper energy production. With thermal energy storage, energy can be produced at times when electricity prices are low instead of producing the energy when it is needed regardless of the price. Furthermore, the thermal energy can be produced at times when the demand is low and used at a time when demand is higher. This will allow for smaller thermal energy generation systems, as the energy stored in the thermal energy storage system will reduce the necessary capacity of a thermal energy generation system, as seen in Figure 13 and Figure 14.

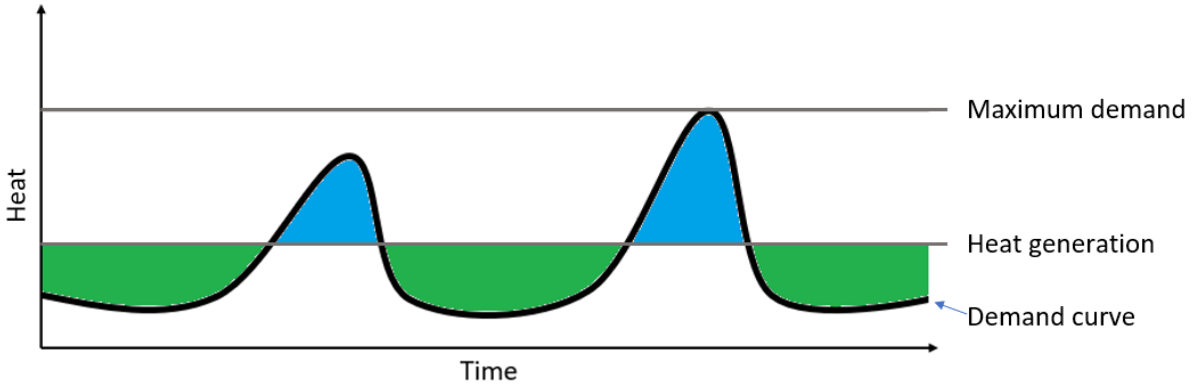

Figure 13: Heat demand and thermal energy generation

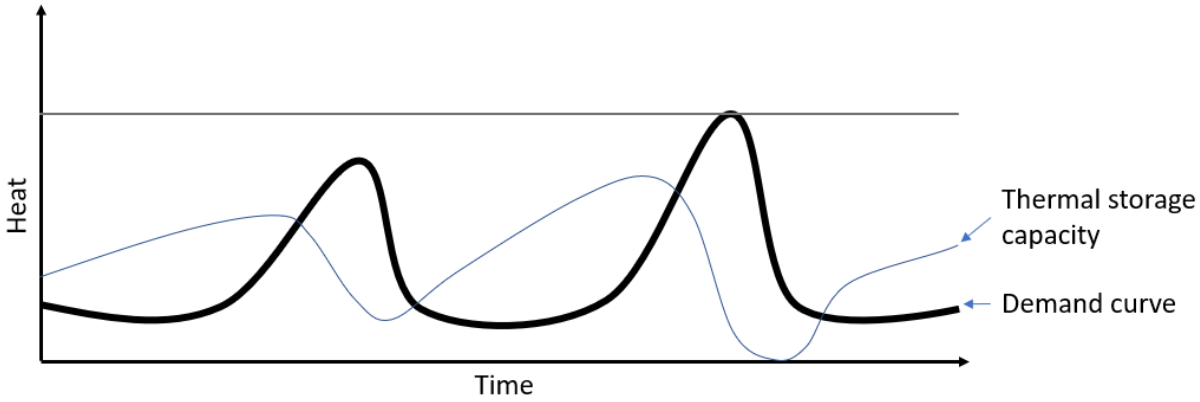

Figure 14: Heat demand and thermal energy storage capacity

Figure 13 shows a possible scenario with thermal energy storage. The thick, black curve illustrated the heat demand throughout a day. The horizontal, grey curve illustrates the heat production throughout the same day. It is assumed that the heat production is uniform at all times of the day. When the demand is lower than the heat production, the excess heat (colored green) will be sent to the heat storage. When the demand is higher than the heat production, the extra heat needed to cover demand will be taken from the heat storage (colored blue). That way, the capacity of the heat production is much lower than the capacity needed to cover demand with no thermal storage. This leads to smaller and cheaper energy production systems. Figure 14 illustrates how the capacity of the thermal energy storage changes throughout the day for the same system as illustrated in Figure 13.

Thermal storage systems can be classified into three categories: Cold storage is typically up to 15°C, warm storage is often 40-50°C, whereas hot storage usually hold temperatures between 70 and 90°C (Sarbu and Sebarchievici, 2018). This paper will focus on hot storage.

Thermal energy storage can use sensible or latent heat transfer. Sensible heat storage systems function by heating or cooling a liquid or a solid medium. Water is commonly used for heat storage in buildings. The heat transfer in sensible heat storage systems is limited to heat transfer without phase change.

Latent heat storage uses phase-changing materials to store energy. The materials change their physical state when energy is absorbed or released, allowing for energy to be stored at the temperature at which the phase changes. Latent heat storage systems

often have higher energy densities than sensible heat storing systems, and they can store the heat at a more constant temperature than sensible systems. The latent heat systems behave like sensible heat systems before phase change occurs. During charging, the temperature increases until the phase change temperature is reached. At this point, the material will melt or evaporate at a constant temperature. Once the material has changed phase, the temperature will continue to increase like in sensible heat storage if the charging process continues. The opposite will happen during discharging. Figure 15 shoes how heat transfer happens in sensible and latent heat storage systems.

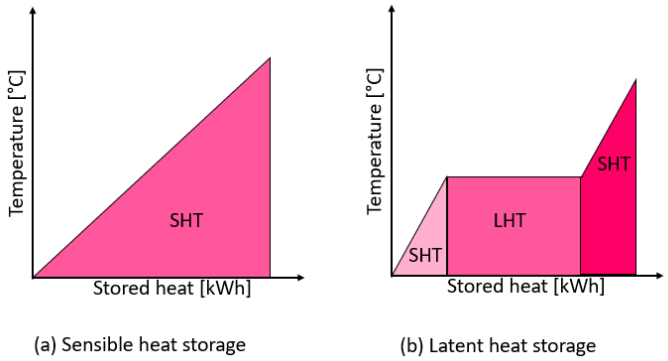

Figure 15: Heat transfer in sensible and latent heat storage systems. SHT = Sensible heat transfer, LHT = latent heat transfer

There are several types of phase changing materials with different melting points and properties. Paraffin is the most common organic materials in commercial thermal energy storage applications. However, pure paraffin is expensive, and technical grade paraffin waxes, which are mixtures of paraffin with different carbon numbers, are often used in practical applications. These waxes have melting temperatures between -5°C and 100°C (Alva et al., 2018). Furthermore, fatty acids and polybasic alcohols are other types of organic materials used in PCM applications. Hydrated salts, molten salts, metal or alloy materials and eutectics are inorganic materials used as PCMs (Fan and Khodadadi, 2011). Inorganic materials are often used in applications with higher temperatures (Alva et al., 2018).

Latent heat is between 50 and 100 times larger than sensible heat, and the energy density of latent heat storage materials is therefore high. This results in more compact systems when PCMs are used than in sensible heat storage systems (Alva et al., 2018). Another important advantage is more stable temperatures, as mentioned above. The main drawback with latent heat storage is that many PCMs used have low thermal conductivity, and that charging and discharging therefore happens slower than with sensible heat storage.

There are clear advantages to using thermal energy storage to better balance heat supply in an integrated energy system. A variety of options exist, so it is clear that installing a thermal energy storage with PCM in the integrated energy system in this project is possible. However, because the thermal storage system will be greatly simplified in this project, the more detailed theory will not be further explored.

Fischer et al. (2014) investigated various strategies for operation of heat pumps in systems with sensible thermal energy storage. They found that increasing the size of the thermal storage system can have a small positive effect on prices, and that in increases

total system flexibility in operation. They also found that if the system includes solar power, a larger TES capacity is favorable because the heat production can take advantage of when power is available. In general, they found that increasing the thermal storage increased the efficiency of the heat pump, but also increased heat losses in the storage tank (Fischer et al., 2014).

Schibuola et al. (2015) investigates demand response management of heat pumps based on electricity prices. They found that if control strategies are properly adapted to the system, it is possible to achieve a high level of energy self-consumption. The costs were also reduced because the control system took advantage of varying electricity prices. However, they found no real effect on energy consumption when varying the size of the thermal energy system (Schibuola et al., 2015).

It is clear that thermal energy storage can provide a more stable heat supply by storing the energy produced when demand is low and using it when demand is higher. It is difficult to compare the storage systems used in literature, as they are designed for very different systems. However, drawbacks related to thermal energy storage cannot be ignored. The main drawback of thermal energy storage is the losses experienced during charging, discharging, and storage.

2.4.3 Solar energy systems

2.4.3.1 Solar photovoltaics

Solar energy is perhaps the most abundant energy source that exists today. Energy from the sun is available across the globe and has been used in the form of lighting and direct heating for millennia. With the technology that exists today, solar energy can also be used for electricity production and more efficient heat production, and in the past few years the price of this technology has been drastically reduced. This project uses solar photovoltaic (PV) systems to produce power, as well as solar thermal systems to provide heat. Other technologies using solar energy will not be discussed. Systems that combine the use of solar PV and solar thermal will be referred to as PVT systems.

Solar PV systems produce electricity without harming the environment in the form of greenhouse gas emissions, air pollution, or depletion of resources. It should be noted that production and disposal of solar PV systems affect the environment by emitting gases and polluting the local environment, and that depletion of the raw materials needed to produce the systems is a potential problem. However, this paper will not go into a life cycle analysis or an economic assessment, instead it will focus on the actual operation of the integrated energy systems.

During operation, however, solar PV systems do not contribute negatively to the climate or the environment. Furthermore, they can be installed in remote areas with little or no access to a stable supply of electricity. There are no moving parts, investment and maintenance costs are low, and PV systems can function unattended over long periods of time. The main disadvantage with PV is that it does not provide a stable electricity supply because it is highly dependent on the weather and the time of day (Singh, 2013).

Solar PV functions by directly converting solar radiation to electricity. A PV cell consists of a semiconductor wafer specially treated, so it is positive on one side and negative on the other, with electrical conductors attached on each side. The electrical conductors form a closed circuit. Additionally, an anti-reflective coating ensures that as much light as possible is absorbed. When the radiation from the sun reaches the wafer, electrons are

knocked loose from the semiconductor and moves to the electrical conductors and then into the electric circuit. In a PV system, multiple cells are connected to form a module, and multiple modules can be connected to form an array (Knier, 2008).

The overall efficiency of PV systems is generally quite low due to losses during the conversion of sunlight to electricity, through regulators, the battery, cables, inverters, and other components (Singh, 2013). Furthermore, the performance of the cells decreases with increasing temperature, and bort electrical efficiency and power output have a linear dependence on operating temperature(Dubey et al., 2013).

2.4.3.2 Solar thermal/PVT

The temperature of the PV cells negatively affects the efficiency of the PV module. The temperature of a PV module is dependent on outside air temperature, but also on the amount of solar radiation. This is because the solar radiation that is absorbed but not turned into electricity increases the temperature of the PV module. To increase the efficiency of the PV modules, the temperature should be reduced. This can be done by integrating a cooling system.

A simple way of cooling the PV modules is by using air circulation. However, this is not very effective when the temperature of the air exceeds 20°C for long time periods (Lamnatou and Chemisana, 2017). Another way to cool the modules is by circulating a refrigerant through a heat exchanger to transfer heat from the PV modules to the refrigerant. The heat transferred to the refrigerant can be used for practical purposes, such as domestic heating if the temperatures are high enough. In heat collected from PV modules is put to practical use, the systems are called Photovoltaic-thermal (PVT) systems. PVT have higher total energy outputs than PV systems, both because the PV efficiency increases and because the heat is being utilized in addition to the generated electricity (Lamnatou and Chemisana, 2017). The heat collected by the PVT system can also be used as a heat source for a heat pump if there is a demand for higher temperatures than what the PVT system can produce.

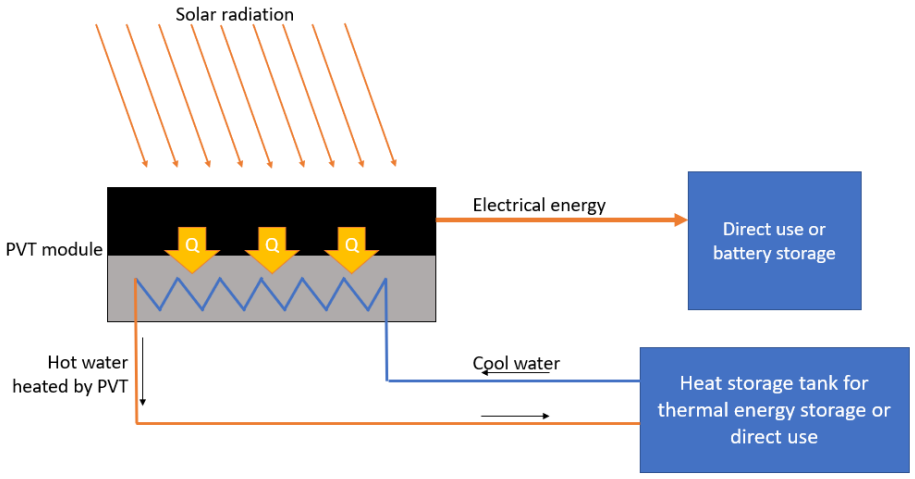

Figure 16: Simple sketch of a PVT module

Figure 16 shows a simplified PVT module. The black part of the module represents the PV cells, which convert solar radiation to electrical energy. The electrical energy is used directly in electrical appliances or stored in batteries. The heat exchanger is found in the

grey part of the PV module, and excess heat is transferred to the refrigerant. In this case, the refrigerant is water.

2.4.4 Batteries

Due to a recent increase in fossil fuel prices coupled with a decrease in prices for solar PV systems with batteries, the solar PV/battery market is growing in many parts of the world. This is especially true for urban areas and areas not connected to an electricity grid (Ayeng'o et al., 2019). PV battery systems can be divided into two main groups: Those that use a charge controller to directly connect the PV system to a battery, and those that connect the PV system and battery with an MPP-Tracker (Ayeng'o et al., 2019). The MPP-Tracker systems are more complex than direct-coupled systems and can always deliver the maximum available PV power. However, they are more expensive than direct-coupled systems, and likelihood of failure as well as investment costs increase. The efficiency of solar batteries can vary greatly, from 70% in lead batteries to more than 90% in Lithium-ion batteries. The lithium-ion batteries can discharge up to 100% of the stored power (Solarwatt, 2020).

The model of the PV battery will be greatly simplified in the simulations in this thesis, and the theory of solar batteries will therefore not be further investigated at this stage of the project.

3 Simulation approach

3.1 Preparations

The focus of this project is a high temperature heat pump in an integrated energy system that can provide heat at above 100°C with a temperature lift of above 50°C and a COP of 3.5 or higher. The Chinese cities Shanghai, Lanzhou and Beijing were selected as locations for the system. The main goal was to investigate how the high-temperature heat pump operates together with the other components in the integrated energy system. This was the focus through the simulations. Consequently, the code created to simulate the system needed to find a balance between complexity and simplicity.

On one hand, the part of the code that represented the heat pump needed to take into account the rest of the system and how the heat pump adapted to ever-changing conditions, including how various variables such as evaporator and condenser temperatures changed throughout a year. On the other hand, the other parts of the system needed to be simplified so that the heat pump operation could be properly evaluated.

In preparation of the master thesis work, a project work was conducted where the effect various system configurations and different types of refrigerants have on the COP was investigated. The results from the project work, as well as the literature review conducted in this project, were used to decide which system configurations would be selected for the heat pump in this system, and which refrigerant that would be most suitable.

3.2 About the model

3.2.1 General

The model was created in Matlab, and refrigerant properties were collected from REFPROP. Meteonorm was used to collect weather data from Shanghai, Lanzhou, and Beijing. The electricity demand of other parts of the system than the heat pump was neglected, including the electricity demand for residential use of electrical appliances and lighting. The heat demand for every hour was calculated based on the outside air temperature. A base demand of 50 kW for water heating was assumed to be constant. Additionally, the heat demand increased with decreasing outside air temperatures. For every degree below 15°C, the heat demand increased with 10.25 kW due to space heating demand. For example, if the outside air temperature were 5°C, the heat demand would be 50 kW for water heating, and 102.5 kW for space heating. The total heat demand would be 152.5 kW.

Prior to making the model for the entire integrated energy system, some parts of the systems were modelled individually to ensure that the codes worked as they should. In the following chapters, the different parts of the combined model will be described separately. Lastly, the combined model will be described before the results are presented.

3.2.2 PV Panels

The panels of the type Jinko Tiger JKM470N-7RL3 from Jinko Solar were chosen for this system (Jinko Solar, 2020). These PV panels have high performance, and technical specifications are easily accessible online. Furthermore, Jinko Solar was selected in part because it is a Chinese company. This is beneficial from an economical and environmental perspective, because using domestically produced PV panels will reduce costs and emissions related to transportation. Moreover, using Chinese products for systems to be installed in China is in line with the "Made in China 2025" initiative.

The values for the maximum power point, module efficiency, and temperature coefficient of the maximum power point have been selected based on the datasheet provided from the producer. Performance ratio is the coefficient that accounts for losses related to the power generation. These losses include inverter losses, temperature losses, cable losses, shading, losses due to dust, and other losses (Photovoltaic Software, 2020). Because of insufficient information to accurately calculate the losses in the PV modules in this report, the performance ratio is assumed to be 75%. This value can vary between 50% and 90%, but 75% is the default value (Photovoltaic Software, 2020).

The surface temperature of the PV panels is assumed to be 20°C higher than the ambient temperature (Power Scout, 2017). Weather data is collected from the program Meteonorm, and the operating efficiency is calculated with Equation 18 based on the information from the datasheet and weather data. Finally, the energy generated by the PV panels is calculated using Equation 19.

To calculate the energy output, the operating efficiency must first be calculated:

Equation 18: Operating efficiency of a PV module

$$r = \eta_{STC} - (T_{STC} - T_{PV}) \times TC$$

r is the operating efficiency [%]
η_{STC} is the module efficiency at standard test conditions [%]
T_{STC} is the temperature at standard test conditions [°C]
T_{PV} is the surface temperature of the PV module [°C]
TC is the temperature coefficient of the maximum power point [%/°C]

The energy output from the PV module can then be calculated:

Equation 19: Electric energy generated by a PV module per hour

$$E = A_{PV} \times r \times H \times PR$$

E is the electric energy generated by the PV module [kWh]
A_{PV} is the surface area of the module [m^2]
r is the operating efficiency [%]
H is the global horizontal radiation per hour [kW/m^2]
PR is the performance ratio [%]

The thermal part of the PVT system was not included in the calculations. The specifications for the PV panels can be found in Table 3.

Maximum power point (P_{max})	470 Wp
Module efficiency at standard test conditions (T_{STC}=20°C)	20.93%
Area of PV panels	4000 m^2
Performance ratio	75%
Temperature coefficient of the maximum power point	0.34%/°C
Temperature at standard test conditions	25°C

Table 3: Solar panel specifications (Jinko Solar, 2020)

3.2.3 Battery Storage

The part of the code that controls the battery storage is also greatly simplified. For every hour, the power added to and removed from the battery is calculated based on the performance of the PV panels and the heat pump. If the power consumption of the compressor is lower than the power produced by the PV panels, the excess power is sent to the battery storage. If the PV panels produce less power than the power consumption of the compressor in a certain time step, the battery will supply the compressor with the remaining power. After calculating the input or output of power in the hourly iteration, the power remaining in the battery is calculated. The efficiency of the battery is set to be 80%, so some power is lost every time the battery is charged or discharged.

3.2.4 Thermal Energy Storage

The thermal energy storage tank is connected to the heat pump and the district heating system. Phase changing materials are used to maintain a temperature slightly above 80°C in the tank, so that the heat supply to the district heating system always stays above 80 °C. No specific PCM is selected for the system in this report because detailed calculations of heat transfer inside the thermal storage system will not be done at this stage of the project. However, $Mg(NO_3)_2{\cdot}6H_2O$ and $Ba(OH)_2{\cdot}8H_2O$ are two examples of inorganic salt hydrates with phase changing temperatures of 89°C and 78°C, respectively, and would be viable potions for this TES system. Rubitherm RT-82 is an organic paraffin with a phase change temperature of 82°C and would also be a good option (Alva et al., 2018). There are several other PCMs that could be used, and the final decision should be based on a thorough evaluation of properties such as melting temperature, thermal conductivity, density, latent heat storage capacity, latent heat, price, and more.

The code for the thermal storage system is simplified compared to an actual system. For every hourly iteration, the energy added to and removed from the thermal storage is calculated, and the hourly thermal storage capacity is determined. The specific heat transfer mechanisms between the water and the phase changing materials are not considered in the code because of the wish to simplify the parts that are not integral to the heat pump.

The tank in this system will store temperatures between 80 and 100°C. Typical charging efficiencies for systems operating in this temperature range is between 75% and 90%, and the power is typically between 0.001 and 1 MW (Hauer, 2013). An efficiency of 90% was selected for the system in this report. The maximum storage capacity was set to be 1000 kWh. The tank is assumed to be fully isolated, and heat transfer through the walls of the storage tank is neglected.

For each hourly iteration, the Matlab code does one of three actions. If the amount of heat produced by the heat pump is higher than the demand, the excess heat is directed to the thermal energy storage. If the heat pump does not produce enough heat, the

remaining heat needed to cover the demand is subtracted from the heat storage. If the heat pump produces exactly the demand, nothing happens to the capacity of the thermal storage. Because the charging/discharging efficiency is set to 90%, 10% of the heat is lost in each charging/discharging cycle. Other losses such as heat transfer through the walls of the tank are neglected, and the focus is the hourly energy input and output to and from the tank, as well as the maximum storage capacity.

3.2.5 District heating

The district heating system is not modelled in this thesis because the types of and number of buildings that will be supplied by the district heating system has not been decided. Instead of modelling the district heating system, the temperature of the supply and return water to and from the district heating system was calculated for every hourly iteration.

3.2.6 Heat pump

3.2.6.1 Code development

Because the heat pump would be the main part of the simulations, the heat pump model was more realistic with fewer simplifications than the other models. The process of developing the code for the heat pump model was divided into several small steps to reduce the risk of code malfunctions.

First, a model of a one-stage simple vapor compression cycle was created. This heat pump model consisted of an evaporator, a compressor, a condenser, and an expansion valve. The one-stage model was implemented to the integrated system, and the code was run to ensure the heat pump model functioned with the other components of the integrated system. Even though the code worked, and the yearly operation of the integrated energy system was simulated with the single-stage heat pump, the COP of the heat pump was too low. The simulation showed a COP of 2.426 for most of the time steps. While this is above 1 and therefore favorable over direct electric heating, it is much lower than the desired value of 3.5. Consequently, the COP needed to be improved.

Once the code worked for the whole system, the heat pump model was therefore updated to increase the efficiency of the heat pump. A second compressor was added in parallel to the first compressor, and instead of one condenser, two condensers were implemented in parallel. The system sketch of the heat pump can be seen in Figure 17.

Two compressors were selected for the heat pump because of the obvious advantages to multi-stage compression. The literature review and previous project work showed that COP significantly increases when compression happens in several stages. This effect is seen even when no other improvements to the system are made. The addition of a second compressor also allowed for a second condenser to be implemented into the system. This led to a more efficient heat exchange process, as the temperature difference between the water entering and leaving the condensers is almost 40 K. With two condensers, the temperature glide in each condenser is lower, which leads to fewer losses in the heat exchangers.

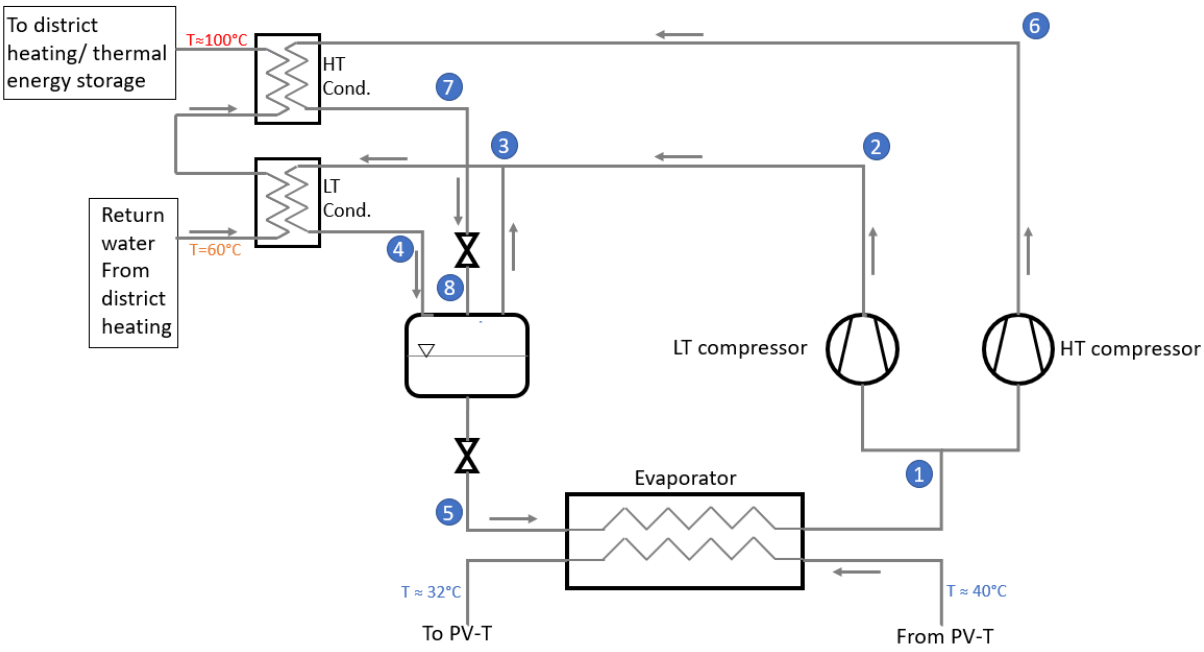

Figure 17: System sketch of two-stage parallel compression heat pump

3.2.6.2 System configurations

The heat source to the evaporator is water heated by the PVT system. The solar thermal system was not part of this simulation, and the inlet temperature of the water entering the evaporator was assumed to be constantly equal to 40°C. This water heats up the refrigerant in the evaporator.

After the refrigerant leaves the evaporator (1), part of in enters the low-temperature (LT) compressor, and the rest of it enters the high temperature (HT) compressor. The LT compressor compresses the refrigerant to an intermediate pressure of about 4160 kPa (2), which corresponds to a condenser temperature of around 80°C. The compressed refrigerant is mixed with the refrigerant in the receiver that is in gaseous state (3), enters the LT condenser, and preheats the water as it condenses. The refrigerant then enters a receiver (4) where it is mixed with the refrigerant from the HT compressor.

The HT compressor compresses the refrigerant to 5780 kPa (6), which corresponds to a condenser temperature of around 96°C. As it condenses, the refrigerant heats the water to its final temperature. After leaving the HT condenser (7), the refrigerant is expanded to a pressure of 4160 kPa (8), which corresponds to the pressure in the LT condenser. The refrigerant from the HT condenser then enters the receiver and is mixed with the rest of the refrigerant.

The fluid in the receiver will mostly be liquid, but because the fluid from the HT condenser has not expanded completely some of it will still be in gaseous state. The gas will be mixed with the refrigerant exiting the LT compressor and entering the LT condenser (3). The liquid refrigerant will leave the receiver and go through an expansion valve and expand back to a pressure of around 990 kPa (5) before it enters the evaporator and the process repeats. A Ph-diagram for the system can be seen in Figure 18.

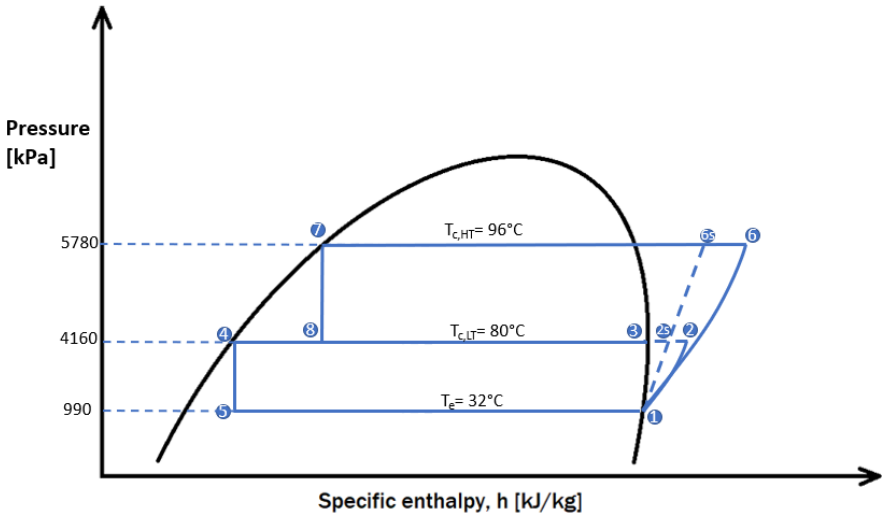

Figure 18: Pressure-enthalpy diagram for two-stage parallel compression heat pump

Among the factors that affect the efficiency of the heat pump are the temperatures and pressures in the condensers and in the evaporator. In a real system, the actual temperatures and pressure levels in the heat exchangers will vary slightly due to changing conditions in the system. To make the simulations as realistic as possible, the pressures and temperatures in the heat exchangers were calculated for every hourly iteration. This will be further described in chapter 3.3.2.

3.2.6.3 Refrigerant selection

The refrigerant was selected based on the literature review and the previous project work. The literature review showed that the refrigerant should be green or natural due to stricter regulations regarding environmental impact and general trends in heat pump development. Several green and natural refrigerants have been successfully used in high-temperature applications. The project works showed that methanol and ethanol provided a high COP for all single-stage and two-stage cycles, as well as cascade systems. However, no examples were found of these refrigerants being used in high-temperature heat pumps. In the instances in literature where ethanol or methanol had been used as refrigerants, they were usually mixed with other substances. Because this research will be continued over the next years, it was desirable to select a refrigerant that surely could be used in practical high-temperature applications. The focus of the report was to show how the heat pump works in the integrated system, and not how to optimize the refrigerant selection. Therefore, methanol and ethanol were discarded.

Water also showed great potential in the project work. However, if water were to be used in this project, the evaporator pressure would be below 1 bar as the evaporating temperature is usually below 40°C. This can be difficult in practical applications, and for this reason, water is usually used in heat pumps operating in higher temperature ranges than the heat pump in this project.

R1233zd(E), R1234ze(Z), and Ammonia are also good options. The literature review showed that these refrigerants have shown promising results in high-temperature applications, and they have low GWP and ODP values. Ammonia is a natural refrigerant, while R1233zd(E) and R1234ze(Z) are synthetic refrigerants. The literature review uncovered that even though the synthetic refrigerants are regarded as having a low

environmental impact, there is still some uncertainty to their actual effect on the environment. Because of this, and because they showed very similar values to Ammonia in the simulations done in the project work, Ammonia was selected as the refrigerant in this project. Ammonia has higher toxicity than the other refrigerants considered (see Table 2) but has been used in commercial heat pumps for many years. As long as necessary safety precautions are taken, the toxicity of ammonia should not be an issue.

3.2.6.4 Values and assumptions

Some assumptions were made in the development of this code. Firstly, any power consumption other than for the operation of the compressor is neglected. Other components such as pumps and valves need electric energy to function, but these components have been neglected when looking at the power consumption of the heat pump. Furthermore, it should be noted that only the energy consumed by the compressor during operation is included in the calculations. More energy is used in the process of starting up, shutting down, or regulating the speed of the compressor. These factors have been neglected.

Secondly, the evaporators of all systems were assumed to be flooded evaporators, so the vapor quality is 1 at the evaporator outlets. The vapor quality at the outlet of the condensers was assumed to be 0. The heat exchange processes, both evaporation and condensation, were assumed to be isobaric and isothermal. Expansion was assumed to be isenthalpic, and expansion losses were neglected. The inlet temperatures of the water entering the heat exchangers was assumed to be constant both for the evaporator and the low temperature condenser.

The U-value was set to be 1400 W/m^{2}K for the evaporator and condensers. This value was selected based on typical U-values for the relevant types of heat exchangers (Engineering ToolBox, 2020). The compressor sizes, areas of the condensers and evaporator, and mass flow rate of the water through the heat exchangers were determined by running the heat pump code for a single time step and modifying the various components to get the desired capacity. The compressor sizes were selected first, and the heat exchanger areas were modified until the heat capacity was satisfactory and the temperature differences across the heat exchangers were small enough.

3.2.7 District heating

The district heating system was not modelled, instead the supply and demand temperatures were calculated based on heat capacity and demand in any given hour. A constant mass flow rate of 2 kg/s through the district heating system was set for every iteration. The temperature of the supply water to the district heating system was based on the performance of the heat pump. If the heat pump produced enough heat to cover the demand, the supply temperature was set to equal the temperature of the water at the outlet of the condenser. If the energy was taken from the thermal storage, the supply temperature was set to equal 80°C.

The temperature of the water returning from the district heating system was calculated with the following equations:

Equation 20: Temperature difference of water through the district heating system

$$\Delta T_{DH} = \frac{D}{\dot{m}_{DH} \times C_{p,DH}}$$

Equation 21: Return temperature of water from the district heating system

$$T_{return} = T_{supply} - \Delta T_{DH}$$

ΔT_{DH} is the temperature difference of the water entering and leaving the district heating system, D is the heat demand, $\dot{m}_{DH}$ and $C_{p,DH}$ are the mass flow rate and specific heat capacity of the water through the district heating system.

3.3 Simulations process

3.3.1 Set-up of the code

A sketch of the whole system can be found in Figure 19.

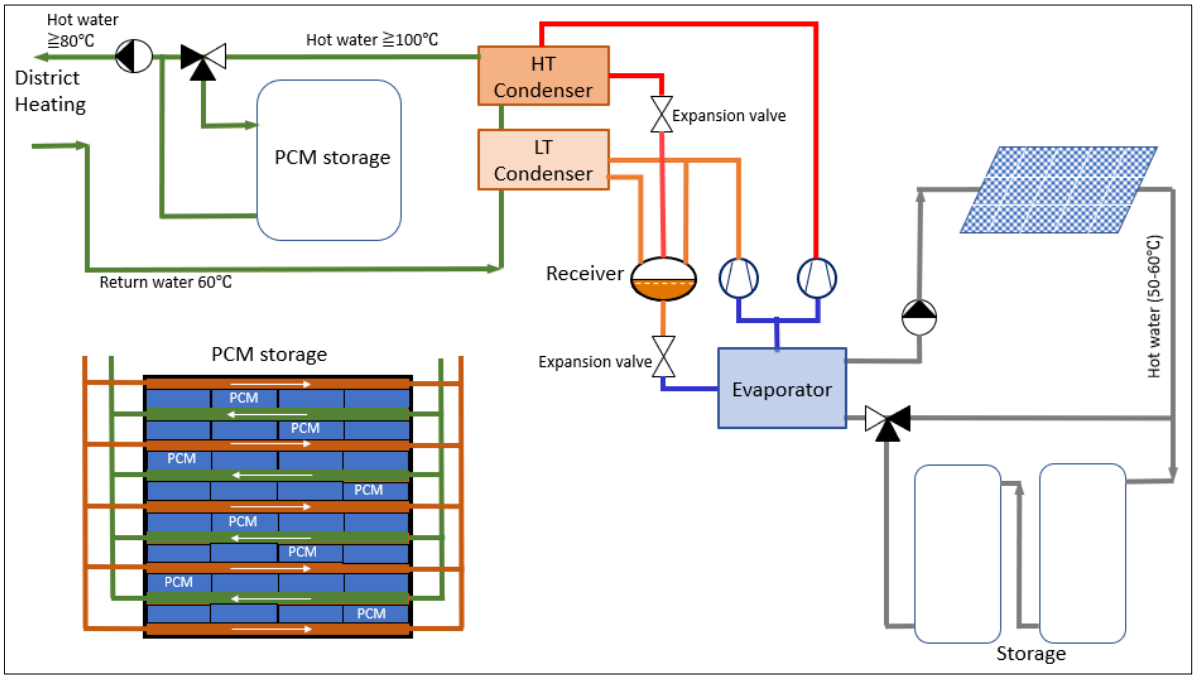

Figure 19: Sketch of the integrated energy system

Weather data from Shanghai, Lanzhou and Beijing was imported to Excel from the program Meteonorm, and the Matlab code collected the data from Excel. The system is simulated for every hour throughout the entire year, which leads to 8760 separate datapoints. The combined code for the integrated energy system was placed inside a for-loop that went through every hour throughout the year. For every hourly time step, values describing the operation and performance of the PV panels, battery, thermal energy storage, and heat pump were calculated.

Some of the values from the previous iteration were used as starting values for certain parameters in the next iteration. For example, the initial guesses of condensing and evaporating temperatures were based on the values for those temperatures in the previous iteration. Matlab does not operate with 0 as a logic identifier, which means that the 0^{th} element of an array cannot be referred to. As a result, the first iteration done by the for-loop had to be the second hour of the year. If the first iteration were for the first hour, the code would refer to the 0^{th} element of sever arrays when referring to values from the previous iteration. This would lead to an error. Therefore, the code begins with the second hour and ends with the 8760^{th} hour. There is a total of 8759 iterations, as the

first hour is disregarded. The code runs through all 8759 iterations before the results are presented. The same code is used for all three locations.

Due to the varying climates in the cities simulated, it was clear that the system would function differently in the different locations. All cities have periods throughout the year with high outside temperatures, resulting in periods of the year with no space heating demand. However, the hot water demand will stay relatively constant throughout the year. Because water must be heated every day of the entire year including the summer months, the heat pump must operate throughout the entire year. There are several possible ways to operate the heat pump when demand varies. In the following paragraphs, the options are discussed.

One way to solve the issue is to program the heat pump to only produce the heat that is in demand at any time. This can be done by adjusting the speed of the compressor, making it run on part load. The heat demand is estimated based on the outside air temperature, and the ratio of heat demand to maximum heat capacity can be used to adjust the mass flow rate of the refrigerant, which is decided by the compressor speed.

A problem with this is the misalignment between available power and maximum heat demand. Because the power is only produced during the day when the sun is up, the highest power supply is in the middle of the day. However, the highest heat demand is when the sun is down, as temperatures tend to be lower at night than during the day. This issue is slightly corrected using batteries that store the electrical energy, so that power is also available at times when the PV panels produce little or no power. However, during colder periods, when temperatures are low over several hours and even days, the heat demand will be high over a large period of time. This may lead to power demands exceeding the available power. However, the thermal storage can reduce this drawback, so it remains a viable option provided the heat demand does not exceed the heat capacity of the heat pump.

Another way to approach the problem is to focus on the thermal storage. If the goal is to always have a full thermal storage system, it is likely that the heat demand will be met for most time steps. However, this will lead to the heat pump turning off and on every other hour or operating on part load. The literature review suggested that intermittent operation with short cycles is inefficient due to the increased power consumption during shutdown and restart. Furthermore, the power supply varies greatly with variations in solar irradiation and battery capacity, so there is no guarantee that there will always be enough power to keep the thermal storage at full capacity.

To prevent the heat pump from running on part load as much as possible, and at the same time prevent it from producing heat that will not be used, a third option is available. The heat pump can be programmed to run on full load whenever there is enough power available if the thermal storage system has not reached full capacity. If the demand is low, the heat pump will produce heat that goes directly to the district heating system, but also heat that recharges the thermal storage. The heat pump will operate with full load until the thermal storage system is full. The heat pump will then turn off, and for the next few hours, the heat will be taken from the storage and the heat pump will be turned off. When there is not enough heat left in the storage to cover the demand, the heat pump is turned back on until the thermal storage is once again filled. This way, the heat pump will run on par load as little as possible, and while it will be turned on and off, this will only happen once every few hours.

3.3.2 Algorithm

In this chapter, the algorithm will be briefly explained before the simulation results are presented in chapter 4. The code starts by importing weather data from Excel and pre-allocating variables that will be calculated in the 8759 iterations. After pre-allocating arrays for the variables, the for-loop begins. Inside the for-loop, the combined code for all components runs for every hourly iteration. The code can be found in 0. The same code is used for all three cities.

Firstly, the power generated by the PV panels is calculated based on the global horizontal radiation and the outside air temperature. Secondly, the heat demand is calculated based on the outside air temperature. Once the demand and available power are calculated, the heat pump loop begins. The heat pump loop is a while-loop that calculates the temperatures in the heat exchangers through several iterations, until the old and new values of condensing temperatures deviate with less than 0.1 K.

The temperatures of the water entering the evaporator and LT condenser are assumed to be constant through every iteration. Initial values for the evaporation and condensation temperatures are guessed in the first iteration, and in the following iterations the initial evaporation and condensation temperatures are set to be the same as the evaporation and condensation temperatures of the previous iteration.

These values are used to calculate the evaporation and condensation pressures, as well as the state properties at all points in the process as seen in Figure 18. The isentropic and volumetric efficiencies of the compressors are important when calculating the state properties. These efficiencies are always dependent on the pressure ratio, but the way in which they are calculated varies depending on the compressor. No specific compressor was selected for this project, so equations from another project was used (Eikevik, 2019). The equations are based on a real case, and the values are therefore realistic.

Equation 22: Isentropic efficiency of the compressors

$$\eta_{is} = -0.00000461 \times \prod^6 + 0.00027131 \times \prod^5 - 0.00628605 \times \prod^4 + 0.07370258 \times \prod^3 - 0.46054399 \times \prod^2 + 1.40653347 \times \prod - 0.87811477$$

Equation 23: Volumetric efficiency of the compressors

$$\eta_{vol} = 0.0011 \times \prod^2 - 0.0487 \times \prod + 0.9979$$

Equation 22 and Equation 23 are used to calculate the isentropic and volumetric efficiencies of both compressors. $\prod$ is the pressure ratio, which is the ratio of the condenser pressure to the evaporator pressure.

Once the state properties are calculated, the properties in the heat exchangers are evaluated. The outlet temperatures of the water being heated by the condensers and cooled by the evaporators are calculated based on the capacities of the heat exchangers (see Equation 11 and Equation 16). The logarithmic mean temperature difference and the outlet temperature of the water are used to calculate new values of the condensation temperature of each condenser and the evaporation temperature of the evaporator. This is done by slightly modifying some of the equations in chapter 2.1.6.2.

First, the LMTD of the condensers and the evaporator are calculated using Equation 12 and Equation 17. Then, the other equations for LMTD are modified so that condensing and evaporating temperatures can be calculated. To calculate the new value for the

condensing temperature, Equation 8, Equation 9, and Equation 10 are modified to the following equation:

Equation 24: New value for condensing temperature

$$T_c = \frac{T_{cw,out} \times e^{\frac{T_{hw,out} - T_{hw,in}}{LMTD_{cond.}}} - T_{cw,in}}{1 - e^{\frac{T_{hw,out} - T_{hw,in}}{LMTD_{cond.}}}}$$

Similarly, Equation 17, Equation 13, and Equation 14 are modified to find the new value for evaporating temperature:

Equation 25: New value for evaporating temperature

$$T_e = \frac{T_{cw,out} - T_{hw,out} \times e^{\frac{T_{hw,out} - T_{hw,in}}{LMTD_{cond.}}}}{e^{\frac{T_{hw,out} - T_{hw,in}}{LMTD_{cond.}}} - 1}$$

Once the new values for the temperatures in the heat exchangers are calculated, the initial values for the next while-loop iteration are calculated. The difference between the initial heat exchanger temperatures and the new heat exchanger temperatures is divided by 2 and then subtracted from the initial values. This makes up the new values for condensation and evaporating temperatures. If the values of the new and old evaporation or condensation temperatures deviate with more than 0.1 K, the calculations are redone with the new values for evaporation and condensation temperatures as the guessed values. This process is repeated until the two temperatures deviate with less than 0.1 K. The values of the last iteration are used in the remaining calculations.

When the heat pump loop is finished, the system has realistic values for the heat pump. The power requirement is compared to the available power from the PV panels and the battery. If the power consumption of the heat pump is lower than the amount of available power, it will run on the conditions found in the heat pump loop. If the PV panels produce more power than the amount consumed by the compressor in any hourly iteration, the remaining power is stored in the battery.

If the power consumption of the heat pump is higher than the available power, the compressor will run on part load. The ratio of heat demand to maximum heating capacity will be calculated, and the speed of the compressor will be reduced so that the heat pump only produces enough heat to cover the demand. In those cases, the heat pump operates on part load.

If the power consumption of the heat pump is still higher than the available power, the load ratio will be further reduced. The load ratio will be reduced by 20%, and the power consumption will once again be compared to the available power. The load ratio is reduced by another 20% until the power consumption is low enough, or until the load ratio is below 20%. In those cases, the heat pump will be shut off completely.

Once the correct operation of the heat pump has been calculated and the power consumption is lower than the available power, the code will calculate how much of the heat that will be sent to the district heating system, and how much that will be sent to thermal energy storage. If the thermal energy storage has reached maximum capacity,

the heat pump will be shut off and the thermal storage will provide the heat for the next hours. The heat pump will be shut off until the thermal storage no longer has the capacity to cover the heat demand. The heat pump will then be turned back on until the thermal storage has once again reached maximum capacity.

If the heat pump is shut off in one iteration, the values for condensation and evaporating temperatures will be set to equal the condensation and evaporating temperatures from the previous iteration. This is done to ensure that the next iteration when the heat pump is turned on will have realistic initial values for temperatures.

4 Results

4.1 Yearly results

In this chapter, selected results from the simulations will be presented. First, results from the whole year will be presented. However, due to the large number of iterations (8759), some of the results can be difficult to interpret if the entire year is studied. Therefore, results from specific months and weeks will be presented as well. Results from winter months, summer months, and spring/autumn months will be presented separately to evaluate different times of year. Some of the graphs and tables presented will only include results from one city, but in those cases the results are representative for all three cities unless otherwise specified.

4.1.1 Temperature and radiation

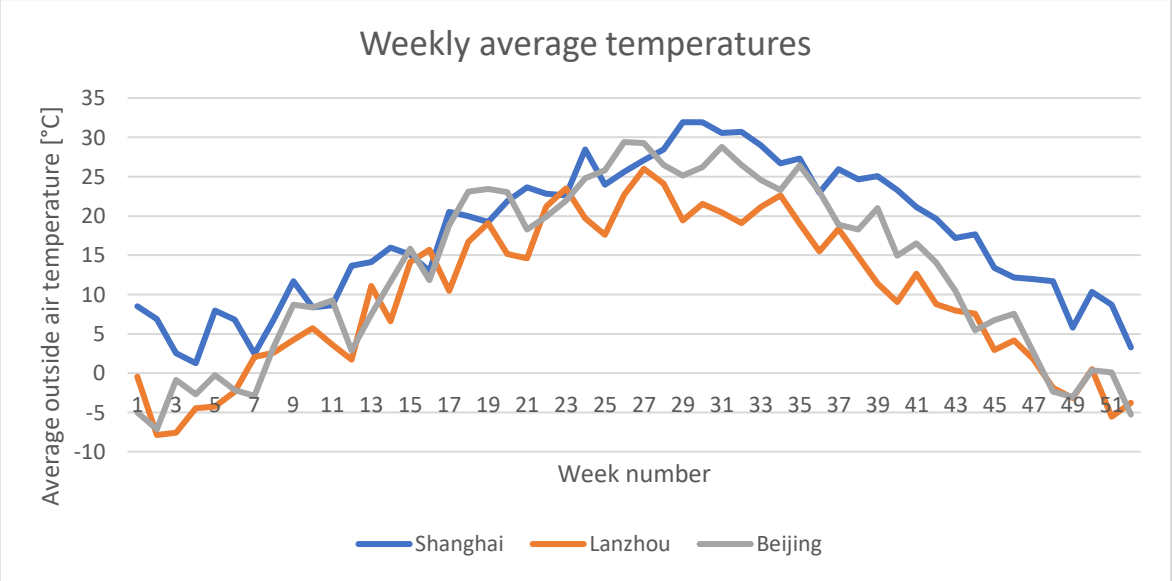

Figure 20: Average outside air temperatures in Shanghai, Lanzhou, and Beijing

Figure 20 shows the weekly average temperatures of Shanghai, Lanzhou, and Beijing in 2005. It is worth noting that this graph shows the weekly average, and that the hourly temperatures can become lower and higher than displayed here. The hourly temperatures reach lows of -4.5 °C in Shanghai, -16.7°C in Lanzhou, and -13.9°C in Beijing.

It should further be noted that the values for temperature and solar radiation are values for a specific year (2005). Because temperature and radiation vary from year to year, the numbers may not be accurate for 2020 or the following years. However, yearly temperatures follow trends and the average temperatures in each month rarely vary with more than two degrees (Michaels et al., 1998). Therefore, the values are assumed to be representative for the simulation at this point in the project.

Because all cities experience winter and summer months throughout the year, their yearly temperature and demand curves have similar shapes. This implies that the trend of how the integrated energy system operates should be similar for all three cities. However, Lanzhou and Beijing experience vastly lower temperatures than Shanghai during the winter months. They also experience longer periods of colder temperatures than Shanghai.

Of the three cities, Shanghai has the highest temperatures. The winters in Shanghai are warm compared to the other cities, and the outside air temperature in Shanghai rarely drops below 0°C. Shanghai has very hot summers, but because there is no cooling in the system in this report, the days with low temperatures and a higher heat demand will be in focus. Lanzhou has the lowest temperatures, with very cold winters and varying temperatures during the summer. Beijing is somewhere between the two cities. Beijing experiences very cold winters, like Lanzhou, but the summers are hot with temperatures close to those in Shanghai.

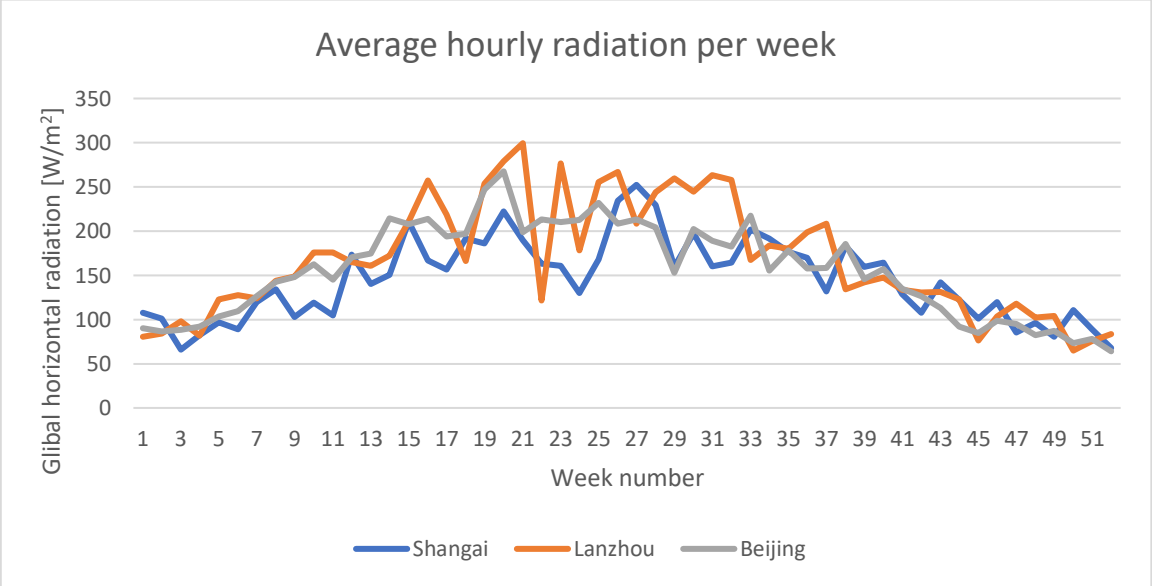

Figure 21: Average hourly radiation per week in Shanghai, Lanzhou, and Beijing

The graph in Figure 21 shows the average hourly solar radiation every week throughout the year in Shanghai, Lanzhou, and Beijing. The weekly averages are calculated using data from every time step, including the hours when the sun has set and the solar radiation is zero. As a result, the average values are much lower than the peak values the cities see during the day. However, this is a relevant representation because the system is simulated for every hour throughout the year. The hourly average will therefore give a representative picture of how much power that can be available every hourly time step.

Again, it should be noted that the values are from the year 2005 and will vary from year to year, especially because weather and cloud coverage have such a significant effect on the values. Consequently, the values for solar radiation vary more from day to day than the values for outside air temperature. The variations between the years may also be greater. Another factor that affects the level of solar radiation is local air pollution (Zhang et al., 2020). The data was collected in 2005, and local air quality has significantly improved in cities across China in the last fifteen years (Zheng et al., 2015). However, this cannot be given significant meaning, especially when the variations are already so

high, and the numbers are more affected by weather than local air pollution. It is assumed that the values from 2005 are representative for 2020 and the following years.

The solar radiation also follows a similar curve for all three cities. It seems that Lanzhou has the least stable values during the summer months, while Shanghai has the least stable values during the winter months. In total, Lanzhou experiences the highest amount of solar irradiation.

4.1.2 Heat pump performance

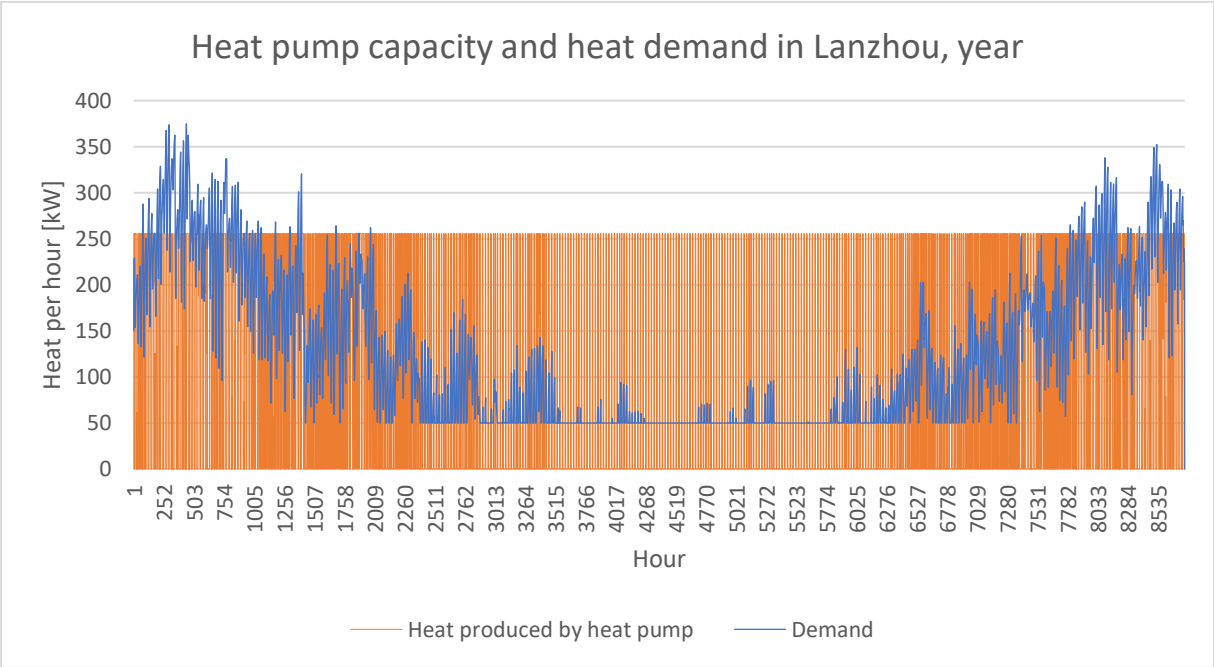

Figure 22: Heat produced by heat pump and heat demand in Lanzhou

Figure 22 shows the hourly heat demand as well as heat produced by the heat pump throughout the entire year in Lnazhou. It is clear that the heat demand greatly exceeds the heat pump capacity in certain hours. However, because of the large number of datapoints the results are difficult to interpret. Please see chapter 4.2 for more data about the winter months.

It is clear that the heat pump mostly operates on maximum capacity when it is not shut off. The heat pump also operates on part load a few hours throughout the year. The maximum capacity of the heat pump is 255.7 kW.

	Number of operating hours heat pump	Percetage of time when heat pump was turned on [%]	Number of operating hours when demand exceeds supply	Percentage of time with insufficient heat [%]	Total amount of insufficient heat [kWh]
SH January	397	53.14	103	13.79	17 863
LZ January	424	56.76	353	47.26	82 112
BJ January	445	59.57	295	39.49	67 731
SH April	194	26.84	0	0	0
LZ April	285	39.64	9	1.25	874
BJ April	227	31.57	1	0.14	82
SH July	162	21.80	0	0	0
LZ July	162	21.80	0	0	0
BJ July	161	21.67	0	0	0
SH year	2757	31.47	283	3.23	44 795
LZ year	3569	40.75	1090	12.4	236 130
BJ year	3351	38.26	856	9.8	187 534

Table 4: Operating hours and supply shortages for selected time periods

Table 4 is a collection of data that describes heat supply and demand for selected time periods. January is colored blue, April is colored green, and July is colored pink to better distinguish between the time periods. The three bottom rows show data for the whole year.

It is interesting to note that the heat pump operates in less than half of the time steps. This means that the heat pump is turned off for more than half of the year. This is true for all three cities, although there is a significant difference between Shanghai and the other two cities. Furthermore, there are many time steps when the heat supply is not high enough to cover the heat demand. The heat supply includes the supply from both the heat pump and the thermal energy storage. The demand exceeds the supply in close to half of the hourly time steps in Lanzhou in January. The number is much lower for Shanghai, where the temperatures are higher in January. The yearly values are much lower than the values for the winter, but the total difference between supply and demand in Lanzhou is 236 130 kWh for the whole year. This is quite a high number.

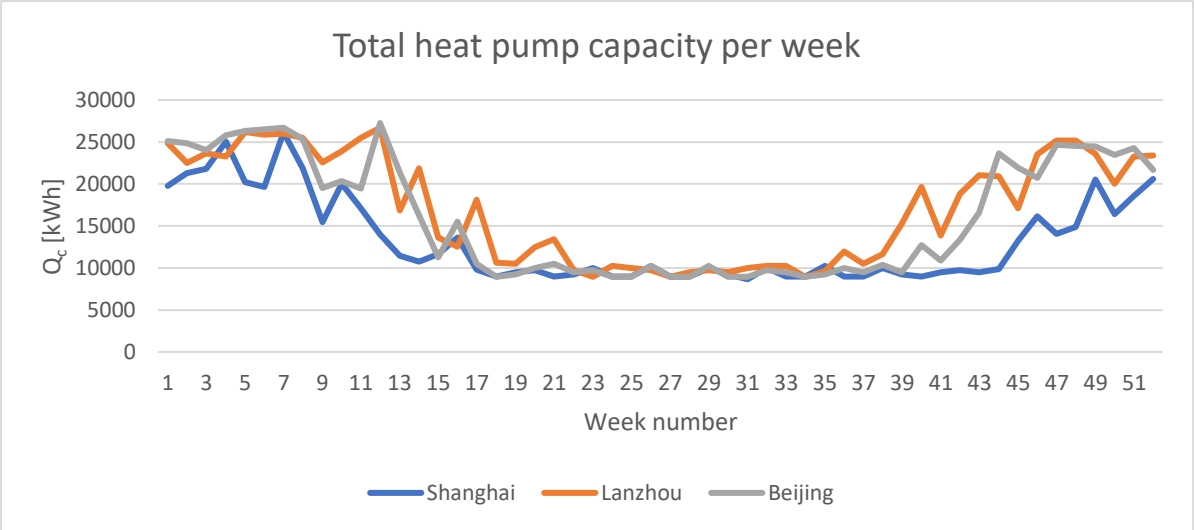

Figure 23: Total heat produced by the heat pump every week in Shanghai, Lanzhou, and Beijing

Figure 23 shows the total heat produced by the heat pump every week. The trends are similar for all three cities, and as expected they are higher in the winter months than the summer months. Whereas the systems produce similar amounts of heat for Beijing and Lanzhou, the values are much lower for Shanghai during the winter weeks. The values for the summer are similar for all three cities.

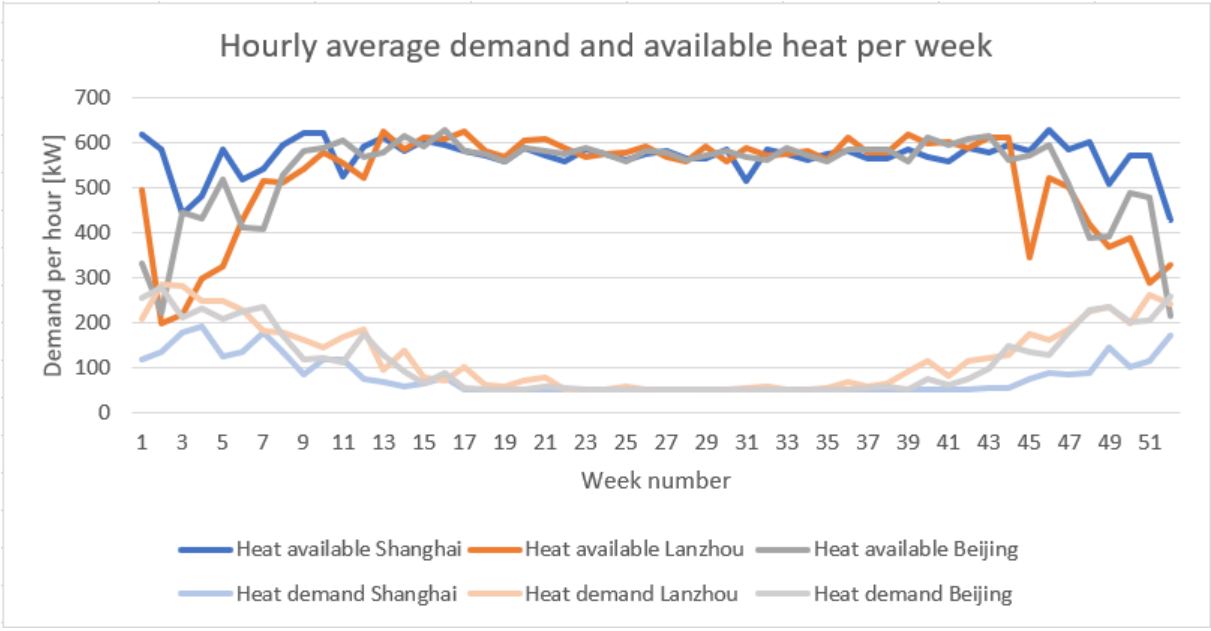

Figure 24: Hourly demand and available heat from heat pump and TES in Shanghai, Lanzhou, and Beijing

The graph in Figure 24 shows the average hourly demand and the average amount of heat available from the heat pump and the thermal storage system combined for every week of the year. It is clear that the heat pump and thermal storage system cover the demand most weeks, however in January and December the demand sometimes exceeds the available heat. As expected, due to temperature variations between the three cities, the heat demand is higher in Beijing and Lanzhou than in Shanghai. It is also interesting to compare the demand curves with the graph showing heat capacity. The heat produced

by the heat pump normally increases when the demand increases, as expected. However, the curves differ slightly, especially in the very beginning of the year. This is likely due to a lack of sufficient power, which means that the heat pump cannot operate despite high demand.

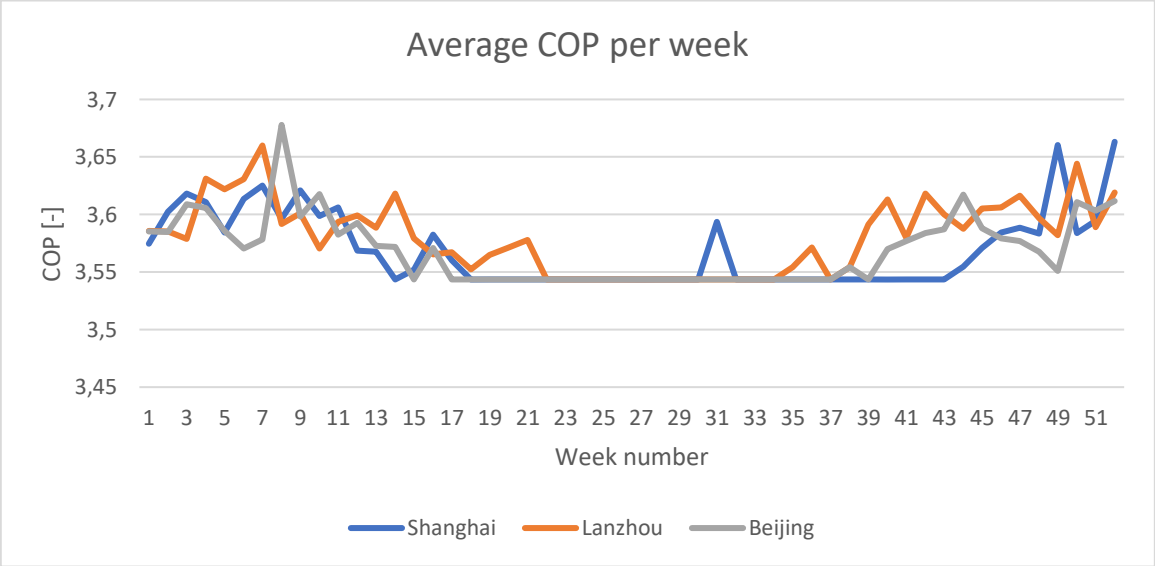

Figure 25: Average COP per week in Shanghai, Lanzhou, and Beijing

Figure 25 shows the average COP per week. The COP is zero when the heat pump is turned off, but to better be able to interpret the data, the COP is set to be equal to the heat pump COP at full load when the heat pump is turned off. The COP is higher during the winter months than in the summer months. However, the average values vary with less than 0.2%.

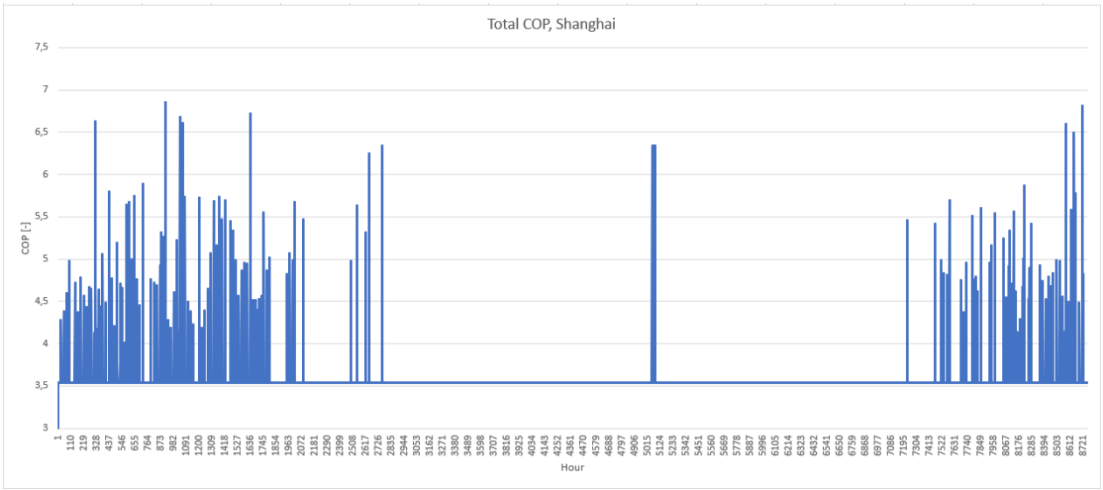

Figure 26: Hourly COP in Shanghai

Figure 26, on the other hand, shows that the hourly COP values vary greatly, and values get as high as 6.68. This only happens in a few time steps, but the results will be further evaluated in the discussion.

The COP is a good measure of the energy efficiency of the heat pump. However, it does not describe the efficiency of the system. The total heating efficiency of the integrated energy system can be found by looking at the relation between the heat delivered to the

district heating system and the power used to produce the heat. In Table 5, the COP and system efficiency are listed together with the total heat production, the total amount of heat delivered to the district heating system, and the total annual power consumption of the compressor.

	Total annual heat production by heat pump [kWh]	Total annual compressor power consumption [kWh]	Total annual heat supplied to the residents [kWh]	Annual COP for the heat pump	Annual system heat efficiency
Shanghai	689 004	192 756	651 021	3.574	3.377
Lanzhou	889 629	248 727	863 523	3.577	3.472
Beijing	840 756	235 513	809 871	3.570	3.439

Table 5: Annual values for COP and system efficiency

The values for heat delivered to the residents are lower than the value of heat produced. This is because of losses in the thermal energy storage system. The system efficiency is lower than the heating COP of the heat pump in all three cities.

In the following chapters, more detailed results of shorter periods of time will be presented. Results for specific months, weeks, and days will be presented to better understand how the heat pump works under different conditions. The results will be divided into three categories: Winter, summer, and spring/autumn. Representative data from each time of year will be selected and presented for each city.

4.2 Winter

Data for January will be presented in this chapter, as January is representative for the winter months January, February, and December. February and December show similar results for January for all three cities.

4.2.1 Heat supply and demand

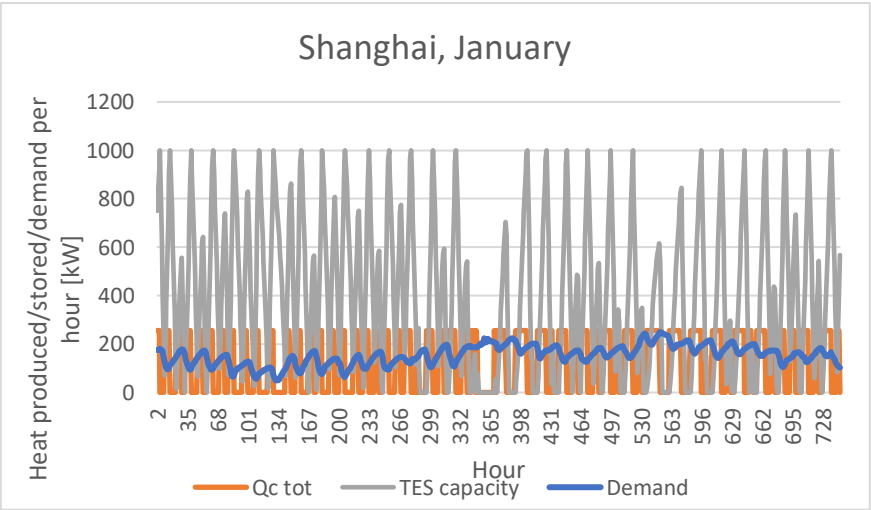

Figure 27: Heat production, thermal energy storage, and heat demand for every hour in January

Figure 27 shows the demand, heat production, and thermal energy storage capacity for every hour in January. The demand stays below the maximum capacity of 255.7 kW for every hourly iteration. The thermal storage capacity reaches the limit of 1000 kWh several times, followed by a shut-down of the heat pump and a heat pump capacity of 0 for the next hours. However, the limit of the thermal storage capacity is not always reached before the heat pump shuts down.

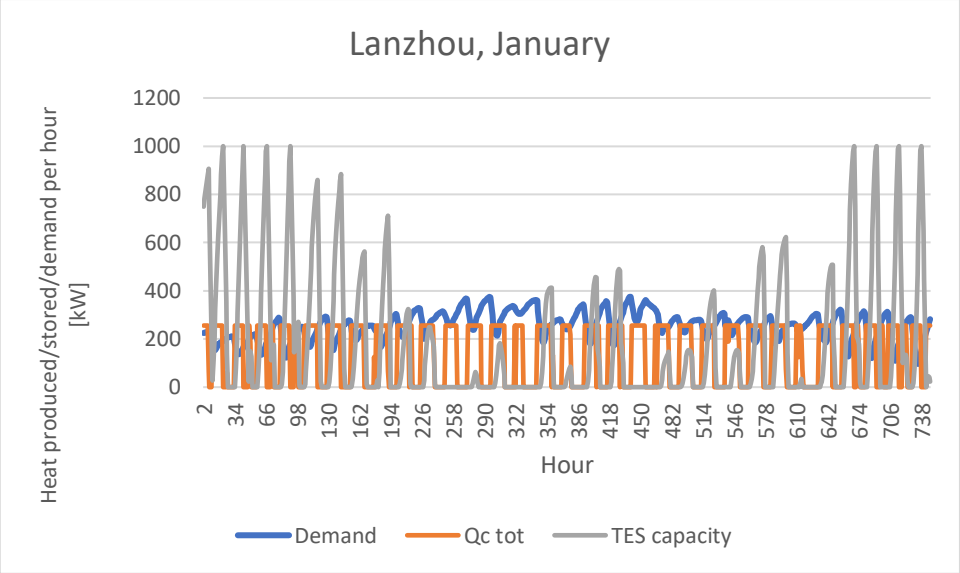

Figure 28: Heat production, thermal energy storage, and heat demand for every hour in January

Figure 28 shows the demand, heat production, and available heat in Lanzhou in January. There is a clear difference in available heat between Shanghai and Lanzhou. Out of 29 recharging cycles, maximum storage capacity is only reached 8 times. The heat demand is quite high throughout the month and reaches values of close to 400 kW certain hours. The thermal storage capacity is very low in the middle weeks of January, and in the same period the demand often exceeds the maximum capacity of the heat pump.

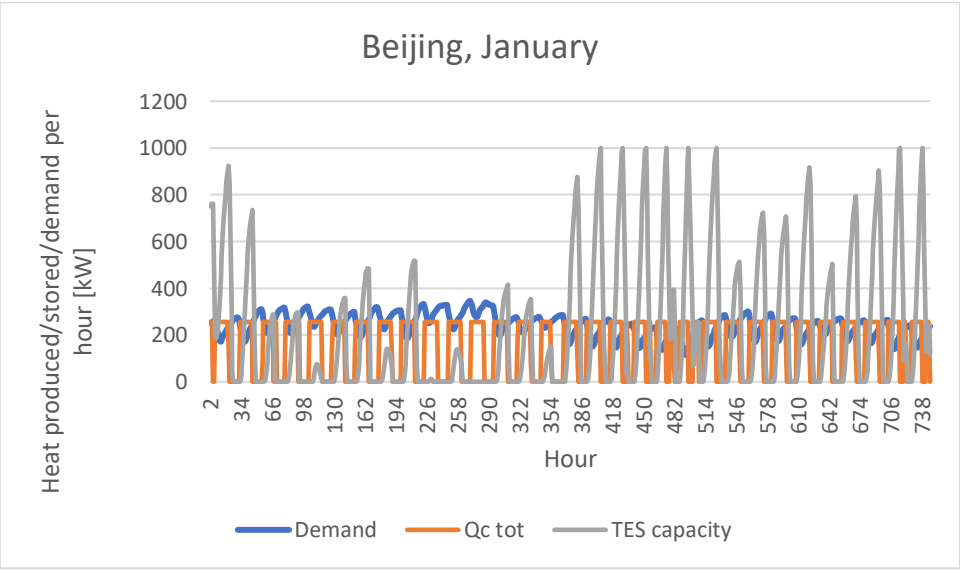

Figure 29: Heat production, thermal energy storage, and heat demand for every hour in January

Figure 29 shows the same as the two pervious figures, but with results from Beijing. The results are quite similar, although Beijing experiences a surge in heat supply earlier in the month than Lanzhou. At the end of the month, the results are closer to the results from Shanghai. Because the graphs are so similar, the weekly results will only be presented from one city. If comparisons are to be made, the results from Shanghai and Lanzhou will be compared without the results from Beijing. This is because Beijing has similar results to the other two cities, so including the results would not provide much added value. The results from Beijing can be found in 104Appendix B:.

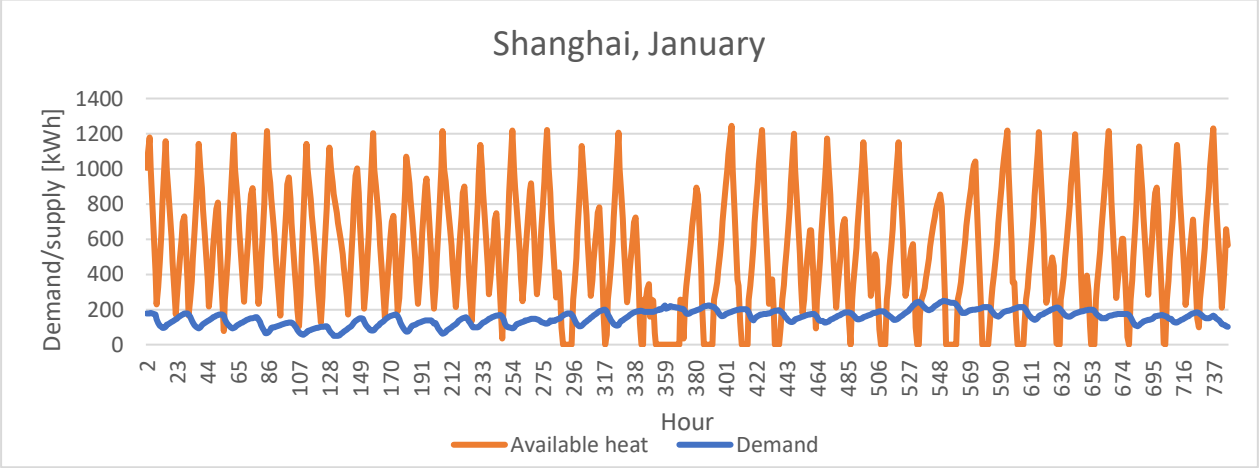

Figure 30: Available heat and heat demand in Shanghai in January

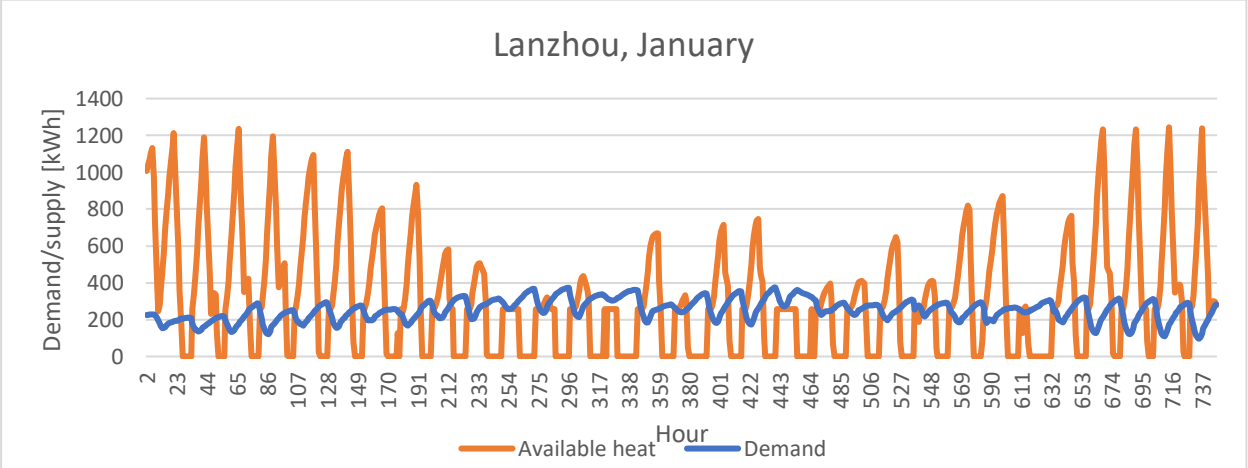

Figure 31: Available heat and heat demand in Lanzhou in January

Figure 30 and Figure 31 show demand and available heat for January in Shanghai and Lanzhou. The heat available in a certain hour is the combined value of the thermal storage capacity and the heat produced by the heat pump in that specific time step. In Shanghai, the demand is normally lower than the available heat, but there are a few exceptions where the demand exceeds the available heat. In Lanzhou on the other hand, demand often exceeds supply. In fact, Table 4 shows that demand exceeds supply as much as 47.26% of the hours during January in Lanzhou, while it only happens 13.79% of the time in Shanghai.

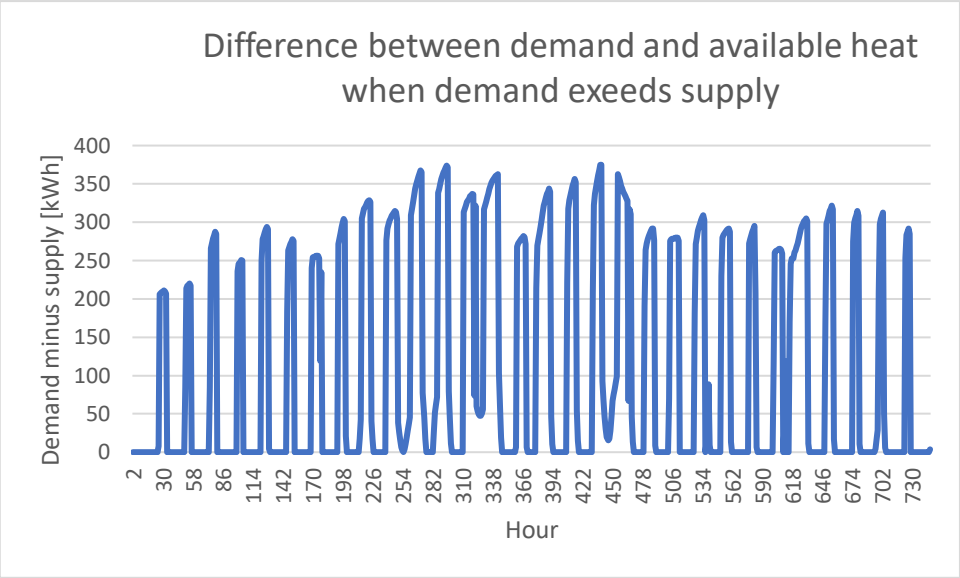

Figure 32: Difference between heat demand and heat supply in time steps when not enough heat is available to meet demand. Lanzhou, January

The graph in Figure 32 displays the demand and available heat (TES + Q_c) in Lanzhou in January. The demand exceeds the available heat 353 times throughout the month, and in certain periods over more than 24 hours. The longest period where the available heat does not meet the demand is a period of 40 hours, between time step 431 and time step 471. Another thing to note is that the difference between supply and demand is usually quite high, sometimes above 350 kWh. In total, 82 112 kWh of demand are not covered in Lanzhou in January. See Table 4 for more data on this for all three cities.

4.2.2 Available power

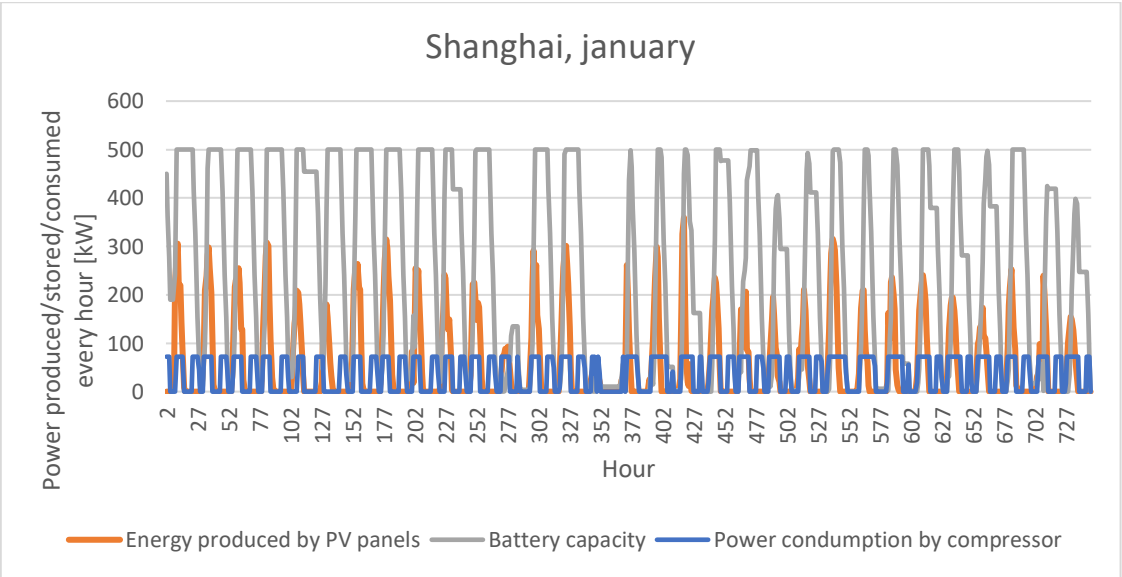

Figure 33: Power production and consumption in Shanghai in January

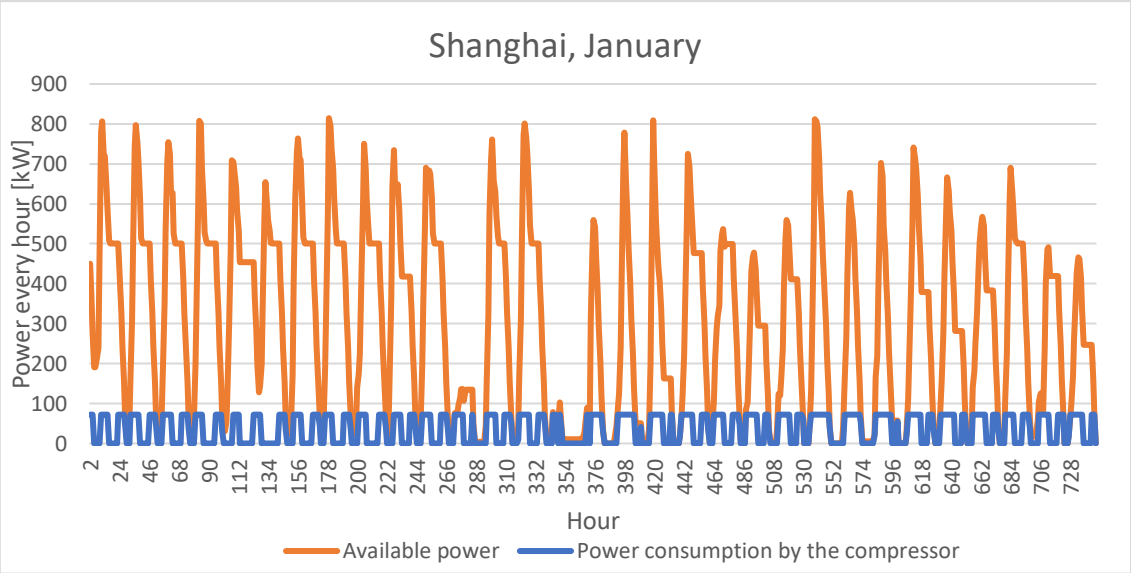

Figure 34: Available power and power consumption by the compressor in Shanghai in January

Figure 33 and Figure 34 show the power produced by the PV panels, stored by the batteries, and consumed by the compressor every hour in January. The power production varies greatly and is noticeably equal to zero for approximately half the day because no power is produced when the sun is down. Furthermore, the amount of power produced varies throughout the month due to varying weather conditions. It is clear that power consumption is never larger than the amount of available power, which suggests that the heat pump shuts off when not enough power is available. This is expected.

Another thing to note is that the battery capacity reaches the maximum capacity of 500 kWh several times throughout the month. This is true for all three cities. When the battery capacity is reached, there is no more storage room if more power is produced and not used.

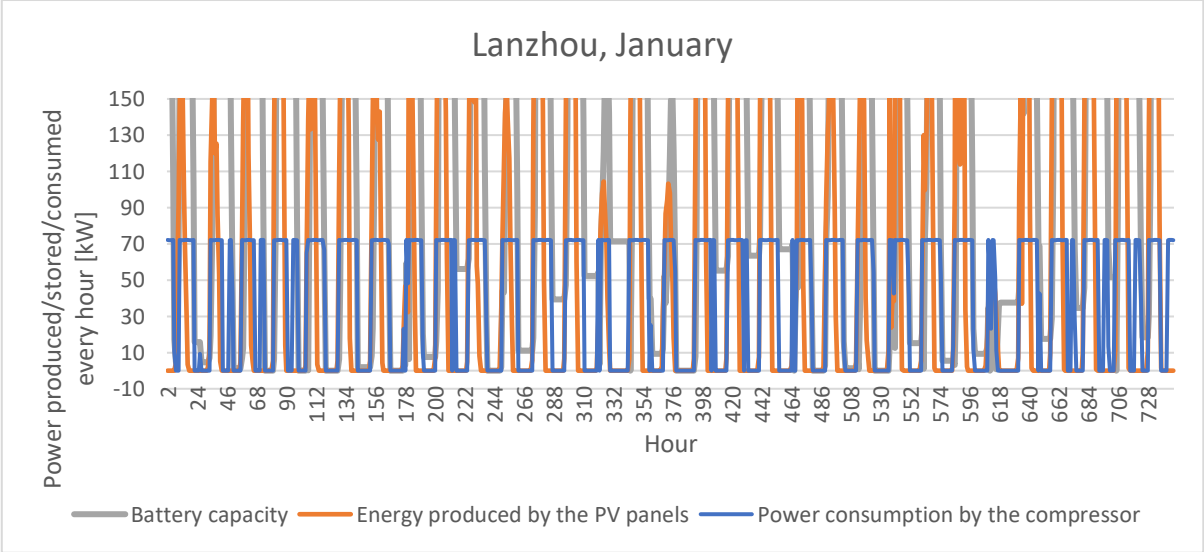

Figure 35: Power consumption and availability in Lanzhou in January. The y axis is cut off at 150 kW to better see the values for the power consumption

Figure 35 displays the same as Figure 33, but for Lanzhou instead of Shanghai. The y axis of the graph is cut off at 150 kW so that the values for power consumption are easier to see. Again, it seems that the values for power consumption never exceed the values for available power, which indicates that the heat pump likely turns off when not enough power is available.

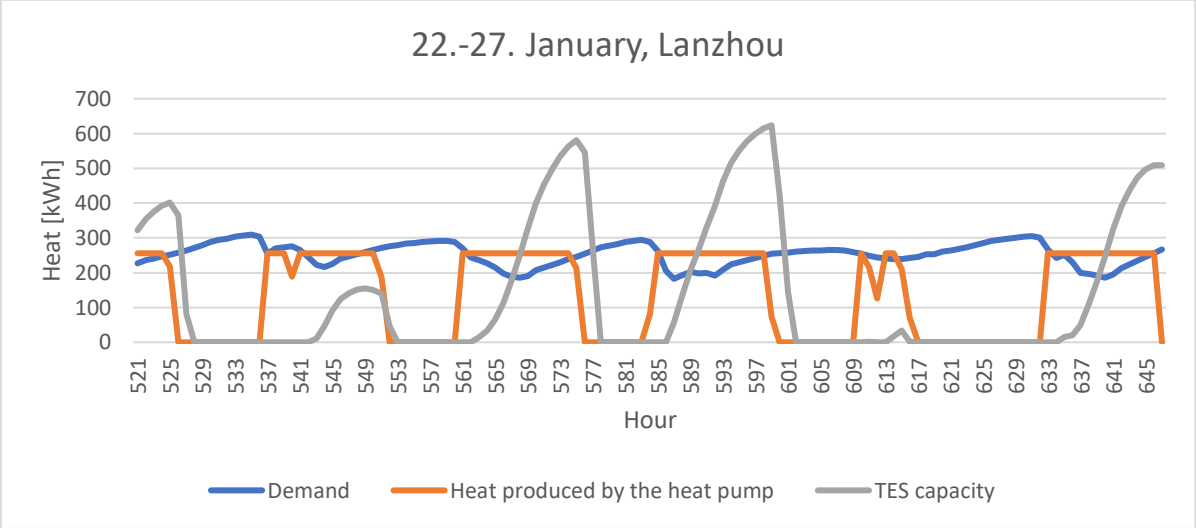

Figure 36: Heat production and demand for five days in January

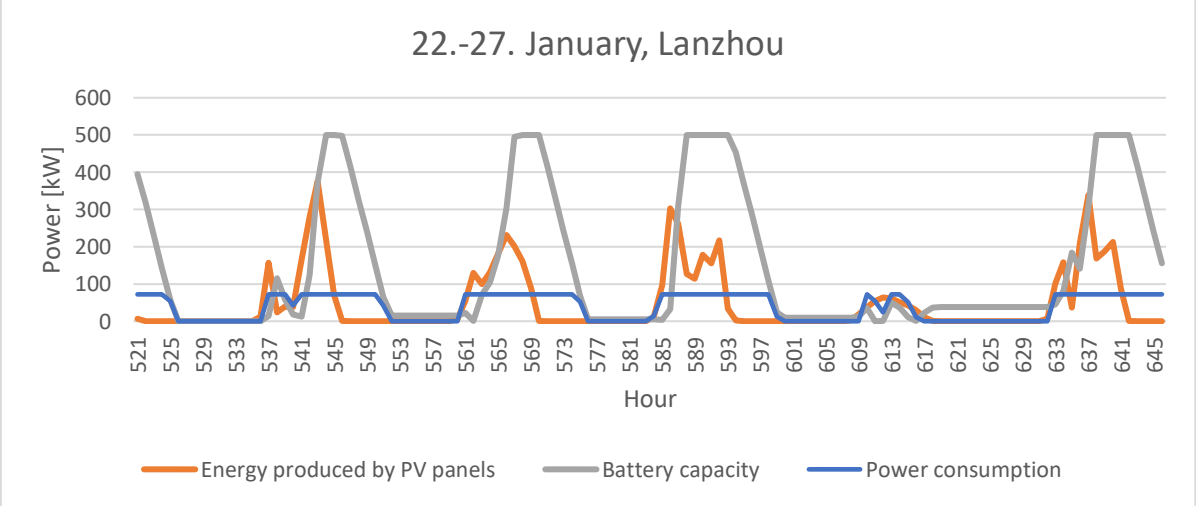

Figure 37: Power production and consumption for five days in January

Figure 36 shows the values for heat demand, heat production and heat storage, and Figure 37 shows the values for power demand, power production and power storage for five days in Lanzhou in the end of January. These days were selected because they include iterations where the heat pump operates on part load. In time steps 525, 540, 551, 584, 599, 612, 615, and 616, the heat capacity of the heat pump is lower than the maximum capacity. The degree to which the system runs on part load varies in the different time steps.

It is interesting to compare the instances with part load operation to the available power. In time step 540, for example, the available power drops below the value needed for maximum capacity, but because more power is produced by the PV panels in time step

541, the heat pump can run on full capacity again rather than shutting off. Consequently, the heat supply is once again high enough to cover the demand in time step 541.

4.2.3 Thermal energy storage

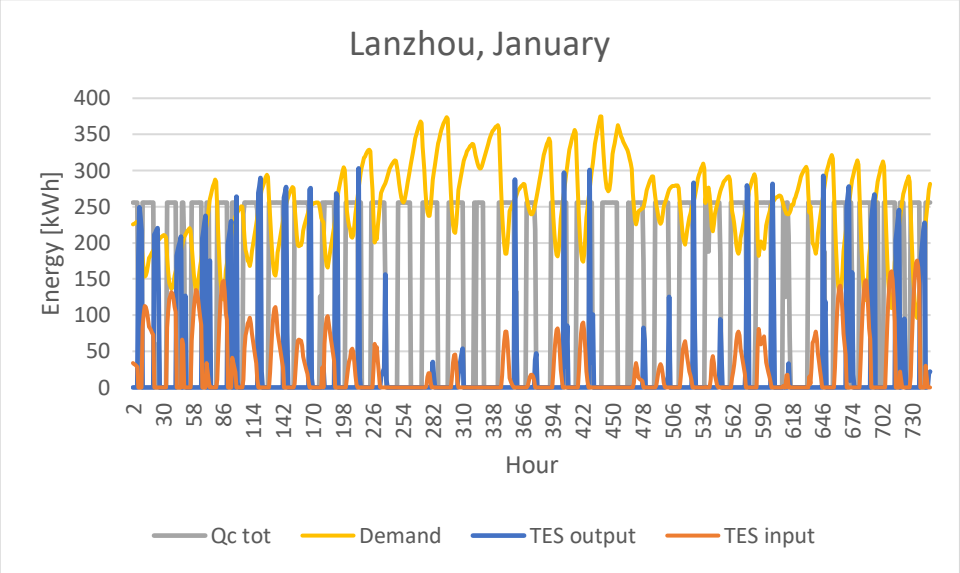

Figure 38: Thermal energy storage in Lanzhou in January

Figure 38 displays the heat production, the input to and output from the thermal energy storage, the heat demand, and the thermal energy storage capacity for January. The thermal energy storage output and input coincide very well with the heat production. This is because heat is added to the thermal storage when excess heat is produced and taken from the storage when the heat pump is turned off or not producing enough heat.

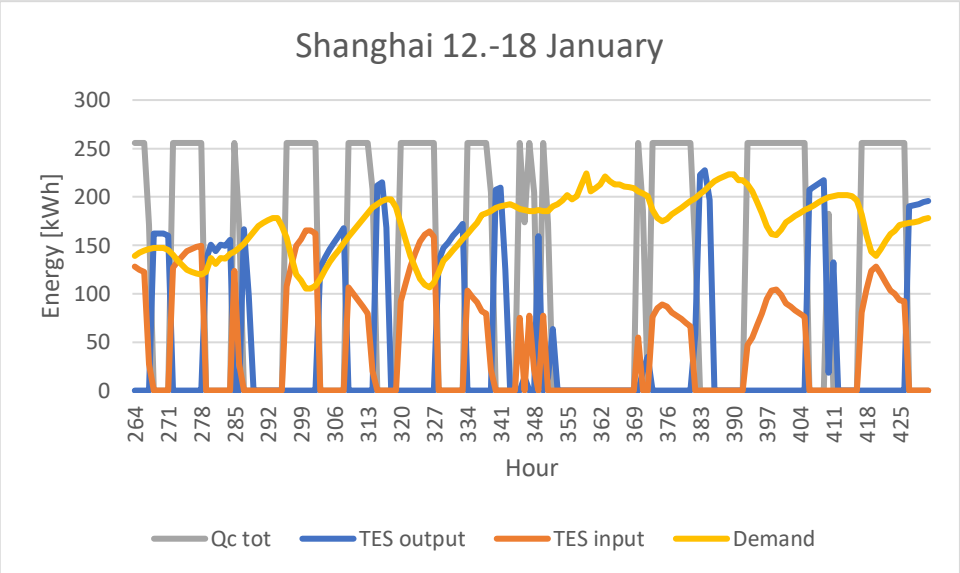

Figure 39: Thermal energy storage in Shanghai between 12.01 and 18.01

Figure 38 shows the same, but for the week between January 12 and January 18 in Shanghai. This image gives a more detailed view of how the thermal storage system behaves. In the beginning of the week, there is sufficient heat to cover the demand. The demand is constantly below the maximum value of the heat pump capacity, and the values for thermal storage input are above 0. When the heat pump is turned off, the

values for heat input to the thermal storage is 0, and the values of heat output are above 0. The values for thermal storage output are slightly higher than the demand. This is to account for the losses during heat transfer that occur because of the 90% efficiency.

4.2.4 Temperatures

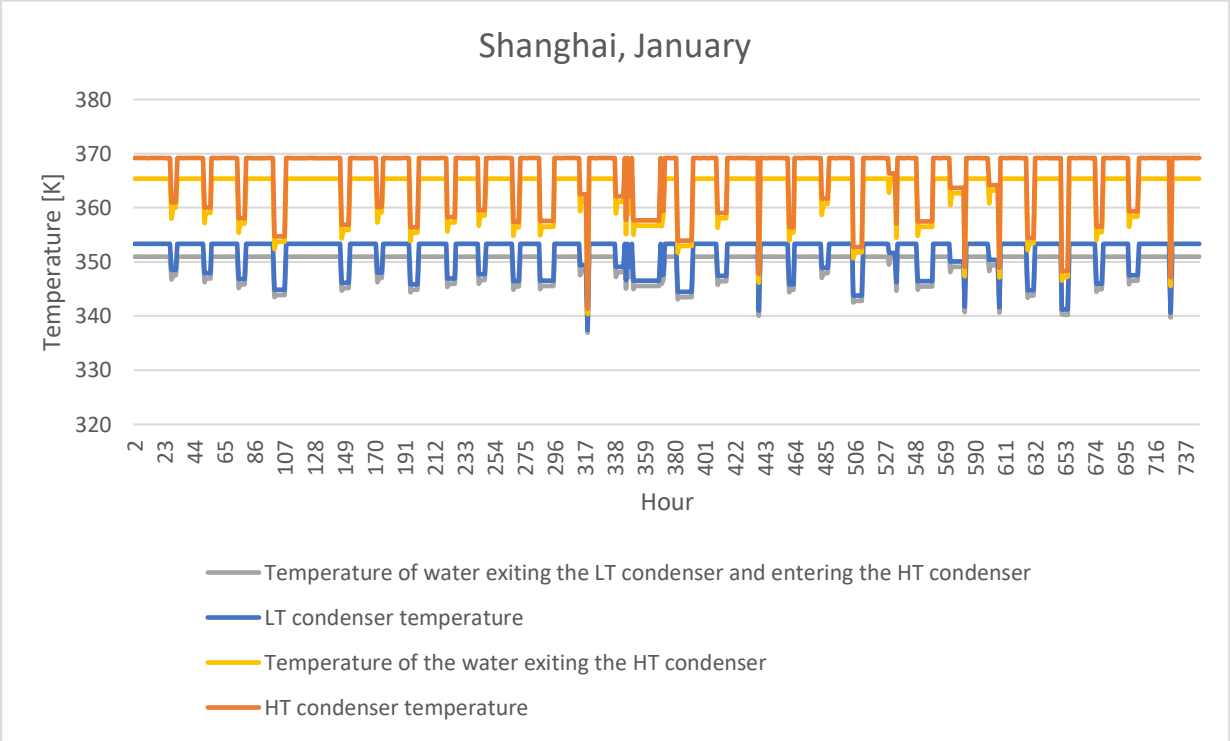

Figure 40: Temperatures in condensers

Figure 40 shows various temperatures in the heat pump throughout January. The red line is the condensation temperature in the high temperature condenser, and the blue line is the condensation temperature in the low temperature condenser. The yellow and grey lines show the temperature of the water heated by the condensers. The grey line shows the water temperature at the outlet of the low temperature condenser and the inlet of the high temperature condenser, while the yellow line shows the temperature at the outlet of the high temperature condenser.

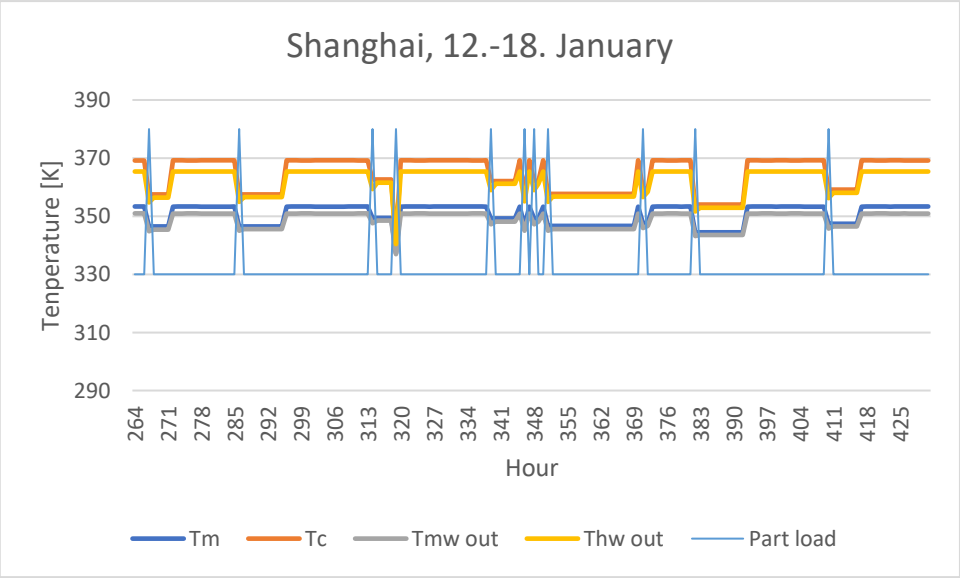

Figure 41: Temperatures in condenser between 12.01 and 18.01

Figure 41 shows the same temperatures, but over the course of the week between January 12 and January 18. This is to better see how the temperatures vary between the time steps. The light blue vertical lines represent the times when the heat pump switches between part load operation and full load operation. When the light blue line is at 330, the heat pump operates on full load. When the line is at 380, it operates on part load. When the heat pump is turned off, the temperatures are set to be the same as in the previous iteration. Therefore, this graph does not illustrate when the heat pump is switched off or on.

The thin blue line was added to illustrate the effect part load operation has on the temperatures in the heat exchangers. The results show that the temperatures are not always the same when the heat pump operates in part load, but that they are always lower than the temperatures when the heat pump functions on full load. The thin blue line does not illustrate the part load ratio, only whether the heat pump operates on part load or not.

The temperature graphs for Lanzhou and Beijing in January are not included because they are very similar to the temperature graph for Shanghai. The difference is that the temperature decreases more often in Beijing and Lanzhou than in Shanghai. However, the percentage of part load operation is higher in Lanzhou and Beijing, and that might be a cause. This is further discussed in chapter 5.

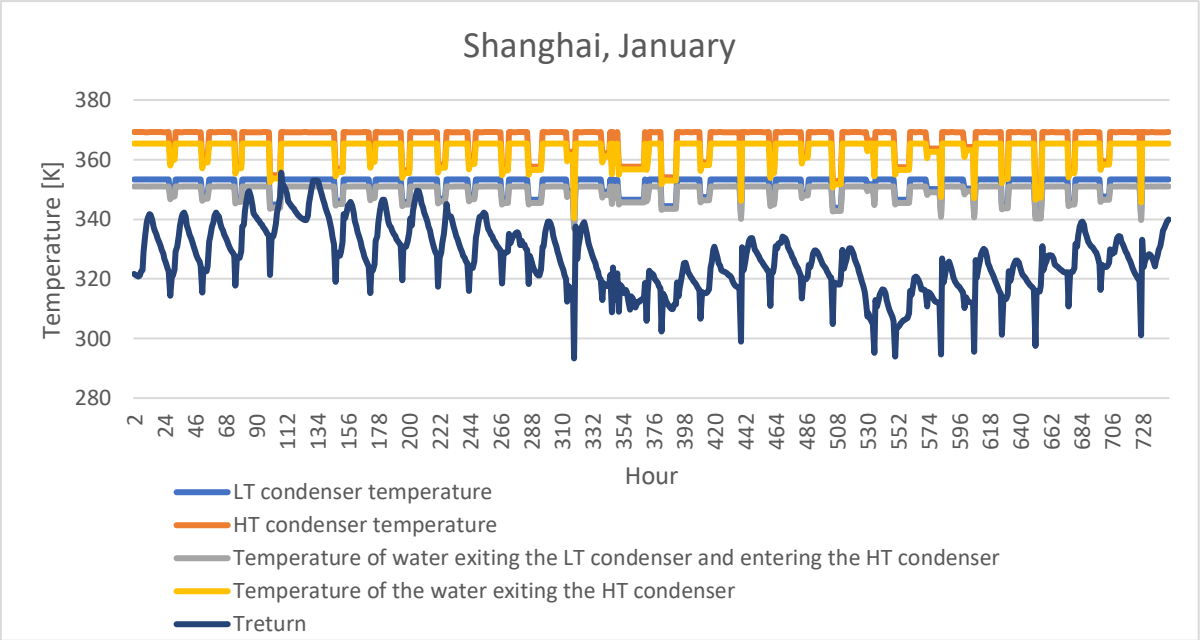

Figure 42: Condenser temperature and return temperature from district heating in Shanghai, January

Figure 42 shows the same as Figure 40, but with the return temperature of the DH water included. The return temperature varies throughout January, with a low of 294 K and a high of 351 K. The return temperature was supposed to equal the water temperature at the LT condenser inlet, however due to the large variations in return temperature this did not work in this code. Instead, the inlet temperature of the water going into the LT condenser was set to 333.15 K (60°C) at all times. In the beginning of the month, the return temperature is slightly above or slightly below this value most times, however the variations are quite large. The variations in return temperature increase even more toward the end of the month.

There is a clear correlation between the dips in condenser temperatures and the dips in return temperature, which is as expected because the temperature of the water at the outlet of the HT condenser is the same as the temperature of the water supplied to the district heating system. It is logical that the return temperatures are lower when the supply temperatures are lower. However, the return temperature varies much more than the condenser temperatures. This might be caused by variations in demand.

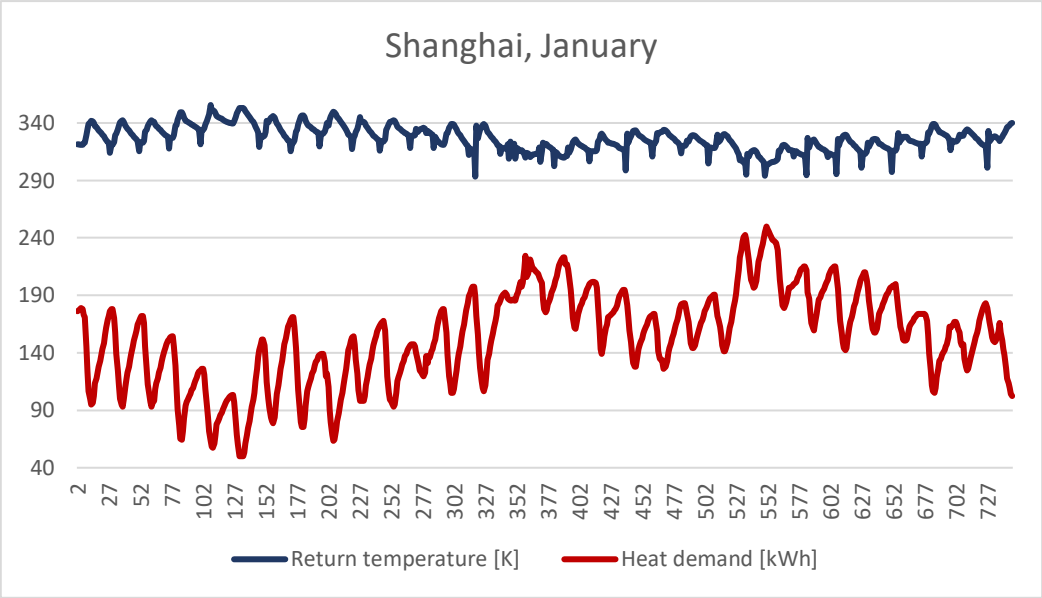

Figure 43: Heat demand and return temperature in Shanghai, January

Figure 43 shows the return temperature in K and the heat demand in kWh for every hour in January. Even though it is difficult to see the details, there is a clear correlation between the two. The return water temperatures are lower when the heat demand is higher, and higher than the heat demand is lower.

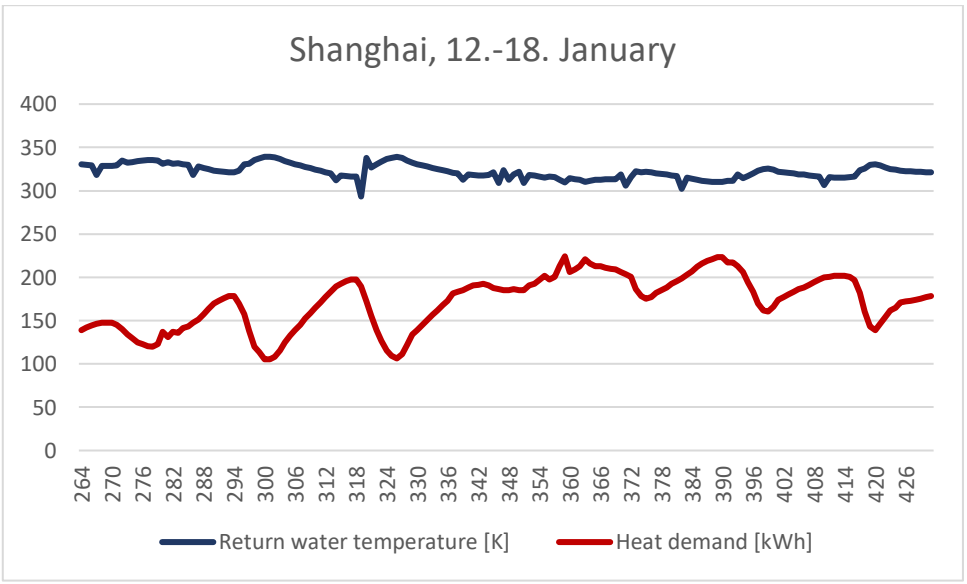

Figure 44: Heat demand and return temperature between January 12 and January 18 in Shanghai, January

This correlation can also be seen in Figure 44, which is more detailed because it shows a shorter time span. The decrease in return water temperature is not completely proportional to the increase in demand, probably due to the variations in condensation temperatures. There is however a clear correlation.

4.2.5 COP

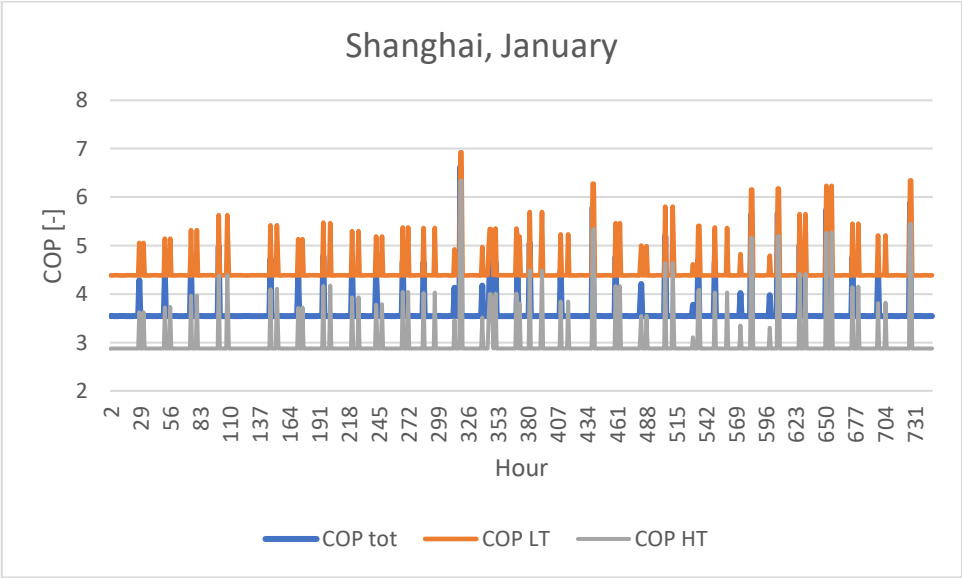

Figure 45: COP for the HT cycle, the LT cycle, and COP for the whole system in Shanghai in January

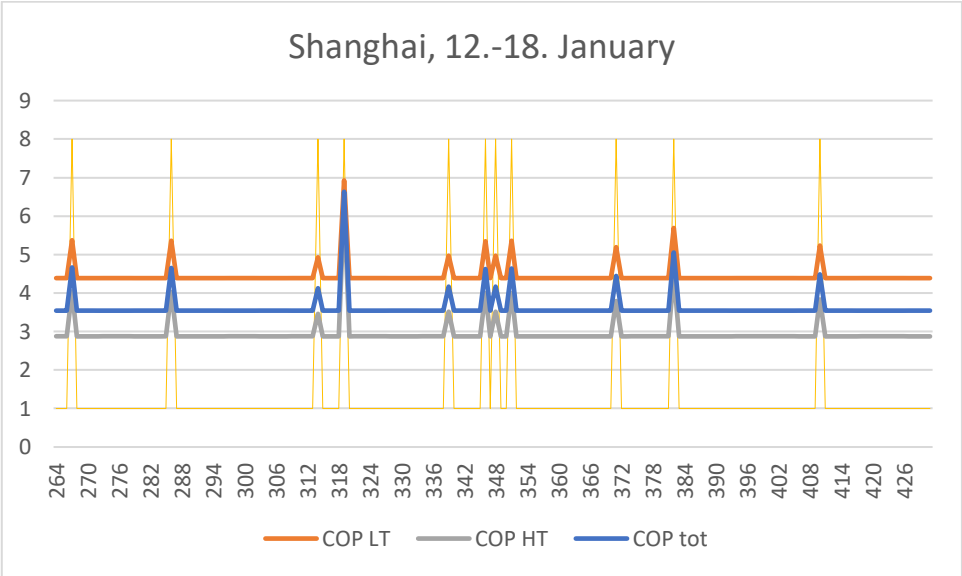

Figure 46: COP for the HT cycle, the LT cycle, and the whole system, as well as indicators of part load operation.

These figures show how the COP varies in January and in the week of 12.-18. January. The total COP normally lies slightly above 3.5, but it sometimes jumps to around 4. In one instance, it jumps to close to 7. Again, the thin yellow line shows when the heat pump operates on part load, and again there seems to be a correlation. The graphs for COP in Lanzhou and Beijing are very similar to those for Shanghai, but with more jumps than Shanghai. It is worth noting that the number of times the heat pump operates on part load is higher in Lanzhou and Beijing.

Hour	5	378	50	360	7	26
Demand	228.35	252.95	207.85	264.23	229.38	17.04
Total heat pump capacity	255.70	218.30	188.44	133.42	67.32	61.01
Load ratio	1.00	0.85	0.74	0.52	0.26	0.24
Total power consumption by the compressors	72.16	54.76	42.84	25.28	10.46	9.31
Available power	276.82	57.18	52.65	39.68	17.04	15.67
LT condenser temperature	353.35	350.28	347.86	343.43	338.24	337.75
HT condenser temperature	369.17	364.01	359.82	352.11	342.80	341.90
Outlet temperature of water heated by the condensers	365.38	360.71	356.97	350.05	341.70	340.90
COP	3.54	3.99	4.40	5.28	6.44	6.55

Table 6: Selected values for various load ratios in Lanzhou in January

Table 6 shows the condenser temperatures, COP, heat pump capacity, power consumption by the compressor, available power, and heat demand for six time steps with different load ratios in Lanzhou in January. The time steps were selected to display a variety of load ratio and the corresponding temperatures and COP. It is clear that the condenser temperatures decrease and that the COP increases with decreasing load ratios.

4.3 Summer

4.3.1 Heat and power

The results for the summer months are almost identical between the three cities, so the results for one city can be used to interpret the operation in the other two cities as well. July is representative for the summer months in all three cities.

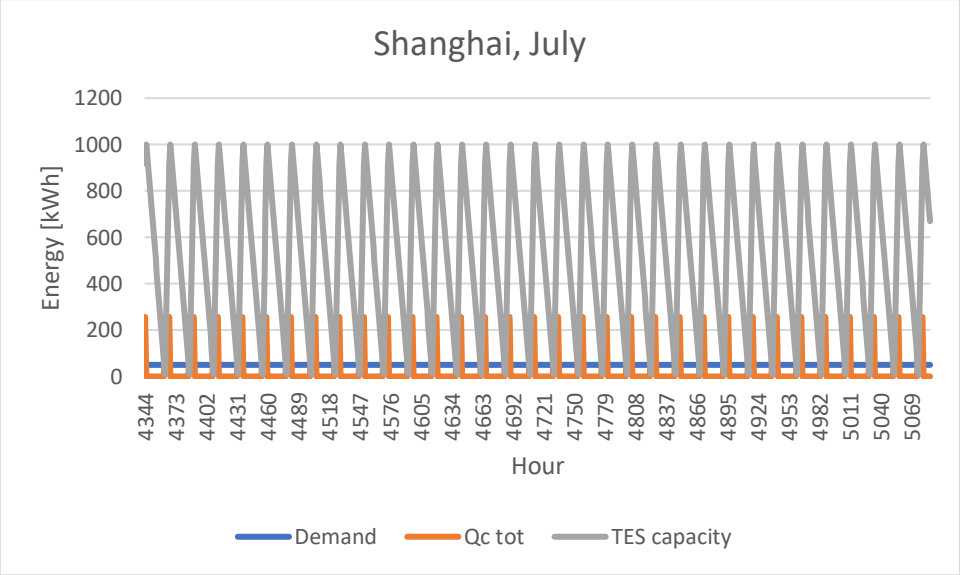

Figure 47: Heat production, storage, and demand in Shanghai in July

The graph in Figure 47: Heat production, storage, and demand in Shanghai in July shows heat demand and available produces and stored heat in Shanghai in July. The temperatures in July are consistently above 15 degrees in Shanghai, so heat demand is

at a stable 50 kW for every hour. There is always sufficient heat available to cover demand. The heat pump functions as expected and works on full capacity until the thermal storage tank is filled up before it shuts off until the thermal storage is no longer sufficient to cover the heat demand.

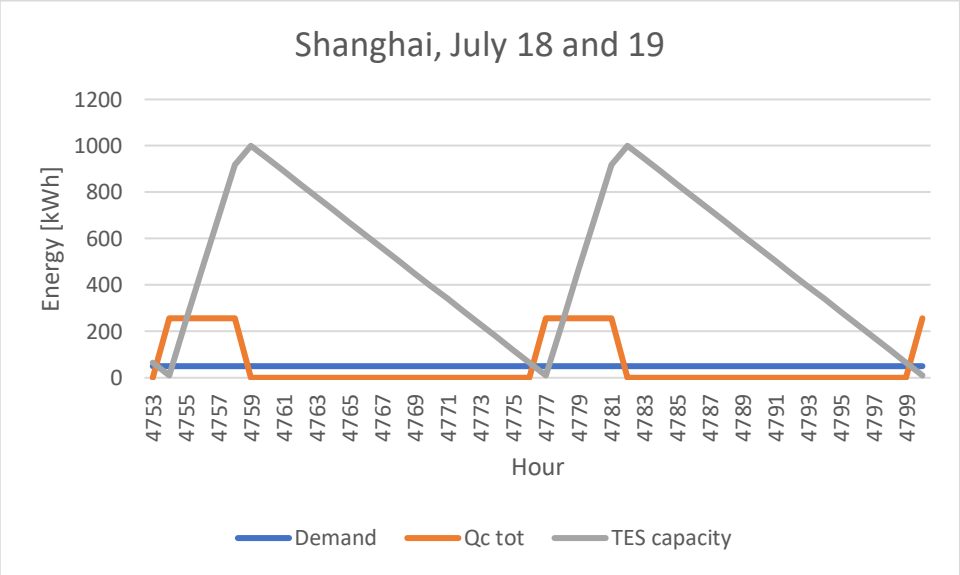

Figure 48: Heat production, storage, and demand in Shanghai on 18.07 and 19.07

Figure 48 shows the system for 48 hours. It is clear that the heat pump is turned on for five hours at a time, and then turned off for 18 hours. The demand is stable during the summer months, so this trend is seen for a long time period.

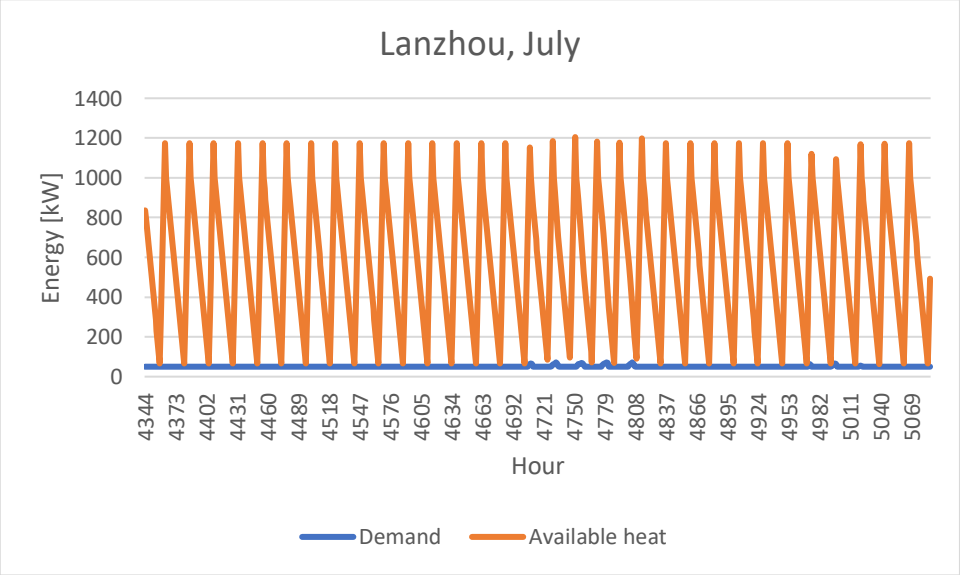

Figure 49: Heat demand an available heat in Lanzhou in July

Figure 49 shows the available heat and the demand in Lanzhou in July. The graph shows that the demand is higher than 50 kW during certain hours. However, this does not seem to affect the heat pump operation notably.

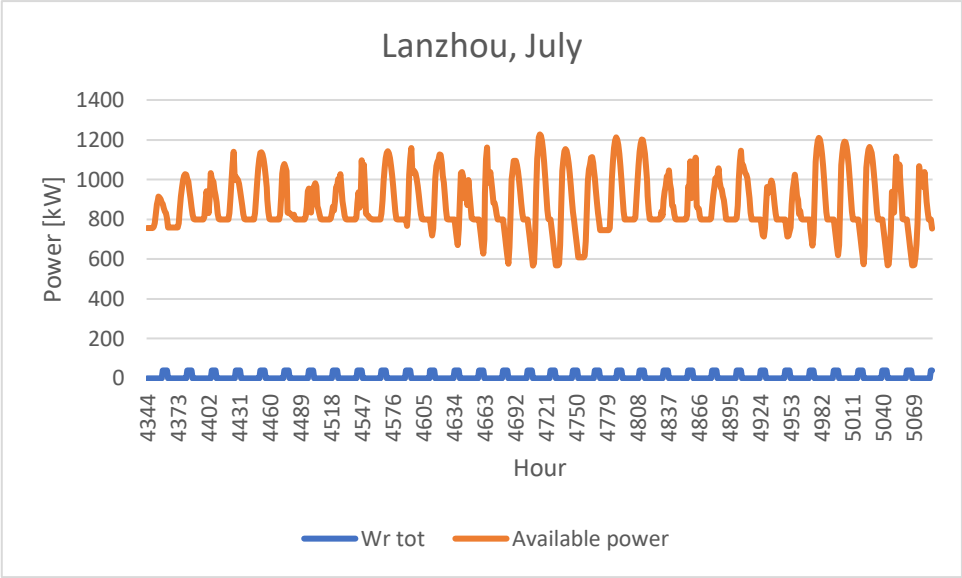

Figure 50: Available power and compressor power consumption in Lanzhou in July

Figure 50 shows the power production during the summer, as well as the power available at all times. Dure to high amounts of solar irradiation during the summer, there is always sufficient power for the heat pump to work at full capacity. No part load is necessary during these times. This is the case for all three cities.

4.3.2 Temperatures

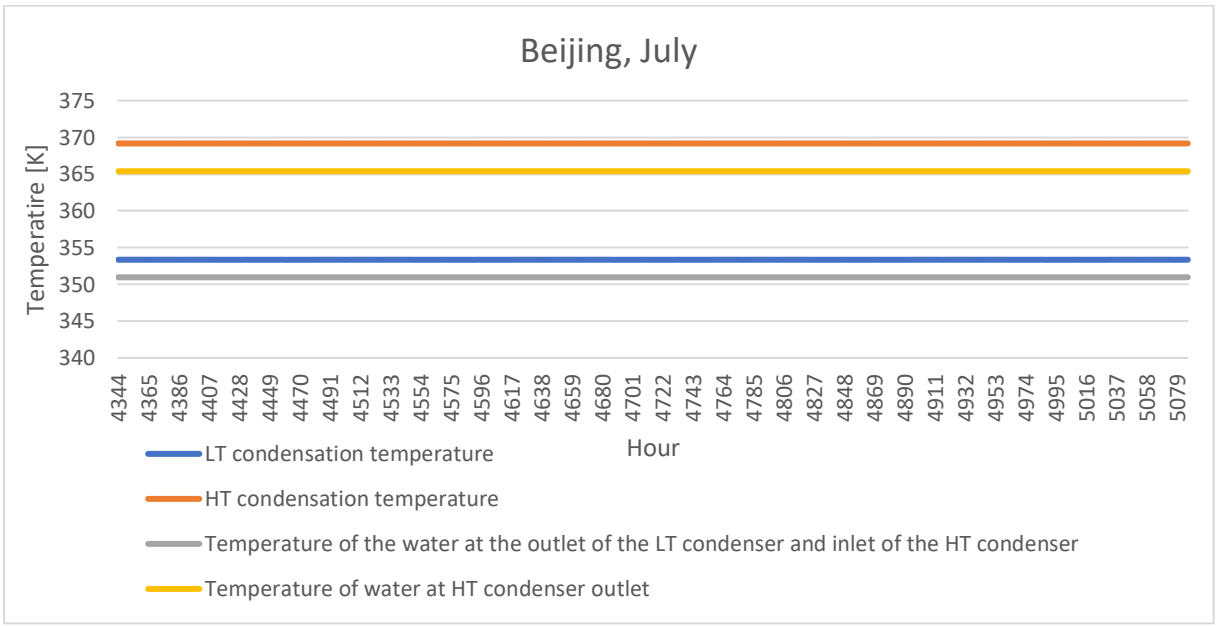

Figure 51: Condenser temperatures in July

The graph in Figure 51 shows the temperatures in Beijing, but it is also representative for Shanghai and Lanzhou in the same period. There are some small variations in the temperatures, but the variations are very small and the temperatures remain relatively constant. As mentioned in chapter 4.3.1, there are no power shortages in any of the cities in July. As a result, the heat pump does not operate on part load in this period.

4.3.3 COP

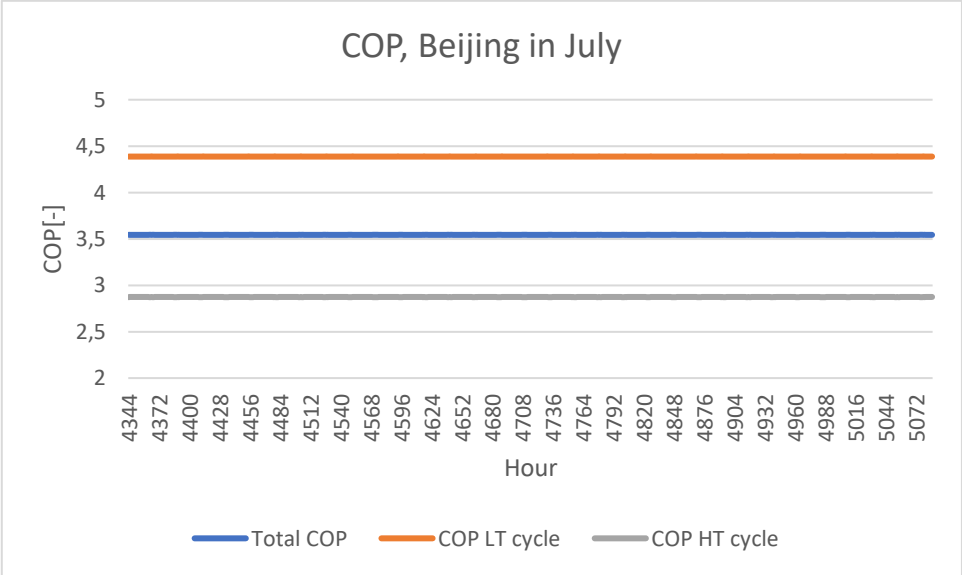

Figure 52: COP for Beijing in July

Like the temperatures, the COP stays rather constant with minor variations that do not have a real significance. They are possibly related to the restarting of the heat pump, but the variations are so small that it does not have the same effect as the variations in COP that was found during the winter months.

4.4 Spring and autumn

In the following pages, some results from April will be presented. The month of April is representative for both spring and autumn, and shows similar results to the months March, October, and November. Only a few results from Beijing will be presented because the results are similar to the results already presented from summer and winter. Results from Beijing will be presented in this chapter, and the results from Shanghai and Lanzhou can be found in Appendix B:.

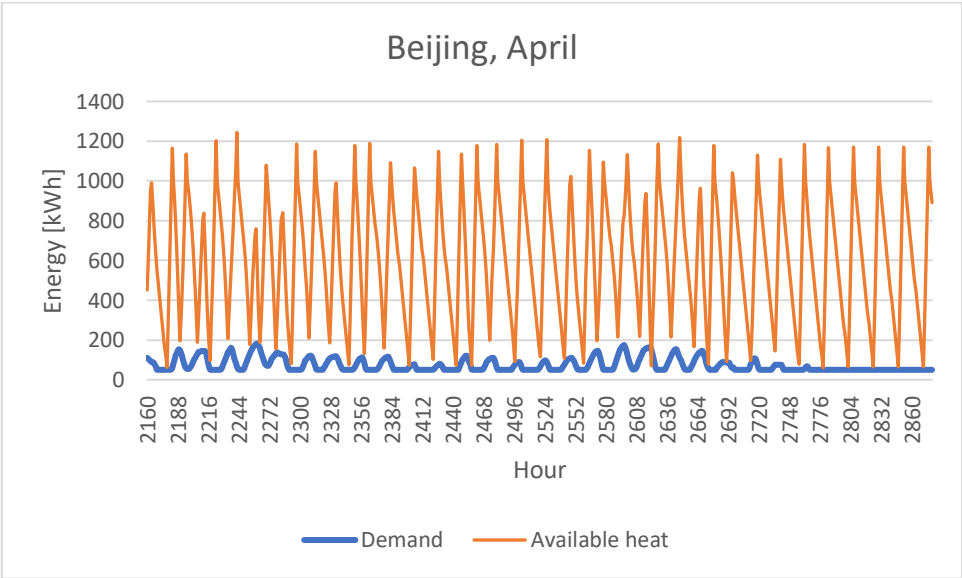

Figure 53: Available heat and demand in Beijing in April

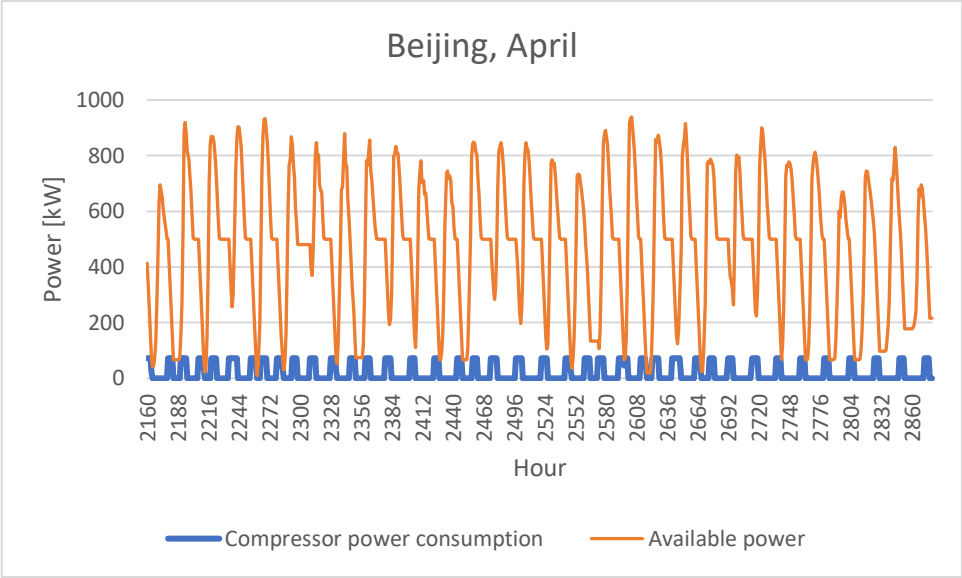

Figure 54: Hourly available power and power consumption by the compressor in Beijing in April

Figure 53 and Figure 54 show the available heat and demand, and the available power and demand in Beijing in April. The available power never reaches zero, and only in very few instances does it drop below the power consumption of the compressor when the heat pump runs on full capacity. The heat demand fluctuates and is somewhere between summer and winter demand. The amount of available power is much steadier than during the winter months, but the values vary more than they do during the summer.

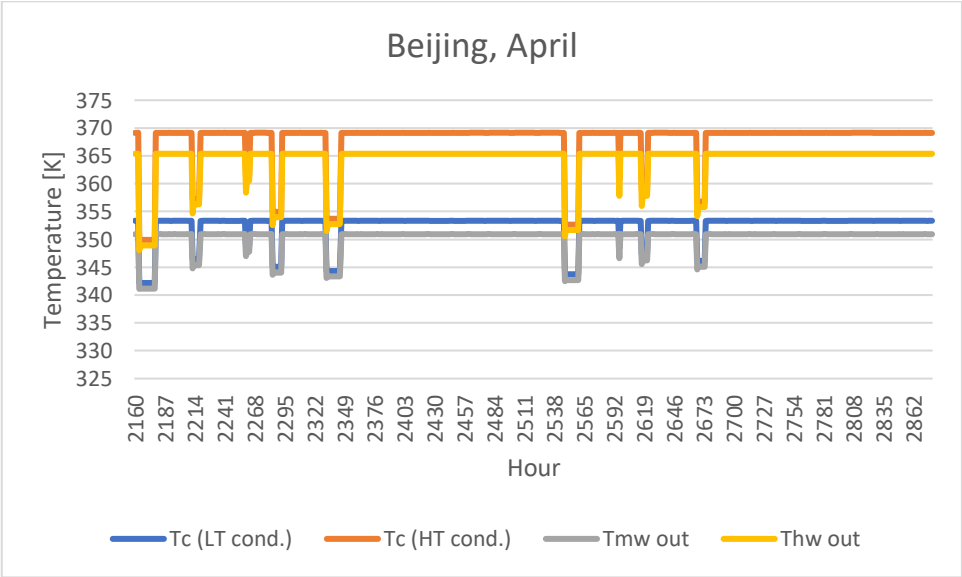

Figure 55: Condensation temperatures in Beijing in April

Figure 55 shows the condensation temperatures and the temperatures of the water being heated by the condensers in April. The results are very similar to those seen for summer and winter, but again, the values are somewhere between the two other seasons. It is clear that the temperatures fluctuate, but not as often as in January. This indicates that the heat pump operates much less on part load in April than in January.

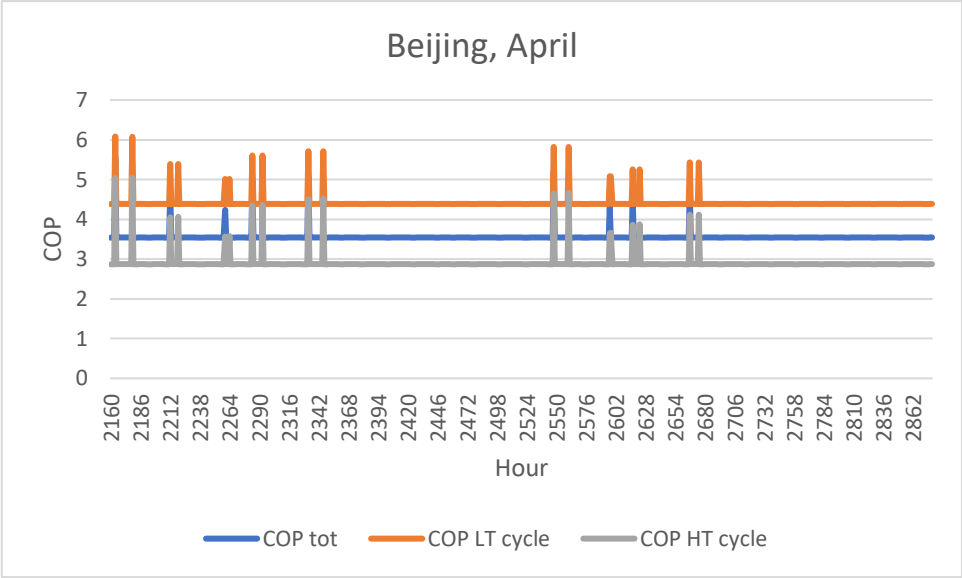

Figure 56: COP for Beijing in April

Figure 56 shows a similar trend as Figure 55. Again, the COP varies at some time instances, but not as often as it does in January.

5 Discussion

5.1 Heat pump performance

Despite differences in heat pump performance between Shanghai, Lanzhou, and Beijing due to variations in temperature and solar irradiation, the trends in heat pump performance were similar for all three cities throughout the year. Consequently, there will not be a separate discussion for each city, but rather a discussion where results from all locations are evaluated at the same time.

5.1.1 Operational mode

The heat pump is programmed to operate on full load until the thermal energy storage reaches full capacity, and then shut off until the thermal storage can no longer cover the heat demand. The results show that the heat pump operates on full capacity in most time steps, however sometimes it operates on part load. When comparing the heat pump capacity and available power for the time steps when the heat pump operates on part load, it is clear that this only happens when there is not sufficient power to for the compressor to run on full load. In those situations, the heat pump is programmed to reduce the capacity until there is sufficient power. The results are therefore in line with what was expected based on the code.

The trends for when the heat pump has sufficient power to operate on full load are similar for all three cities. During the summer, there is little or no part load operation, likely due to high amounts of solar radiation and therefore sufficient power production, and due to lower heat demand in the summer months. In the warm months, the heat pump operates in stable intervals, and the operational patterns are equal for all three cities in the month of July. Lanzhou experienced a few hours of lower temperatures than 15°C in July, but this only happened for a few hours during nighttime, and the temperatures never dropped below 13°C. Therefore, the impact on the heat pump operation was minimal, and the only effect was that the thermal storage filled up slightly slower when the temperature dropped. The temperature drops had no real impact on the operation of the heat pump.

In the winter months, on the other hand, the operation was more unstable. There was less available power for the compressor and a higher and less stable heat demand, which in turn led to less stable operation. The trend for January was that the intervals when the heat pump is turned on were longer than the intervals when the heat pump is turned off. The most common pattern was that the heat pump was turned on for 15 hours, and then turned off for 10 hours. However, sometimes the heat pump was only turned off four as little as four hours, which indicates that when the heat pump was turned off for a longer period it might be due to a lack of available power.

In Lanzhou, the heat pump was turned on 56.7% of the time in January. In Beijing it was 59.6% of the time, and in Shanghai it was turned on 53% of the time. Beijing and Lanzhou experienced longer periods of insufficient heat supply because the heat pump was turned off due to a lack of power more often than in Shanghai. Therefore, the percentage of times when the heat pump was turned on would have been higher if

enough power had always been available. Table 4 shows that Beijing and Lanzhou experienced a much larger heat shortage in January than Shanghai did.

This implies that either the heat pump or the thermal storage should have a larger capacity than they do in this simulation, especially in Beijing and Lanzhou. The total difference between demand and supply in January was 17 863 kWh in Shanghai, 82 112 kWh in Lanzhou, and 67 731 kWh in Beijing. It is likely that these numbers would be lower if the maximum limit for the thermal storage capacity was higher, as the thermal storage would be able to fill up more when there was available power. However, there are several instances when the demand exceeds the available heat for longer periods of time. The longest period is 40 hours. Even if the maximum thermal storage capacity were more than 1000 kW, it is likely that it would discharge completely in that period.

Therefore, a safer way to secure demand would be to install a larger heat pump with a higher capacity. This would of course require more power, so more PV panels would need to be installed, or the heat pump would need to be connected to an alternative power source. However, if an alternative power source were available, it is possible that the existing heat pump could supply sufficient heat.

The total heat demand in Lanzhou in January was 188 222 kWh. The total amount of heat produced by the heat pump was 105 630 kWh. If the heat pump had been at full capacity for every time step in the duration of January, it would have produced 190 497 kWh. This is slightly more than the total demand, and in theory it is enough to cover the heat demand in January. However, this assumes a steady heat demand or a higher maximum thermal storage capacity. If the heat demand had been right below 250 kW every hour, the heat pump would always be able to send the heat directly to the district heating system and cover heat demand. But since the heat demand varies and sometimes approaches 400 kW in Beijing and Lanzhou, it is necessary that the thermal storage unit supplies the heat pump in the hours with the highest demand. To ensure that this can happen, the thermal storage system must have a high enough capacity to save all the excess heat for the heat pump. Furthermore, the efficiency of the thermal energy storage limits the amount of heat that is actually available. The thermal energy storage system operates with a 90% efficiency during charging and discharging, so 10% of the heat is lost in the process. In reality, there are additional heat losses through the walls of the thermal storage system, although those losses have been neglected in this simulation. This means that even if the heat pump operated on full capacity with no breaks every hour throughout January, and even if the thermal storage system had an unlimited capacity, the heat pump in this system would likely not be able to supply the residents in Lanzhou with enough heat to cover their heat demand in January.

Beijing has a slightly lower total heat demand, and it might have been possible to cover this heat demand if an alternative power source was connected to the system, and if the thermal storage capacity was higher. The heat shortage in Shanghai in January was 64 249 kWh lower than in Lanzhou, and the heat demand never exceeds 255 kW in any hourly time step. Consequently, the heat pump would be able to cover the total heat demand if an alternative power source were connected so that the heat pump could always operate on full capacity.

If the thermal storage capacity is not increased, a larger heat pump would need to be installed to cover the heat demand in January. As mentioned, this would require more power supply, either for more PV panels or an alternative power source. The problem is

that a larger heat pump leads to increased costs related to materials, installation, maintenance, operation, and more. A larger heat pump would also take up more space.

When discussing the option of installing a larger heat pump, the operating time of the existing heat pump throughout the year should be evaluated. One reason to change other parts of the system, such as the area of the PV modules or the capacity of the battery or thermal storage, before changing the heat pump, is the total operating hours of the heat pump throughout the year. Table 4 illustrates that on a yearly basis, the heat pump was turned on less than half the time for all three cities. In the summer months, it ran just over 21% of the hourly iterations. If the size of the heat pump increased, this number would be even larger because it would take less time to recharge the thermal storage system during warmer months. This would lead to increased costs related to operation.

Instead, the PV area and battery storage capacity could be enhanced so that more electricity would be available. This would allow for the heat pump to operate for longer during the winter months without installing a large heat pump that barely operates during the summer. The excess electricity could be used to power electrical appliances or sent out to the local power grid to avoid waste.

However, it is clear that the current heat pump does not meet the heat demand in Lanzhou in January, and that it would not meet the demand even with a stable electricity supply and a larger thermal storage capacity due to losses in the TES system. Therefore, to meet the demand in Lanzhou in January, a larger heat pump or an auxiliary heating system must be installed.

If electricity demand had been factored into the code, the operational mode would likely have been different. Less power would have been available in the times when electricity consumption by the residents was high, so the heat pump would likely operate more during the times when electricity consumption was low. Typical peak hours for electricity consumption are mornings and evenings, so the heat pump would probably operate more during the day and during the night.

5.1.2 Temperatures

5.1.2.1 Temperatures in the condensers

The condensation temperatures vary greatly throughout the year. However, the variations in temperature coincide with the load ratio of the heat pump. When the heat pump works on full load, the heat exchanger temperatures remain relatively constant. While they may vary slightly, they normally stabilize around 353.35 K, or 80.20°C in the low-temperature condenser, and 369.17 K or 96.02°C in the high-temperature condenser. This leads to an outgoing water temperature of 350.97 K (77.82°C) from the low-temperature condenser and 365.38 K (92.23°C) from the high-temperature condenser. These temperatures are consistent for all three cities.

However, in the beginning and end of the year, the temperatures drop quite frequently. As previously mentioned, there appears to be a correlation between the temperature drops and the load ratio of the heat pump. This is also consistent with research in the literature review. The graph in Figure 41 shows that the load ratio decreases every time the temperatures drop. It can therefore be concluded that the temperatures are reduced when the heat pump works on part load. Table 6 shows that temperatures are higher when the load ratio is higher, and that they are lower with increasingly low load ratio.

5.1.2.2 Outgoing water temperatures

The outgoing water temperature from the high-temperature condenser normally stays above 353.15 K (80°C), even when the heat pump operates on part load. This is important, because the outgoing water temperature to the district heating system is designed to be 80°C. The system will therefore be less efficient and able to transfer less heat to the district heating system if the outgoing water temperature is below 80°C. In the system sketch, the outgoing temperature from the heat pump was set to be ≥100°C. The heat pump in this system does not quite reach this temperature, and this should be improved in a later stage of the project. However, the outgoing water temperature is much higher than 80°C and is assumed to be high enough for the thermal storage tank.

A problem occurs when the outgoing water temperature is lower than 80°C, which happens in certain time steps. This happens 431 times (4.9%) in Shanghai, 505 times (5.76%) in Lanzhou, and 308 times (3.51%). It happens in less than 5% of the cases, however this should be avoided to ensure the district heating system receives enough heat. To avoid this, the heat pump system must be modified so that the condensation temperature of the high-temperature condenser is higher. Because the water temperatures are directly related to the load ratio, this problem can also be avoided by limiting the load ratio. It seems that the outgoing water temperature drops below 80°C when the load ratio is below 70%. If the heat pump is programmed to shut off when the load ratio drops below 70% rather than going on part load, this problem could be avoided and the outgoing water temperatures would be above 80°C at all times.

Another option is to connect a heating coil to the system, after the water has passed through both condensers. In this case, there could be a temperature sensor after the high-temperature condenser, and if the temperature is lower than a specified value, for example 80°C, the heating coil could be turned on. However, this heating coil would require a power source, preferably electricity. The problem is that the heating coil would only be necessary when the heat pump operates on part load, and the heat pump only operates on part load when there is not enough power for the heat pump to operate on full load. This means that there probably would not be enough power to heat the heating coil when it was needed. Another drawback is that the heating coil would have a COP below 1 if all losses are accounted for, and the heating coil would therefore reduce the efficiency of the system as a whole.

5.1.2.3 Evaporator temperatures and heat source temperatures

The temperatures in the evaporator also vary with the load ratio of the heat pump. The evaporator temperature normally stabilizes around 31.7°C when the heat pump runs on full load, and the outgoing water temperature is 28.5°C. However, during part load operation the evaporator temperature increases. This does not have a large effect on the heating capacity of the heat pump, and will not be thoroughly investigated in this report.

However, it is worth mentioning that the outgoing water from the evaporator is supposed to be used for cooling of the PVT system. This has not been investigated in this report, but it should be noted that lower evaporation temperatures will lead to more cooling and therefore higher efficiencies for the PVT system. This will allow the PV panels to produce more power due to an increased efficiency, which will lead to more available power for the compressor and the rest of the integrated energy system.

Because the water used in the evaporator is supposed to be used for cooling in the PVT system, the inlet temperature of the water going into the evaporator should depend on the temperature in the PVT system. This has not been accounted for in this simulation,

instead the inlet temperature of the water to the evaporator is 40°C for every hourly iteration. This is due to a lack of knowledge about how much the PVT system realistically could heat the water. This should be changed in a later stage of this project to get a more realistic simulation.

If the inlet temperature of the water to the evaporator had been dependent on the heating from the PVT system instead of being a constant value, the heat pump operation should have been programmed differently. In that case, the heat pump would have a higher COP during the day due to higher heat source temperatures, so the heat pump should operate more during the day than during the night to minimize the power consumption. This would have to be balanced with other factors such as the amount of available power.

5.1.2.4 Return water from DH and inlet temperature of water to the condensers

The inlet temperature of the water to the condenser has also been given a constant value of 60°C for every iteration. This is not accurate, and in reality, the temperature should be equal to the temperature of the water returning from the district heating system. Figure 43 and Figure 44 show the return temperatures in Shanghai in February. There is a clear correlation with both condenser temperature and heat demand. The condenser temperature affects how much the water is heated by the condensers, and therefore it affects the supply temperature of the water going to the district heating system. Because the demand is not affected by the supply temperature, there might be a high heat demand even if the supply temperature is low. As a result, the temperature of the return water will be lower when the temperature of the supply water is low.

Another correlation was found between the return water temperature and the heat demand. Even in periods when the supply water temperature was constant, the return water temperature could vary due to varying demand. The heat transferred to the district heating system, and therefore the temperature difference between the inlet and outlet, is dependent on the heat demand (see Equation 20). If the demand is high, a large amount of heat will need to be transferred to the district heating system, which will result in a larger temperature difference. This will result in a lower return temperature. The opposite is true in instances with a low heat demand.

This results in a large range of return temperatures. While it can reach values of 355 K when the demand is low, the return temperature can be as low as 293 K when the demand is high. The temperature can get even lower in Beijing and Lanzhou, where heat demand is higher. These values are not always realistic. This is because the water is being used to supply heat to the district heating system. In order to supply heat, there must be a certain temperature difference between the cold and hot sides. With a counterflow heat exchanger, the outlet temperature of the cold side can be warmer than the outlet temperature of the hot side, but there is a limit to how low the temperatures can get. The inlet temperature of the water on the hot side cannot be lower than the inlet temperature of the water on the cold side, so there exists a lower limit. This limit is not set, because of limited knowledge about the district heating system. The temperatures in the system are unknown, and as a result more detailed calculations about temperatures in the district heating system cannot be performed.

Because of the large variation in return temperatures, the system could not be simulated if the inlet temperature of the water going to the LT condenser was equal to the return temperature. This is because the return temperature became too low. Because of this, a constant value of 60°C was set as the inlet temperature to the LT condenser. This is

equal to 333 K, and the results show that the return temperature often is around this value. If the actual return temperatures were to be used, they would have to become more realistic. This could have been done by making the district heating system slightly more complex, for example by adjusting the mass flow rate instead of having a constant mass flow rate throughout the entire year. By increasing or decreasing the mass flow rate, the heat transfer to the district heating system could be adapted to the temperatures at any moment, so that the temperature difference between the supply water and return water would be smaller. It would then be possible to use the more realistic return temperatures as input temperatures to the LT condenser.

The same is true for the mass flow rate of the water used to cool the PVT system and provide the evaporator with heat. If the mass flow rate is regulated throughout the year, the temperatures can be more easily controlled. Regulation of mass flow rate is possible if accumulation tanks are installed.

5.1.3 COP and efficiency

5.1.3.1 COP and part load operation

While the COP values are relatively stable during the summer months, they vary more at the beginning and end of the year. The COP stabilizes at 3.544 during the summer in all three cities but can reach values close to 7 in the colder months. In the beginning of the year, the COP varies the least in Shanghai and most in Beijing, and the average COP increases at a later stage in Shanghai than in Lanzhou and Beijing. The trends are clear in Figure 25, where the weekly average COP values are displayed. While the weekly averages are clearly higher in the summer months, the highest average value is 3.678, which is only 0.134 less than the lowest average value. This suggests that the high COP surges only happen in a few time steps every week.

The graph in Figure 46 shows the COP for the low temperature cycle, the high temperature cycle, and the total COP for one week in January. The load ratio of the heat pump is also indicated in this graph, and there is a clear correlation between the load ratio and the change in total COP. When the load ratio is lower than one, that is when the heat pump operates on part load, the COPs for both the low temperature and the high temperature cycles increase. As a result, the total COP increases as well.

The literature review showed various relations between COP and part load operation/startup and shutoff. In certain studies, the COP increased during part load operation, and certain studies saw a decrease. Intermittent operation seemed to have a high efficiency, but often with increased power consumption during shutdown and startup.

In this simulation, the increase in COP that is observed when the heat pump runs on part load may be explained by the variations in temperature. As explained in the previous chapter, the temperature in the condensers decrease and the temperature in the evaporator increases when the heat pump runs on part load. This was also seen in some cases in the literature review. As a result, the pressure ratios in the compressors decrease, which leads to higher efficiencies in the compressors. The compressor work necessary to bring the refrigerant to the condensing temperatures decreases, which will increase the COP. The heat capacity decreases as well, but it appears that the compressor work decreases more, leading to a higher overall COP.

5.1.3.2 Increasing the COP

The COP is never below 3.54, thus it satisfies the requirement of a COP higher than 3.5. The COP of this system is much higher than the COP of a single-stage system, which stabilized at 2.43 when the heat pump ran at full load. This illustrates how various system configurations can significantly increase the COP of a system, as described in chapter 2.3. The literature review showed that increasing the number of compressors to compress the working fluid in several stages rather than just once was one of the most effective ways to increase system efficiency. The results of the simulation confirm that using two compressors was much more efficient than using one. It is likely that the system COP would be further increased if more stages were added, up to a certain point. It would also have been interesting to see the effect on the system if the two compressors were in connected in series rather than in parallel. It would likely still have increased from the single-stage system, but in that case the two condensers would have had to function in a different way and the heat transfer process would have been different.

The two condensers in this system allowed for the hot water to be heated in two stages. First, it was heated from 60°C to around 77°C, and then from 77°C to around 92°C. This is leads to a more efficient heat transfer in the condensers, because the difference between the condensing temperature and inlet water temperature is lower for both condensers than it would have been if only one condenser were to heat the water more than 30°C.

It is clear that the low-temperature cycle has a much higher COP than the high-temperature cycle. The COP of the high-temperature cycle stabilizes at 2.87, whereas the COP of the low-temperature cycle stabilizes at 4.38. The total COP if the system would likely increase if the ratio of refrigerant going through the low-temperature compressor to refrigerant going through the high-temperature compressor was optimized. In the current simulation, the same amount of refrigerant goes through both compressors. If more refrigerant went through the LT compressor without compromising the capacity of the heat pump, the COP could likely be further increased. This was not done in this report because the focus was to find the trends in how the heat pump operates with the system as a whole rather than optimizing specific details of the heat pump. However, it should be done at a later stage of the project.

Numerous things can be done to further increase the system COP. Firstly, the ratio of refrigerant that flows through the LT compressor to the refrigerant that flows through the HT compressor could be optimized, as mentioned above. Secondly, the heat pump configurations could be changed. Based on the results from the literature review and the project work, it is likely that the COP would be further increased if a third compressor, and perhaps a third condenser, were installed. Other configurations such as an ejector could also increase the COP. Optimizing and varying the mass flow rates of the refrigerant as well as the water going through the heat exchangers can also increase the COP according to the literature review. This would require the additions of various sensors and regulating valves, as well as accumulation tanks

5.1.3.3 Limitations related to the COP calculations

As mentioned above, the inlet temperatures of the water going to the evaporator and the LT condenser was set to a constant value instead of the actual return temperature values. Using the actual values instead of the same values in every iteration would likely have a very large effect on the COP. The COP would decrease when the inlet temperature

of the water going to the condenser was low and increase when the inlet temperature increased. This is because a lower temperature lift is necessary with a higher heat source temperature. There would likely be a larger variation in COP throughout the day, as the heat source temperature would be higher when the PVT system is heated by the sun. During the night, the heat source temperature would be lower as it would not have been heated by the PVT system. Similarly, the COP would be much higher during the summer months when the temperature and solar radiation is higher, and lower during the winter months. It is possible that the water providing heat to the evaporator would need to be heated by another heat source than the PVT system during the night on the coldest days, especially in Beijing and Lanzhou where temperatures can go below -10°C.

Lastly, it must be noted that the calculation of COP is simplified. In this simulation, only the power consumption by the compressor during operation has been accounted for. Power surges during shutdown/startup and reduction in compressor speed have not been calculated. The power used by pumps that drive the refrigerant and other electrically driven components has not been calculated and has been neglected in all calculations. As a result, the simulations do not give an accurate image of the COP. The overall COP is likely lower, especially during part load operation. According to the literature review, other components than the compressor make up a larger share of the electricity consumption during part load operation, which decreases the heat pump efficiency. These effects should be looked at more closely at a later stage in the project.

5.1.3.4 Overall system heating efficiency

The discussion above has been about the COP of the heat pump. However, it is also possible to measure the heating efficiency of the whole system. Table 5 shows the yearly average COP of the heat pump and the average heating efficiency. The heating efficiency is calculated by dividing the total heat sent to the district heating system by the total power consumed by the compressor. Some of the heat sent to the district heating comes directly from the heat pump, while some of the heat goes through the thermal energy storage system first. The system heating efficiency is lower than the heat pump COP for all three cities. This is because the thermal storage has an efficiency of 90%, which means that 10% of the heat going through the thermal energy storage is lost. The heat going directly from the heat pump to the district heating is assumed to have an efficiency of 100%. A larger thermal storage capacity would lead to more heat going through the thermal storage system, and a larger amount of heat loss throughout the year. However, if a larger heat storage capacity would render an auxiliary heating device unnecessary, it would likely be beneficial because the efficiency of an auxiliary heating device would have been much lower than the system efficiency.

5.2 Power/batteries

As expected, the results show that the power production from the PV panels varies greatly throughout the day and year. There is no power generation at night, and there is less solar irradiation during the winter due to shorter days and less intense radiation. The amount of power produced by the PV panels depend on the solar irradiation and outside air temperature, as the efficiency of the PV panels decreases with increasing temperatures. However, even though the temperatures in the summer get very high and the efficiency of the PV panels get as low as 9.472%, the amounts of radiation are still high enough to produce sufficient power during the hot days. This is likely both because of the radiation, and because the power consumption of the compressor decreases as the heat demand decreases. Even though the heat pump still operates on full load, it is

turned off for longer periods of time during summer because the thermal storage tank can provide heat for longer when the heat demand is low.

For most time steps, the battery capacity and power production make up a much higher value than the compressor needs. However, because the PV panels and batteries are part of an integrated energy system that will provide energy to a small-scale neighborhood or large building, the excess power will go to other electric appliances. This report has only considered heat demand and not electricity demand, so the use of excess electricity could be investigated further in another stage of the project. If there is still excess electricity left after all appliances are powered, the system could be connected to the local power grid and sell the excess power to the grid.

If the power production part of the system is to be fully utilized, the size of the batteries should be more thoroughly investigated. The batteries reach maximum capacity 50.27% of the year in Shanghai, 46.21% of the year in Lanzhou, and 49.16% of the year in Beijing. In this report, the maximum battery capacity was selected with only the heat pump in mind, and with no regard for further utilization of the power from the PV panels. The PV panels continue to produce power even when the battery capacity is full, which leads to waste if the power demand at the specific time step where battery capacity is full is lower than the power production. Because the battery is full around 50% of the time in all three cities, this indicates that a lot of power is wasted when the battery capacity is only 500 kWh. Therefore, the batteries should be sized to better fit the system.

A higher battery capacity could also lead to fewer instances of the heat pump being shut off or working on part load due to insufficient power supply. All three cities experienced instances with insufficient heat supply because not enough power was available for the heat pump to operate on full capacity. If the battery capacity were higher, some of these instances would likely be avoided, because the batteries would be able to save more of the power produced by the PV panels on days with large amounts of solar radiation.

An alternative way to solve the problem of power shortages is to connect the system to an alternative power source. This could be another renewable power source such as wind energy, which could contribute with power during the night and other times with little or no solar irradiation. The system could also be connected to the local power grid to have access to a more stable power source.

5.3 Limitations

Several limitations to the simulations have been addressed in the discussion. The most notable limitation is the lack of accuracy due to simplified models of the PVT system, the battery, the thermal energy storage, and the district heating. The results showed trends that reflect the trends that would have been seen in a real situation, but due to the many simplifications the numbers are not accurate enough. The heat pump model also has certain limitations, especially the neglection of power consumption from other components than the compressor and the constant values of inlet temperatures to the heat exchangers.

Because the limitations were addressed and discussed in the previous chapters, they will not be further evaluated here. Suggestions for further work to improve the model can be found in chapter 7.

6 Conclusion

In this thesis, an integrated energy system has been evaluated as part of the project «Key technologies and demonstration of combined cooling, heating, and power generation for low-carbon neighborhoods/buildings with clean energy – ChiNoZEN». The integrated energy system consisted of a PVT system, a battery, a high-temperature heat pump, a thermal storage system, and it was connected to a district heating system. The thesis simulated the integrated energy system using Matlab and investigated how the high-temperature heat pump functioned with the other components every hour over the course of one year. The system was simulated for three locations: The Chinese cities Shanghai, Lanzhou, and Beijing.

The results were similar for all three cities during the summer months. There were similarities between the locations during the winter months as well, but larger variations were observed during winter months due to lower temperatures in Lanzhou and Beijing. The results showed that the system operated very differently in the summer than it did in the winter. The operation during the summer was constant and predictable, and the heat pump was either shut off or operated on full capacity. In the winter months, on the other hand, more part load operation was observed. This was due to less available power during the winter months, and consequently the heat pump would not always operate on full load.

The results from the winter months showed that there were several time steps when the heat pump was shut off even though the thermal energy storage was empty, and the heat demand was high. This happened when there was no available power left for the heat pump to operate. This resulted in a large heat shortage. By evaluating the total amount of heat shortage and the potential total heat pump capacity during January, it was found that the heat pump could have supplied Beijing and Shanghai with sufficient heat if some changes were made to the system. A larger thermal storage capacity, and more available power would allow the heat pump to operate for longer periods of time, and the total demand in Beijing and Shanghai could have been covered. This could have been achieved by increasing the battery storage capacity as well as expanding the area of the PV modules or connecting the system to an alternative power source such as wind power or the local power grid. To cover the January demand in Lanzhou, however, a larger heat pump would have to be installed. This illustrates that an integrated energy system such as this one should be specifically adapted to the location.

The temperatures in the condensers and the COP varied with the load ratio of the heat pump. It was found that in the instances where the heat pump operated on part load, the temperatures in the condensers were reduced. This led to a higher COP, but a less stable heat supply to the district heating system. Many parts of the integrated energy system were greatly simplified in these simulations. This was done because the focus was to see the trends in the heat pump operation throughout a year. In further development of this project, however, these simplifications should be looked into and the system should be more realistically modelled. However, the initial simulations done in this thesis provide a good initial understanding of how a high-temperature heat pump can operate in an integrated energy system and what challenges need to be solved when designing such a system.

7 Further work

In the further work on this project, there are several things that need to be improved from the model in this thesis.

First of all, the heat pump model should be updated with fewer simplifications. Instead of assuming a constant temperature of the water entering the heat exchangers, the real water temperatures should be used. In order to do this, the models for the PVT system and district heating system need to be updated. The temperature of the return water from the district heating system must be thoroughly regulated, and the mass flow rates of water and refrigerant should be adjusted to various scenarios. The temperature of the water from the PVT-system must also be monitored and perhaps regulated, especially during colder periods and when the solar radiation levels are low.

The sizes of various components such as heat exchanges and compressors should be optimized to improve the COP. A detailed model of each component should be created to fully understand how the heat pump functions. The total energy use of the heat pump should be calculated rather than just including the energy consumption of the compressors during operation. Furthermore, the system configurations of the heat pump should be evaluated to see if it is possible to increase the efficiency by modifying the heat pump.

Secondly, the PVT system should be more thoroughly investigated and modelled with fewer simplifications. The necessary area of the PV modules should be evaluated to better understand how much power that will be available at all times. The temperatures of the modules should be calculated so that an accurate model for cooling of the PV modules can be created. This will ensure a more accurate calculation of the efficiency of the PVT system, and more accurate inlet temperatures of the water entering the evaporator. The placement of the modules should also be evaluated, including the angle of the PV modules, shading, and other factors.

The electricity consumption of the residents in the homes where the integrated energy system is installed should also be calculated. By knowing when the electricity use is at its peak, the heat pump can be programmed to not operate, or to operate on part load, when the electricity demand for other electrical appliances is high. Using load peak shaving technology will allow for a more stable electricity consumption in the system.

The battery capacity and operation should also be further researched. It is important that the battery has a high enough capacity to provide a stable electricity supply to the heat pump and the residents, but it should not be larger than necessary. The losses in the battery should also be further evaluated to get an accurate idea of the available energy.

The thermal energy storage system should be more thoroughly researched and modelled with fewer simplifications. Heat transfer through the walls should be accounted for, and the heat transfer mechanisms between the water and the phase changing materials should be evaluated. The storage size should be calculated, and the material used for latent heat storage should be selected. A dynamic model of the thermal storage should be created. The thermal storage capacity necessary to ensure that heat demand is covered should also be evaluated.

A more accurate model for predicting heat demand should also be created. The model should account for the design of the buildings being heated by the integrated energy system. A program such as IDA ICE should be used to evaluate the temperatures inside the buildings heated by the integrated energy system, by calculating heat transfer rate through the walls. Insulation, size of rooms, thermal mass, activity from residents, and other factors should be included to get an accurate picture of the actual heat demand.

The cooling part of the integrated energy system should be added to the model in the continuation of this project. All three cities experience very high temperatures during the summer months, and cooling is necessary. By calculation the cooling COP, it will be possible to get better values for total system efficiency.

In addition to relying on historic data, forecasts and measurements of temperature and radiation should determine the operation of the system. If the temperature in the next week is forecasted to be lower than expected based on historical data, more heat should be produced to ensure that demand is met. If the radiation levels over the past week have been lower than expected, the system should determine how to best use the electricity available. Such analyses are complicated because of the need to analyze real-time data as well as predicted future values, but in order for a system to provide the necessary energy, it is important that real information is evaluated so that the system adapts to the current situation rather than how the weather was fifteen years ago.

In addition to creating a more advanced and complete model of the system, an economic analysis and an environmental impact study should be conducted. There will be no interest in installing this system if the total cost is higher than it would if conventional methods were used. The costs related to production and installation as well as costs related to operation, maintenance and disposal should be calculated. A pay-back time analysis should be conducted.

A life-cycle assessment of the system as a whole should be conducted to understand the environmental impact of the system. One of the reasons behind installing an integrated energy system that uses renewable energy is to lower the negative impacts that energy production and consumption have on the environment, so it is important that the impact on pollution, depletion of resources, local air quality, and other factors is evaluated.

In general, many things should be improved with this system. More detailed models need to be created, and the components need to be evaluated and optimized individually and with the other components to find a realistic and efficient way to operate the integrated energy system.

References

ABAS, N., KALAIR, A. R., KHAN, N., HAIDER, A., SALEEM, Z. & SALEEM, M. S. 2018. Natural and synthetic refrigerants, global warming: A review. *Renewable and Sustainable Energy Reviews,* 90**,** 557-569.

ALVA, G., LIN, Y. & FANG, G. 2018. An overview of thermal energy storage systems. *Energy,* 144**,** 341-378.

ARPAGAUS, C., BLESS, F., UHLMANN, M., SCHIFFMANN, J. & BERTSCH, S. S. 2018. High temperature heat pumps: Market overview, state of the art, research status, refrigerants, and application potentials. *Energy,* 152**,** 985-1010.

AYENG'O, S. P., AXELSEN, H., HABERSCHUSZ, D. & SAUER, D. U. 2019. A model for direct-coupled PV systems with batteries depending on solar radiation, temperature and number of serial connected PV cells. *Solar Energy,* 183**,** 120-131.

BAMIGBETAN, O., EIKEVIK, T., NEKSÅ, P. & BANTLE, M. Evaluation of natural working fluids for the development of high temperature heat pumps. 12th IIR Gustav Lorentzen Conference on Natural Refrigerants (GL2016), Edinburgh, United Kingdom, 2016.

BAMIGBETAN, O., EIKEVIK, T., NEKSÅ, P. & BANTLE, M. 2017. Extending Ammonia High Temperature Heat Pump Using Butane in a Cascade System. *7th IIR Conference: Ammonia and CO2 Refrigeration Technologies.* Ohrid.

BAMIGBETAN, O., EIKEVIK, T., NEKSÅ, P., BANTLE, M. & SCHLEMMINGER, C. 2019. The development of a hydrocarbon high temperature heat pump for waste heat recovery. *Energy,* 173**,** 1141-1153.

BLESS, F., ARPAGAUS, C., BERTSCH, S. S. & SCHIFFMANN, J. 2017. Theoretical analysis of steam generation methods-Energy, CO2 emission, and cost analysis. *Energy,* 129**,** 114-121.

BRODAL, E. & JACKSON, S. 2019. A comparative study of CO2 heat pump performance for combined space and hot water heating. *International Journal of Refrigeration,* 108**,** 234-245.

CAO, X.-Q., YANG, W.-W., ZHOU, F. & HE, Y.-L. 2014. Performance analysis of different high-temperature heat pump systems for low-grade waste heat recovery. *Applied thermal engineering,* 71**,** 291-300.

CONNOR, N. 2019. *What is Logarithmic Mean Temperature Difference - LMTD - Definition* [Online]. Available: https://www.thermal-engineering.org/what-is-logarithmic-mean-temperature-difference-lmtd-definition/ [Accessed 01.12.2020 2020].

DEMIR, H., MOBEDI, M. & ÜLKÜ, S. 2008. A review on adsorption heat pump: Problems and solutions. *Renewable and Sustainable Energy Reviews,* 12**,** 2381-2403.

DUBEY, S., SARVAIYA, J. N. & SESHADRI, B. 2013. Temperature dependent photovoltaic (PV) efficiency and its effect on PV production in the world–a review. *Energy Procedia,* 33**,** 311-321.

EFCTC. 2011. *Hydrofluoroolefins (HFOs)* [Online]. Available: https://www.fluorocarbons.org/publication/hydrofluoroolefins-hfos/#.Xny1vYhKg2w [Accessed 28.11 2019].

EIKEVIK, T. 2019. Heat Pumping Processes and Systems. NTNU.

ENGINEERING TOOLBOX. 2020. *Heat Exchanger Heat Transfer Coefficients* [Online]. Available: https://www.engineeringtoolbox.com/heat-transfer-coefficients-exchangers-d_450.html [Accessed 05.08.2020 2020].

FAN, L. & KHODADADI, J. M. 2011. Thermal conductivity enhancement of phase change materials for thermal energy storage: a review. *Renewable and sustainable energy reviews,* 15**,** 24-46.

FISCHER, D., TORAL, T. R., LINDBERG, K. B., WILLE-HAUSSMANN, B. & MADANI, H. 2014. Investigation of thermal storage operation strategies with heat pumps in German multi family houses. *Energy Procedia,* 58**,** 137-144.
FUKUDA, S., KONDOU, C., TAKATA, N. & KOYAMA, S. 2014. Low GWP refrigerants R1234ze (E) and R1234ze (Z) for high temperature heat pumps. *International journal of Refrigeration,* 40**,** 161-173.
FUKUDA, S., KONDOU, C., TAKATA, N. & KOYAMA, S. Thermodynamic Analysis on High Temperature Heat Pump cycles using Low-GWP refrigerants for Heat recovery. Proceedings of the Twelfth IEA Heat Pump Conference, 2017.
HAN, D., CHANG, Y. S. & KIM, Y. 2016. Performance analysis of air source heat pump system for office building. *Journal of Mechanical Science and Technology,* 30**,** 5257-5268.
HAUER, A. 2013. *Thermal Energy Storage* [Online]. IEA- ETSAP. Available: https://iea-etsap.org/E-TechDS/PDF/E17IR%20ThEnergy%20Stor_AH_Jan2013_final_GSOK.pdf [Accessed 10.09.2020 2020].
HU, B., WU, D., WANG, L. & WANG, R. 2017a. Exergy analysis of R1234ze (Z) as high temperature heat pump working fluid with multi-stage compression. *Frontiers in Energy,* 11**,** 493-502.
HU, B., XU, S., WANG, R., LIU, H., HAN, L., ZHANG, Z. & LI, H. 2019. Investigation on advanced heat pump systems with improved energy efficiency. *Energy Conversion and Management,* 192**,** 161-170.
HU, B., YAN, Y. & WANG, R. 2017b. Comparison on Low GWP Refrigerants for High Temperature Heat Pump. *TPTPR2017.* Seoul.
IEA. 2019. *Renewables 2019* [Online]. Available: https://www.iea.org/reports/renewables-2019/heat [Accessed 28.01 2020].
INDUSTRIAL HEAT PUMPS. 2019a. *Absorption Heat Pump* [Online]. Available: http://industrialheatpumps.nl/en/how_it_works/absorption_heat_pump/ [Accessed 09.03 2020].
INDUSTRIAL HEAT PUMPS. 2019b. *Adsportion Heat Pumps* [Online]. Available: http://industrialheatpumps.nl/en/how_it_works/adsorption_heat_pump/). [Accessed 09.03 2020].
JINKO SOLAR 2020. Tiger Mono-facial 450- 470 Watt. Jinko Solar.
KARLSSON, F. & FAHLÉN, P. 2007. Capacity-controlled ground source heat pumps in hydronic heating systems. *International Journal of Refrigeration,* 30**,** 221-229.
KIM, D. H., PARK, H. S. & KIM, M. S. 2013. Optimal temperature between high and low stage cycles for R134a/R410A cascade heat pump based water heater system. *Experimental thermal and fluid science,* 47**,** 172-179.
KLEIN, S. & NELLIS, G. 2012. *Thermodynamics,* Cambridge, Cambridge University Press.
KNIER, G. 2008. *How do Photovoltaics work?* [Online]. NASA. Available: https://science.nasa.gov/science-news/science-at-nasa/2002/solarcells [Accessed 02.07.2020 2020].
KONDOU, C. & KOYAMA, S. 2015. Thermodynamic assessment of high-temperature heat pumps using Low-GWP HFO refrigerants for heat recovery. *International Journal of Refrigeration,* 53**,** 126-141.
LAMNATOU, C. & CHEMISANA, D. 2017. Photovoltaic/thermal (PVT) systems: A review with emphasis on environmental issues. *Renewable energy,* 105**,** 270-287.
LI, G., ZHANG, R., JIANG, T., CHEN, H., BAI, L., CUI, H. & LI, X. 2017. Optimal dispatch strategy for integrated energy systems with CCHP and wind power. *Applied energy,* 192**,** 408-419.
LI, M., MU, H., LI, N. & MA, B. 2016. Optimal design and operation strategy for integrated evaluation of CCHP (combined cooling heating and power) system. *Energy,* 99**,** 202-220.
LIANGDONG, M., ZHANG, J. & SHUYAN, Z. Thermodynamic cycle performances analysis of high temperature refrigerants in a multi-stage heat pump system. 2010 International Conference on Mechanic Automation and Control Engineering, 2010. IEEE, 1515-1520.

LONGO, G. A., MANCIN, S., RIGHETTI, G., ZILIO, C. & BROWN, J. S. 2019. Assessment of the low-gwp refrigerants r600a, r1234ze (z) and r1233zd (e) for heat pump and organic rankine cycle applications. *Applied Thermal Engineering*, 114804.
MA, X., ZHANG, Y., FANG, L., YU, X., LI, X., SHENG, Y. & ZHANG, Y. 2018. Performance analysis of a cascade high temperature heat pump using R245fa and BY-3 as working fluid. *Applied Thermal Engineering,* 140, 466-475.
MAN, Y., YANG, H., WANG, J. & FANG, Z. 2012. In situ operation performance test of ground coupled heat pump system for cooling and heating provision in temperate zone. *Applied Energy,* 97, 913-920.
MATEU-ROYO, C., NAVARRO-ESBRÍ, J., MOTA-BABILONI, A., AMAT-ALBUIXECH, M. & MOLÉS, F. 2018. Theoretical evaluation of different high-temperature heat pump configurations for low-grade waste heat recovery. *International Journal of Refrigeration,* 90, 229-237.
MICHAELS, P. J., BALLING JR, R. C., VOSE, R. S. & KNAPPENBERGER, P. C. 1998. Analysis of trends in the variability of daily and monthly historical temperature measurements. *Climate Research,* 10, 27-33.
NASA. 2019. *The Causes of Climate Change* [Online]. Available: https://climate.nasa.gov/causes/ [Accessed 22.01 2020].
NASA. 2020. *Climate Change: How Do We Know?* [Online]. NASA. Available: https://climate.nasa.gov/evidence/ [Accessed 21.01 2020].
NAWAZ, K., SHEN, B., ELATAR, A., BAXTER, V. & ABDELAZIZ, O. 2017. R1234yf and R1234ze (E) as low-GWP refrigerants for residential heat pump water heaters. *International Journal of Refrigeration,* 82, 348-365.
NEKSÅ, P., REKSTAD, H., ZAKERI, G. R. & SCHIEFLOE, P. A. 1998. CO2-heat pump water heater: characteristics, system design and experimental results. *International Journal of refrigeration,* 21, 172-179.
NORD, J. H., KOOHANG, A. & PALISZKIEWICZ, J. 2019. The Internet of Things: Review and theoretical framework. *Expert Systems with Applications,* 133, 97-108.
NTNU DEPARTMENT OF ENERGY AND PROCESS ENGINEERING. 2020. *Key technologies and demonstration of combined cooling, heating and power generation for low-carbon neighbourhoods/buildings with clean energy (ChiNoZEN)* [Online]. Available: https://www.ntnu.edu/ept/chinozen#/view/about [Accessed 22.10.2020 2020].
PALM, B. 2008. Hydrocarbons as refrigerants in small heat pump and refrigeration systems–a review. *International journal of refrigeration,* 31, 552-563.
PEUREUX, J., SICARD, F. & BOBELIN, D. French industrial heat pump developments applied to heat recovery. 11th IEA Heat Pump conference, May 12, 2014, Montréal, Canada, 2014.
PHOTOVOLTAIC SOFTWARE. 2020. *How to calculate the annual solar energy output of a photovoltaic system?* [Online]. Available: https://photovoltaic-software.com/principle-ressources/how-calculate-solar-energy-power-pv-systems [Accessed 12.07.2020 2020].
POWER SCOUT. 2017. *How to Calculate Solar Panel Output* [Online]. Available: https://powerscout.com/site/how-to-calculate-solar-panel-output#:~:text=Most%20solar%20panels%20have%20efficiency,(measured%20in%20square%20meters). [Accessed 12.07.2020 2020].
REFRIGERANTHQ. 2019. *What are CFC and HCFC refrigerants?* [Online]. Available: https://refrigeranthq.com/f-a-q/what-are-cfc-refrigerants/ [Accessed 04.12 2019].
RITCHIE, H. & ROSER, M. 2020. *Renewable Energy* [Online]. Our World in Data. Available: https://ourworldindata.org/renewable-energy [Accessed 23.01 2020].
SARBU, I. & SEBARCHIEVICI, C. 2018. A comprehensive review of thermal energy storage. *Sustainability,* 10, 191.
SARKAR, J. 2012. Ejector enhanced vapor compression refrigeration and heat pump systems—A review. *Renewable and Sustainable Energy Reviews,* 16, 6647-6659.

SCHIBUOLA, L., SCARPA, M. & TAMBANI, C. 2015. Demand response management by means of heat pumps controlled via real time pricing. *Energy and Buildings,* 90**,** 15-28.
SINGH, G. K. 2013. Solar power generation by PV (photovoltaic) technology: A review. *Energy,* 53**,** 1-13.
SOLARWATT. 2020. *Solar Batteries* [Online]. Available: https://www.solarwatt.com/solar-batteries#:~:text=System%20efficiency%3A%20The%20system%20efficiency,leading%20to%20unnecessary%20extra%20costs. [Accessed 14.07.2020 2020].
STAFFELL, I., BRETT, D., BRANDON, N. & HAWKES, A. 2012. A review of domestic heat pumps. *Energy & Environmental Science,* 5**,** 9291-9306.
STANDARD NORGE. 2017. *NS-EN 378-1:2016* [Online]. Available: https://www.standard.no/nettbutikk/sokeresultater/?search=NS-EN+378-1%3a2016&subscr=1 [Accessed 06.04 2020].
TARAS, M. F. & LIFSON, A. 2007. Heat pump with reheat and economizer functions. Google Patents.
U.S. DEPARTMENT OF ENERGY. 2018. *Heat Pump Systems* [Online]. Available: https://www.energy.gov/energysaver/heat-and-cool/heat-pump-systems [Accessed 18.01 2020].
UHLMANN, M. & BERTSCH, S. S. 2012. Theoretical and experimental investigation of startup and shutdown behavior of residential heat pumps. *International Journal of Refrigeration,* 35**,** 2138-2149.
WORLD GREEN BUILDING COUNCIL. 2017. *Global Status Report 2017* [Online]. Available: https://www.worldgbc.org/news-media/global-status-report-2017 [Accessed 22.01 2020].
WORLD GREEN BUILDING COUNCIL. 2019. *New report: the building and construction sector can reach net zero carbon emissions by 2050* [Online]. Available: https://www.worldgbc.org/news-media/WorldGBC-embodied-carbon-report-published#_ftn1 [Accessed 22.01 2020].
WU, D., HU, B. & WANG, R. 2018. Performance simulation and exergy analysis of a hybrid source heat pump system with low GWP refrigerants. *Renewable energy,* 116**,** 775-785.
ZHANG, C., SHEN, C., YANG, Q., WEI, S., LV, G. & SUN, C. 2020. An investigation on the attenuation effect of air pollution on regional solar radiation. *Renewable Energy,* 161**,** 570-578.
ZHENG, S., YI, H. & LI, H. 2015. The impacts of provincial energy and environmental policies on air pollution control in China. *Renewable and Sustainable Energy Reviews,* 49**,** 386-394.

Appendix A: Matlab code

```
WeatherData=readtable('Beijing_hour_year.xlsx');

OutsideTemp=WeatherData{:,10};
%Variables
hours_onBJ=0;
hours_partloadBJ=0;
dT_dh=zeros(1,length(OutsideTemp));
T_supply=zeros(1,length(OutsideTemp));
T_return=zeros(1,length(OutsideTemp));
T_hw_in=zeros(1,length(OutsideTemp));
T_PV=zeros(1,length(OutsideTemp));
r=zeros(1,length(OutsideTemp));
E=zeros(1,length(OutsideTemp));
load_ratio=zeros(1,length(OutsideTemp));
lowpwr=[];
lwheat=[];
partload=[];
ninetyprheat=[];
eightyprheat= [];
seventyprheat=[];
sixtyprheat= [];
fourtyprheat=[];
twentyprheat=[];
eightypr=[];
sixtypr=[];
fourtypr=[];
fullon=[];

battery_input=zeros(1,length(OutsideTemp));
battery_capacity=zeros(1,length(OutsideTemp));
battery_output=zeros(1,length(OutsideTemp));
Q_sup=250+zeros(1,length(OutsideTemp));
TES_input=zeros(1,length(OutsideTemp));
TES_output=zeros(1,length(OutsideTemp));
TES_capacity=zeros(1,length(OutsideTemp));
```

```
T_c=(273.15+110)+zeros(1,length(OutsideTemp));
T_m=(273.15+80)+zeros(1,length(OutsideTemp));
T_e=(273.15+40)+zeros(1,length(OutsideTemp));
P_c=zeros(1,length(OutsideTemp));
P_m=zeros(1,length(OutsideTemp));
P_e=zeros(1,length(OutsideTemp));
W_r_ht=zeros(1,length(OutsideTemp));

W_r_mt=zeros(1,length(OutsideTemp));
W_r_tot=zeros(1,length(OutsideTemp));
Q_c_ht=zeros(1,length(OutsideTemp));
Q_c_mt=zeros(1,length(OutsideTemp));
Q_c_tot=zeros(1,length(OutsideTemp));
Q_e=zeros(1,length(OutsideTemp));
```

```
COP_ht=zeros(1,length(OutsideTemp));
COP_mt=zeros(1,length(OutsideTemp));
COP_tot=zeros(1,length(OutsideTemp));

T_mw_out=zeros(1,length(OutsideTemp));
dT_lmtd_cond_mt=zeros(1,length(OutsideTemp));
T_m2=zeros(1,length(OutsideTemp));
T_hw_out=zeros(1,length(OutsideTemp));
dT_lmtd_cond_ht=zeros(1,length(OutsideTemp));
T_cw_out=zeros(1,length(OutsideTemp));
dT_lmtd_evap=zeros(1,length(OutsideTemp));
T_e2=zeros(1,length(OutsideTemp));

dTe=zeros(1,length(OutsideTemp));
dTc=zeros(1,length(OutsideTemp));
dTm=zeros(1,length(OutsideTemp));

T_1=zeros(1,length(OutsideTemp));
h_1=zeros(1,length(OutsideTemp));
rho_1=zeros(1,length(OutsideTemp));
s_1=zeros(1,length(OutsideTemp));
h_2s=zeros(1,length(OutsideTemp));
h_2=zeros(1,length(OutsideTemp));
s_2=zeros(1,length(OutsideTemp));
T_2=zeros(1,length(OutsideTemp));
T_3=zeros(1,length(OutsideTemp));
h_3=zeros(1,length(OutsideTemp));
s_3=zeros(1,length(OutsideTemp));
h_4=zeros(1,length(OutsideTemp));
s_4=zeros(1,length(OutsideTemp));
Pr_rat_ht=zeros(1,length(OutsideTemp));
Pr_rat_mt=zeros(1,length(OutsideTemp));
eta_comp_ht=zeros(1,length(OutsideTemp));
eta_comp_mt=zeros(1,length(OutsideTemp));
vol_eff_ht=zeros(1,length(OutsideTemp));
vol_eff_mt=zeros(1,length(OutsideTemp));
compressor_load=zeros(1,length(OutsideTemp));
W_r_max=zeros(1,length(OutsideTemp));
heat_ratio=zeros(1,length(OutsideTemp));

output_from_TES=zeros(1,length(OutsideTemp));
heat_from_TES_to_DH=zeros(1,length(OutsideTemp));
input_to_TES=zeros(1,length(OutsideTemp));
heat_from_HP_to_TES=zeros(1,length(OutsideTemp));
output_from_battery=zeros(1,length(OutsideTemp));
power_from_battery_to_HP=zeros(1,length(OutsideTemp));
input_to_battery=zeros(1,length(OutsideTemp));
power_from_PV_to_battery=zeros(1,length(OutsideTemp));
```

```
T_7=zeros(1,length(OutsideTemp));
h_7=zeros(1,length(OutsideTemp));
s_7=zeros(1,length(OutsideTemp));
h_8=zeros(1,length(OutsideTemp));
s_8=zeros(1,length(OutsideTemp));
h_5=zeros(1,length(OutsideTemp));
s_5=zeros(1,length(OutsideTemp));
m_r_ht=zeros(1,length(OutsideTemp));
m_r_mt23=zeros(1,length(OutsideTemp));
```

```
h_6=zeros(1,length(OutsideTemp));
h_6s=zeros(1,length(OutsideTemp));
T_6=zeros(1,length(OutsideTemp));
s_6=zeros(1,length(OutsideTemp));
T_4=zeros(1,length(OutsideTemp));
m_r_mt483=zeros(1,length(OutsideTemp));
m_r_mt34=zeros(1,length(OutsideTemp));
x_8=zeros(1,length(OutsideTemp));
```

```
hour=(1:length(OutsideTemp));
hour2=[hour 8760];
Demand=zeros(1,length(OutsideTemp));
T_c2=zeros(1,length(OutsideTemp));

for i =2:length(OutsideTemp)

    T_supply(1)=80+273.15;
    T_c(1)=110+273.15;
    T_m(1)=80+273.15;
    T_e(1)=40+273.15;
    E(1)=0;
    W_r_tot(1)=0;
    TES_capacity(1)=750;
    TES_capacity(2)=750;
    Demand(1)=150;
```

```
%PV
Pmax=470; %Wp
Eff_STC= 0.2093; %Module efficiency STC, 20.93%
T_coeff=-0.0034; %[0.34%/degC], temperature coeff. of Pmax

%Other values
A_pv= 4000; %[m^2]. Total solar panel area. 5000. 1500 funker
PR= 0.75; %[75%], performance ratio, coeff. for losses. 0.75 is default
T_STC=25; %Standard test conditions temperture, 25degC

T_col=WeatherData{:,10}; %[deg C]
H_col=WeatherData{:,5}; %Global horizontal radiation, W/m2
hr_col=WeatherData{:,4};

%Calculations
T_PV(i)=T_col(i)+20; %Temperature of PV panels. Air temperature + 20 K
r(i)=Eff_STC-(T_STC-T_PV(i))*T_coeff; %Operating efficiency, takes temp into account
E(i)=A_pv*r(i)*H_col(i)*PR/1000; %E= Energy in kW

%Battery
battery_input(1)=0;
battery_capacity(1)=450;
battery_output(1)=0;
battery_capacity(2)=450;
battery_capacity_max=500;

%DH
m_dh=2; %kg/s
Cp_dh=2011.6/1000; %kJ/kgK
TES_capacity_max=1000;
```

```
%Demand
dT_heat=15-T_col(i);
if dT_heat>=0
    Demand(i)=50+dT_heat*10.25;
else
    Demand(i)=50;
end

dT_dh(i-1)=Demand(i-1)/(m_dh*Cp_dh); %Temp difference of water entering and leaving DH system

T_return(i-1)=T_supply(i-1)-dT_dh(i-1);

T_mw_in(i)=273.15+60;
if TES_capacity(i)>TES_capacity_max
    TES_capacity(i)=TES_capacity_max;
end
if TES_capacity(i)<0
    TES_capacity(i)=0;
end

if battery_capacity(i)>battery_capacity_max
    battery_capacity(i)=battery_capacity_max;
end
if battery_capacity(i)<0
    battery_capacity(i)=0;
end

%%%%%%%%%%%%%%%%%%%%%%%%%%%%%%%%%%%%%%%%%%%%%%%%%%%%%%%%%%%%%%%%%%%%%%%%%%%%%%%%%%%%%%%%%%%%%%%%%%%%
%HEAT PUMP MAIN LOOP%
%%%%%%%%%%%%%%%%%%%%%%%%%%%%%%%%%%%%%%%%%%%%%%%%%%%%%%%%%%%%%%%%%%%%%%%%%%%%%%%%%%%%%%%%%%%%%%%%%%%%

%Set values (No need to incude in every iteration)
%1. General
Ref= 'Ammonia';
comp_size_ht=60; %m^3/h
comp_size_mt=63;
heat_ratio(i)=Demand(i)/255;

%2. MT Condenser
rho_mw=refpropm('D','T',(273.15+60),'Q',1,'Water');
Cp_mw=refpropm('C','T',(273.15+60),'Q',1,'Water'); % J/kgK.
U_cond_mt=1400; %W/m^2K
A_cond_mt=12; %m^2
UA_cond_mt=U_cond_mt*A_cond_mt;
m_mw=4; %kg/s

%3. HT Condenser
U_cond_ht=1400; %W/m^2K
A_cond_ht=9; %m^2
UA_cond_ht=U_cond_ht*A_cond_ht;
m_hw=4; %kg/s

%4. Evaporator
T_cw_in=273.15+40;
rho_cw=refpropm('D','T',T_cw_in,'Q',1,'Water');
Cp_cw=refpropm('C','T',T_cw_in,'Q',1,'Water');
U_evap=1600; %W/m^2K
A_evap=10; %m^2
```

```
UA_evap=U_evap*A_evap;
m_cw=12;

%First loop: Full load
%Initial values
T_c(1)=273.15+110;
T_m(1)=273.15+80;
T_e(1)=273.15+35;
T_c2(1)=273.15+105;
T_mw_in(1)=273.15+60;

T_c(i)=T_c(i-1);
T_m(i)=T_m(i-1);
T_e(i)=T_e(i-1);


if (T_c(i)-T_c2(i))<=0.1
    T_c2(i)=T_c2(i)-1;
%
end

while (T_c(i)-T_c2(i))>0.1

P_c(i)= refpropm('P','T',T_c(i),'Q',0,Ref);
P_m(i)= refpropm('P','T',T_m(i),'Q',0,Ref);
P_e(i)= refpropm('P','T',T_e(i),'Q',1,Ref);
Pr_rat_ht(i)=P_c(i)/P_e(i);
Pr_rat_mt(i)=P_m(i)/P_e(i);

eta_comp_ht(i)=-0.00000461*Pr_rat_ht(i)^6+0.00027131*Pr_rat_ht(i)^5-
0.00628605*Pr_rat_ht(i)^4+0.07370258*Pr_rat_ht(i)^3-
0.46054399*Pr_rat_ht(i)^2+1.40653347*Pr_rat_ht(i)-0.87811477;
eta_comp_mt(i)=-0.00000461*Pr_rat_mt(i)^6+0.00027131*Pr_rat_mt(i)^5-
0.00628605*Pr_rat_mt(i)^4+0.07370258*Pr_rat_mt(i)^3-
0.46054399*Pr_rat_mt(i)^2+1.40653347*Pr_rat_mt(i)-0.87811477;
vol_eff_ht(i)=0.0011*Pr_rat_ht(i)^2-0.0487*Pr_rat_ht(i)+0.9979;
vol_eff_mt(i)=0.0011*Pr_rat_mt(i)^2-0.0487*Pr_rat_mt(i)+0.9979;

%State properies
T_1(i)=T_e(i);
x_1=1;
h_1(i)=refpropm('H','T',T_1(i),'Q',x_1,Ref); % J/kg
rho_1(i)=refpropm('D','T',T_1(i),'Q',x_1,Ref);
s_1(i)=refpropm('S','T',T_1(i),'Q',x_1,Ref);  %J/kgK

h_2s(i)=refpropm('H','P',P_m(i),'S',s_1(i),Ref);
h_2(i)=h_1(i)+(h_2s(i)-h_1(i))/eta_comp_mt(i);
s_2(i)=refpropm('S','H',h_2(i),'P',P_m(i),Ref);
T_2(i)=refpropm('T','P',P_m(i),'H',h_2(i),Ref);

T_4(i)=T_m(i);
h_4(i)=refpropm('H','T',T_4(i),'P',P_m(i),Ref);
s_4(i)=refpropm('S','H',h_4(i),'P',P_m(i),Ref);

h_6s(i)=refpropm('H','P',P_c(i),'S',s_1(i),Ref);
h_6(i)=h_1(i)+(h_6s(i)-h_1(i))/eta_comp_ht(i);
s_6(i)=refpropm('S','H',h_6(i),'P',P_c(i),Ref);
T_6(i)=refpropm('T','P',P_c(i),'H',h_6(i),Ref);
```

```
T_7(i)=T_c(i);
h_7(i)=refpropm('H','T',T_7(i),'P',P_c(i),Ref);
s_7(i)=refpropm('S','H',h_7(i),'P',P_c(i),Ref);

h_8(i)=h_7(i);
s_8(i)=refpropm('S','H',h_8(i),'P',P_m(i),Ref);

h_5(i)=h_4(i);
s_5(i)=refpropm('S','H',h_5(i),'P',P_e(i),Ref);

%x-greier
m_r_ht(i)=rho_1(i)*(comp_size_ht/3600)*vol_eff_ht(i);
m_r_mt23(i)=rho_1(i)*(comp_size_mt/3600)*vol_eff_mt(i);

h_3(i)=refpropm('H','P',P_m(i),'Q',1,Ref);
x_8(i)=(h_7(i)-h_4(i))/(h_3(i)-h_4(i));

m_r_mt483(i)=m_r_ht(i)*x_8(i);
m_r_mt34(i)=m_r_mt23(i)+m_r_mt483(i);
%Vedier
W_r_ht(i)=m_r_ht(i)*(h_6(i)-h_1(i))/1000; %kW
W_r_mt(i)=m_r_mt23(i)*(h_2(i)-h_1(i))/1000; %kW
W_r_tot(i)=W_r_mt(i)+W_r_ht(i);
Q_c_ht(i)=m_r_ht(i)*(h_6(i)-h_7(i))/1000; %kW, Capacity of HT condenser
Q_c_mt(i)=m_r_mt34(i)*(h_2(i)-h_4(i))/1000; %kW, Capacity of MT condenser
Q_c_tot(i)=Q_c_ht(i)+Q_c_mt(i);
Q_e(i)=(m_r_ht(i)+m_r_mt23(i))*(h_1(i)-h_5(i))/1000; %kW
COP_ht(i)=Q_c_ht(i)/W_r_ht(i);
COP_mt(i)=Q_c_mt(i)/W_r_mt(i);
COP_tot(i)=(Q_c_ht(i)+Q_c_mt(i))/(W_r_ht(i)+W_r_mt(i));

%LT Condenser
T_mw_out(i)=T_mw_in(i)+Q_c_mt(i)/(Cp_mw/1000*m_mw);
dT_lmtd_cond_mt(i)=Q_c_mt(i)*1000/UA_cond_mt;
A(i)=exp((T_mw_out(i)-T_mw_in(i))/dT_lmtd_cond_mt(i));
T_m2(i)=(T_mw_in(i)-T_mw_out(i)*A(i))/(1-A(i));

%HT Condenser
T_hw_in(i)=T_mw_out(i); %inlet temerature of water to be heated (coolant)
rho_hw=refpropm('D','T',T_hw_in(i),'Q',1,'Water');
Cp_hw=refpropm('C','T',T_hw_in(i),'Q',1,'Water'); % J/kgK.
T_hw_out(i)=T_hw_in(i)+Q_c_ht(i)/(Cp_hw/1000*m_hw);

dT_lmtd_cond_ht(i)=Q_c_ht(i)*1000/UA_cond_ht;
B(i)=exp((T_hw_out(i)-T_hw_in(i))/dT_lmtd_cond_ht(i));
T_c2(i)=(T_hw_in(i)-T_hw_out(i)*B(i))/(1-B(i));

%Evaporator
T_cw_out(i)=T_cw_in-Q_e(i)/(Cp_cw/1000*m_cw);
dT_lmtd_evap(i)=Q_e(i)*1000/UA_evap;
T_e2(i)=(T_cw_out(i)*exp((T_cw_in-T_cw_out(i))/dT_lmtd_evap(i))-T_cw_in)/(exp((T_cw_in-
T_cw_out(i))/dT_lmtd_evap(i))-1);

%New values
dTe(i)= (T_e(i)-T_e2(i))/2;
dTc(i)=(T_c(i)-T_c2(i))/2;
dTm(i)=(T_m(i)-T_m2(i));
```

```
T_c(i)=T_c(i)-dTc(i);
T_e(i)=T_e(i)-dTe(i);
T_m(i)=T_m(i)-dTm(i);

end %while. Finished main loop with no part load.
% %

if (E(i)+battery_capacity(i))<W_r_tot(i) %if part load
% %%%%%%%%%%%%%%%%%%%%%%%%%%%%%%%%%%%%%%%%%%%%%%%%%%%%%%%%%%%%%%%%%%%%%%%%%%%%%%%
% %New loop, part load to meet demand

if (T_c(i)-T_c2(i))<=0.1
    T_c2(i)=T_c2(i)-1;
%
end

while (T_c(i)-T_c2(i))>0.1

P_c(i)= refpropm('P','T',T_c(i),'Q',0,Ref);
P_m(i)= refpropm('P','T',T_m(i),'Q',0,Ref);
P_e(i)= refpropm('P','T',T_e(i),'Q',1,Ref);
Pr_rat_ht(i)=P_c(i)/P_e(i);
Pr_rat_mt(i)=P_m(i)/P_e(i);

eta_comp_ht(i)=-0.00000461*Pr_rat_ht(i)^6+0.00027131*Pr_rat_ht(i)^5-
0.00628605*Pr_rat_ht(i)^4+0.07370258*Pr_rat_ht(i)^3-
0.46054399*Pr_rat_ht(i)^2+1.40653347*Pr_rat_ht(i)-0.87811477;
eta_comp_mt(i)=-0.00000461*Pr_rat_mt(i)^6+0.00027131*Pr_rat_mt(i)^5-
0.00628605*Pr_rat_mt(i)^4+0.07370258*Pr_rat_mt(i)^3-
0.46054399*Pr_rat_mt(i)^2+1.40653347*Pr_rat_mt(i)-0.87811477;
vol_eff_ht(i)=0.0011*Pr_rat_ht(i)^2-0.0487*Pr_rat_ht(i)+0.9979;
vol_eff_mt(i)=0.0011*Pr_rat_mt(i)^2-0.0487*Pr_rat_mt(i)+0.9979;

%State properies
T_1(i)=T_e(i);
x_1=1;
h_1(i)=refpropm('H','T',T_1(i),'Q',x_1,Ref); % J/kg
rho_1(i)=refpropm('D','T',T_1(i),'Q',x_1,Ref);
s_1(i)=refpropm('S','T',T_1(i),'Q',x_1,Ref);  %J/kgK

h_2s(i)=refpropm('H','P',P_m(i),'S',s_1(i),Ref);
h_2(i)=h_1(i)+(h_2s(i)-h_1(i))/eta_comp_mt(i);
s_2(i)=refpropm('S','H',h_2(i),'P',P_m(i),Ref);
T_2(i)=refpropm('T','P',P_m(i),'H',h_2(i),Ref);

T_4(i)=T_m(i);
h_4(i)=refpropm('H','T',T_4(i),'P',P_m(i),Ref);
s_4(i)=refpropm('S','H',h_4(i),'P',P_m(i),Ref);

h_6s(i)=refpropm('H','P',P_c(i),'S',s_1(i),Ref);
h_6(i)=h_1(i)+(h_6s(i)-h_1(i))/eta_comp_ht(i);
s_6(i)=refpropm('S','H',h_6(i),'P',P_c(i),Ref);
T_6(i)=refpropm('T','P',P_c(i),'H',h_6(i),Ref);

T_7(i)=T_c(i);
h_7(i)=refpropm('H','T',T_7(i),'P',P_c(i),Ref);
s_7(i)=refpropm('S','H',h_7(i),'P',P_c(i),Ref);
```

```
h_8(i)=h_7(i);
s_8(i)=refpropm('S','H',h_8(i),'P',P_m(i),Ref);

h_5(i)=h_4(i);
s_5(i)=refpropm('S','H',h_5(i),'P',P_e(i),Ref);

%x-greier
m_r_ht(i)=rho_1(i)*(comp_size_ht/3600)*vol_eff_ht(i)*heat_ratio(i);
m_r_mt23(i)=rho_1(i)*(comp_size_mt/3600)*vol_eff_mt(i)*heat_ratio(i);

h_3(i)=refpropm('H','P',P_m(i),'Q',1,Ref);
x_8(i)=(h_7(i)-h_4(i))/(h_3(i)-h_4(i));

m_r_mt483(i)=m_r_ht(i)*x_8(i);
m_r_mt34(i)=m_r_mt23(i)+m_r_mt483(i);
%Vedier
W_r_ht(i)=m_r_ht(i)*(h_6(i)-h_1(i))/1000; %kW
W_r_mt(i)=m_r_mt23(i)*(h_2(i)-h_1(i))/1000; %kW
W_r_tot(i)=W_r_mt(i)+W_r_ht(i);
Q_c_ht(i)=m_r_ht(i)*(h_6(i)-h_7(i))/1000; %kW, Capacity of HT condenser
Q_c_mt(i)=m_r_mt34(i)*(h_2(i)-h_4(i))/1000; %kW, Capacity of MT condenser
Q_c_tot(i)=Q_c_ht(i)+Q_c_mt(i);
Q_e(i)=(m_r_ht(i)+m_r_mt23(i))*(h_1(i)-h_5(i))/1000; %kW
COP_ht(i)=Q_c_ht(i)/W_r_ht(i);
COP_mt(i)=Q_c_mt(i)/W_r_mt(i);
COP_tot(i)=(Q_c_ht(i)+Q_c_mt(i))/(W_r_ht(i)+W_r_mt(i));

%LT Condenser
T_mw_out(i)=T_mw_in(i)+Q_c_mt(i)/(Cp_mw/1000*m_mw);
dT_lmtd_cond_mt(i)=Q_c_mt(i)*1000/UA_cond_mt;
A(i)=exp((T_mw_out(i)-T_mw_in(i))/dT_lmtd_cond_mt(i));
T_m2(i)=(T_mw_in(i)-T_mw_out(i)*A(i))/(1-A(i));

%HT Condenser
T_hw_in(i)=T_mw_out(i); %inlet temerature of water to be heated (coolant)
rho_hw=refpropm('D','T',T_hw_in(i),'Q',1,'Water');
Cp_hw=refpropm('C','T',T_hw_in(i),'Q',1,'Water'); % J/kgK.
T_hw_out(i)=T_hw_in(i)+Q_c_ht(i)/(m_hw *Cp_hw/1000);

dT_lmtd_cond_ht(i)=Q_c_ht(i)*1000/UA_cond_ht;
B(i)=exp((T_hw_out(i)-T_hw_in(i))/dT_lmtd_cond_ht(i));
T_c2(i)=(T_hw_in(i)-T_hw_out(i)*B(i))/(1-B(i));

%Evaporator
T_cw_out(i)=T_cw_in-Q_e(i)/(Cp_cw/1000*m_cw);
dT_lmtd_evap(i)=Q_e(i)*1000/UA_evap;
T_e2(i)=(T_cw_out(i)*exp((T_cw_in-T_cw_out(i))/dT_lmtd_evap(i))-T_cw_in)/(exp((T_cw_in-
T_cw_out(i))/dT_lmtd_evap(i))-1);

%New values
dTe(i)= (T_e(i)-T_e2(i))/2;
dTc(i)=(T_c(i)-T_c2(i))/2;
dTm(i)=(T_m(i)-T_m2(i));
T_c(i)=T_c(i)-dTc(i);
T_e(i)=T_e(i)-dTe(i);
T_m(i)=T_m(i)-dTm(i);

end %while. Finished main loop with part load.
```

```
if W_r_tot(i-1)>battery_capacity(i-1)+E(i-1) && W_r_tot(i)>W_r_tot(i-1)

    Q_c_tot(i)=Q_c_tot(i-1);
    W_r_tot(i)=W_r_tot(i-1);
    COP_tot(i)=COP_tot(i-1);
end

end %if part load

if (E(i)+battery_capacity(i))<W_r_tot(i) %if 80
% %%%%%%%%%%%%%%%%%%%%%%%%%%%%%%%%%%%%%%%%%%%%%%%%%%%%%%%%%%%%%%%%%%%%%%%%%%%%%%%
% %New loop, reduce to 80% of load ratio

if (T_c(i)-T_c2(i))<=0.1
    T_c2(i)=T_c2(i)-1;
%
end

while (T_c(i)-T_c2(i))>0.1

P_c(i)= refpropm('P','T',T_c(i),'Q',0,Ref);
P_m(i)= refpropm('P','T',T_m(i),'Q',0,Ref);
P_e(i)= refpropm('P','T',T_e(i),'Q',1,Ref);
Pr_rat_ht(i)=P_c(i)/P_e(i);
Pr_rat_mt(i)=P_m(i)/P_e(i);

eta_comp_ht(i)=-0.00000461*Pr_rat_ht(i)^6+0.00027131*Pr_rat_ht(i)^5-
0.00628605*Pr_rat_ht(i)^4+0.07370258*Pr_rat_ht(i)^3-
0.46054399*Pr_rat_ht(i)^2+1.40653347*Pr_rat_ht(i)-0.87811477;
eta_comp_mt(i)=-0.00000461*Pr_rat_mt(i)^6+0.00027131*Pr_rat_mt(i)^5-
0.00628605*Pr_rat_mt(i)^4+0.07370258*Pr_rat_mt(i)^3-
0.46054399*Pr_rat_mt(i)^2+1.40653347*Pr_rat_mt(i)-0.87811477;
vol_eff_ht(i)=0.0011*Pr_rat_ht(i)^2-0.0487*Pr_rat_ht(i)+0.9979;
vol_eff_mt(i)=0.0011*Pr_rat_mt(i)^2-0.0487*Pr_rat_mt(i)+0.9979;

%State properies
T_1(i)=T_e(i);
x_1=1;
h_1(i)=refpropm('H','T',T_1(i),'Q',x_1,Ref); % J/kg
rho_1(i)=refpropm('D','T',T_1(i),'Q',x_1,Ref);
s_1(i)=refpropm('S','T',T_1(i),'Q',x_1,Ref);  %J/kgK

h_2s(i)=refpropm('H','P',P_m(i),'S',s_1(i),Ref);
h_2(i)=h_1(i)+(h_2s(i)-h_1(i))/eta_comp_mt(i);
s_2(i)=refpropm('S','H',h_2(i),'P',P_m(i),Ref);
T_2(i)=refpropm('T','P',P_m(i),'H',h_2(i),Ref);

T_4(i)=T_m(i);
h_4(i)=refpropm('H','T',T_4(i),'P',P_m(i),Ref);
s_4(i)=refpropm('S','H',h_4(i),'P',P_m(i),Ref);

h_6s(i)=refpropm('H','P',P_c(i),'S',s_1(i),Ref);
h_6(i)=h_1(i)+(h_6s(i)-h_1(i))/eta_comp_ht(i);
s_6(i)=refpropm('S','H',h_6(i),'P',P_c(i),Ref);
T_6(i)=refpropm('T','P',P_c(i),'H',h_6(i),Ref);
```

```
T_7(i)=T_c(i);
h_7(i)=refpropm('H','T',T_7(i),'P',P_c(i),Ref);
s_7(i)=refpropm('S','H',h_7(i),'P',P_c(i),Ref);

h_8(i)=h_7(i);
s_8(i)=refpropm('S','H',h_8(i),'P',P_m(i),Ref);

h_5(i)=h_4(i);
s_5(i)=refpropm('S','H',h_5(i),'P',P_e(i),Ref);

%x-greier
m_r_ht(i)=rho_1(i)*(comp_size_ht/3600)*vol_eff_ht(i)*heat_ratio(i)*0.8;
m_r_mt23(i)=rho_1(i)*(comp_size_mt/3600)*vol_eff_mt(i)*heat_ratio(i)*0.8;

h_3(i)=refpropm('H','P',P_m(i),'Q',1,Ref);
x_8(i)=(h_7(i)-h_4(i))/(h_3(i)-h_4(i));

m_r_mt483(i)=m_r_ht(i)*x_8(i);
m_r_mt34(i)=m_r_mt23(i)+m_r_mt483(i);
%Vedier
W_r_ht(i)=m_r_ht(i)*(h_6(i)-h_1(i))/1000; %kW
W_r_mt(i)=m_r_mt23(i)*(h_2(i)-h_1(i))/1000; %kW
W_r_tot(i)=W_r_mt(i)+W_r_ht(i);
Q_c_ht(i)=m_r_ht(i)*(h_6(i)-h_7(i))/1000; %kW, Capacity of HT condenser
Q_c_mt(i)=m_r_mt34(i)*(h_2(i)-h_4(i))/1000; %kW, Capacity of MT condenser
Q_c_tot(i)=Q_c_ht(i)+Q_c_mt(i);
Q_e(i)=(m_r_ht(i)+m_r_mt23(i))*(h_1(i)-h_5(i))/1000; %kW
COP_ht(i)=Q_c_ht(i)/W_r_ht(i);
COP_mt(i)=Q_c_mt(i)/W_r_mt(i);
COP_tot(i)=(Q_c_ht(i)+Q_c_mt(i))/(W_r_ht(i)+W_r_mt(i));

%LT Condenser
T_mw_out(i)=T_mw_in(i)+Q_c_mt(i)/(Cp_mw/1000*m_mw);
dT_lmtd_cond_mt(i)=Q_c_mt(i)*1000/UA_cond_mt;
A(i)=exp((T_mw_out(i)-T_mw_in(i))/dT_lmtd_cond_mt(i));
T_m2(i)=(T_mw_in(i)-T_mw_out(i)*A(i))/(1-A(i));

%HT Condenser
T_hw_in(i)=T_mw_out(i); %inlet temerature of water to be heated (coolant)
rho_hw=refpropm('D','T',T_hw_in(i),'Q',1,'Water');
Cp_hw=refpropm('C','T',T_hw_in(i),'Q',1,'Water'); % J/kgK.
T_hw_out(i)=T_hw_in(i)+Q_c_ht(i)/(m_hw *Cp_hw/1000);

dT_lmtd_cond_ht(i)=Q_c_ht(i)*1000/UA_cond_ht;
B(i)=exp((T_hw_out(i)-T_hw_in(i))/dT_lmtd_cond_ht(i));
T_c2(i)=(T_hw_in(i)-T_hw_out(i)*B(i))/(1-B(i));

%Evaporator
T_cw_out(i)=T_cw_in-Q_e(i)/(Cp_cw/1000*m_cw);
dT_lmtd_evap(i)=Q_e(i)*1000/UA_evap;
T_e2(i)=(T_cw_out(i)*exp((T_cw_in-T_cw_out(i))/dT_lmtd_evap(i))-T_cw_in)/(exp((T_cw_in-
T_cw_out(i))/dT_lmtd_evap(i))-1);

%New values
dTe(i)= (T_e(i)-T_e2(i))/2;
dTc(i)=(T_c(i)-T_c2(i))/2;
dTm(i)=(T_m(i)-T_m2(i));
T_c(i)=T_c(i)-dTc(i);
```

```
T_e(i)=T_e(i)-dTe(i);
T_m(i)=T_m(i)-dTm(i);

end %while.

eightyprheat=[eightyprheat i];
if W_r_tot(i-1)>battery_capacity(i-1)+E(i-1) && W_r_tot(i)>W_r_tot(i-1)

    Q_c_tot(i)=Q_c_tot(i-1);
    W_r_tot(i)=W_r_tot(i-1);
    COP_tot(i)=COP_tot(i-1);
end

end %if 80

if (E(i)+battery_capacity(i))<W_r_tot(i) %if 60
% %%%%%%%%%%%%%%%%%%%%%%%%%%%%%%%%%%%%%%%%%%%%%%%%%%%%%%%%%%%%%%%%%%%%%%%%%%%%%%%
% %New loop, reduce to 60% of part load

if (T_c(i)-T_c2(i))<=0.1
    T_c2(i)=T_c2(i)-1;
%
end

while (T_c(i)-T_c2(i))>0.1

P_c(i)= refpropm('P','T',T_c(i),'Q',0,Ref);
P_m(i)= refpropm('P','T',T_m(i),'Q',0,Ref);
P_e(i)= refpropm('P','T',T_e(i),'Q',1,Ref);
Pr_rat_ht(i)=P_c(i)/P_e(i);
Pr_rat_mt(i)=P_m(i)/P_e(i);

eta_comp_ht(i)=-0.00000461*Pr_rat_ht(i)^6+0.00027131*Pr_rat_ht(i)^5-
0.00628605*Pr_rat_ht(i)^4+0.07370258*Pr_rat_ht(i)^3-
0.46054399*Pr_rat_ht(i)^2+1.40653347*Pr_rat_ht(i)-0.87811477;
eta_comp_mt(i)=-0.00000461*Pr_rat_mt(i)^6+0.00027131*Pr_rat_mt(i)^5-
0.00628605*Pr_rat_mt(i)^4+0.07370258*Pr_rat_mt(i)^3-
0.46054399*Pr_rat_mt(i)^2+1.40653347*Pr_rat_mt(i)-0.87811477;
vol_eff_ht(i)=0.0011*Pr_rat_ht(i)^2-0.0487*Pr_rat_ht(i)+0.9979;
vol_eff_mt(i)=0.0011*Pr_rat_mt(i)^2-0.0487*Pr_rat_mt(i)+0.9979;

%State properies
T_1(i)=T_e(i);
x_1=1;
h_1(i)=refpropm('H','T',T_1(i),'Q',x_1,Ref); % J/kg
rho_1(i)=refpropm('D','T',T_1(i),'Q',x_1,Ref);
s_1(i)=refpropm('S','T',T_1(i),'Q',x_1,Ref);  %J/kgK

h_2s(i)=refpropm('H','P',P_m(i),'S',s_1(i),Ref);
h_2(i)=h_1(i)+(h_2s(i)-h_1(i))/eta_comp_mt(i);
s_2(i)=refpropm('S','H',h_2(i),'P',P_m(i),Ref);
T_2(i)=refpropm('T','P',P_m(i),'H',h_2(i),Ref);

T_4(i)=T_m(i);
h_4(i)=refpropm('H','T',T_4(i),'P',P_m(i),Ref);
s_4(i)=refpropm('S','H',h_4(i),'P',P_m(i),Ref);

h_6s(i)=refpropm('H','P',P_c(i),'S',s_1(i),Ref);
```

```
h_6(i)=h_1(i)+(h_6s(i)-h_1(i))/eta_comp_ht(i);
s_6(i)=refpropm('S','H',h_6(i),'P',P_c(i),Ref);
T_6(i)=refpropm('T','P',P_c(i),'H',h_6(i),Ref);

T_7(i)=T_c(i);
h_7(i)=refpropm('H','T',T_7(i),'P',P_c(i),Ref);
s_7(i)=refpropm('S','H',h_7(i),'P',P_c(i),Ref);

h_8(i)=h_7(i);
s_8(i)=refpropm('S','H',h_8(i),'P',P_m(i),Ref);

h_5(i)=h_4(i);
s_5(i)=refpropm('S','H',h_5(i),'P',P_e(i),Ref);

%x-greier
m_r_ht(i)=rho_1(i)*(comp_size_ht/3600)*vol_eff_ht(i)*heat_ratio(i)*0.6;
m_r_mt23(i)=rho_1(i)*(comp_size_mt/3600)*vol_eff_mt(i)*heat_ratio(i)*0.6;

h_3(i)=refpropm('H','P',P_m(i),'Q',1,Ref);
x_8(i)=(h_7(i)-h_4(i))/(h_3(i)-h_4(i));

m_r_mt483(i)=m_r_ht(i)*x_8(i);
m_r_mt34(i)=m_r_mt23(i)+m_r_mt483(i);
%Vedier
W_r_ht(i)=m_r_ht(i)*(h_6(i)-h_1(i))/1000; %kW
W_r_mt(i)=m_r_mt23(i)*(h_2(i)-h_1(i))/1000; %kW
W_r_tot(i)=W_r_mt(i)+W_r_ht(i);
Q_c_ht(i)=m_r_ht(i)*(h_6(i)-h_7(i))/1000; %kW, Capacity of HT condenser
Q_c_mt(i)=m_r_mt34(i)*(h_2(i)-h_4(i))/1000; %kW, Capacity of MT condenser
Q_c_tot(i)=Q_c_ht(i)+Q_c_mt(i);
Q_e(i)=(m_r_ht(i)+m_r_mt23(i))*(h_1(i)-h_5(i))/1000; %kW
COP_ht(i)=Q_c_ht(i)/W_r_ht(i);
COP_mt(i)=Q_c_mt(i)/W_r_mt(i);
COP_tot(i)=(Q_c_ht(i)+Q_c_mt(i))/(W_r_ht(i)+W_r_mt(i));

%LT Condenser
T_mw_out(i)=T_mw_in(i)+Q_c_mt(i)/(Cp_mw/1000*m_mw);
dT_lmtd_cond_mt(i)=Q_c_mt(i)*1000/UA_cond_mt;
A(i)=exp((T_mw_out(i)-T_mw_in(i))/dT_lmtd_cond_mt(i));
T_m2(i)=(T_mw_in(i)-T_mw_out(i)*A(i))/(1-A(i));

%HT Condenser
T_hw_in(i)=T_mw_out(i); %inlet temerature of water to be heated (coolant)
rho_hw=refpropm('D','T',T_hw_in(i),'Q',1,'Water');
Cp_hw=refpropm('C','T',T_hw_in(i),'Q',1,'Water'); % J/kgK.
T_hw_out(i)=T_hw_in(i)+Q_c_ht(i)/(m_hw *Cp_hw/1000);

dT_lmtd_cond_ht(i)=Q_c_ht(i)*1000/UA_cond_ht;
B(i)=exp((T_hw_out(i)-T_hw_in(i))/dT_lmtd_cond_ht(i));
T_c2(i)=(T_hw_in(i)-T_hw_out(i)*B(i))/(1-B(i));

%Evaporator
T_cw_out(i)=T_cw_in-Q_e(i)/(Cp_cw/1000*m_cw);
dT_lmtd_evap(i)=Q_e(i)*1000/UA_evap;
T_e2(i)=(T_cw_out(i)*exp((T_cw_in-T_cw_out(i))/dT_lmtd_evap(i))-T_cw_in)/(exp((T_cw_in-
T_cw_out(i))/dT_lmtd_evap(i))-1);

%New values
```

```
dTe(i)= (T_e(i)-T_e2(i))/2;
dTc(i)=(T_c(i)-T_c2(i))/2;
dTm(i)=(T_m(i)-T_m2(i));
T_c(i)=T_c(i)-dTc(i);
T_e(i)=T_e(i)-dTe(i);
T_m(i)=T_m(i)-dTm(i);

end %while.

sixtyprheat=[sixtyprheat i];
if W_r_tot(i-1)>battery_capacity(i-1)+E(i-1) && W_r_tot(i)>W_r_tot(i-1)

    Q_c_tot(i)=Q_c_tot(i-1);
    W_r_tot(i)=W_r_tot(i-1);
    COP_tot(i)=COP_tot(i-1);
end

end %if 60

if (E(i)+battery_capacity(i))<W_r_tot(i) %if 40
% %%%%%%%%%%%%%%%%%%%%%%%%%%%%%%%%%%%%%%%%%%%%%%%%%%%%%%%%%%%%%%%%%%%%%%%%%%%%%%%
% %New loop, reduce to 40% of part load

if (T_c(i)-T_c2(i))<=0.1
    T_c2(i)=T_c2(i)-1;
%
end

while (T_c(i)-T_c2(i))>0.1

P_c(i)= refpropm('P','T',T_c(i),'Q',0,Ref);
P_m(i)= refpropm('P','T',T_m(i),'Q',0,Ref);
P_e(i)= refpropm('P','T',T_e(i),'Q',1,Ref);
Pr_rat_ht(i)=P_c(i)/P_e(i);
Pr_rat_mt(i)=P_m(i)/P_e(i);

eta_comp_ht(i)=-0.00000461*Pr_rat_ht(i)^6+0.00027131*Pr_rat_ht(i)^5-
0.00628605*Pr_rat_ht(i)^4+0.07370258*Pr_rat_ht(i)^3-
0.46054399*Pr_rat_ht(i)^2+1.40653347*Pr_rat_ht(i)-0.87811477;
eta_comp_mt(i)=-0.00000461*Pr_rat_mt(i)^6+0.00027131*Pr_rat_mt(i)^5-
0.00628605*Pr_rat_mt(i)^4+0.07370258*Pr_rat_mt(i)^3-
0.46054399*Pr_rat_mt(i)^2+1.40653347*Pr_rat_mt(i)-0.87811477;
vol_eff_ht(i)=0.0011*Pr_rat_ht(i)^2-0.0487*Pr_rat_ht(i)+0.9979;
vol_eff_mt(i)=0.0011*Pr_rat_mt(i)^2-0.0487*Pr_rat_mt(i)+0.9979;

%State properies
T_1(i)=T_e(i);
x_1=1;
h_1(i)=refpropm('H','T',T_1(i),'Q',x_1,Ref); % J/kg
rho_1(i)=refpropm('D','T',T_1(i),'Q',x_1,Ref);
s_1(i)=refpropm('S','T',T_1(i),'Q',x_1,Ref);  %J/kgK

h_2s(i)=refpropm('H','P',P_m(i),'S',s_1(i),Ref);
h_2(i)=h_1(i)+(h_2s(i)-h_1(i))/eta_comp_mt(i);
s_2(i)=refpropm('S','H',h_2(i),'P',P_m(i),Ref);
T_2(i)=refpropm('T','P',P_m(i),'H',h_2(i),Ref);

T_4(i)=T_m(i);
```

```
h_4(i)=refpropm('H','T',T_4(i),'P',P_m(i),Ref);
s_4(i)=refpropm('S','H',h_4(i),'P',P_m(i),Ref);

h_6s(i)=refpropm('H','P',P_c(i),'S',s_1(i),Ref);
h_6(i)=h_1(i)+(h_6s(i)-h_1(i))/eta_comp_ht(i);
s_6(i)=refpropm('S','H',h_6(i),'P',P_c(i),Ref);
T_6(i)=refpropm('T','P',P_c(i),'H',h_6(i),Ref);

T_7(i)=T_c(i);
h_7(i)=refpropm('H','T',T_7(i),'P',P_c(i),Ref);
s_7(i)=refpropm('S','H',h_7(i),'P',P_c(i),Ref);

h_8(i)=h_7(i);
s_8(i)=refpropm('S','H',h_8(i),'P',P_m(i),Ref);

h_5(i)=h_4(i);
s_5(i)=refpropm('S','H',h_5(i),'P',P_e(i),Ref);

%x-greier
m_r_ht(i)=rho_1(i)*(comp_size_ht/3600)*vol_eff_ht(i)*heat_ratio(i)*0.4;
m_r_mt23(i)=rho_1(i)*(comp_size_mt/3600)*vol_eff_mt(i)*heat_ratio(i)*0.4;

h_3(i)=refpropm('H','P',P_m(i),'Q',1,Ref);
x_8(i)=(h_7(i)-h_4(i))/(h_3(i)-h_4(i));

m_r_mt483(i)=m_r_ht(i)*x_8(i);
m_r_mt34(i)=m_r_mt23(i)+m_r_mt483(i);
%Vedier
W_r_ht(i)=m_r_ht(i)*(h_6(i)-h_1(i))/1000; %kW
W_r_mt(i)=m_r_mt23(i)*(h_2(i)-h_1(i))/1000; %kW
W_r_tot(i)=W_r_mt(i)+W_r_ht(i);
Q_c_ht(i)=m_r_ht(i)*(h_6(i)-h_7(i))/1000; %kW, Capacity of HT condenser
Q_c_mt(i)=m_r_mt34(i)*(h_2(i)-h_4(i))/1000; %kW, Capacity of MT condenser
Q_c_tot(i)=Q_c_ht(i)+Q_c_mt(i);
Q_e(i)=(m_r_ht(i)+m_r_mt23(i))*(h_1(i)-h_5(i))/1000; %kW
COP_ht(i)=Q_c_ht(i)/W_r_ht(i);
COP_mt(i)=Q_c_mt(i)/W_r_mt(i);
COP_tot(i)=(Q_c_ht(i)+Q_c_mt(i))/(W_r_ht(i)+W_r_mt(i));

%LT Condenser
T_mw_out(i)=T_mw_in(i)+Q_c_mt(i)/(Cp_mw/1000*m_mw);
dT_lmtd_cond_mt(i)=Q_c_mt(i)*1000/UA_cond_mt;
A(i)=exp((T_mw_out(i)-T_mw_in(i))/dT_lmtd_cond_mt(i));
T_m2(i)=(T_mw_in(i)-T_mw_out(i)*A(i))/(1-A(i));

%HT Condenser
T_hw_in(i)=T_mw_out(i); %inlet temerature of water to be heated (coolant)
rho_hw=refpropm('D','T',T_hw_in(i),'Q',1,'Water');
Cp_hw=refpropm('C','T',T_hw_in(i),'Q',1,'Water'); % J/kgK.
T_hw_out(i)=T_hw_in(i)+Q_c_ht(i)/(m_hw *Cp_hw/1000);

dT_lmtd_cond_ht(i)=Q_c_ht(i)*1000/UA_cond_ht;

B(i)=exp((T_hw_out(i)-T_hw_in(i))/dT_lmtd_cond_ht(i));
T_c2(i)=(T_hw_in(i)-T_hw_out(i)*B(i))/(1-B(i));


%Evaporator
```

```
T_cw_out(i)=T_cw_in-Q_e(i)/(Cp_cw/1000*m_cw);
dT_lmtd_evap(i)=Q_e(i)*1000/UA_evap;
T_e2(i)=(T_cw_out(i)*exp((T_cw_in-T_cw_out(i))/dT_lmtd_evap(i))-T_cw_in)/(exp((T_cw_in-
T_cw_out(i))/dT_lmtd_evap(i))-1);

%New values
dTe(i)= (T_e(i)-T_e2(i))/2;
dTc(i)=(T_c(i)-T_c2(i))/2;
dTm(i)=(T_m(i)-T_m2(i));
T_c(i)=T_c(i)-dTc(i);
T_e(i)=T_e(i)-dTe(i);
T_m(i)=T_m(i)-dTm(i);

end %while.

fourtyprheat=[fourtyprheat i];
if W_r_tot(i-1)>battery_capacity(i-1)+E(i-1) && W_r_tot(i)>W_r_tot(i-1)

    Q_c_tot(i)=Q_c_tot(i-1);
    W_r_tot(i)=W_r_tot(i-1);
    COP_tot(i)=COP_tot(i-1);
end

end %if 40

if (E(i)+battery_capacity(i))<W_r_tot(i)
% %%%%%%%%%%%%%%%%%%%%%%%%%%%%%%%%%%%%%%%%%%%%%%%%%%%%%%%%%%%%%%%%%%%%%%%%%%%%%%%
% %Reduce to 20% of part load

if (T_c(i)-T_c2(i))<=0.1
    T_c2(i)=T_c2(i)-1;
%
end

while (T_c(i)-T_c2(i))>0.1

P_c(i)= refpropm('P','T',T_c(i),'Q',0,Ref);
P_m(i)= refpropm('P','T',T_m(i),'Q',0,Ref);
P_e(i)= refpropm('P','T',T_e(i),'Q',1,Ref);
Pr_rat_ht(i)=P_c(i)/P_e(i);
Pr_rat_mt(i)=P_m(i)/P_e(i);

eta_comp_ht(i)=-0.00000461*Pr_rat_ht(i)^6+0.00027131*Pr_rat_ht(i)^5-
0.00628605*Pr_rat_ht(i)^4+0.07370258*Pr_rat_ht(i)^3-
0.46054399*Pr_rat_ht(i)^2+1.40653347*Pr_rat_ht(i)-0.87811477;
eta_comp_mt(i)=-0.00000461*Pr_rat_mt(i)^6+0.00027131*Pr_rat_mt(i)^5-
0.00628605*Pr_rat_mt(i)^4+0.07370258*Pr_rat_mt(i)^3-
0.46054399*Pr_rat_mt(i)^2+1.40653347*Pr_rat_mt(i)-0.87811477;
vol_eff_ht(i)=0.0011*Pr_rat_ht(i)^2-0.0487*Pr_rat_ht(i)+0.9979;
vol_eff_mt(i)=0.0011*Pr_rat_mt(i)^2-0.0487*Pr_rat_mt(i)+0.9979;

%State properies
T_1(i)=T_e(i);
x_1=1;
h_1(i)=refpropm('H','T',T_1(i),'Q',x_1,Ref); % J/kg
rho_1(i)=refpropm('D','T',T_1(i),'Q',x_1,Ref);
s_1(i)=refpropm('S','T',T_1(i),'Q',x_1,Ref);  %J/kgK
```

```
h_2s(i)=refpropm('H','P',P_m(i),'S',s_1(i),Ref);
h_2(i)=h_1(i)+(h_2s(i)-h_1(i))/eta_comp_mt(i);
s_2(i)=refpropm('S','H',h_2(i),'P',P_m(i),Ref);
T_2(i)=refpropm('T','P',P_m(i),'H',h_2(i),Ref);

T_4(i)=T_m(i);
h_4(i)=refpropm('H','T',T_4(i),'P',P_m(i),Ref);
s_4(i)=refpropm('S','H',h_4(i),'P',P_m(i),Ref);

h_6s(i)=refpropm('H','P',P_c(i),'S',s_1(i),Ref);
h_6(i)=h_1(i)+(h_6s(i)-h_1(i))/eta_comp_ht(i);
s_6(i)=refpropm('S','H',h_6(i),'P',P_c(i),Ref);
T_6(i)=refpropm('T','P',P_c(i),'H',h_6(i),Ref);

T_7(i)=T_c(i);
h_7(i)=refpropm('H','T',T_7(i),'P',P_c(i),Ref);
s_7(i)=refpropm('S','H',h_7(i),'P',P_c(i),Ref);

h_8(i)=h_7(i);
s_8(i)=refpropm('S','H',h_8(i),'P',P_m(i),Ref);

h_5(i)=h_4(i);
s_5(i)=refpropm('S','H',h_5(i),'P',P_e(i),Ref);

%x-greier
m_r_ht(i)=rho_1(i)*(comp_size_ht/3600)*vol_eff_ht(i)*heat_ratio(i)*0.2;
m_r_mt23(i)=rho_1(i)*(comp_size_mt/3600)*vol_eff_mt(i)*heat_ratio(i)*0.2;

h_3(i)=refpropm('H','P',P_m(i),'Q',1,Ref);
x_8(i)=(h_7(i)-h_4(i))/(h_3(i)-h_4(i));

m_r_mt483(i)=m_r_ht(i)*x_8(i);
m_r_mt34(i)=m_r_mt23(i)+m_r_mt483(i);
%Vedier
W_r_ht(i)=m_r_ht(i)*(h_6(i)-h_1(i))/1000; %kW
W_r_mt(i)=m_r_mt23(i)*(h_2(i)-h_1(i))/1000; %kW
W_r_tot(i)=W_r_mt(i)+W_r_ht(i);
Q_c_ht(i)=m_r_ht(i)*(h_6(i)-h_7(i))/1000; %kW, Capacity of HT condenser
Q_c_mt(i)=m_r_mt34(i)*(h_2(i)-h_4(i))/1000; %kW, Capacity of MT condenser
Q_c_tot(i)=Q_c_ht(i)+Q_c_mt(i);
Q_e(i)=(m_r_ht(i)+m_r_mt23(i))*(h_1(i)-h_5(i))/1000; %kW
COP_ht(i)=Q_c_ht(i)/W_r_ht(i);
COP_mt(i)=Q_c_mt(i)/W_r_mt(i);
COP_tot(i)=(Q_c_ht(i)+Q_c_mt(i))/(W_r_ht(i)+W_r_mt(i));

%LT Condenser
T_mw_out(i)=T_mw_in(i)+Q_c_mt(i)/(Cp_mw/1000*m_mw);
dT_lmtd_cond_mt(i)=Q_c_mt(i)*1000/UA_cond_mt;
A(i)=exp((T_mw_out(i)-T_mw_in(i))/dT_lmtd_cond_mt(i));
T_m2(i)=(T_mw_in(i)-T_mw_out(i)*A(i))/(1-A(i));

%HT Condenser
T_hw_in(i)=T_mw_out(i); %inlet temerature of water to be heated (coolant)
rho_hw=refpropm('D','T',T_hw_in(i),'Q',1,'Water');
Cp_hw=refpropm('C','T',T_hw_in(i),'Q',1,'Water'); % J/kgK.
T_hw_out(i)=T_hw_in(i)+Q_c_ht(i)/(m_hw *Cp_hw/1000);

dT_lmtd_cond_ht(i)=Q_c_ht(i)*1000/UA_cond_ht;
```

```
B(i)=exp((T_hw_out(i)-T_hw_in(i))/dT_lmtd_cond_ht(i));
T_c2(i)=(T_hw_in(i)-T_hw_out(i)*B(i))/(1-B(i));

%Evaporator
T_cw_out(i)=T_cw_in-Q_e(i)/(Cp_cw/1000*m_cw);
dT_lmtd_evap(i)=Q_e(i)*1000/UA_evap;
T_e2(i)=(T_cw_out(i)*exp((T_cw_in-T_cw_out(i))/dT_lmtd_evap(i))-T_cw_in)/(exp((T_cw_in-
T_cw_out(i))/dT_lmtd_evap(i))-1);

%New values
dTe(i)= (T_e(i)-T_e2(i))/2;
dTc(i)=(T_c(i)-T_c2(i))/2;
dTm(i)=(T_m(i)-T_m2(i));
T_c(i)=T_c(i)-dTc(i);
T_e(i)=T_e(i)-dTe(i);
T_m(i)=T_m(i)-dTm(i);

end %while.

twentyprheat=[twentyprheat i];
if W_r_tot(i-1)>battery_capacity(i-1)+E(i-1) && W_r_tot(i)>W_r_tot(i-1)

    Q_c_tot(i)=Q_c_tot(i-1);
    W_r_tot(i)=W_r_tot(i-1);
    COP_tot(i)=COP_tot(i-1);
end

end %if 20

if (E(i)+battery_capacity(i))<W_r_tot(i)

    T_c(i)=T_c(i-1);
    T_m(i)=T_m(i-1);
    T_e(i)=T_e(i-1);
    T_hw_out(i)=365.3838;
    T_mw_out(i)=350.9679;
    Q_c_ht(i)=0;
    Q_c_mt(i)=0;
    Q_c_tot(i)=0;
    Q_e(i)=0;
    W_r_ht(i)=0;
    W_r_mt(i)=0;
    W_r_tot(i)=0;
    COP_ht(i)=2.8743;
    COP_mt(i)=4.3872;
    COP_tot(i)=3.5435;
end


if TES_capacity(i)>=Demand(i) && TES_capacity(i)<TES_capacity(i-1)
    compressor_load(i)=0;

    T_c(i)=T_c(i-1);
    T_m(i)=T_m(i-1);
    T_e(i)=T_e(i-1);
    T_hw_out(i)=365.3838;
    T_mw_out(i)=350.9679;
    Q_c_ht(i)=0;
```

```
    Q_c_mt(i)=0;
    Q_c_tot(i)=0;
    Q_e(i)=0;
    W_r_ht(i)=0;
    W_r_mt(i)=0;
    W_r_tot(i)=0;
    COP_ht(i)=2.8743;
    COP_mt(i)=4.3872;
    COP_tot(i)=3.5435;
elseif TES_capacity(i)>=TES_capacity_max
    compressor_load(i)=0;

    T_c(i)=T_c(i-1);
    T_m(i)=T_m(i-1);
    T_e(i)=T_e(i-1);
    T_hw_out(i)=365.3838;
    T_mw_out(i)=350.9679;
    Q_c_ht(i)=0;
    Q_c_mt(i)=0;
    Q_c_tot(i)=0;
    Q_e(i)=0;
    W_r_ht(i)=0;
    W_r_mt(i)=0;
    W_r_tot(i)=0;
    COP_ht(i)=2.8743;
    COP_mt(i)=4.3872;
    COP_tot(i)=3.5435;

end %lager nullverdier

T_supply(i)=T_hw_out(i);
if Q_c_tot==0
    T_supply(i)=273.15+80;
end

TES_output(i)=(Demand(i)-Q_c_tot(i))*1.1;
TES_capacity(i+1)=(TES_capacity(i)-TES_output(i));
battery_output(i)=(W_r_tot(i)-E(i))*1.2;
battery_capacity(i+1)=(battery_capacity(i)-battery_output(i));

load_ratio(i)=Q_c_tot(i)/255;

if TES_output(i)>=TES_capacity(i)
    TES_output(i)=TES_capacity(i);
end
if battery_output(i)>=battery_capacity(i)
    battery_output(i)=battery_capacity(i);
end


if TES_output(i)>0
    output_from_TES(i)=TES_output(i);
    heat_from_TES_to_DH(i)=(TES_output(i)/1.1)*0.9;
elseif TES_output(i)<0
    input_to_TES(i)=-TES_output(i);
    heat_from_HP_to_TES(i)=(-TES_output(i)/1.1)*0.9;
end
```

```
if battery_output(i)>0
    output_from_battery(i)=battery_output(i);
    power_from_battery_to_HP(i)=(battery_output(i)/1.2)*0.8;
elseif battery_output(i)<0
    input_to_battery(i)=-battery_output(i);
    power_from_PV_to_battery(i)=(-battery_output(i)/1.2)*0.8;
end

if Q_c_tot(i)>0
    hours_onBJ=hours_onBJ+1;
elseif Q_c_tot(i)<255 &&Q_c_tot(i)>0
    hours_partloadBJ=hours_partloadBJ+1;
end

if Q_c_tot(i)>Demand(i)
    energy_to_dh(i)=Demand(i);
elseif Q_c_tot(i)+TES_capacity(i)>=Demand(i)
    energy_to_dh(i)=Demand(i);
elseif Q_c_tot(i)+TES_capacity(i)<Demand(i)
    energy_to_dh(i)=Q_c_tot(i)+TES_capacity(i);
else
    energy_to_dh(i)=0;
end


end%for
figure(1)
plot(hour,Q_c_tot)

figure(2)
plot(hour,T_c,hour,T_m,hour,T_hw_out,hour,T_mw_out)
legend('Tc','Tm','Thw','Tmw')

% figure(3)
% plot(hour,COP_tot)


combined_energyBJ=[Demand 0;Q_c_tot 0;TES_capacity];
combined_powerBJ=[W_r_tot 0;E 0;battery_capacity];
combined_watertempBJ=[T_m;T_c;T_mw_out;T_hw_out;T_e;T_cw_out;T_return];
combined_COPBJ=[COP_tot;COP_mt;COP_ht];
combined_TESBJ=[output_from_TES;input_to_TES;heat_from_TES_to_DH;heat_from_HP_to_TES];
combined_battBJ=[output_from_battery;input_to_battery;power_from_battery_to_HP;power_from_PV_t
o_battery];
```

```
Warning: Variable names were modified to make them valid MATLAB identifiers. The
original names are saved in the VariableDescriptions property.
```

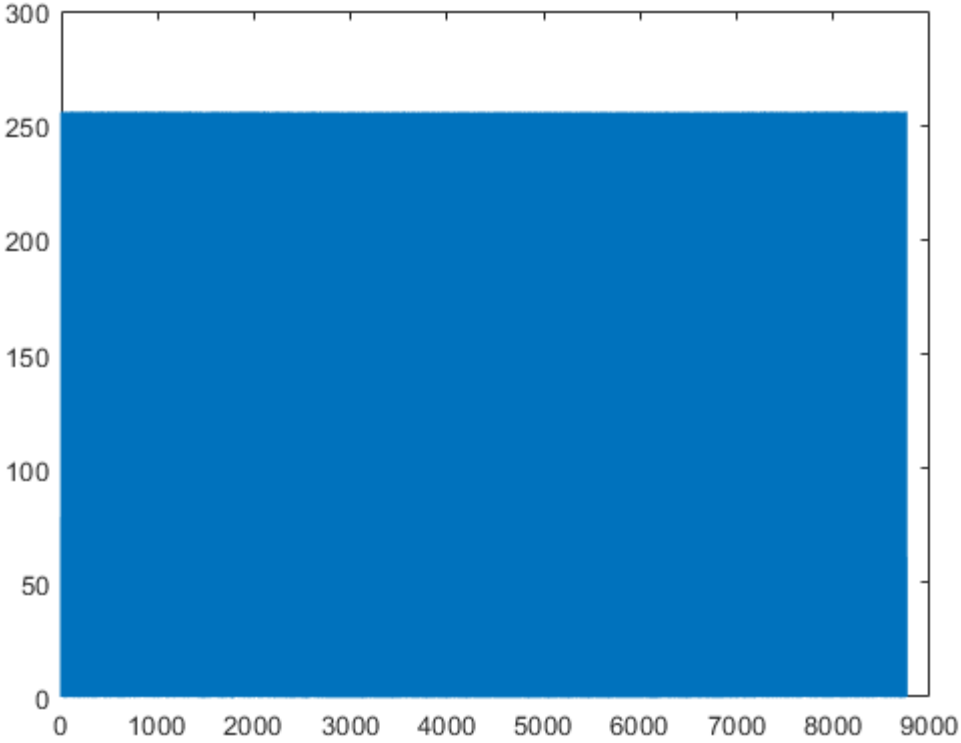

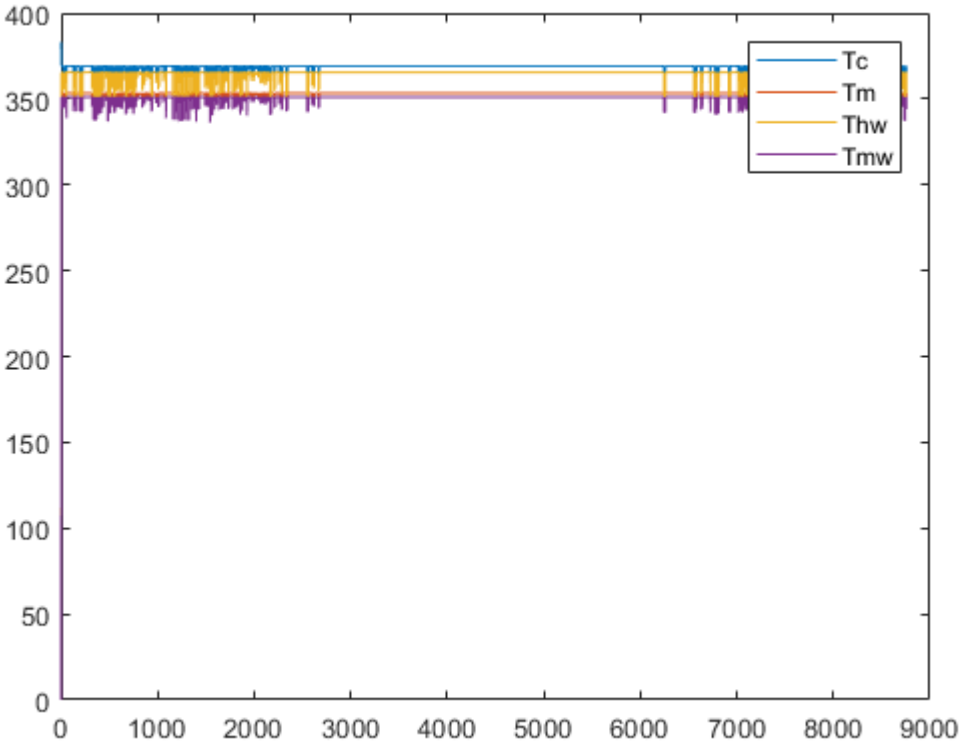

Published with MATLAB® R2017b

Appendix B: Results from simulations

Hourly heat capacity, thermal storage, and heat demand in Beijing, January:

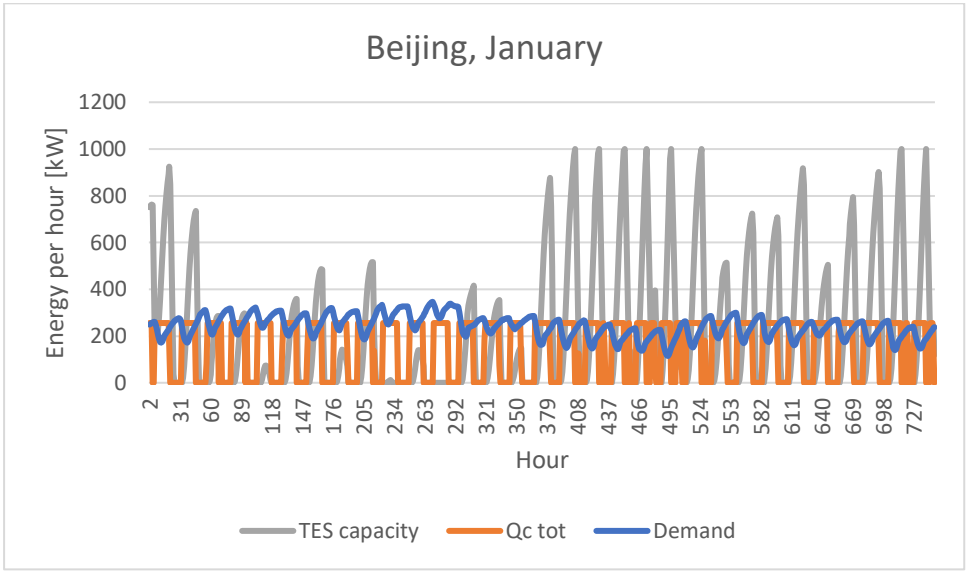

Hourly heat demand and available heat in Beijing, January:

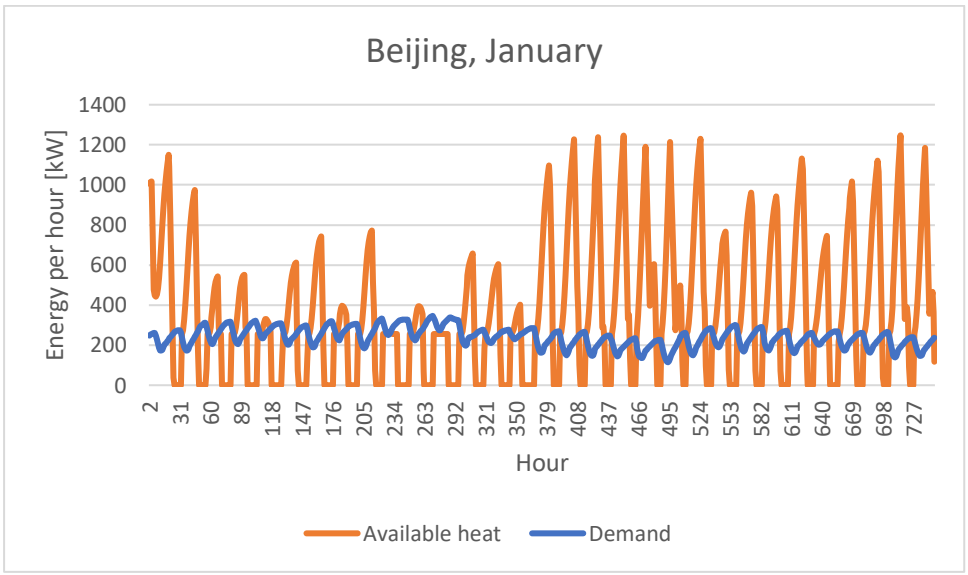

Hourly energy produced by PV, battery capacity, and power consumption of the compressor in Beijing, January:

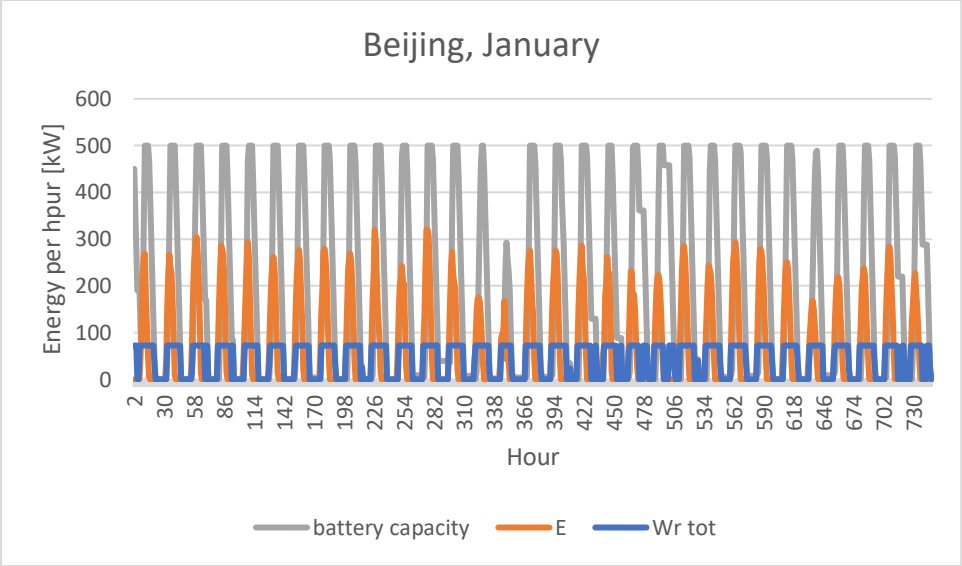

Hourly available power and energy consumption by the compressor in Beijing, January:

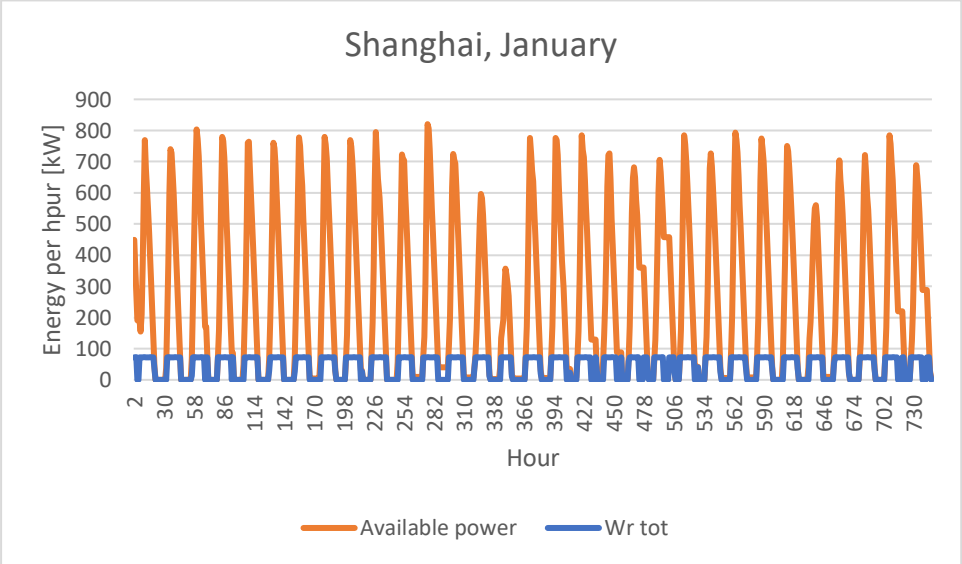

Hourly heat capacity, thermal storage, and heat demand in Lanzhou, January:

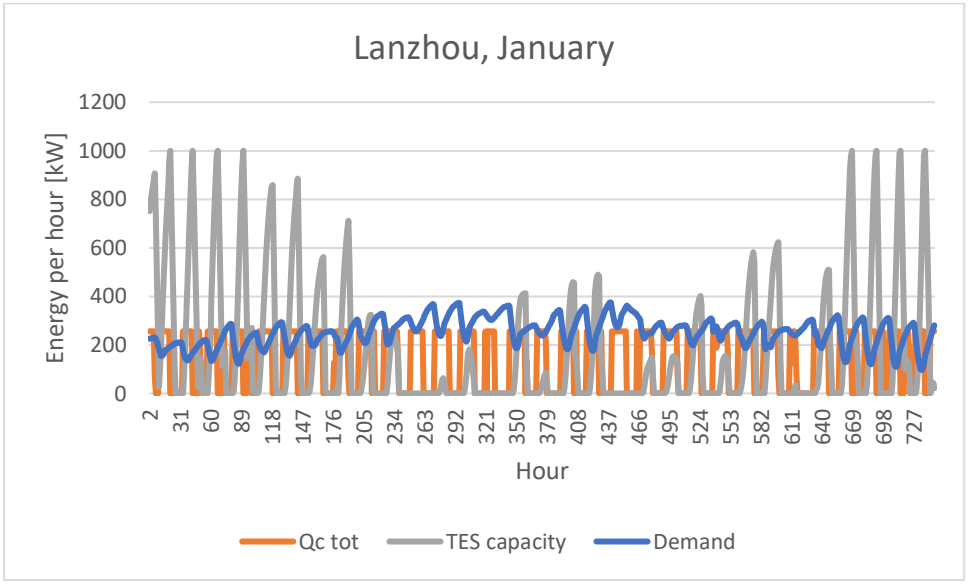

Hourly heat demand and available heat in Lanzhou, January:

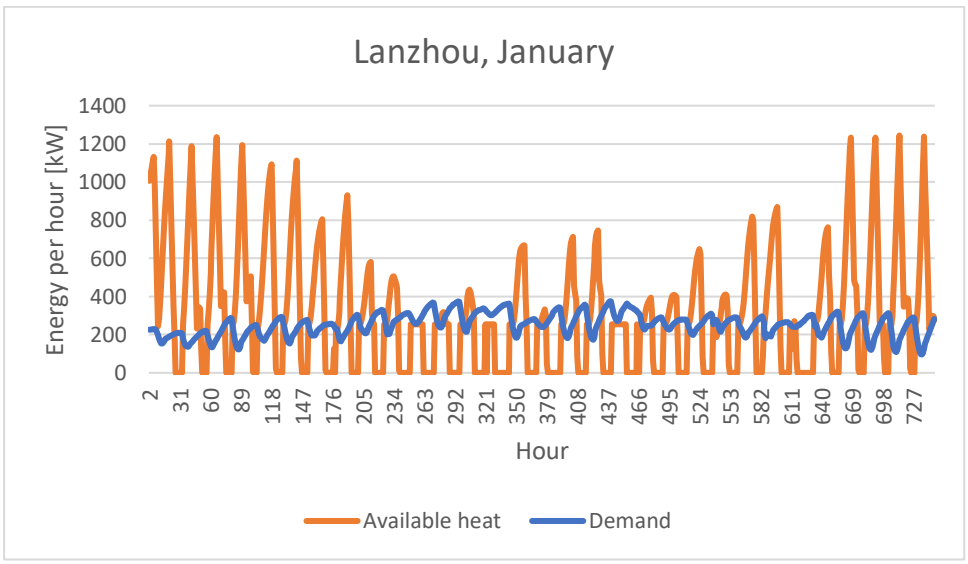

Hourly energy produced by PV, battery capacity, and power consumption of the compressor in Lanzhou, January:

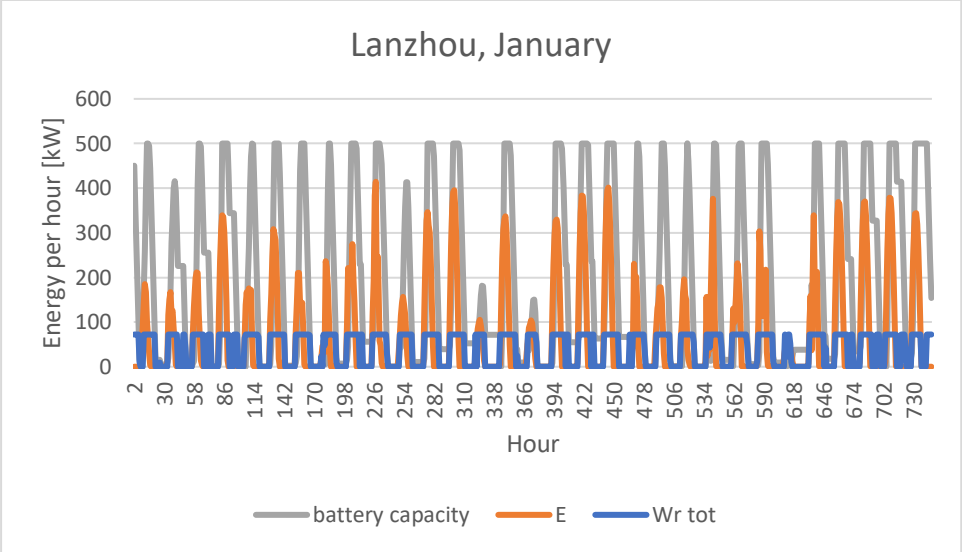

Hourly available power and energy consumption by the compressor in Lanzhou, January:

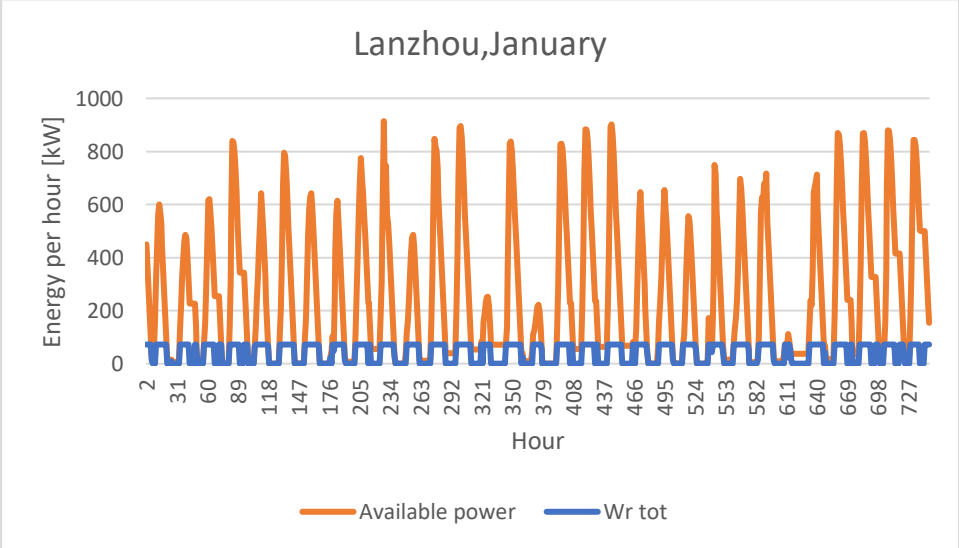

Hourly heat demand and available heat in Shanghai, January12-18

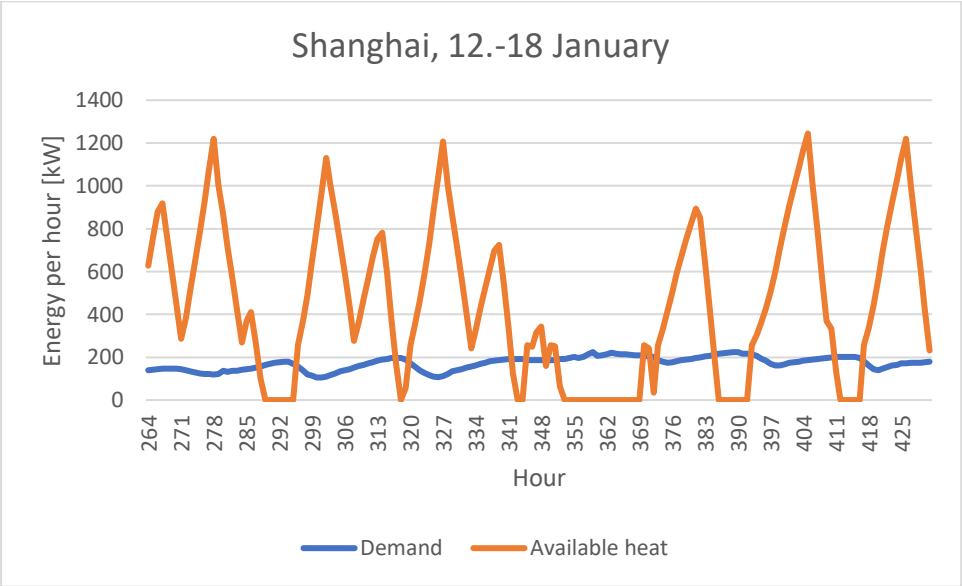

Hourly available power and energy consumption by the compressor in Shanghai, January 12-18:

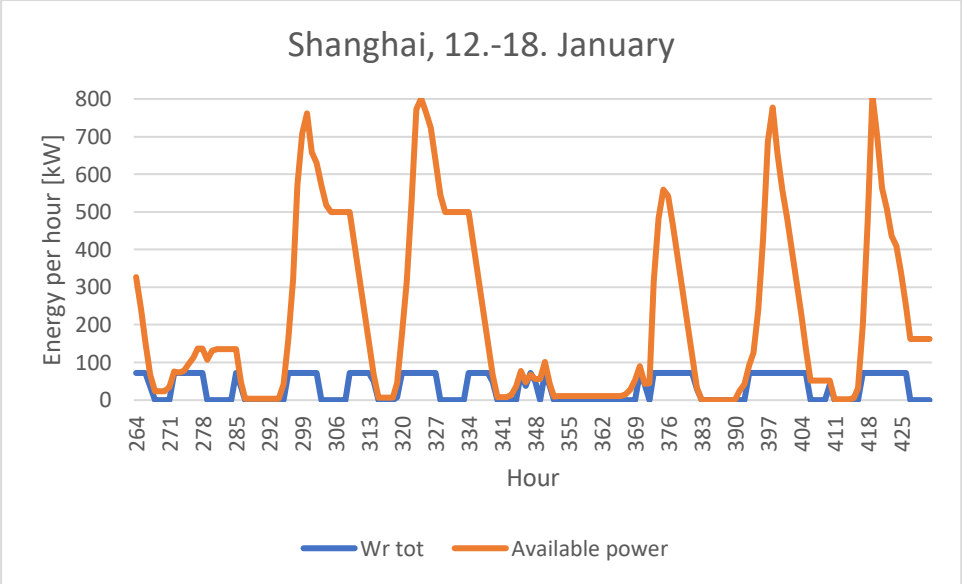

Hourly heat demand and available heat in Beijing, January12-18

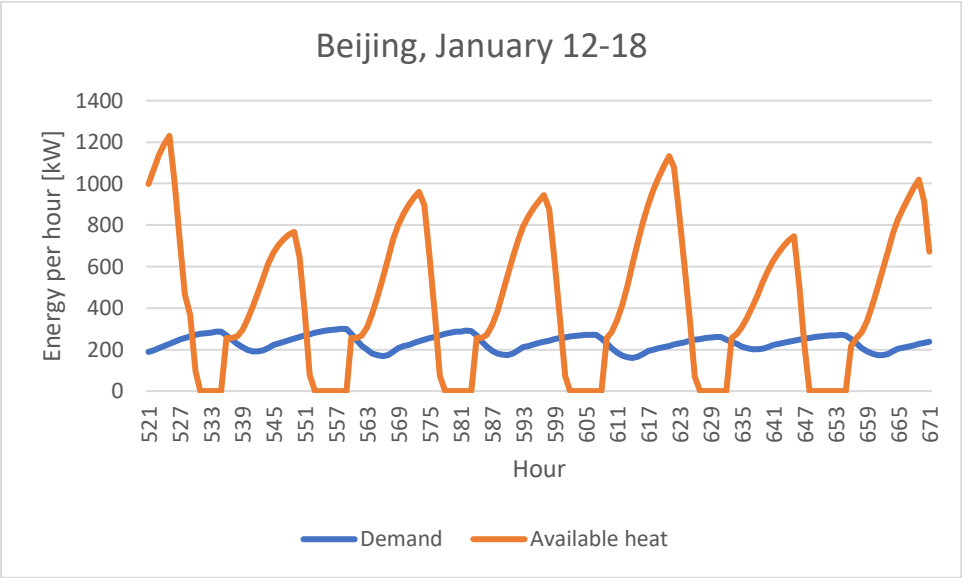

Hourly available power and energy consumption by the compressor in Beijing, January 12-18:

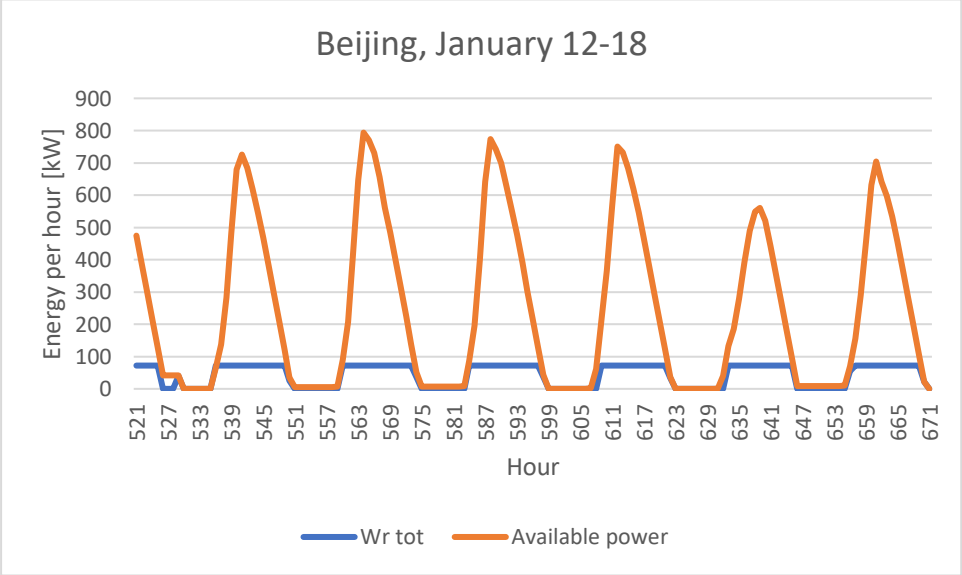

Hourly temperatures in the condensers in Lanzhou, January

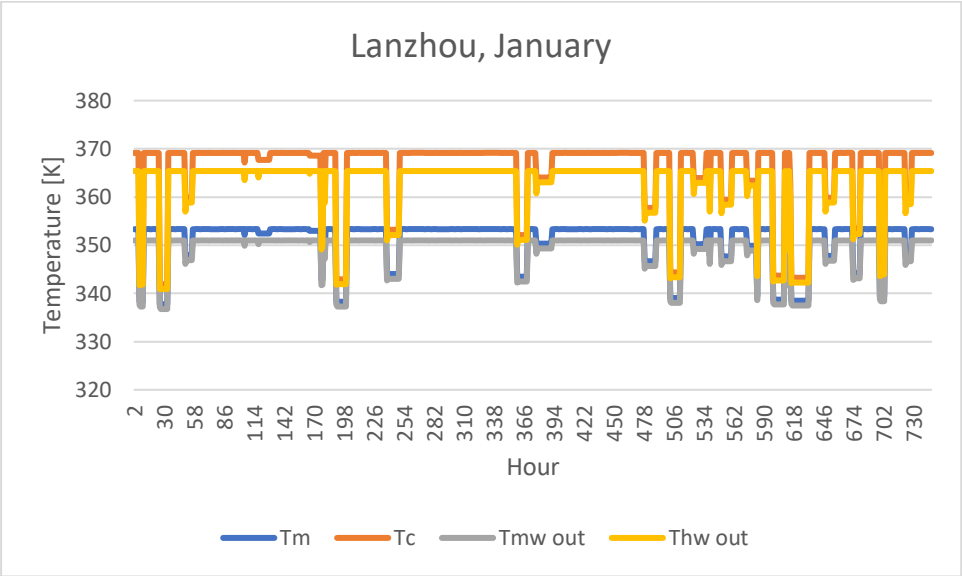

Hourly temperatures in the condensers in Beijing, January

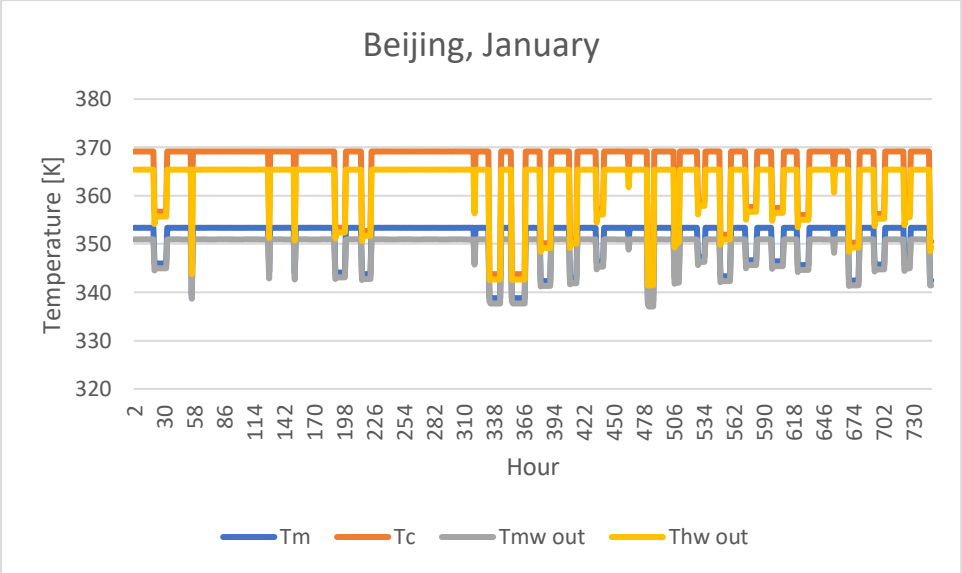

Hourly COP in Lanzhou, January

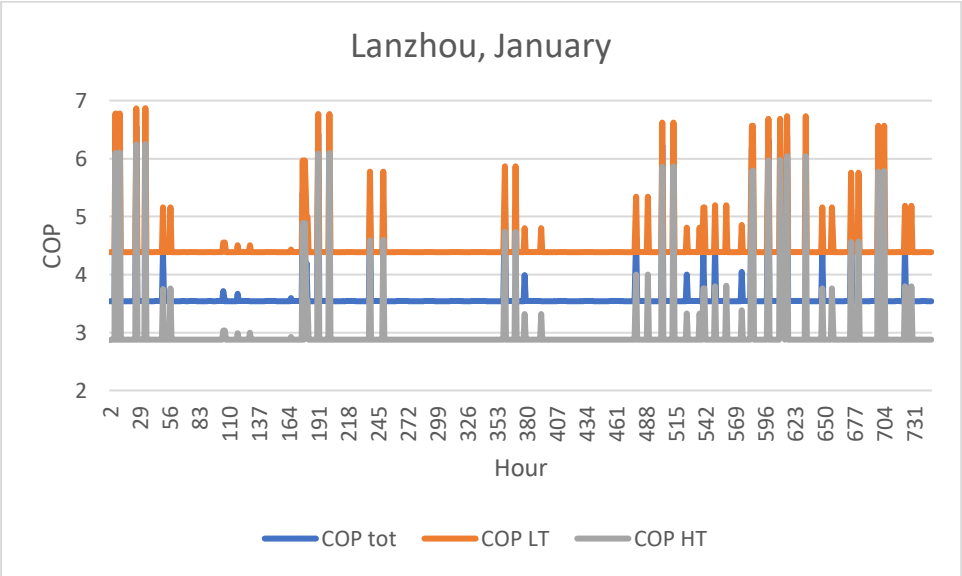

Hourly COP in Beijing, January

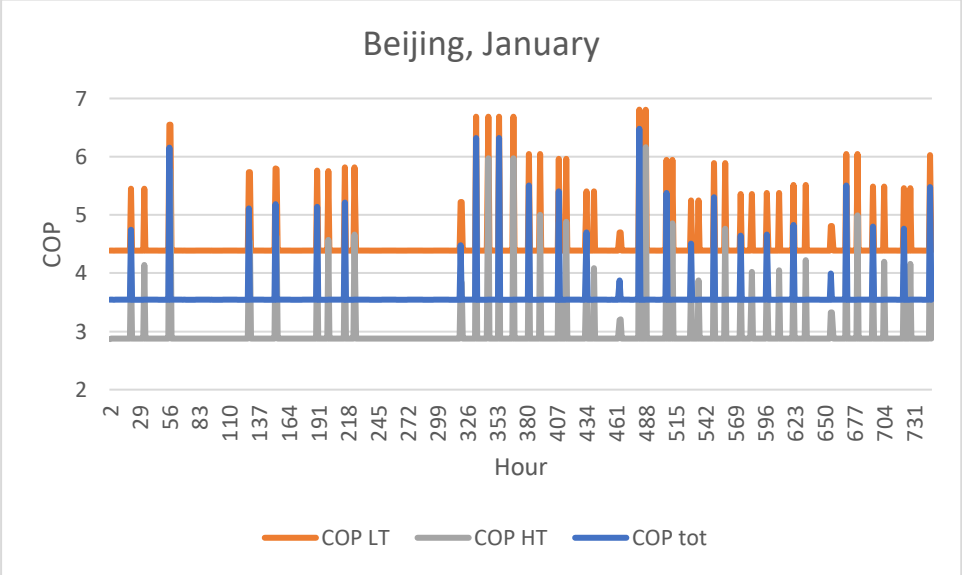

Hourly heat capacity, thermal storage, and heat demand in Shanghai, July:

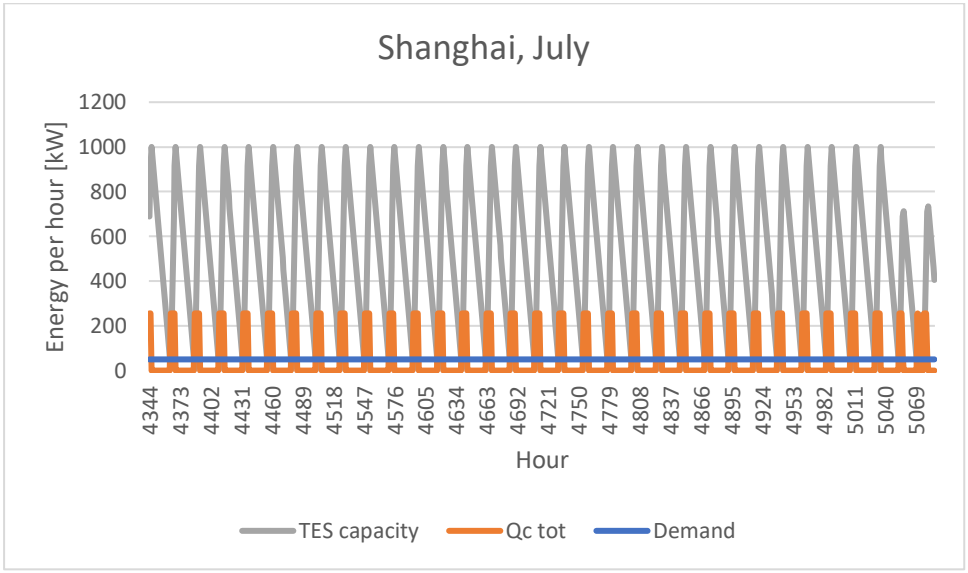

Hourly heat demand and available heat in Shanghai, July:

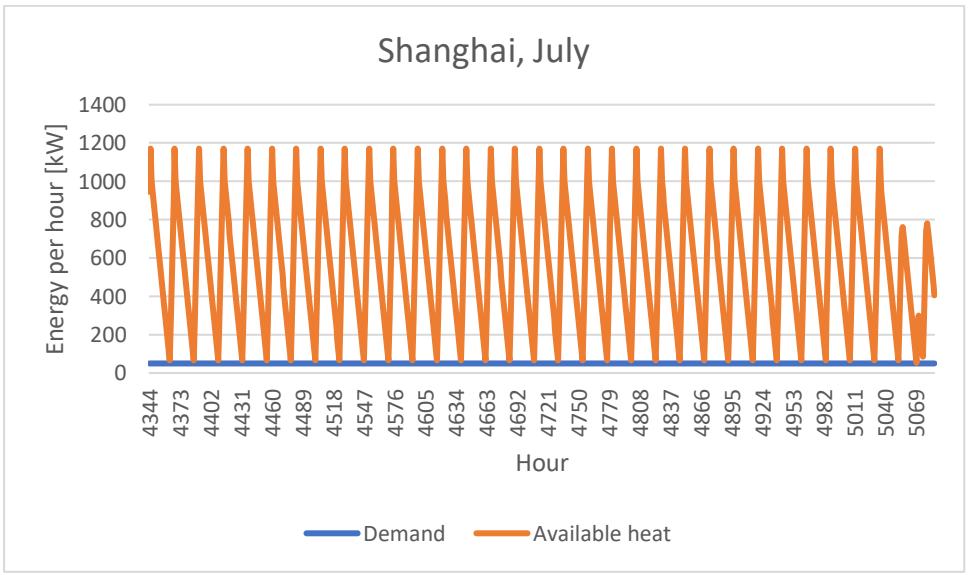

Temperatures in condenser in Shanghai in July

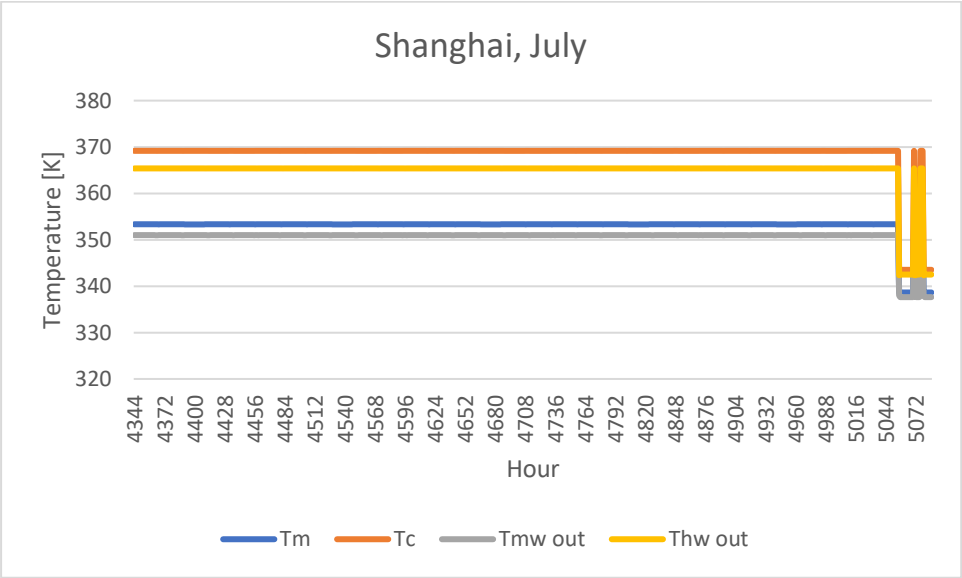

Temperatures in the condenser in Lanzhou in July

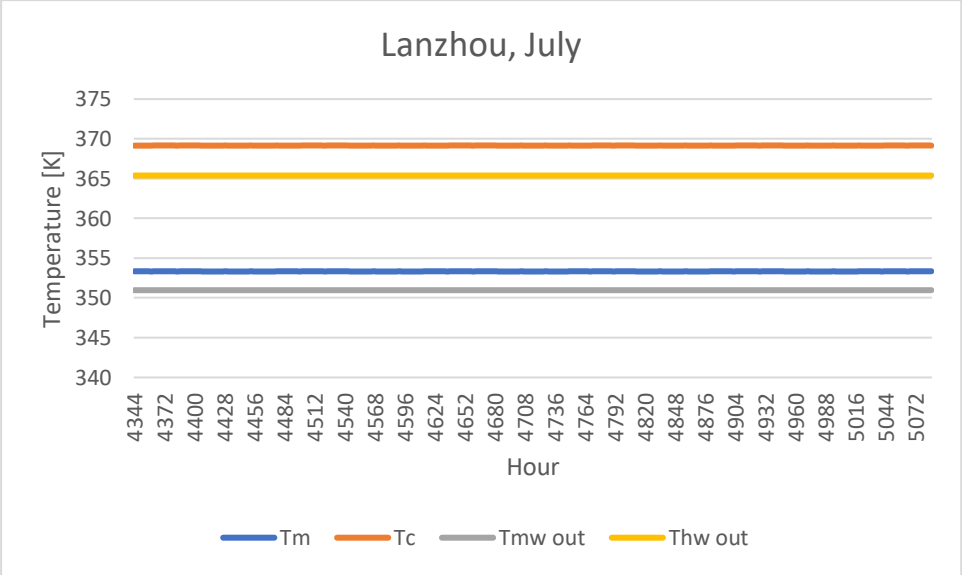

COP in Shanghai, July

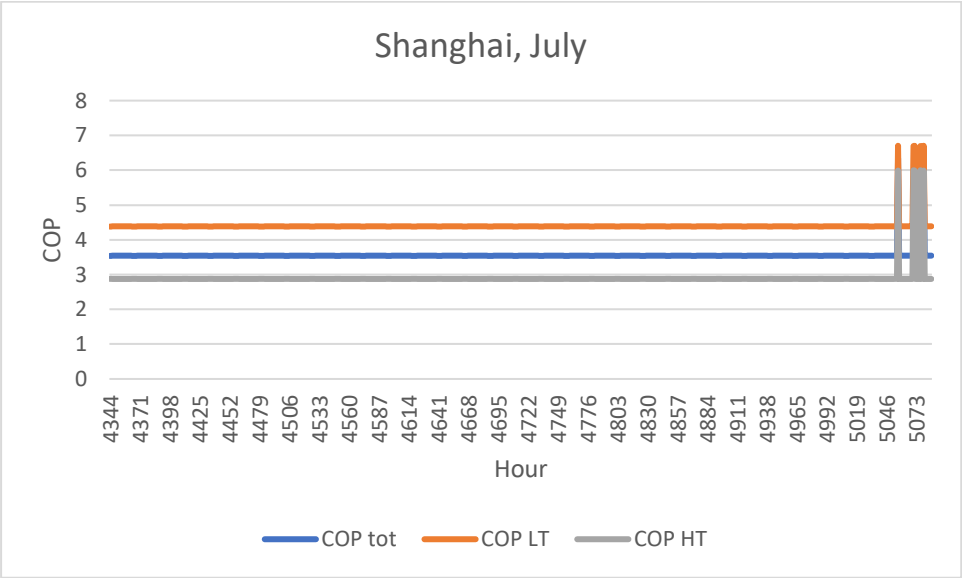

COP in Lanzhou, July

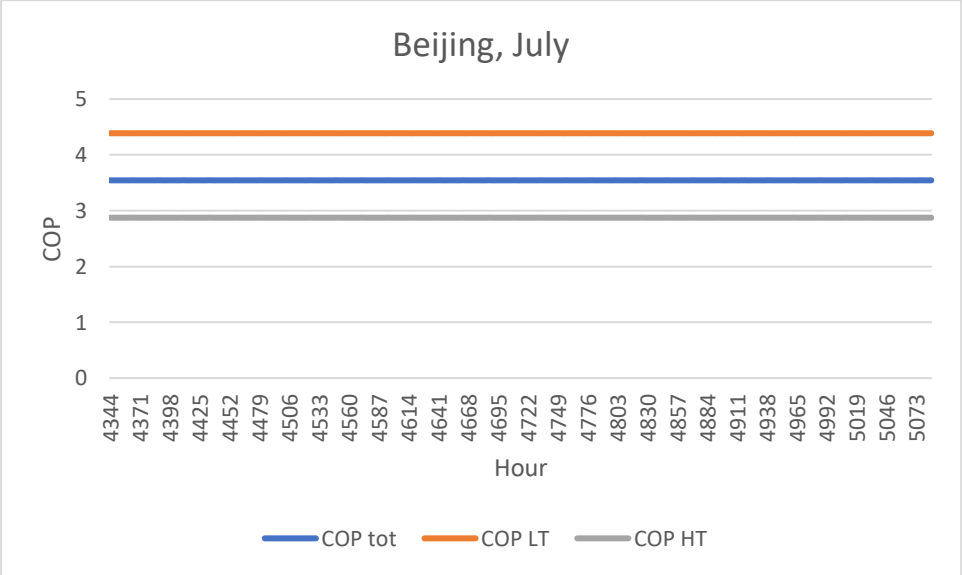

Hourly energy produced by PV, battery capacity, and power consumption of the compressor in Shanghai, July:

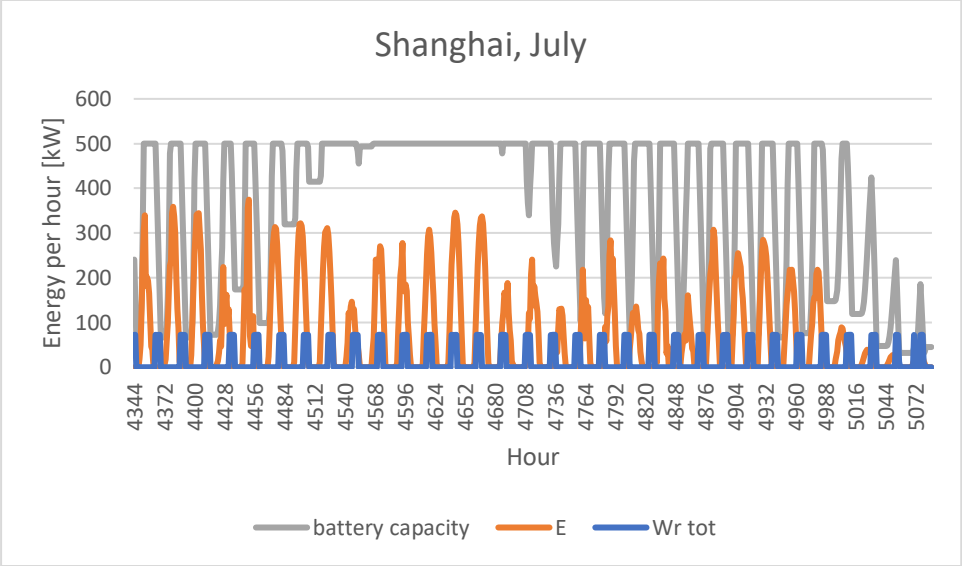

Hourly available power and energy consumption by the compressor in Shanghai, July:

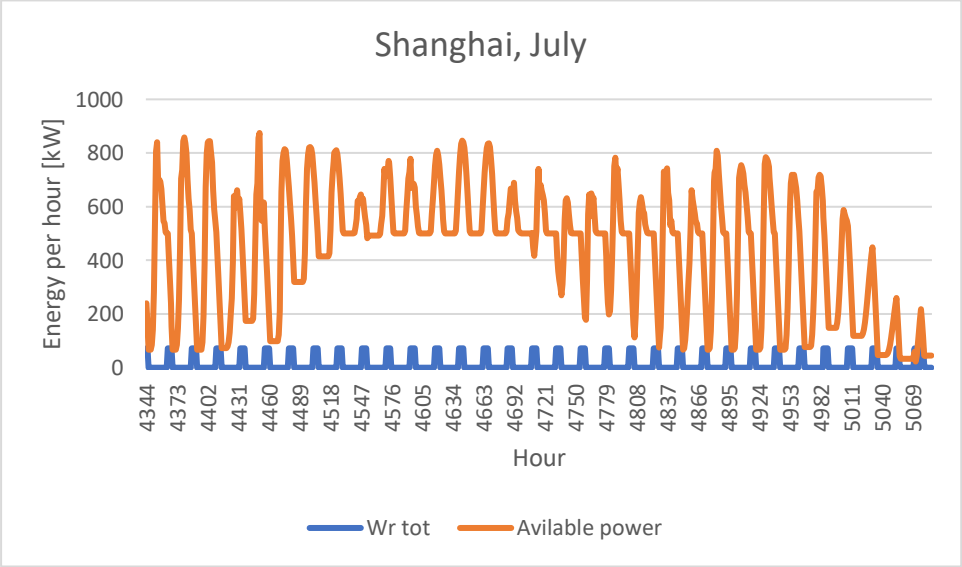

Hourly heat capacity, thermal storage, and heat demand in Beijing, July:

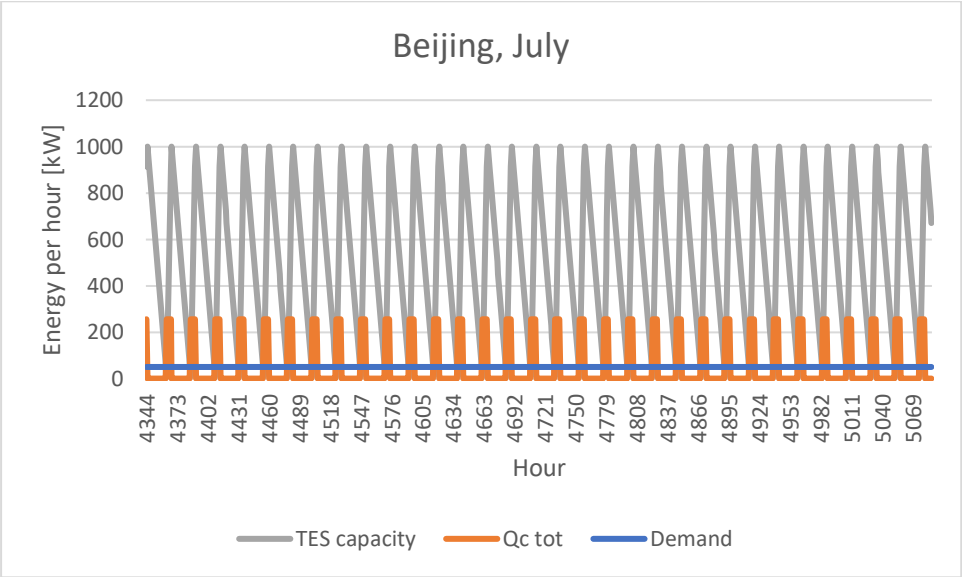

Hourly heat demand and available heat in Beijing, July:

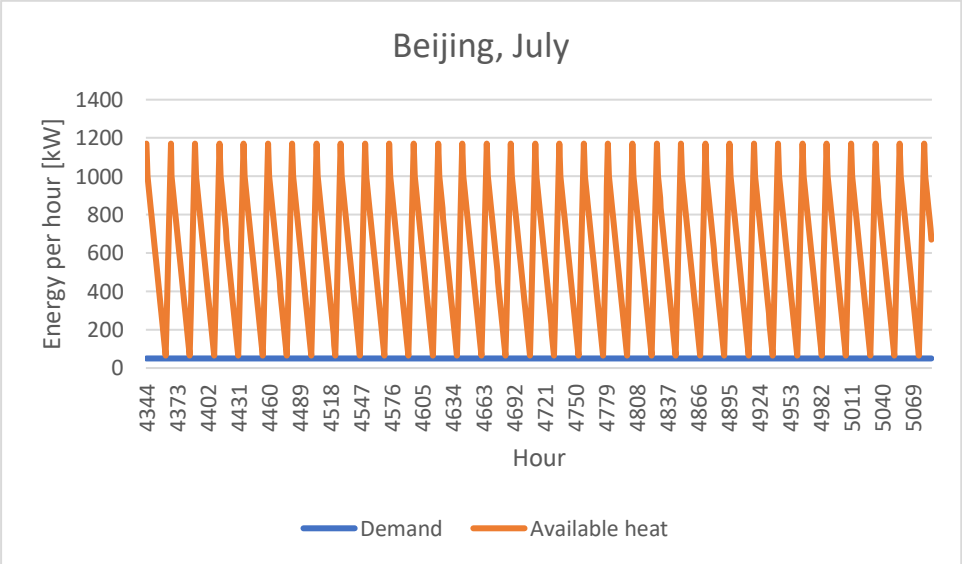

Hourly energy produced by PV, battery capacity, and power consumption of the compressor in Beijing, July:

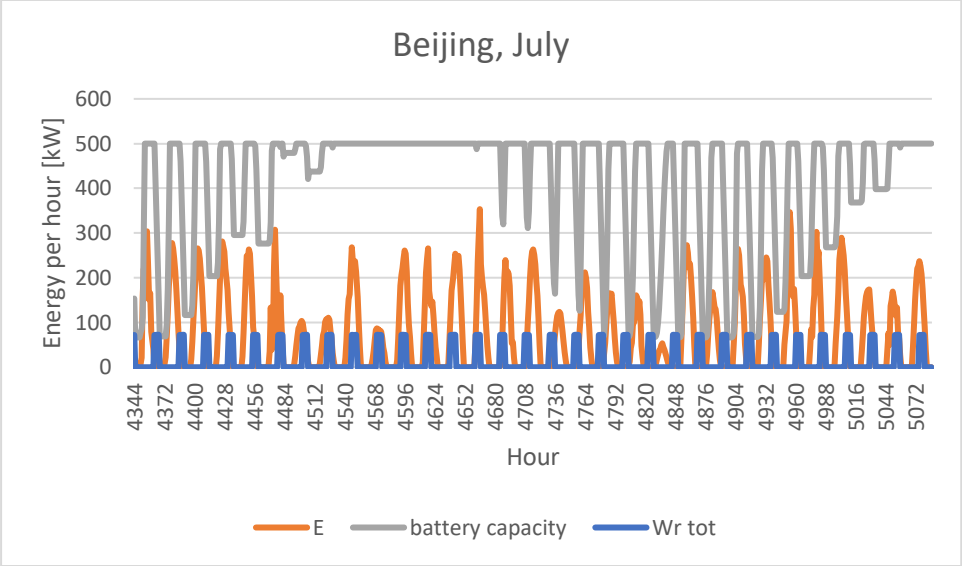

Hourly available power and energy consumption by the compressor in Beijing, July:

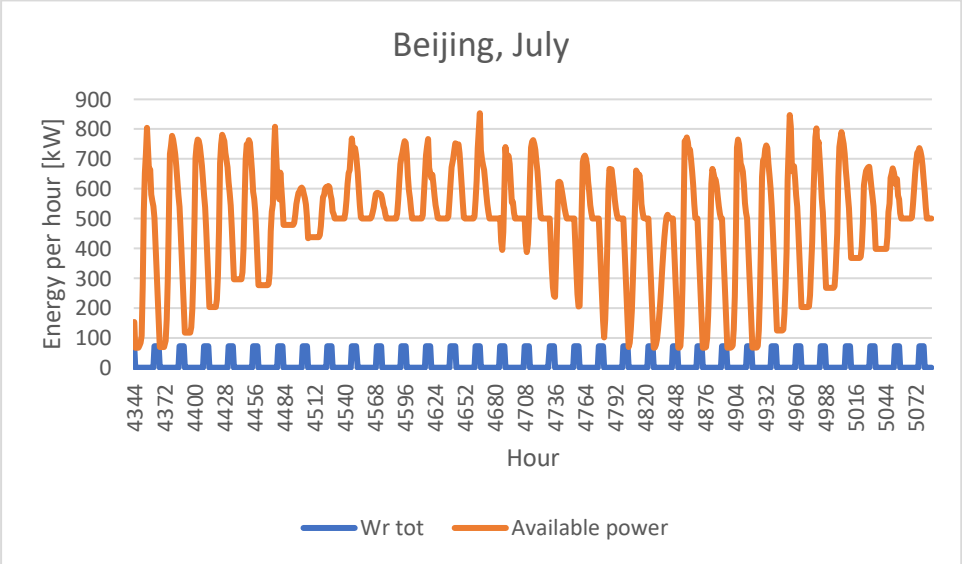

Hourly heat capacity, thermal storage, and heat demand in Lanzhou, April:

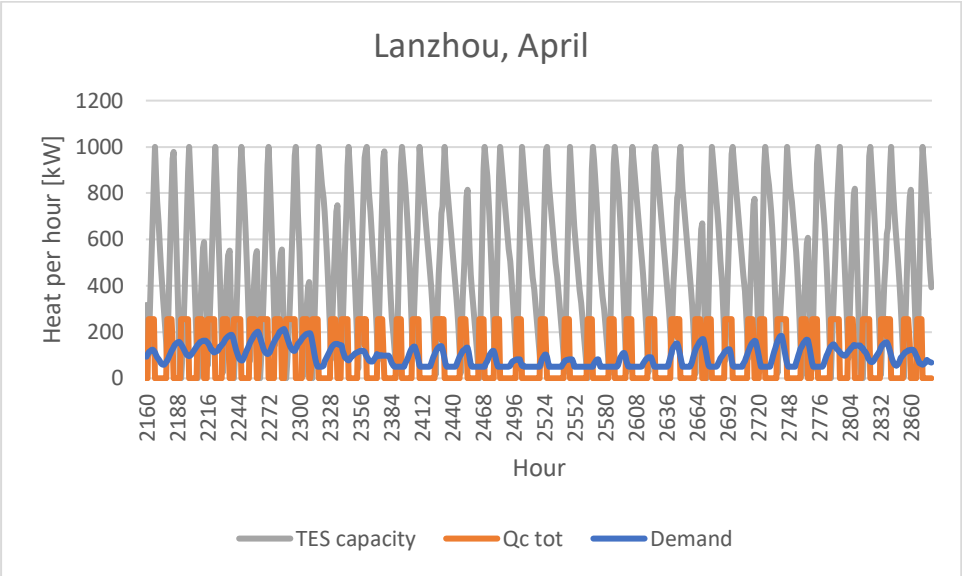

Hourly heat demand and available heat in Lanzhou, April:

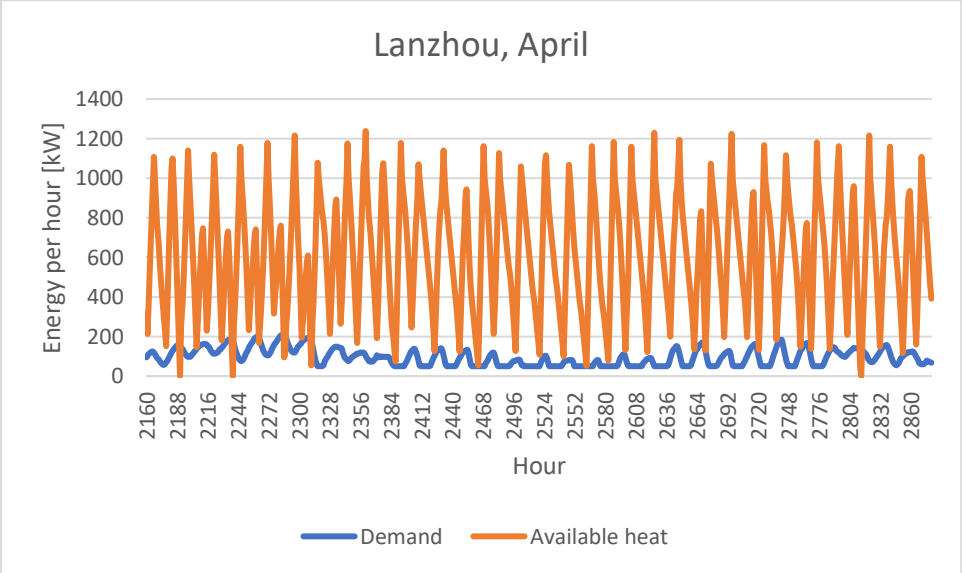

Hourly energy produced by PV, battery capacity, and power consumption of the compressor in Lanzhou, April:

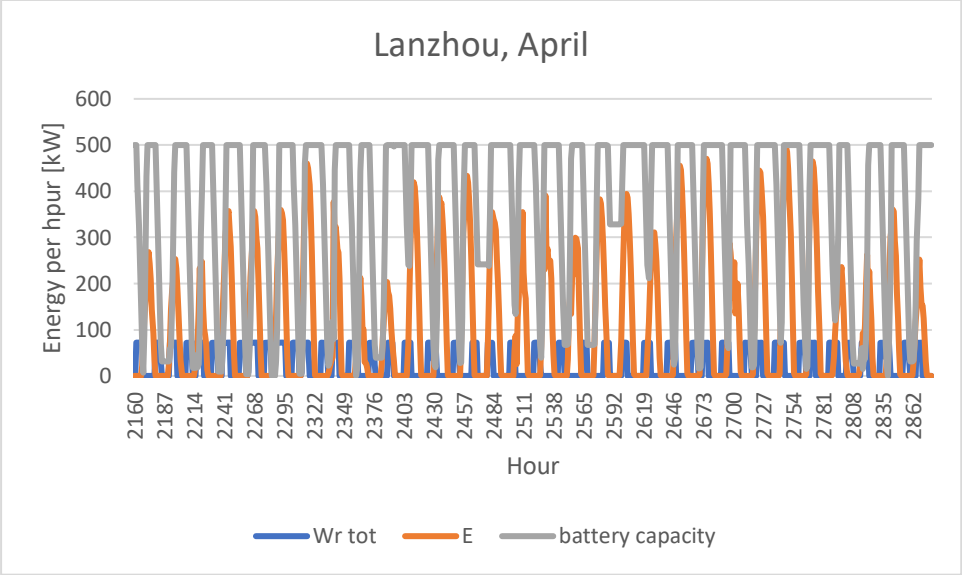

Hourly available power and energy consumption by the compressor in Lanzhou, April:

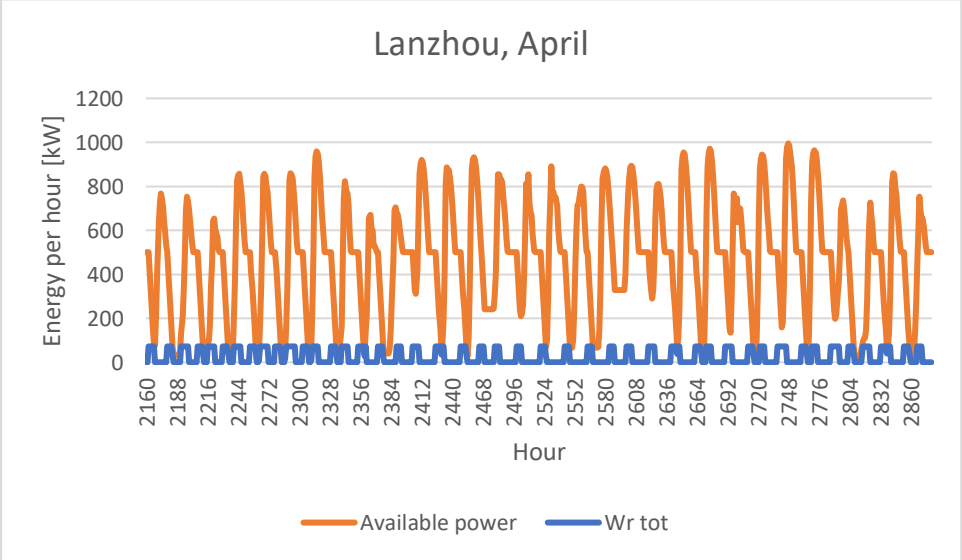

Hourly heat capacity, thermal storage, and heat demand in Shanghai, April:

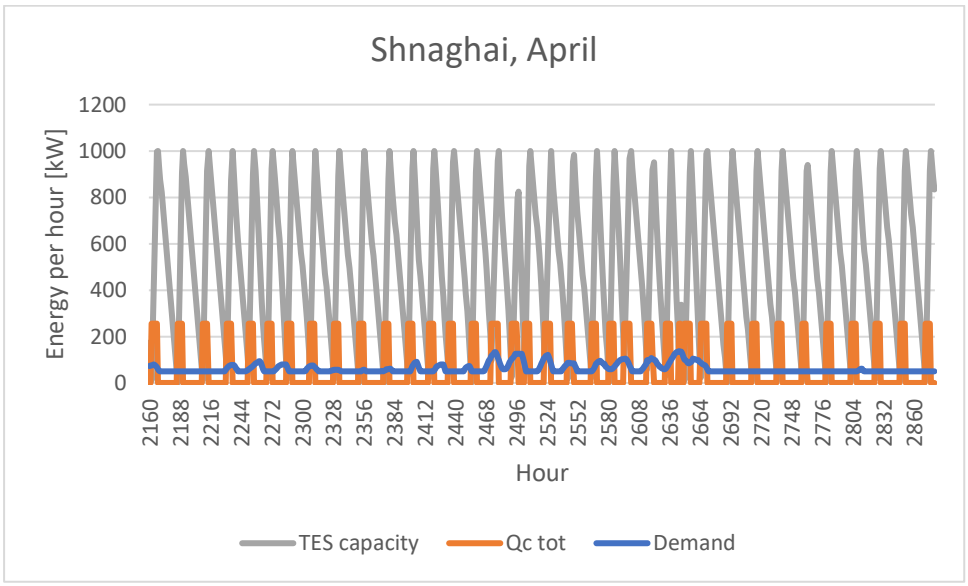

Hourly heat demand and available heat in Shanghai, April:

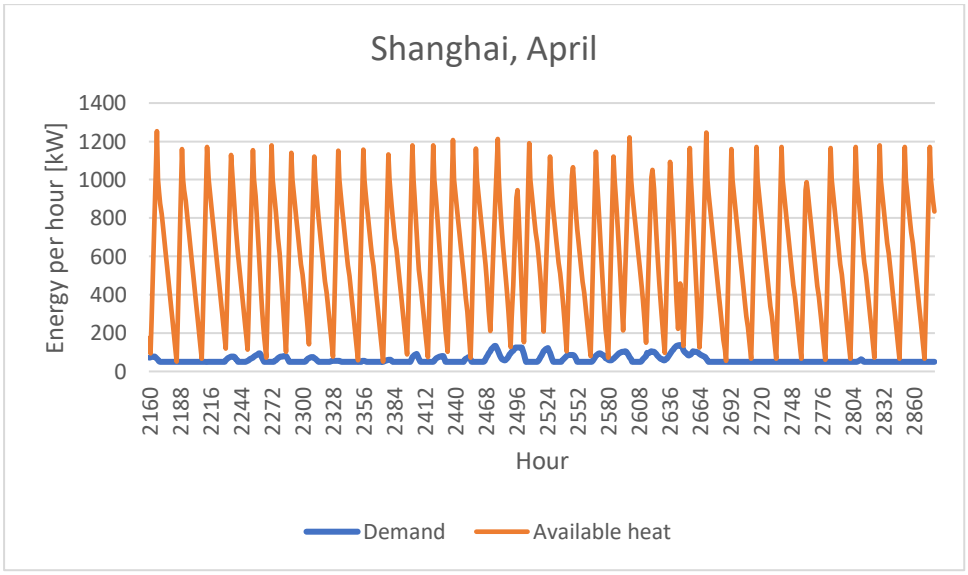

Hourly energy produced by PV, battery capacity, and power consumption of the compressor in Shanghai, April:

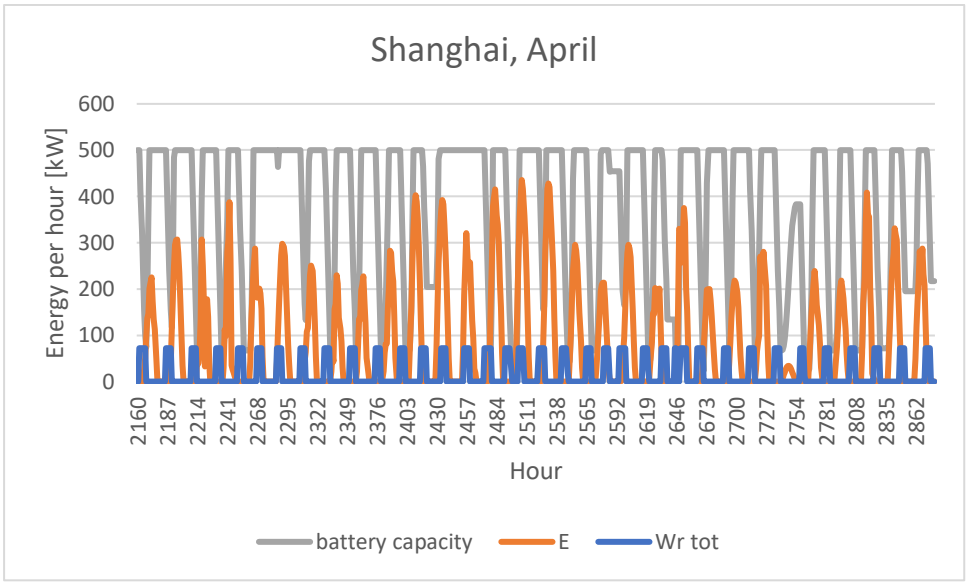

Hourly available power and energy consumption by the compressor in Shanghai, April:

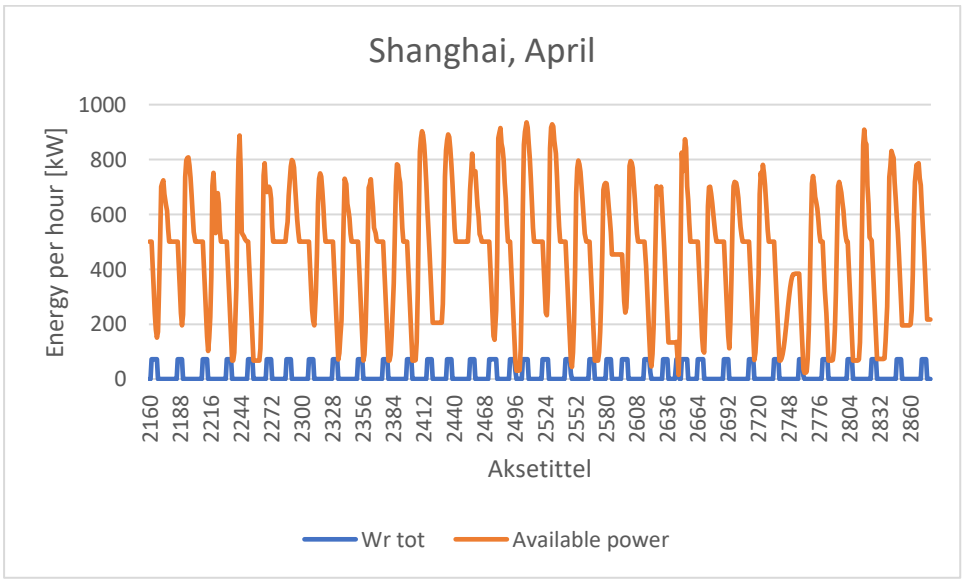

Temperatures in the condenser and return water temperatures in Beijing, April:

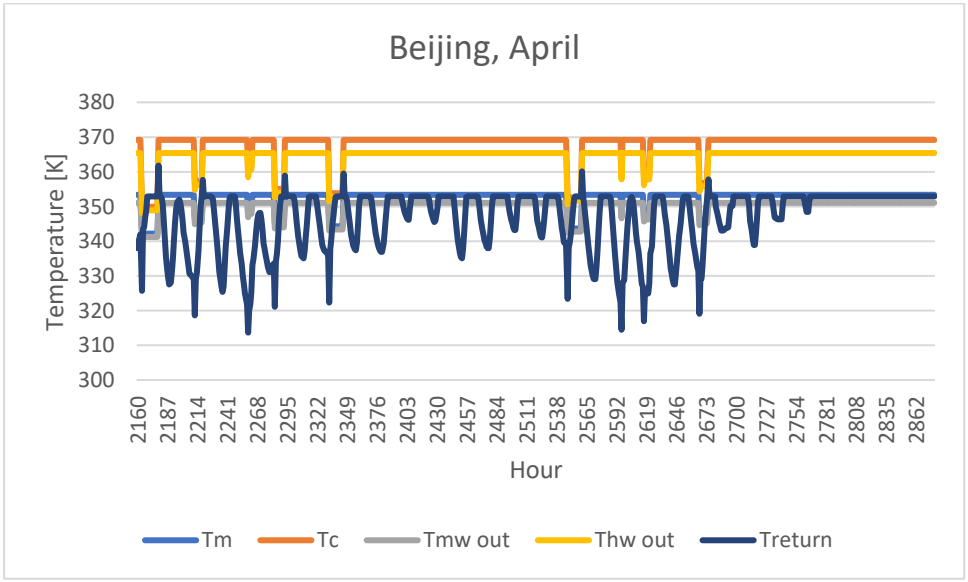

COP in Beijing, April:

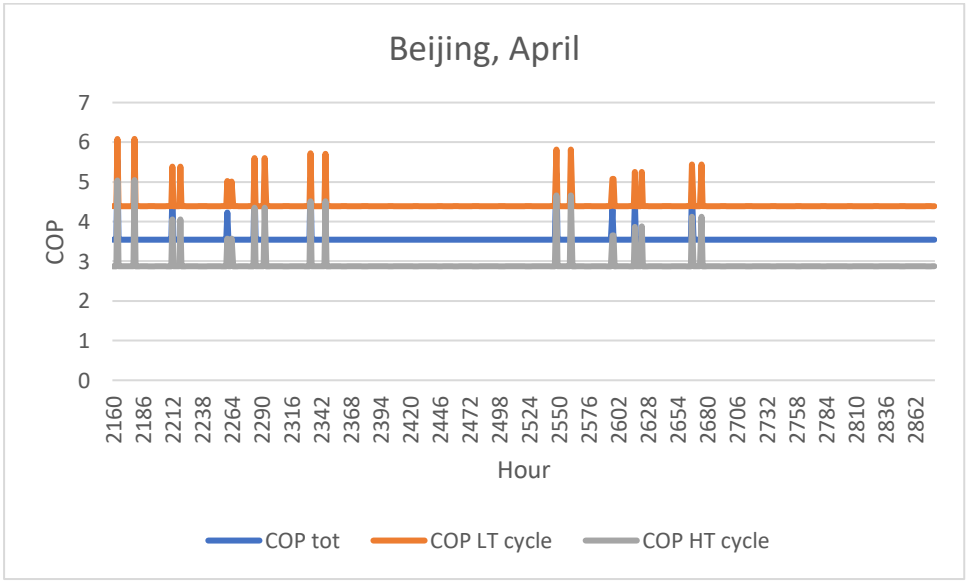

Appendix C: Draft Scientific Paper

Simulation of a high-temperature ammonia heat pump in an integrated energy system

Signe Truyen Ryssdal[1,2], Trygve M. Eikevik[1], Ruzhu Wang[2], Bin Hu[2]
[1] Department of Energy and Process Engineering, Norwegian University of Science and Technology, Trondheim, Norway
[2] Institute of Refrigeration and Cryogenics, Shanghai, Jiao Tong University, Shanghai, China

Email:
signetr@stud.ntnu.no

Received xxxxxx
Accepted for publication xxxxxx
Published xxxxxx

Abstract

A high-temperature ammonia heat pump with a COP of 3.55, a condensation temperature of 96°C and a temperature lift of 72°C was modelled as part of an integrated energy system. In addition to the high-temperature heat pump, the integrated energy system consisted of a PVT-system, a battery for electrical power, a thermal energy storage system, and district heating. The operation of the system was simulated for one year in three Chinese cities: Shanghai, Lanzhou, and Beijing. The heat pump had a maximum capacity of 255.7 kW, and the thermal storage had a maximum capacity of 1000 kWh. The results from the simulations showed that the system behaved similarly in the three cities during the summer months when temperatures were high and there was little or no demand for space heating. In the colder months, the heat demand in Lanzhou and Beijing was higher than in Shanghai. The heat pump did not provide enough energy to cover the heat demand in any of the three cities in the winter months, but the gap between available heat and demand was largest in Lanzhou and Beijing. It was found that the area of the PV panels should be increased to produce more power so that the heat pump operation would not be limited by lack of available power. An alternative power source could also be installed to provide more power. Furthermore, the capacity of the battery storage and the thermal energy storage should be increased to provide a more stable supply of heat and electric power than the system currently experiences.

Keywords: High-temperature heat pump, ammonia refrigerant, integrated energy system, combined cooling, heating and power system

1. Introduction

Since the late 1800s, the average surface temperature of Earth has risen about 0.9°C, and most of the warming has taken place during the past 35 years [1]. According to the Global Status Report from the International Energy Agency in 2017, buildings and construction account for 36% of global energy use and 39% of energy related CO_2 emissions [2]. Operational emissions, that is emissions from heating, cooling, and lighting of buildings, account for 28% of global emissions [3]. As the world is becoming more developed, the demand for heating and cooling will likely rise, as more people will be financially able to equip their residences with heating and cooling systems.

According to the IEA, heat accounted for 50% of final global energy consumption in 2018, and 40% of global CO_2 emissions. 46% of the heat produced was used in buildings, mainly for space and water heating. 50% was used in industrial processes, and the last 4% was used in agriculture. Of all the heat produced in 2018, only 10% came from renewable energy sources [4]. Increasing this share by replacing old heating systems with greener, more efficient technologies can contribute greatly to a

decrease in global greenhouse gas emissions. Many alternatives exist today, such as district heating systems, solar heaters, and heat pumps.

Another way to reduce emissions related to energy production and consumption is to install an integrated energy system, where various smaller energy systems are connected, communicate, and operate interdependently of one another. Typical integrated energy systems consist of combined cooling, heating, and power (CCHP), but other combinations also exist. Two of the main benefits of integrated energy systems are the reduced overall cost if the system is properly controlled and the reduced environmental impact due to the higher overall efficiency. To further reduce the environmental impact, renewable energy sources can be integrated into these energy systems.

This paper is part of the project «Key technologies and demonstration of combined cooling, heating, and power generation for low-carbon neighborhoods/buildings with clean energy – ChiNoZEN». The operation of an integrated energy system is simulated for one year in the three Chinese cities Shanghai, Lanzhou, and Beijing. The focus of the simulations is the operation of the heat pump, and the goal is to investigate how the heat pump operates with the other components of the integrated energy system over the course of one year.

2. Methodology

2.1 About the model

The model was created in Matlab, and refrigerant properties were collected from REFPROP. Meteonorm was used to collect weather data from Shanghai, Lanzhou, and Beijing. The electricity demand of other parts of the system than the heat pump was neglected, including the electricity demand for residential use of electrical appliances and lighting. The heat demand for every hour was calculated based on the outside air temperature. A base demand of 50 kW for water heating was assumed to be constant. Additionally, the heat demand increased with decreasing outside air temperatures.

The system consists of four main components: The PVT system, the electrical energy storage, the high-temperature heat pump, and the thermal energy storage. Additionally, the integrated energy system is connected to district heating.

The system is illustrated in Figure 1.

Figure 1:System sketch of the integrated energy system

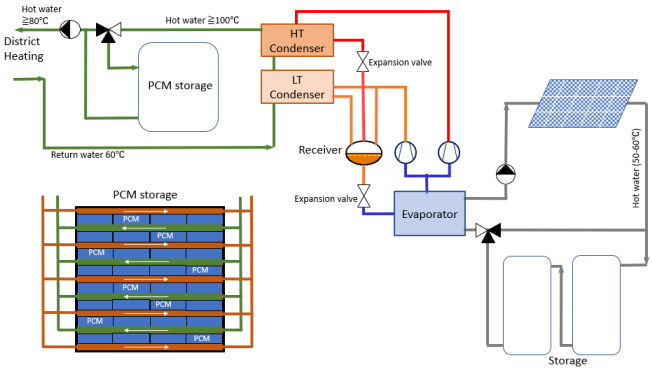

2.2 PVT model

The PVT system was simplified in this model. The effects from the solar thermal system were neglected, and only the PV system was modelled. PV panels of the type Jinko Tiger JKM470N-7RL3 from Jinko Solar were used in the model, and values used in calculations were taken from the datasheet [5]. The total PV area was assumed to be 4000 m^2, and the performance ratio was assumed to be 75%.

The model of the PV panels consisted of simple calculations that determined the energy output every hour. The modules were assumed to be horizontal, and the hourly values for global horizontal radiation were assumed to accurately represent the radiation the PV system would be exposed to every hour. Any shading effects were neglected.

To calculate the energy output, the operating efficiency was first calculated:

Equation 1: Operating efficiency of a PV module

$$r = \eta_{STC} - (T_{STC} - T_{PV}) \times TC$$

r is the operating efficiency [%]
η_{STC} is the module efficiency at standard test conditions [%]
T_{STC} is the temperature at standard test conditions [°C]
T_{PV} is the surface temperature of the PV module [°C]
TC is the temperature coefficient of the maximum power point [%/°C]

The energy output from the PV module can then be calculated:

Equation 2: Electric energy generated by a PV module per hour

$$E = A_{PV} \times r \times H \times PR$$

E is the electric energy generated by the PV module [kWh]

A_{PV} is the surface area of the module [m^2]
r is the operating efficiency [%]
H is the global horizontal radiation per hour [kW/m^2]
PR is the performance ratio [%]

2.3 Battery model

The code for the battery storage is greatly simplified. The power added to or removed from the battery is calculated every hour based on power production by the PV system and power consumption of the compressor. If the power consumption of the compressor exceeds the power produced by the batteries, the remaining power demand is taken from the battery. If the power consumption is lower than the power production, the excess power is sent to the battery. The charging and discharging efficiencies are assumed to be 80%, and the maximum storage capacity is 500 kWh.

2.4 Thermal energy storage model

The thermal energy storage tank is connected to the heat pump and the district heating system. Phase changing materials are used to maintain a temperature slightly above 80°C in the tank, so that the heat supply to the district heating system always stays above 80 °C. The specific heat transfer mechanisms between the phase changing materials and the water are not evaluated. For each hourly iteration, the heat demand is evaluated. The thermal energy system is either charged by receiving energy from the heat pump or discharged by providing energy to the district heating system. Whether the energy storage is charged or discharged depends on whether or not the heat demand exceeds the amount of heat produced by the heat pump. The charging and discharging efficiencies are 90%, and other heat losses are neglected. The maximum storage capacity is 1000 kWh.

2.5 Heat pump model

The heat pump is a vapor compression cycle with an evaporator, and expansion valve, two condensers at different temperature and pressure levels, and two compressors in series. A system sketch can be found in Figure 2 and a pressure-enthalpy diagram is illustrated in Figure 3.

Figure 2: System sketch of the high-temperature heat pump

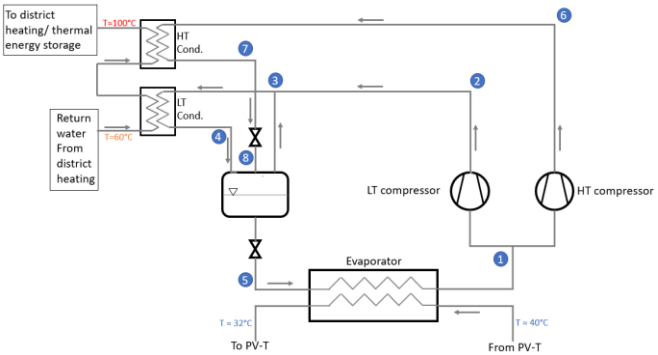

Figure 3: Pressure-enthalpy diagram of the high-temperature heat pump

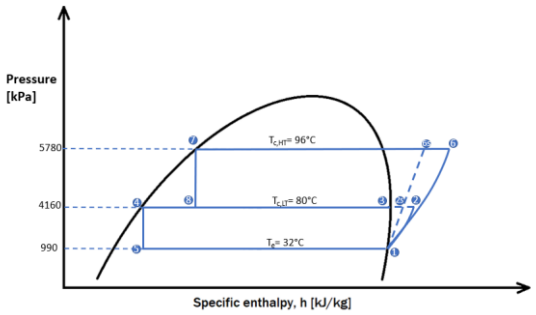

For every hourly iteration, the evaporation and condensation temperatures are calculated as well as power consumption, heating capacity, COP, and other properties. The calculations start with initial guesses of the evaporation and condensation temperatures. The refrigerant properties are calculated, and the heat capacity is found using the following equation:

Equation 3: Heating capacity

$$\dot{Q}_C = \dot{m}_{R,LT} \cdot (h_4 - h_2) + \dot{m}_{R,HT} \cdot (h_7 - h_6)$$

Where $\dot{Q}_C$ is the total heating capacity in [kW], $\dot{m}_{R,LT}$ and $\dot{m}_{R,HT}$ are the mass flow rates of the refrigerant through the low-temperature compressor and the high-temperature compressor, respectively, in [kg/s]. h_4 and h_7 refer to the enthalpies at the outlet of the condensers in [kJ/kg], where stage 4 is the outlet of the low-temperature condenser and stage 7 is the outlet of the high-temperature condenser. h_2 and h_6 refer to the enthalpies at the inlet of the low-temperature and high-temperature condensers.

The power consumption, or work done by the compressors in [kW] is calculated and coefficient of performance are calculated with the following equations:

Equation 4: Work done by the compressor

$$\dot{W} = \dot{m}_{R,LT} \cdot (h_2 - h_1) + \dot{m}_{R,HT} \cdot (h_6 - h_1)$$

Equation 5: Heating COP

$$COP = \frac{\dot{Q}_C}{\dot{W}}$$

Once these values are determined, new values for condensation and evaporation temperatures are calculated. First, the logarithmic mean temperature difference [K] is found:

Equation 6: Logarithmic mean temperature difference in the condenser

$$LMTD_{Condenser} = \frac{\dot{Q}_c}{U \times A}$$

Where U is the U-value, which is a coefficient that describes the heat transfer through the walls of the heat exchangers in [kW/m^{2}K]. A is the heat exchanger surface area in [m^2]. These equations can also be rearranged, combined, and used to find other values such as $\dot{Q}_c$ or T_c.

The outlet temperature of the water heated by the condenser is calculated:

Equation 7: Outlet temperature of hot water

$$T_{hw,out} = T_{hw,in} + \frac{\dot{Q}_c}{C_{p,hw} \times \dot{m}_{hw}}$$

$C_{p,hw}$ is the specific heat capacity of the hot water at constant pressure, in [kJ/kgK]. $\dot{m}_{hw}$ is the mass flow rate of the hot water through the condenser in kg/s, and $\dot{Q}_c$ is the heat capacity. The unit for all temperatures is [K].

Using these values, a new value for the condensation temperature can be found:

Equation 8: New value for condensing temperature

$$T_c = \frac{T_{cw,out} \times e^{\frac{T_{hw,out} - T_{hw,in}}{LMTD_{cond.}}} - T_{cw,in}}{1 - e^{\frac{T_{hw,out} - T_{hw,in}}{LMTD_{cond.}}}}$$

The same is done for the evaporator. If the new value for the condensing temperature deviates from the old value with more than 0.1 K, the heat pump loop starts again, with the new initial guess for condenser temperature equal the old value plus half of the difference between the old and the new value. This continues until the difference between the old and new value is less than 0.1 K.

The heat pump is programmed to operate on full load whenever possible. However, when the thermal storage system reaches full capacity, the heat pump is shut off. It remains off until the thermal storage is completely discharged, or until the storage capacity is lower than the demand. The heat pump is then turned back on and operates on full capacity until the thermal storage is full. However, if the power consumption of the compressor exceeds the available power in the battery and from the PVT system, the heat pump will operate on part load. The load will be as high as possible with the available power supply. The load ratio (LR) describes the ratio of the current heating capacity to the maximum capacity:

Equation 9: Load ratio

$$LR = \frac{\dot{Q}_{c,actual}}{\dot{Q}_{c,max}}$$

3. Results and discussion

3.1 Heat pump performance and power production

The system was simulated for the three Chinese cities Shanghai, Lanzhou, and Beijing. Shanghai has the highest annual temperatures of the three, and Lanzhou has the lowest temperatures. Due to the large number of iterations, some results will be presented by month or week rather than by year. January is a representative winter month, April is representative for spring and autumn, and July is representative for the summer months. Average temperatures, as well as maximum and minimum values, are displayed in Table 1.

	Max. temp.	**Min. temp.**	**Average temp. January**	**Average temp. April**	**Average temp. July**
SH	38.7	-4.5	4.78	14.56	26.28
LZ	34.5	-16.7	-5.10	11.87	22.61
BJ	38.7	-13.9	-3.92	11.68	27.74

Table 1: Temperatures in Shanghai, Lanzhou, and Beijing. All temperatures are in [°C].

Despite large temperature differences during the winter months, the cities have similar temperature and demand curves over a year. Consequently, the same results from all three cities will not be presented. Instead, results from one city will be presented, and the similarities and differences between the three cities will be explained.

Figure 4 shows the total heat pump capacity and demand for every hour through the year in Lanzhou. The curves are similar for Shanghai and Beijing, although the hourly demand never exceeds 250 kW in Shanghai. It is clear that the heat demand greatly exceeds the heat pump capacity in certain hours. The

heat pump mostly operates on maximum capacity or is shut off. Furthermore, the heat pump operates on part load a few hours throughout the year. The maximum capacity of the heat pump is 255.7 kW.

Figure 4: Heat capacity and heat demand in Lanzhou in January

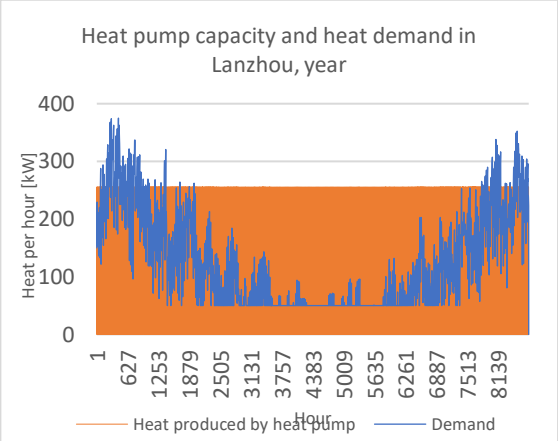

Figure 5 shows the hourly average heat demand and available heat from the heat pump and thermal energy storage per week. This graph shows that the heat supply exceeds the demand most weeks, however, the heat supply is sometimes insufficient during the winter months. The table below presents the number of hours with insufficient heat supply.

Figure 5: Hourly average heat demand and heat supply

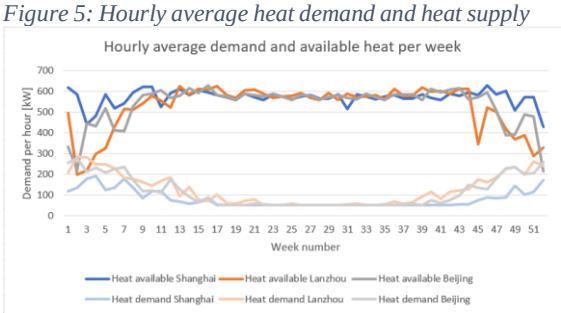

Table 2 is a collection of data that describes heat supply and demand for selected time periods. The heat pump operates in less than half the time steps, which means that the heat pump is turned off for more than half the time. In January, the heat pump is turned on for a larger percentage of the time than on a yearly basis, due to a higher demand during winter months. However, the heat pump is turned off for more than 40% of the time in all three cities, even though all cities experience heat shortages. The most notable heat shortage is found in Lanzhou, where the heat demand is not met 47.26% of January.

	Number of operating hours heat pump	Percentage of time when heat pump was turned on [%]	Number of hours when demand exceeds supply	Percentage of time with insufficient heat [%]	Total amount of insufficient heat [kWh]
SH Jan.	397	53.14	103	13.79	17 863
LZ Jan.	424	56.76	353	47.26	82 112
BJ Jan.	445	59.57	295	39.49	67 731
SH April	194	26.84	0	0	0
LZ April	285	39.64	9	1.25	874
BJ April	227	31.57	1	0.14	82
SH July	162	21.80	0	0	0
LZ July	162	21.80	0	0	0
BJ July	161	21.67	0	0	0
SH year	2757	31.47	283	3.23	44 795
LZ year	3569	40.75	1090	12.4	236 130
BJ year	3351	38.26	856	9.8	187 534

Table 2: Heat shortages

Figure 6 shows the heat production, thermal storage capacity, and heat demand in Lanzhou in January. There is a notable period during the middle of the month where the thermal storage capacity is low or empty, and demand exceed the amount of heat produced by the heat pump.

The graph also shows that the heat pump is turned off for several time steps while demand is high. This is because of a lack of available power in those time steps.

Figure 6: Heat production, heat demand, and thermal energy storage capacity in Lanzhou in January

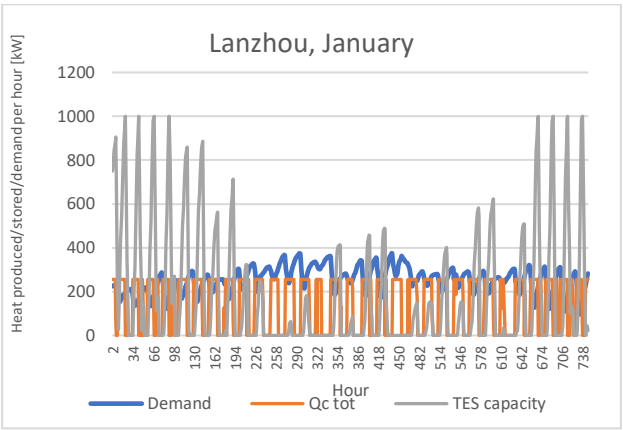

To better see the relation between the lack of heat despite high demand and a lack of power, the following figures will show data for five days in January.

Figure 7: Heat production, heat demand, and thermal energy storage capacity in Lanzhou, January 22-27

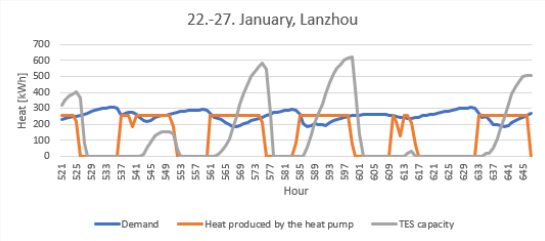

Figure 8: Power production, power consumption, and battery capacity in Lanzhou, January 22-27

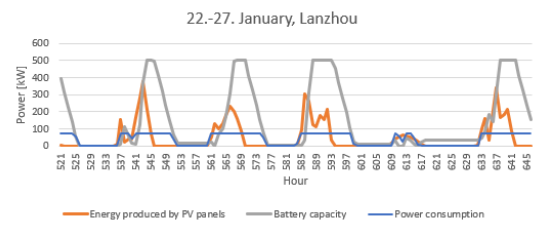

There is a clear correlation between the heat pump operation and the available power. The time steps when the heat pump is shut off or is at part load even though demand is high are the same time steps when there is little or no available power for the compressor. This is seen throughout the year and the same results are found in the simulations for Shanghai and Beijing.

To increase the number of operating hours for the heat pump, the amount of available power must be increased. This can be achieved by increasing the area of the PV modules, or by enhancing the battery storage capacity. Figure 8 displays four separate instances where the PV system produces power even when the mattery has reached maximum capacity, so increasing the battery capacity would elongate the heat pump operating cycles. Because the battery reaches maximum capacity so many times, increasing the PV area would have little effect without an increase in battery capacity as well. An alternative is to add an auxiliary power supply, for example wind power or a connection to the local power grid. This would give a more stable power supply, but prices and emissions related to power production would increase.

Thermal storage capacity or heat pump capacity should also increase if the demand during winter months is to be met. This must be done together with an increase in available power.

The total heat demand in Lanzhou in January was 188 222 kWh. The total amount of heat produced by the heat pump was 105 630 kWh. If the heat pump has been at full capacity for every time step in the duration of January, the heat pump would have produced 190 497 kWh. This is slightly more than the total demand, and in theory it is enough to cover the heat demand in January. However, this assumes a steady heat demand or a higher maximum thermal storage capacity. If the heat demand had been right below 250 kW every hour, the heat pump would always be able to send the heat directly to the district heating system and cover heat demand. But since the heat demand varies and sometimes approaches 400 kW, it is necessary that the thermal storage unit supplies the heat pump in the hours with the highest demand. To ensure that this can happen, the thermal storage system must have a high enough capacity to save all the excess heat for the heat pump. Furthermore, the efficiency of the thermal energy storage limits the amount of heat that is available. The thermal energy storage system operates with a 90% efficiency during charging and discharging, so 10% of the heat is lost in the process. There are additional heat losses through the walls of the thermal storage system, although those losses have been neglected in this simulation. This means that even if the heat pump operated on full capacity with no breaks every hour throughout January, and even if the thermal storage system had an unlimited capacity, the heat pump in this system would likely not be able to supply the residents in Lanzhou with enough heat to cover their heat demand in January.

Beijing has a slightly lower total heat demand, and it might have been possible to cover this heat demand if an alternative power source was connected to the system, and if the thermal storage capacity was higher. The heat shortage in Shanghai in January was 64 249 kWh lower than in Lanzhou, and the heat demand never exceeds 255 kW in any hourly time step. Consequently, the heat pump would be able to cover the total heat demand if an alternative power source were connected so that the heat pump could always operate on full capacity.

The heat supply and power demand in July are stable, as can be seen in Figure 9. The results from July and other summer months are very similar for all three cities.

Figure 9: Heat demand and available heat in Lanzhou in July

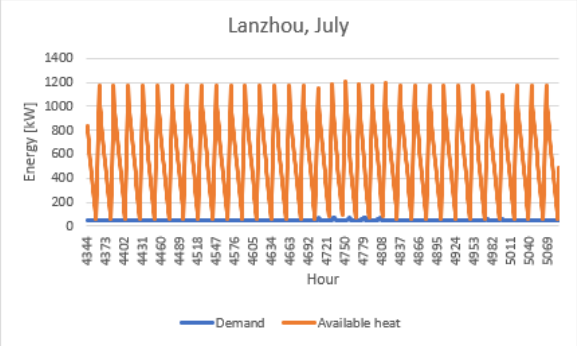

3.2 Temperatures and efficiencies

The condensation temperatures vary greatly throughout the year. However, it appears that the variations in temperature coincide with the load ratio of the heat pump. When the heat pump works on full load, the heat exchanger temperatures remain relatively constant. While they may vary slightly, they normally stabilize around 353.35 K, or 80.20°C in the low-temperature condenser, and 369.17 K or 96.02°C in the high-temperature condenser. This leads to an outgoing water temperature of 350.97 K (77.82°C) from the low-temperature condenser and 365.38 K (92.23°C) from the high-temperature condenser. These temperatures are consistent for all three cities.

However, in the beginning and end of the year, the temperatures drop quite frequently. Figure 10 displays the temperatures in the two condensers in Shanghai during one week in January. Similar results to the ones displayed in this graph are found throughout the colder periods in all three cities, but the week of January 12 to January 18 was selected to better be able to interpret the results.

Figure 10: Temperatures in the condensers in Shanghai, January 12-18

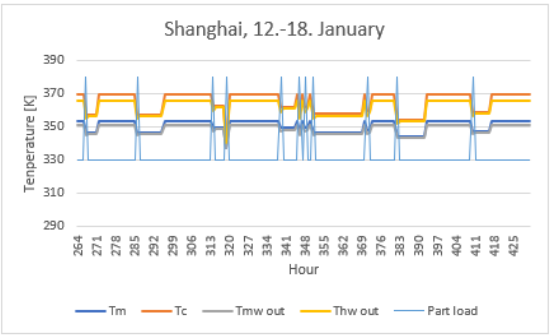

As previously mentioned, there appears to be a correlation between the temperature drops and the load ratio of the heat pump. This is also consistent with literature [6]. The thin blue, vertical lines show the time steps when the heat pump operates on part load.

An effect on the load ratio is also seen when studying the COP of the heat pump in the various time steps. This is displayed in Figure 11.

Figure 11: Coefficients of performance in the LT cycle, the HT cycle and the total COP for Shanghai, January 12-18

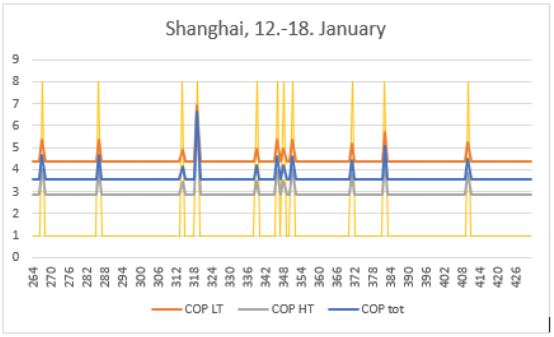

In Table 3, data from six different time steps are presented. ll time steps are sorted from largest to smallest load ratio. All the data points are from Lanzhou in January, but similar results are found in the simulation data from the other cities as well. The same results are found during the spring and autumn, but with a lower frequency than the winter months.

Hour	**5**	**378**	**50**	**360**	**7**	**26**
Demand	228.35	252.95	207.85	264.23	229.38	17.04
Total heat pump capacity	255.70	218.30	188.44	133.42	67.32	61.01
Load ratio	1.00	0.85	0.74	0.52	0.26	0.24
Total power consumption by the compressors	72.16	54.76	42.84	25.28	10.46	9.31
Available power	276.82	57.18	52.65	39.68	17.04	15.67
LT condenser temperature	353.35	350.28	347.86	343.43	338.24	337.75
HT condenser temperature	369.17	364.01	359.82	352.11	342.80	341.90
Outlet temp. of water from HT condenser	365.38	360.71	356.97	350.05	341.70	340.90
COP	3.54	3.99	4.40	5.28	6.44	6.55

Table 3: Values for temperature, efficiency, heat production, and power at various load ratios

There is a clear correlation between the changes in condenser temperatures and COP and the load ratio. The temperatures decrease with the load ratio, while COP increases as load ratio is reduced.

The outgoing water temperature from the high-temperature condenser normally stays above 353.15 K (80°C), even when the heat pump operates on part

load. This is important, because the outgoing water temperature to the district heating system is designed to be 80°C. The system will therefore be less efficient and able to transfer less heat to the district heating system if the outgoing water temperature is below 80°C.

A problem occurs when the outgoing water temperature is lower than 80°C, which happens in certain time steps. This happens in less than 5% of the cases, however this should be avoided to ensure the district heating system receives enough heat. To avoid this, the heat pump system must be modified so that the condensation temperature of the high-temperature condenser is higher. Because the water temperatures are directly related to the load ratio, this problem can also be avoided by limiting the load ratio. It seems that the outgoing water temperature drops below 80°C when the load ratio is below 70%. If the heat pump is programmed to shut off when the load ratio drops below 70% rather than going on part load, this problem could be avoided, and the outgoing water temperatures would be above 80°C at all times.

Another option is to connect a heating coil to the system, after the water has passed through both condensers. In this case, there could be a temperature sensor after the high-temperature condenser, and if the temperature is lower than a specified value, for example 80°C, the heating coil could be turned on. However, this heating coil would require a power source, preferably electricity. The problem is that the heating coil would only be necessary when the heat pump operates on part load, and the heat pump only operates on part load when there is not enough power for the heat pump to operate on full load. This means that there probably would not be enough power to heat the heating coil when it was needed. Another drawback is that the heating coil would have a COP below 1 if all losses are accounted for, and the heating coil would therefore reduce the COP of the system as a whole.

The increase in COP can be explained by the temperature reduction. Lower condenser temperatures lead to smaller temperature lifts, and less power is needed by the compressor. This results in a higher COP when the condensing temperatures are lower. However, the calculations of COP are not completely accurate due to assumptions and simplifications.

The temperature of the heat source is assumed to be constant. In reality, it is dependent on the ambient temperature and the temperature of the PVT system. The heat source temperature will be higher on hot days and days with a high amount of solar radiation, which leads to a smaller temperature lift and a higher COP. This effect was neglected in the simulations.

Moreover, the inlet temperature of the water going to the condensers is assumed to be constant. The actual temperature is dependent on the return temperature from the district heating system, which will be affected by mass flow rates and heat demand.

Lastly, the power consumption of other components than the compressor is neglected. This includes pumps and other electrical components which need power during heat pump operation. When the heat pump operates on part load, these components make up a larger part of the total power consumption and will lead to a reduced COP [7]. Power consumption also increases during shutdown and start up, but this effect is neglected.

4. Conclusions

The siulations of the integrated energy system showed sismilar trends for Shanghai, Lanzhou, and Beijing thrughout the year, however the heat demand was much higher in Lanzhou and Beijing than Shanghai during the winter months. This suggests that the energy system should be adapted to the city where it is located. The optimal operation of the system in Shnaghai might be different than if the system is located in Lanzhou.

Because the heat pump needs electrical power to operate, it is crucial that the power production part of the integrated energy system can produce enough power. The existing system does not have a high enough capacity, and the area of the PV modules must be improved or an auxiliary power source must be connected to the system. This is especially important during the winter months, when heat demand and therefore compressor power consumption is high and the solar radiation is low.

The capacities of the battery storage and thermal energy storage must also be enhanced. This will reduce the number of hours with insufficient heat demand, and reduce the amount of electrical power produced by the PV system that is wasted due to a full battery capacity.

The heat pump mostly operates on full load, but when there is not enough power for full load operation, the heat pumpoperates on part load. This leads to a higher COP due to lower condenser temperatures. However, lower condenser temperatures lead to lower temperatures in the heat sink, which can result in loess available heat to the district heating system.

The values for COP are not completely accurate due to assumptions about water temperatures and power consumptions. There is a need for a more

detailed model of the heat pump and the other components in the integrated energy system in order to get more accurate and realistic values and a better understanding of how the heat pump operates in the integrated energy system. However, the simulations presented in this paper have uncovered certain trends that are important to be aware of in future work on this project.

Acknowledgements

This research work was funded by the Chinese-Norwegian collaboration project on Energy (ChiNoZEN) and National Key R&D Program of China (SQ2019YFE010256). The authors also gratefully acknowledge the financial support from the Research Council of Norway and user partners of High EFF (Centre for an Energy Efficient and Competitive Industry for the Future, an 8-year Research Centre under the FME-scheme).

References

1. NASA. *Climate Change: How Do We Know?* 2020 [cited 2020 21.01]; Available from: https://climate.nasa.gov/evidence/.
2. World Green Building Council. *Global Status Report 2017*. 2017 11.12.2017 [cited 2020 22.01]; Available from: https://www.worldgbc.org/news-media/global-status-report-2017.
3. World Green Building Council. *New report: the building and construction sector can reach net zero carbon emissions by 2050*. 2019 23.09.2019 [cited 2020 22.01]; Available from: https://www.worldgbc.org/news-media/WorldGBC-embodied-carbon-report-published#_ftn1.
4. IEA. *Renewables 2019*. 2019 [cited 2020 28.01]; Available from: https://www.iea.org/reports/renewables-2019/heat.
5. Jinko Solar, *Tiger Mono-facial 450- 470 Watt*. 2020, Jinko Solar.
6. Karlsson, F. and P. Fahlén, *Capacity-controlled ground source heat pumps in hydronic heating systems.* International Journal of Refrigeration, 2007. **30**(2): p. 221-229.
7. Han, D., Y.S. Chang, and Y. Kim, *Performance analysis of air source heat pump system for office building.* Journal of Mechanical Science and Technology, 2016. **30**(11): p. 5257-5268.

Signe Truyen Ryssdal

High Temperature Heat Pumps in Integrated Energy Systems

NTNU
Norwegian University of
Science and Technology